Creating Novel Ligand Libraries from Air-Stable, Chiral Primary Phosphines

PhD Thesis Submitted by

Arne Ficks

Supervisor
Dr. Lee J. Higham

School of Chemistry
Faculty of Science, Agriculture and Engineering
Newcastle University, Newcastle upon Tyne
NE1 7RU, United Kingdom
April 2013

Thesis Abstract

The fearsome reputation of primary phosphines, many of which are toxic and highly reactive towards atmospheric oxygen, has constrained the use of these versatile compounds in synthetic chemistry. However, a few examples of user-friendly stable primary phosphines have been reported which owe their stability to high steric encumbrance or is as yet unexplained. Recently an electronic stabilisation has allowed for the synthesis of novel MOP-type phosphorus ligands with previously inaccessible architectures that have potential applications in homogeneous asymmetric catalysis; an introduction into the topic is given in Chapter 1.

The first air-stable chiral primary phosphines **1a**,**b** were developed in our labs. We subsequently simplified and improved the synthetic approach to afford these and previously unreported synthons on a multigram scale, which is described in Chapter 2.

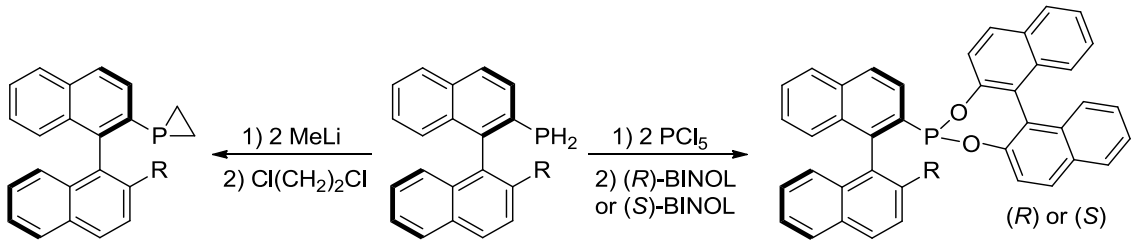

14a,**b** **1a**,**b** (R = H, OMe) **33a**,**b** (*R*) **34a**,**b** (*S*)

Phosphiranes are highly strained heterocycles with a small sum of bond angles at the phosphorus (Σ°(P): <260). They act as ligands with interesting properties upon metal complexation due to the unusual electronics they possess as a result of the imposed ring strain; this leads to high *s*-character at the phosphorus and both lowered HOMO and LUMO energy levels compared to their acyclic counterparts. In Chapter 3 we report the synthesis of chiral binaphthyl-phosphirane ligands **14a**,**b** offering high thermal and air stability, as well as the synthesis and solid state structures of their platinum(II) dichloride complexes. Initial findings for the application of the phosphiranes in the palladium catalysed asymmetric hydrosilylation of styrene are discussed.

Furthermore, we were able to synthesise MOP-dimethylphosphine, MOP-bis(dimethyl-amino)phosphine and MOP-dimethylphosphonite ligands in one-pot reactions from **1a**,**b**. Their peculiar structural and electronic parameters, in addition to those of MOP-phosphiranes **14a**,**b**, are discussed in Chapter 4. The coordination chemistry of these compounds was investigated on platinum(II) and palladium(II) metals elucidating their *cis*/*trans* influences

and aryl side-on coordination respectively. We also carried out comparative studies in the allylic alkylation of (*rac*)-(*E*)-1,3-diphenylallyl acetate and the hydrosilylation of styrene, utilising palladium complexes of those MOP-type ligands as asymmetric catalysts.

In Chapter 5 we report the efficient synthesis of novel MOP-phosphonite hybrid ligands **33a**,**b** and **34a**,**b** which incorporate two binaphthyl groups around the single phosphonite P-donor. We present their methallylpalladium complexes, which were studied in detail both in the solid-state and in solution. The palladium catalysed asymmetric hydrosilylation of styrene was again carried out and the results analysed in view of the molecular structure of the ligands. Furthermore, rhodium complexes of the same ligands were investigated, in particular with a view to examining their binding behaviour towards the metal. An unusual aromatic side-on binding mode was revealed by X-ray crystallography and further elucidated in solution by extended NMR experiments. Solution NMR studies also revealed a dynamic behaviour of these complexes, triggered by the hemilabile binding of the ligands towards the metal centre.

Finally, we describe the synthesis of novel MOP-phosphonodichalcogenoite and MOP-phosphaalkene ligands in Chapter 6. Their corresponding gold(I) complexes were prepared and representative examples were characterised by X-ray diffraction. For the MOP-phosphonodiselenoite derivatives we also report the characteristic ^{77}Se NMR data.

About the Author

Arne Ficks studied chemistry at the University of Göttingen, Germany, where he obtained his Diplom (MSc equivalent degree) in June 2009 under the supervision of Prof. Dr. Franc Meyer. His research was focused on the synthesis of C_2-symmetric pyrazole bridged bis(oxazoline) ligands and their use in transition metal catalysis. He joined the research group of Dr. Lee J. Higham at Newcastle University in October 2009 to work on applications of primary phosphines in asymmetric catalysis.

Acknowledgement

I am most grateful to my supervisor Dr. Lee Higham who gave me the opportunity to come to Newcastle and join his research group. I am glad for his guidance that made me most aware of what experiments to focus on, but I also appreciated the freedom that I was granted to develop some of my own ideas and to incorporate them into the overall research theme. In addition, I am thankful for the financial support that was provided by Lee through his EPSRC grant, which allowed me to present my work at the *ACS National Meeting 2011* in Anaheim (CA, USA), and the *Dalton Transactions Younger Researchers Symposium 2011* at the University of Warwick (UK); I was also able to get funding awarded by PhoSciNet (COST action CM0802) to deliver an oral presentation at the *9th European Workshop on Phosphorus Chemistry 2012* in Rennes (France).

I would like to thank all the present and past members of the Lee Higham research group, in particular my fellow PhD students Manuel Abelairas-Edesa, Connor Sibbald, James Fleming, Jennifer Wallis and Laura Davies, who have contributed immensely to the excellent working atmosphere in our shared lab and office, for their friendship, mutual advice and help of any kind. For the same reasons my thanks also extend to the vast majority of co-workers in the Johnston Lab and the Chemistry Department in general.

There are a number of people in the Chemistry Department that I would like to thank for providing various types of services that strongly facilitated the work on my research project: Prof. William McFarlane, Dr. Corinne Wills (NMR); Dr. Ross Harrington, Dr. Ulrich Baisch, Prof. William Clegg (X-ray); Claire Nicoll (Administration); Dr. Jerry Hagon (Computing); Dr. Beverly Stewart, Prof. Anthony Harriman (DFT-Calculations); Christopher Burrow, Geoffrey Reah (Electrical Workshop); John Corner, Gary Day (Mechanical Workshop); James Baron (Elemental Analysis); Robyn Hare, William McCormack (Glassblowing); Robin Ingleton (Stores). Furthermore, I would like to acknowledge the EPSRC NMSSC in Swansea for providing the mass spectrometric measurements.

Lastly, I would like to thank my parents for the remarkable support they have given me throughout my life.

List of Publications

Parts of this thesis have been published in the following scientific papers (in chronological order).

I. R. M. Hiney, A. Ficks, H. Müller-Bunz, D. G. Gilheany, L. J. Higham*, Air-stable Chiral Primary Phosphines: Part (i) Synthesis, Stability and Reactivity, in *Specialist Periodical Reports - Organometallic Chemistry*. (Eds. I. J. S. Fairlamb, J. M. Lynam), RSC, 2011, *37*, pp.27–45.

II. A. Ficks, I. Martinez-Botella, B. Stewart, R. W. Harrington, W. Clegg, L. J. Higham*, Taming Functionality: Easy-to-handle Chiral Phosphiranes, *Chem. Commun.* **2011**, *47*, 8274–8276.

III. A. Ficks, R. M. Hiney, R. W. Harrington, D. G. Gilheany, L. J. Higham*, MOP-Phosphonites: A Novel Ligand Class for Asymmetric Catalysis, *Dalton Trans.* **2012**, *41*, 3515–3522.

IV. A. Ficks, C. Sibbald, S. Ojo, R. W. Harrington, W. Clegg, L. J. Higham*, Efficient Multigram Syntheses of Air-Stable, Chiral Primary Phosphine Ligand Precursors via Palladium-Catalyzed Phosphonylation of Aryltriflates, *Synthesis* **2013**, *45*, 265–271.

V. A. Ficks, R. W. Harrington, L. J. Higham*, Chiral MOP-Phosphonite Ligands: Synthesis, Characterisation and Interconversion of η^1,η^6-(σ-P, π-arene) Chelated Rhodium(I) Complexes, *Dalton Trans.* **2013**, *42*, 6302–6305.

VI. A. Ficks, R. W. Harrington, L. J. Higham*, Chiral MOP-Type Ligands: Structural and Electronic Impact in Palladium(II) and Platinum(II) Complexes; Applications in Asymmetric Hydrosilylation and Allylic Alkylation, manuscript in preparation.

List of Abbreviations

Ac	acetyl
acac	acetylacetone
Ar	aryl
BArF	$B[3,5\text{-}(CF_3)_2C_6H_3]_4^-$
br	broad
BABARphos	specific type of polycyclic phosphirane ligand (**LIV**; Figure 3.2)
BINAP	2,2'-bis(diphenylphosphino)-1,1'-binaphthyl
BINOL	1,1'-bi-2-naphthol
Bn	benzyl
BSA	bis(trimethylsilyl)acetamide
Bu	butyl
CAMP	*o*-anisylcyclohexylmethylphosphine
cod	1,5-cyclooctadiene
COSY	two-dimensional correlation spectroscopy (NMR)
Cy	cyclohexyl
d	doublet (NMR)
DABCO	1,4-diazabicyclo[2.2.2]octane
DCM	dichloromethane
DFT	density functional theory
DIOP	2,3-*o*-isopropylidene-2,3-dihydroxy-1,4-bis-(diphenylphosphino)butane
DiPAMP	(2-methoxyphenyl)-[2-[(2-methoxyphenyl)-phenylphosphanyl]ethyl]-phenylphosphine
DIPEA	*N*,*N*-diisopropylethylamine
DMAP	4-dimethylaminopyridine
DMSO	dimethyl sulfoxide
DPPB	1,4-bis(diphenylphosphino)butane
DPPE	1,2-bis(diphenylphosphino)ethane
DPPF	1,1'-bis(diphenylphosphino)ferrocene
DPPP	1,3-bis(diphenylphosphino)propane
DuPHOS	1,2-bis(phospholano)benzene
EDC	1,2-dichloroethane
E	energy

ee	enantiomeric excess
Et	ethyl
Josiphos	ferrocene based chiral diphosphine ligand (Figure 1.2)
J	spin-coupling constant (NMR)
HMBC	two-dimensional heteronuclear multiple bond correlation (NMR)
HOMO	highest occupied molecular orbital
HPLC	high-performance liquid chromatography
HRMS	high resolution mass spectrometry
HSQC	two-dimensional heteronuclear single quantum coherence (NMR)
^{i}Pr	*iso*-propyl
IR	infra-red
L	arbitrary ligand
L_P	arbitrary phosphorus ligand
L-DOPA	L-3,4-dihydroxyphenylalanine
LUMO	lowest unoccupied molecular orbital
M	metal
m	multiplet (NMR), medium (IR)
MAP	2'-(diphenylphosphino)-*N*,*N*-dimethyl-[1,1'-binaphthalen]-2-amine
Me	methyl
Men	menthyl
MOP	[1,1'-binaphthalen]-2-yldiphenylphosphine
MP	melting point
MPPP	methyl(phenyl)(*n*-propyl)phosphine
MS	mass spectrometry
NMDPP	neomenthyldiphenylphosphine
NMR	nuclear magnetic resonance
nOe	nuclear Overhauser effect
NOESY	two dimensional nuclear Overhauser effect spectroscopy (NMR)
OR	optical rotation
PA	proton affinity
PAMP	(2-methoxyphenyl)(methyl)(phenyl)phosphine
Ph	phenyl
PPF	ferrocene based chiral monophosphine ligand (Figure 1.3)
q	quartet (NMR)

R	arbitrary organic substituent
R_f	retardation factor
s	singlet (NMR); strong (IR)
S4	symmetric deformation coordinate
SOMO	singly occupied molecular orbital
T	temperature
t	triplet (NMR)
Tf	trifluoromethane sulfonyl
THF	tetrahydrofuran
tht	tetrahydrothiophene
TLC	thin layer chromatography
TMS	trimethylsilyl
Ts	tosyl
UV	ultraviolet
w	width
w	weak (IR)
X	arbitrary halogen substituent
$[\alpha]_D^{20}$	specific angle of rotation
δ	chemical shift (NMR)
η	hapticity
θ_T	cone angle
v	wavenumber
Ξ	frequency of the specified nucleus relative to ^1H at 100MHz (NMR)

Table of Contents

Chapter 1 — Asymmetric Catalysis Using Monodentate P-Ligands

Transition metal catalysts provide a versatile approach to the synthesis of a variety of chemical compounds. Common homogeneous catalytic systems contain a metal-centre decorated with a suitable ligand scaffold. In chemical reactions these catalysts activate substrates by lowering activation barriers to transition states. In an asymmetric environment, *e.g.* when using a chiral ligand, catalysts can orientate pro-chiral substrates selectively in a certain way so that the formation of one enantiomer product is favoured. Thus, asymmetric catalysis is a convenient way to synthesise large amounts of optically active material from achiral substrates using only small fractions of chiral catalysts to start with. An important class of ligands used in homogeneous catalysis are the phosphines. They are organo-phosphorus compounds that can act as Lewis bases by utilising their free electron pair on the P(III)-atom in order to coordinate onto metals.

1.1 A Brief Historic Overview

Homogeneous catalysis utilising monodentate phosphine ligands was introduced by Wilkinson and co-workers in 1965, who showed that [$RhCl(PPh_3)_3$] catalysed the hydrogenation of alkenes.[1] It was the first time that a homogeneous catalyst showed comparable high catalytic activity to their, at the time already well-known, heterogeneous counterparts. Homogeneous catalysis may offer better selectivity, milder reaction conditions and better variation possibilities than heterogeneous processes; disadvantages normally lie in catalyst/product separation and lower thermal stability of the catalyst.[2] For his contributions in the area of organometallic chemistry Wilkinson was awarded the Nobel Prize in chemistry in 1973 (shared with E. O. Fischer).[3]

Later in 1965, Vaska *et al.* used their *trans*-[$IrCl(CO)(PPh_3)_2$] complex as a homogeneous catalyst for the reduction of alkenes.[4] Horner and co-workers, who were investigating the influence of different phosphine ligands on the catalytic activity of Wilkinson's rhodium complex, reported in 1968 that they were planning to use chiral tertiary phosphines (the synthesis of which they had published back in 1961)[5] in order to achieve stereospecific hydrogenations.[6] In October of the same year Knowles *et al.* were the first to utilise an optically active phosphine ligand MePPh(*i*Pr) (Figure 1.1) on rhodium so that they could prepare hydratropic acid in 15% optical yield.[7]

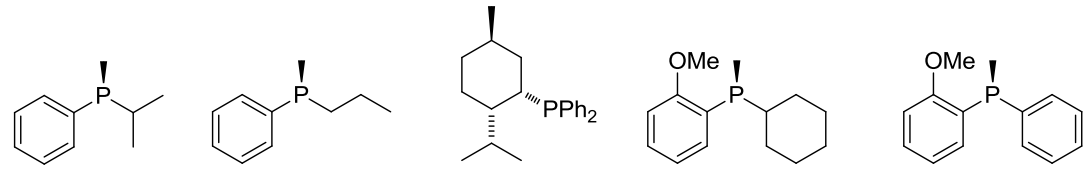

Figure 1.1 Early examples of chiral monophosphine ligands.

The ligand that was used is chiral by virtue of its three different substituents on the P-atom; the inversion barrier of phosphines, 29–31 kcal/mol for methyl(phenyl)(*n*-propyl)phosphine (MPPP, Figure 1.1), lies sufficiently high to prevent racemisation.[8] Horner and co-workers published their contribution to asymmetric catalytic hydrogenations in December 1968, showing that prochiral styrene derivatives can be hydrogenated in up to 8% optical yield by using MPPP (Figure 1.1) as the P-chiral ligand.[9] In 1971 Morrison and co-workers synthesised neomenthyldiphenylphosphine (NMDPP, Figure 1.1) from menthyl chloride, a readily available chiral precursor.[10] Although the chirality of the ligand is located away from the P-atom, it gave up to 61% *ee* in rhodium catalysed hydrogenations.[11] The enantio-selectivity of this reaction could be further enhanced in 1972 when Knowles and co-workers accomplished up to 90% *ee* in the reduction of α-(acylamino)acrylic acids utilising their chiral CAMP and PAMP ligands (Figure 1.1).[12]

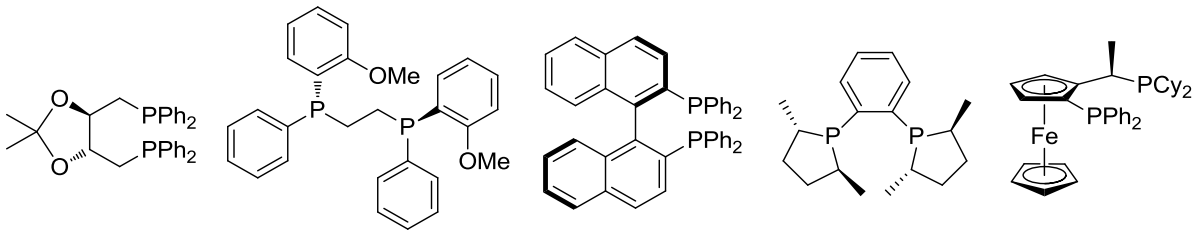

Figure 1.2 Selection of bidentate chiral phosphine ligands.

For the next 25 years the development of phosphine ligands focused mainly on the synthesis of bidentate derivatives. The first chiral diphosphine ligand DIOP (Figure 1.2) was developed by Kagan *et al.* in 1971; the ligand was prepared from naturally occurring (+)-tartaric acid and used in several asymmetric reductions giving optical yields of up to 72%.[13] In 1975 Knowles and co-workers reported the bidentate DiPAMP phosphine (Figure 1.2) which was derived from the monodentate PAMP ligand.[14]

DiPAMP was employed by the Monsanto Company for the commercial synthesis of L-DOPA (a drug for the treatment of Parkinson's disease), thus providing the first example of an asymmetric organometallic catalyst being used on an industrial scale (Scheme 1.1).[15] For his pioneering work in the field of asymmetric hydrogenations, Knowles was eventually awarded the Nobel Prize in chemistry in 2001 (shared with Noyori and Sharpless).[16]

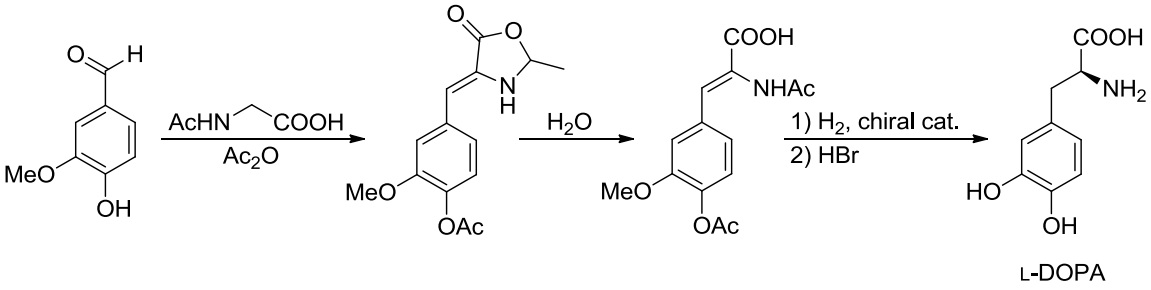

Scheme 1.1 Monsanto L-DOPA synthesis using (*R*,*R*)-DiPAMP as chiral ligand in the hydrogenation step.

Another milestone in the development of bidentate phosphine ligands was the discovery of BINAP by Noyori in 1980 (Figure 1.2, page 2).[17] This atropisomeric C_2-symmetrical bisphosphine ligand worked well in Rh(I) and Ru(II) catalysed asymmetric hydrogenations (for atropisomerism see Chapter 1.3.1). The scope of the reaction was greatly extended so that the catalytic hydrogenation worked with a wide range of functionalised alkenes.[18] Dupont's DuPHOS-Rh catalysts achieved the effective synthesis of various unnatural α-amino acids in asymmetric hydrogenations from their α-enamide substrates;[19] the DuPHOS ligand (Figure 1.2) was first reported by Burk in 1991.[20]

JosiPhos (Figure 1.2) is a successful bidentate ligand that features planar chirality (the chiral plane is on the substituted ring) in addition to its chiral centre. It is based on a ferrocene ligand motif that was first used by Hayashi in the early 1980s (*vide infra*). The ligand was developed by Togni and co-workers in the research laboratories of Ciba-Geigy in 1994. The company is now known as Solvias and currently sells 40 ligand derivatives of the JosiPhos family.[21]

While many new bidentate ligands were developed and applied in asymmetric transformations in the 1980s and 1990s, the field of chiral monophosphine ligands remained relatively unexplored for a number of years. Nevertheless, a few examples of ligands that were capable of achieving high levels of enantioselectivities were synthesised. In particular Hayashi and co-workers contributed in this field. They reported the PPF-OMe ligand containing ferrocene-based planar chirality,[22] the axially chiral OMe-MOP ligand[23] and a variety of different substituted derivatives (Figure 1.3).[24]

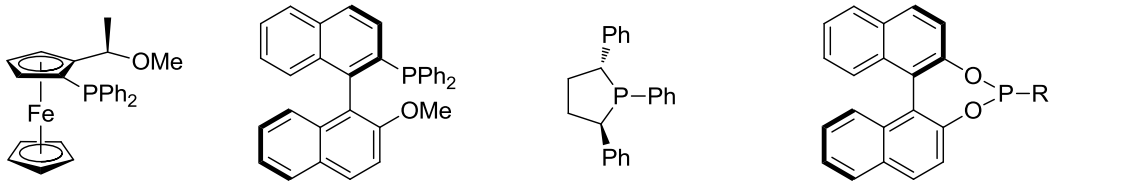

(R,S_{Fc})-PPF-OMe
Hayashi
1982

(*R*)-OMe-MOP
Hayashi
1992

phospholane
Fiaud
1991/1999

phosphonite (R = *t*Bu), *Pringle*
phosphite (R = (*R*)-OCH(Me)Ph), *Reetz*
phosporamidite (R = NMe_2), *Feringa*
2000

Figure 1.3 Selection of chiral monophosphorus ligands.

The renaissance of monodentate phosphorus ligands was finally initiated in the year 2000, whereby the conventional wisdom at the time, that *"efficient asymmetric hydrogenation will generally require the use of chelating (bidentate) ligands"*, was revolutionised.[25] A monodentate species of the DuPHOS ligand had been published by Fiaud and co-workers (Figure 1.3)[26] which gave 82% *ee* in the asymmetric hydrogenation of methyl *N*-acetylphenyl-dehydroalaninate.[27] Subsequently three different research groups independently reported monodentate phosphorus ligands based on the BINOL binaphthyl-backbone that could achieve high turnover numbers and high selectivities of up to >99% *ee* in similar reactions. These efforts by Pringle's,[28] Reetz's,[29] and Feringa's[30] research groups (Figure 1.3) were later highlighted by Komarov and Börner.[31] Also published in 2000 was a review by Lagasse and Kagan in which the authors stated that monophosphines *"will play a role of increasing importance in many aspects of organometallic catalysis"*.[32] Indeed, phosphoramidite ligands turned out to have a significant academic and commercial impact with their applications as chiral catalysts in a variety of asymmetric transformations.[33] Consequently these and other monodentate phosphorus ligands were further developed and refined. Today, a large number of derivatives of each of the discussed ligands are available, as well as completely new ligand scaffolds relying on a single phosphorus donor atom.[34]

1.2 Electronic and Steric Parameters of Phosphorus Ligands

Ligands play a key role in organometallic chemistry as their electronic and steric parameters significantly impact the overall properties of transition-metal complexes. The development and optimisation of homogeneous organometallic catalysts therefore often requires the screening of a number of possible ligand candidates. Having a deeper understanding about the effects that a specific ligand might have on the outcome of a catalytic reaction can help focus experimental efforts and guide further experiments in that optimisation process.[35]

The quantitative measurement of electronic and steric properties of phosphorus ligands was most prominently rationalised by Tolman, whose key contribution from 1977 has been cited more than 3500 times as of January 2013.[36] Two parameters were defined to describe ligand effects separating electronic and steric contributions. It is important to notice that this separation is somewhat arbitrary as the two effects can be closely related to each other. For example, large substituents on the P-atom normally decrease the pyramidalisation of the structure which results in a lower s-character of the phosphorus lone pair.[37,38]

1.2.1 Steric Parameters

The Tolman cone angle θ_T is most commonly used to describe the steric effects of phosphorus ligands. It was introduced after it became apparent that the coordination equilibrium in NiL_4 complexes (Table 1.1) was inexplicable by solely relying on electronic properties.[39] Instead, the dissociation constant K_d increases with the growing steric encumbrance around the phosphorus atom and is thereby almost unaffected by the electronic character.

Table 1.1 Equilibrium constant K_d of NiL_4 in relation to the ligand parameters θ_T and S4.

$$NiL_4 \overset{K_d}{\rightleftharpoons} NiL_3 + L$$

entry	L	K_d [a]	θ_T [a]	S4 [b]
1	$P(OEt)_3$	$< 10^{-10}$ [c]	109°	43.2°
2	PMe_3	$< 10^{-9}$ [c]	118°	38.9°
3	PEt_3	$1.2 * 10^{-2}$	132°	38.2°
4	$PMePh_2$	$5.0 * 10^{-2}$	136°	33.4°
5	PPh_3	– [d]	145°	31.2°

[a] Selected values (K_d at 25 °C in benzene) from ref. 36. [b] Values from ref. 46a. [c] At 70 °C. [d] No $Ni(PPh_3)_4$ was detected.

The θ_T parameter was originally determined using a mechanical angle measuring device and was defined as the apex angle of a cylindrical cone centred at a distance of 2.28 Å from the donor atom; the sides of the cone just touch the van der Waals surfaces of the outermost atoms.[39] This relatively simple model has some limitations, mainly based on approximations made to determine the lowest energy conformation and the van der Waals surface. For unsymmetrically substituted phosphorus compounds the half-angles θ_i can be used to define an average effective cone angle θ_T. However, if the substituent groups of the phosphorus ligand differ greatly, the values obtained may not reflect the actual properties of the compound.[40] The cone angle concept was modified and extended to overcome some limitations of the original model; cone angles were calculated based on X-ray structure

data.[40,41] The geometrical determination from crystallographic data according to Mingos *et al.* is shown in Figure 1.4.[42] The following relationships apply:

$$\theta_i = \alpha + \frac{180}{\pi} * sin^{-1}\left(\frac{r_H}{d}\right) \quad (1.1)$$

$$\theta_T = \frac{2}{3}\sum_i^3 \theta_i \quad (1.2)$$

where r_H is the van der Waals radius of hydrogen.

Rather than being based on an idealised molecular model, this methodology leads to cone angles of individual structurally characterised molecules.[40,41,42] Alternatively, the utilisation of quantum chemical calculations may be desirable to obtain the necessary structural data.[43]

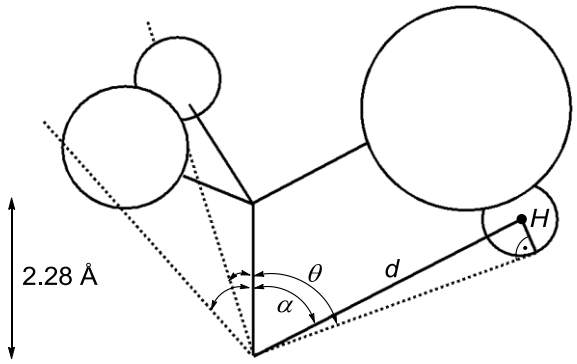

Figure 1.4 Cone angle determination from crystallographic data based on geometric relationships.

Geometric deformations in phosphorus fragments may be more directly described using the symmetric deformation coordinate S4' which was first introduced by Orpen and co-workers.[44] As a measure of flattening or pyramidality around the phosphorus, S4' is defined as the sum of Z-P-R angles (α_i) minus the sum of R-P-R angles (β_i), with Z describing the coordinated atom of the PR_3 ligand (Figure 1.5). A modified descriptor coined S4 is given for free ligands, where Z is a perpendicular vector to the plane containing the three substituents of the phosphorus atom.[45] The descriptor is part of a computational ligand knowledge base that was developed by Fey, Harvey, Orpen and co-workers;[46] selected S4 values are listed in Table 1.1 on page 5.

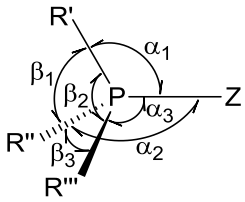

Figure 1.5 Definition of angles for the calculation of S4' = ($\alpha_1 + \alpha_2 + \alpha_3$) – ($\beta_1 + \beta_2 + \beta_3$).

1.2.2 Electronic Parameters

In order to quantify the electronic effects of phosphorus ligands, Tolman chose to use IR spectroscopy to determine the symmetric stretching frequency of $[Ni(CO)_3L]$ complexes.[36] The resonance of the carbonyl groups is very sensitive towards alteration of L and its magnitude depends on the electronic properties of the complex. The phosphine ligand normally acts as a σ-donor and increases the electron density on the metal. The increased electron count is transferred through π-back-bonding into anti-bonding orbitals of the carbonyl group, which reduces the bond order of CO (Figure 1.6). Thus, good net-donor ligands are indicated by a shift of the CO stretching frequency to lower wavenumbers (lower in energy). The value is thereby almost unaffected by the specific size of the ligand or steric crowding on the metal.

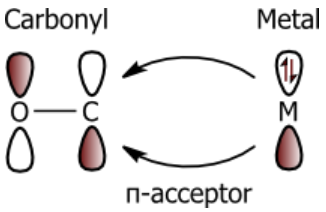

Figure 1.6 Back-donation into anti-bonding orbitals reduces the bond order of the carbonyl group.

Other transition-metal carbonyl complexes can be used as alternatives to $[Ni(CO)_3L]$ to gain quantitative insights into the electronic structure of phosphorus ligands.[47] Tolman himself stated that *"We could have chosen some other carbonyl complex, but Ni(CO₃)L forms readily […] even if L is very large."*[36] Rhodium(I) complexes of the general structure *trans*-$[RhCl(CO)(L)_2]$ have been studied in this context, which have an advantage in their safety of preparation ($Ni(CO)_4$ is highly toxic) and their high degree of stability.[48] The values correlate fairly well with those obtained from Ni(0) complexes; selected wavenumbers for both types of carbonyl complexes are given in Table 1.2.

In addition to IR measurements, coupling constants between phosphorus and selenium have been used to evaluate the electronics of phosphorus ligands.[49] It was demonstrated that the $^1J_{PSe}$ coupling in a phosphine selenide is inversely correlated to the σ-donor strength of the parent phosphine.[50] According to Bent atoms tend to concentrate their s-character in orbitals directed towards electropositive groups.[51] For ligands that carry electron-donating substituents, the s-character of the phosphorus hybrid orbital forming the P-Se σ-bond is therefore decreased. The reduced Fermi-contact between the bond-forming s-orbitals manifests itself in a smaller coupling constant. Values for a selection of phosphorus ligands

can be found in Table 1.2. The synthesis of phosphine selenides can be achieved from the respective phosphines by reaction with selenium or potassium selenocyanate.[49,52]

Table 1.2 IR data for the $[Ni(CO)_3L]$ and *trans*-$[RhCl(CO)(L)_2]$ complexes and NMR data for [(L)Se].

entry	L	$\nu(CO_{Ni})/cm^{-1}$ [a]	$\nu(CO_{Rh})/cm^{-1}$ [a]	$^1J_{P,Se}/Hz$ [b]
1	P(*p*-Cl-Ph)$_3$	2072.8	1983	746.9
2	PPh_3	2068.9	1979	728.9
3	P(*p*-Me-Ph)$_3$	2066.7	1976	717.6
4	P(*o*-Me-Ph)$_3$	2066.6	1974	704.6
5	$PPhCy_2$	2060.6	1964	701.2
6	PCy_3	2056.4	1943	672.9

[a] Values (in CH_2Cl_2) from ref. 48a. [b] Values (in $CDCl_3$) from ref. 50.

1.3 MOP Ligands and Derivatives

The OMe-MOP ligand (Figure 1.3, page 4) is based on the chiral 1,1'-binaphthyl backbone which also forms the basic skeleton of the successful BINAP ligand family.[17] The synthesis of MOP-type ligands was first reported by Hayashi and co-workers,[24] starting from 1,1'-binaphthyl-2,2'-diol (BINOL) that is commercially available in its enantiopure forms.[53] The configuration of the molecule is normally retained during the synthetic route to the desired MOP-type ligand. The binaphthyl backbone of these ligands is capable of forming hemilabile binding interactions with various metals; palladium and ruthenium complexes of this type have been studied to some extent, mainly by Pregosin and co-workers.[54]

1.3.1 Axial Chirality and Nomenclature

In MOP-type ligands the rotation around the bonding of the two naphthyl groups is restrained due to the interfering hydrogen atoms on the rear aromatic rings. Therefore, the binaphthyl backbone possesses an axis of chirality, also referred to as atropisomerism.[55] To determine the absolute configuration of molecules with axial chirality, sequence rules apply along the chiral axis (Figure 1.7, left).[56] In the Newman projection the atoms in the front have a higher priority than those in the back (Figure 1.7, middle and right). The priority increases with the rise of the atomic number; the clockwise progression of the priority is assigned as (*R*)-configuration, whereas an anti-clockwise progression is assigned as (*S*)-configuration. The absolute configuration of **1a** and **1b** in Figure 1.7 is reversed (despite the same orientation on the backbone) because of the different order of priorities of the substituents.[57]

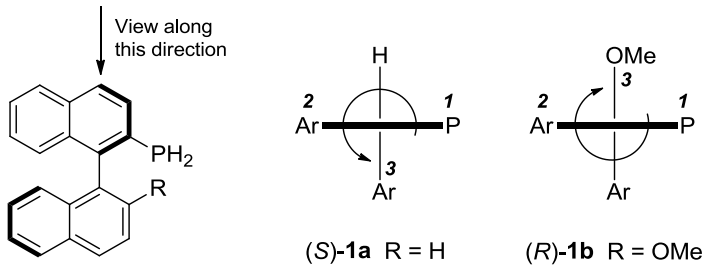

Figure 1.7 Assignment of the absolute configuration of (*S*)-**1a** and (*R*)-**1b**.

1.3.2 Synthesis

The H-MOP ligand bears no substituent at the 2'-position and was originally prepared starting from monotriflate **I** (Scheme 1.2).[58] The starting material was available by monotriflation of BINOL using Tf_2NPh and 2,4,6-trimethylpyridine, a procedure developed by Katsuki and co-workers.[59] The following hydrogenolysis and subsequent sulfonylation of the resulting hydroxy-binaphthyl gave monotriflate **II** in 92% yield. The palladium catalysed phosphinylation was carried out using an *in situ* generated Pd-dppb complex as catalyst. The phosphine oxide **III** was reduced with trichlorosilane yielding enantiopure H-MOP.

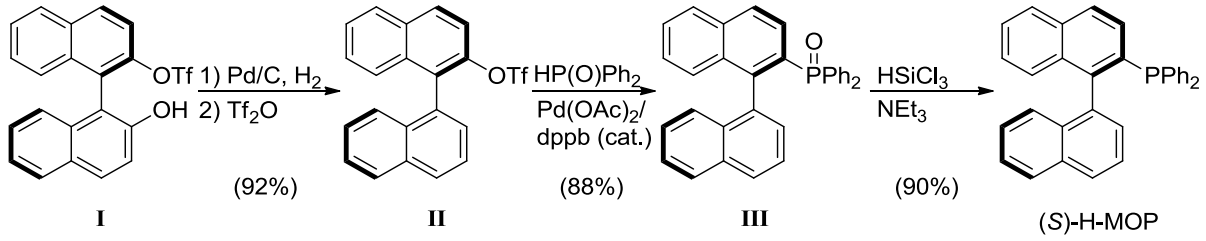

Scheme 1.2 Synthetic procedure to H-MOP.

The introduction of a variety of substituents in the 2'-position is possible and was achieved starting from 1,1'-binaphthyl-2,2'-ditriflate (**IV**, Scheme 1.3).[60] The selective monophosphinylation of **IV** was first described by Morgans *et al.* in 1990,[61] and was found to be a convenient method of preparing monophosphine compounds. The reaction of the remaining triflate group in **V** is prevented in the palladium catalysed reaction because of the steric bulk of the diphenylphosphinyl group in the 2-position. It is however a convenient functional group for the introduction of other various types of substituents. The methoxy group in OMe-MOP was introduced in two steps from **V** as shown in Scheme 1.3.[60] Subsequent reduction of the phosphine oxide **VI** finally led to the desired phosphine in excellent yields.

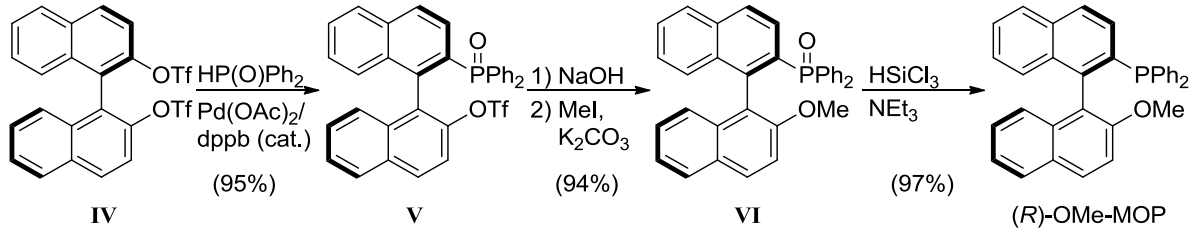

Scheme 1.3 Synthetic procedure to OMe-MOP.

Different 2'-substituted MOP derivatives were obtained from **V** by comparable reaction sequences (Figure 1.8). For example, triflate **V** was reacted with Grignard reagents in a nickel catalysed cross-coupling reaction to give 2'-alkyl-substituted compounds such as (*S*)-Et-MOP.[60] Nickel catalysis was also used for the introduction of the cyano group in (*R*)-CN-MOP, which could be further transformed to obtain (*R*)-CH_2NMe_2-MOP.[58] The hydroxy derivative (*R*)-OH-MOP was obtained by missing out the alkylation step of the corresponding phosphine oxide.

The aryl-backbone of the MOP ligand was also modified (Figure 1.8); (*R*)-MOP-phen was prepared from 3,3'-dihydroxy-4,4'-biphenanthryl in analogy to the binaphthyl synthesis which had given OMe-MOP.[62] The biaryl derivative **VII** was synthesised from its 2,6-bistriflate precursor by a palladium catalysed enantioposition-selective cross-coupling reaction.[63]

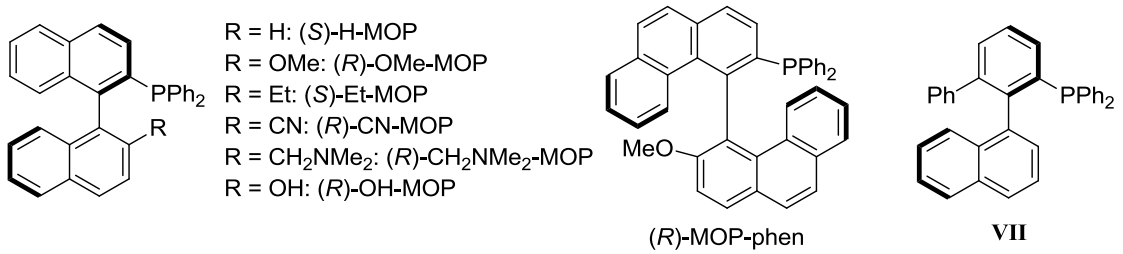

Figure 1.8 MOP-type ligands with different 2'-substituents (left) or a modified aryl-backbone (middle/right).

The P-aryl substituents of the H-MOP ligand were changed using a slightly modified reaction procedure compared to the original synthesis by varying the diarylphosphine oxide. Good to excellent yields were obtained for the palladium catalysed phosphinylation of **II** and the subsequent reduction (Scheme 1.4).[64] In the case of P-aryl substituted OMe-MOP derivatives an alternative synthetic route has been developed because some of the bulky diarylphosphine oxides failed to undergo the phosphinylation reaction with **IV**.[65] Access to these derivatives was achieved *via* diethylphosphonate **VIII**, subsequent conversion to the dichloride using thionyl chloride, and further treatment with an excess of the appropriate aryl Grignard reagent

(Scheme 1.4).[65] The final alkylation and reduction steps followed the usual procedures that were known from the synthesis of OMe-MOP (*cf.* Scheme 1.3 on page 10).

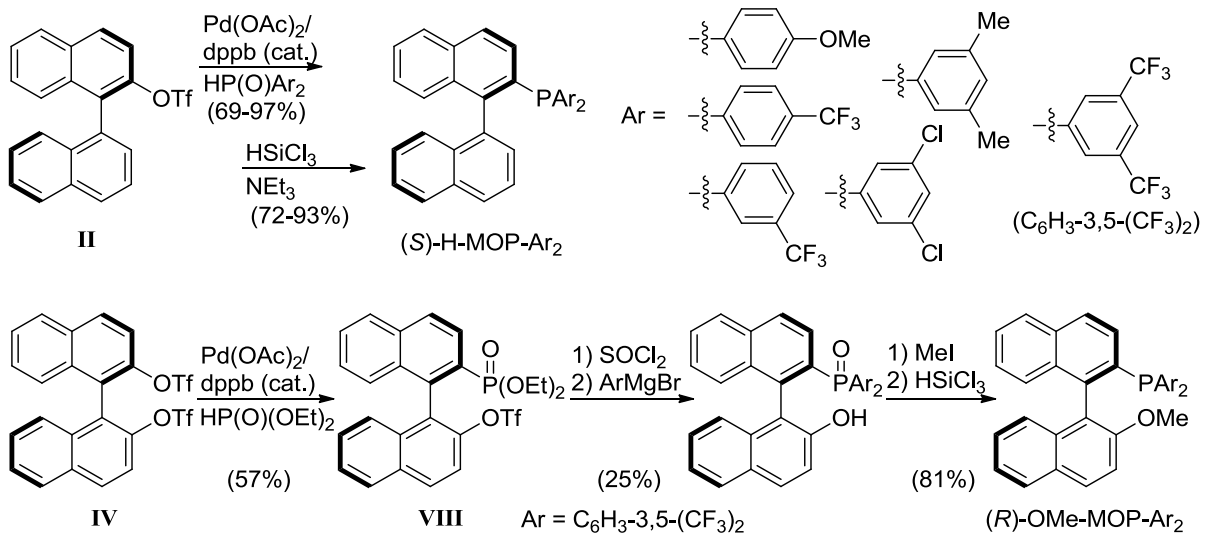

Scheme 1.4 MOP-type ligands with modified P-aryl substituents.

The preparation of electron-rich P-alkyl substituted MOP ligands was reported by Buchwald and co-workers using the palladium catalysed phosphinylation reaction in analogy to Hayashi's method (Scheme 1.5).[66] Good yields were achieved in the case of the diisopropyl-phosphine (R' = *i*Pr) but conversions were rather low for the more sterically demanding dicyclohexyl derivative (R' = Cy). The MOP-dimethylphosphine (R' = Me) was prepared by another research group (Shi *et al.*) using similar reaction conditions, but no yields were reported.[67]

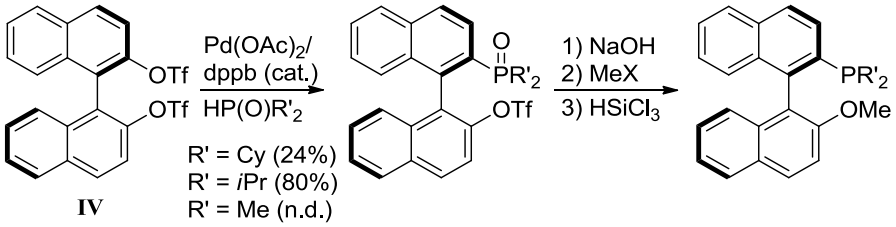

Scheme 1.5 Electron-rich MOP-type ligands bearing different P-alkyl substituents.

An alternative synthesis of electron-rich MOP derivatives was described by Zhang and co-workers, whereby the use of precious metals and triflic anhydride was completely avoided (Scheme 1.6).[68] Dinaphthofuran **IX** was obtained by dehydration of BINOL with an HY zeolite. This reaction step required elevated temperatures of 180 °C and therefore is unsuitable for the synthesis of single enantiomer products. The heterocycle was opened with lithium metal to afford the intermediate dilithium salt **X**. This was further reacted with chloro-

dicyclohexylphosphine to give MOP-phosphine **XI**. Due to the vulnerability of **XI** towards oxidation, the alkylation was achieved in a sequence of four reaction steps *via* the phosphine oxide.

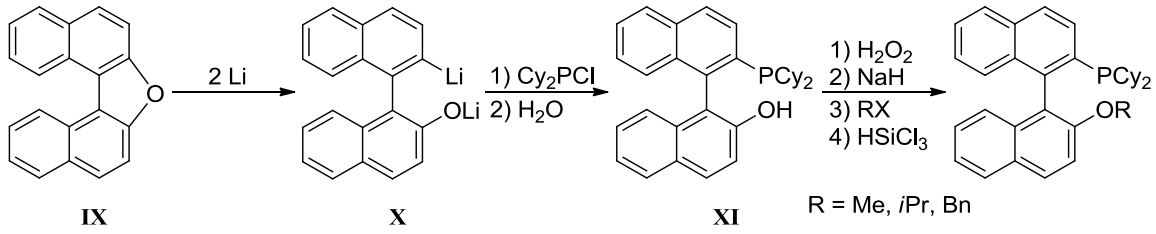

Scheme 1.6 Alternative synthetic route to MOP-type ligands which avoids the use of precious metals.

Gilheany and co-workers reported the synthesis of the P-chiral MOP analogue **XIII** (Scheme 1.7).[69,70] The direct phosphinylation of triflate **XII** was achieved using nickel catalysis under reaction conditions that were first described by Cai *et al.* for the synthesis of BINAP.[71] The two resulting diastereomers of the MOP-phosphine were separated in the form of their protected phosphine boranes by column chromatography. The deprotection of the borane adducts was carried out in a basic environment with diethylamine.

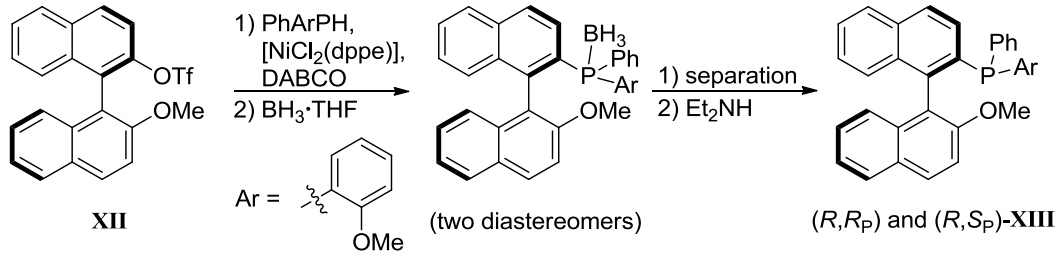

Scheme 1.7 Synthesis of P-chiral MOP-type ligands. The two diastereomers were separated on silica media by column chromatography.

The heterocyclic MOP derivative **XVI** was synthesised by RajanBabu and co-workers (Scheme 1.8).[72] Primary phosphine **XV** was obtained from reduction of phosphonate **XIV**, which was then reacted with a cyclic sulfate to give MOP-phospholane **XVI**. The reported yields for these reactions were rather low; however the reduction of **XIV** can be achieved in very good yield using both $LiAlH_4$ and Me_3SiCl as reducing agents, as shown by Higham, Gilheany and co-workers.[73] An optimised large scale synthesis of this and other chiral primary phosphine precursors is described in more detail in Chapter 2.

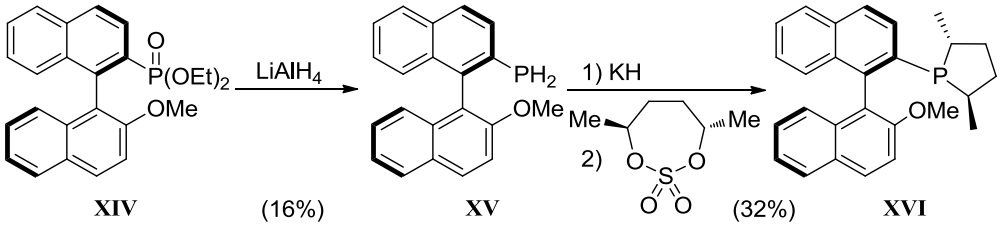

Scheme 1.8 Synthesis of a MOP-phospholane ligand *via* its primary phosphine precursor.

1.3.3 Aryl Side-on Coordination of Binaphthyl Ligands

In addition to their P-atom, the atropisomeric MOP-type ligands are capable of using their aromatic backbone as donors to stabilise coordinatively unsaturated metal complexes; in particular palladium and ruthenium metal-complexes of this kind have been investigated in some detail.[54] The chelating ligand fragments are often described as hemilabile; in contrast to the P-donor, the arene is usually only weakly bonded. The MeO-MOP Pd(I) dinuclear salt **XVII** provides an example of η^2-arene interactions (Figure 1.9); its crystal structure shows that the naphthyl groups are acting as bridging diene fragments across the Pd–Pd bond.[74] The complex was obtained from the reaction of two MeO-MOP ligands with $[Pd_2(MeCN)_6](BF_4)_2$.

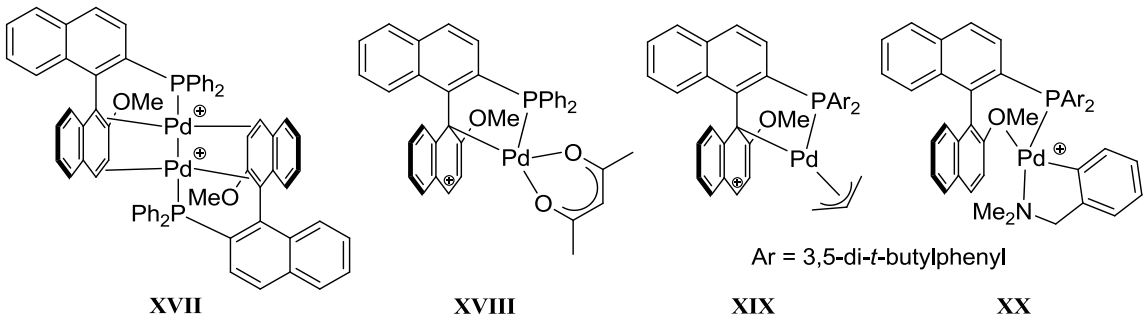

Figure 1.9 Aryl η^1- and η^2-binding modes of the MeO-MOP ligand on palladium.

When the same ligand was reacted with $[Pd(acac)(MeCN)_2]BF_4$ it formed an η^1-arene coordinated complex **XVIII** exhibiting a σ-bond to the 1'-carbon of the binaphthyl fragment.[75] The positive charge is thereby delocalised on the naphthyl moiety. The similarly coordinated compound **XIX** was obtained from the reaction of a slightly modified OMe-MOP ligand (Ar = 3,5-di-*t*-butylphenyl), allylpalladium dimer, and subsequent treatment with NaBArF.[76] An alternative η^2-arene π-coordination mode for an allylpalladium complex using the OMe-MOP ligand was postulated by Kocovsky and co-workers.[77] Finally, coordination of the methoxy-oxygen (rather than the aryl backbone of the MOP ligand) was observed in complex **XX**.[74] The favoured coordination of the oxygen atom was interpreted as a result of the increased *trans* influence of the σ-bonded carbon donor, in contrast to the η^3-allyl group in **XIX**.[54a]

In general, both σ- and π-bonding to the arene can occur, mostly depending on the MOP substituent in the 2'-position. H-MOP ligand derivatives have been analysed for their side-on coordination behaviour; compared to their OMe-MOP counterparts subtle differences in coordination modes were found (Figure 1.10). Allylpalladium complex **XXI** shows π-coordination to the MOP aryl-backbone (*cf.* **XIX** in Figure 1.9).[76] In **XXII** the metal is coordinated to the 2'-binaphthyl-carbon in a η^1-σ-bound fashion (*cf.* **XX** in Figure 1.9).[74]

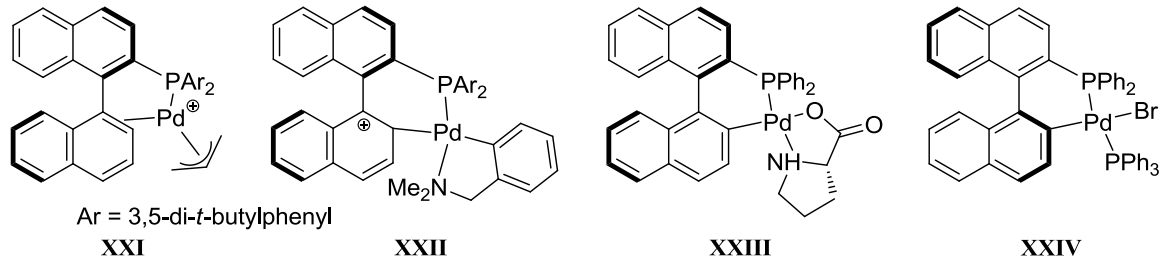

XXI **XXII** **XXIII** **XXIV**

Figure 1.10 Aryl binding modes in H-MOP-type Pd-complexes.

Complex **XXIII** was synthesised from H-MOP and $Pd(OAc)_2$ with subsequent addition of proline sodium salt.[78] The H-MOP ligand was thereby deprotonated in the 2'-position during the initial reaction step. A comparable palladium complex was obtained from the oxidative addition of bromobenzene to $(BINAP)_2Pd$, initially giving (BINAP)Pd(Ph)(Br). The resulting palladacyclic structure **XXIV** was formed when the reaction mixture was heated to 65 °C overnight under elimination of benzene.[79]

The most common aryl bonding mode for ruthenium is η^6 as shown in Scheme 1.9.[80] The H-MOP complexes **XXVI** and **XXVII** are easily accessible from BINAP complex **XXV** under acidic conditions and in the presence of water. The P–C bond cleavage of one PPh_2 group leads to the cationic MOP-complex **XXVI**. Phenyl migration to **XXVII** is possible in methanol; the P–C bond splitting and P–O bond making reactions are stereospecific and give rise to a single diastereomer.

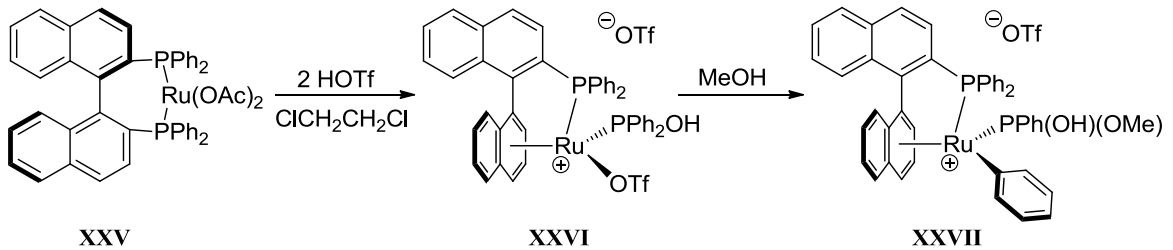

XXV **XXVI** **XXVII**

Scheme 1.9 Synthesis of binaphthyl ruthenium complexes with η^6-aryl coordination.

In a synthetic approach that is also reliant on P–C cleavage of BINAP, the rhodium complex **XXIX** was synthesised *via* phosphonium salt **XXVIII** (Scheme 1.10).[81] Migration of the PPh_2Me group onto the metal is achieved in refluxing ethanol. According to the proposed mechanism the binaphthyl ligand is protonated by oxidation of the ethanol solvent to acetaldehyde. The η^4-aryl-coordiantion mode was described based on ^{13}C NMR data, although the authors were unable to obtain a crystal structure.

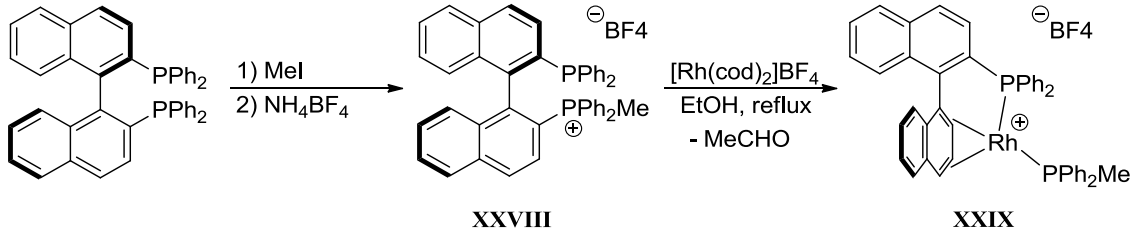

XXVIII **XXIX**

Scheme 1.10 The H-MOP ligand in a proposed η^4-aryl coordinated rhodium complex (**XXIX**).

Coordination studies with other transition-metals have been investigated for related bi- and terphenyl derivatives but not for MOP-type ligands themselves. Metal-arene interactions of various strengths have been found for biphenylphosphines in their copper(I), silver(I), and gold(I) complexes, as exemplarily shown for **XXX** in Figure 1.11.[82] Side-on aryl coordination to nickel(I) was reported for a terphenyldiphosphine derivative in complex **XXXI**.[83]

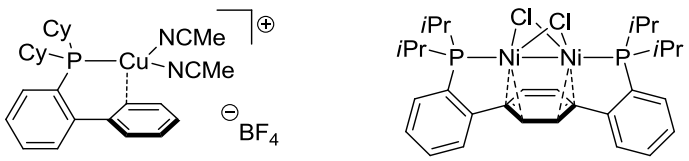

XXX **XXXI**

Figure 1.11 Copper(I) and nickel(I) aryl side-on coordination has been investigated for biphenyl- and terphenyl derivatives **XXX** and **XXXI**, but not for MOP-type ligands.

1.3.4 Palladium Catalysed Allylic Alkylation

The allylic alkylation reaction has been studied in great detail and is nowadays a common transformation used in organic synthesis.[84] The palladium catalysed asymmetric version with 1,3-diphenylallyl acetate (Scheme 1.11, R = Ph) has become a common benchmark reaction to test the activity and selectivity of new chiral ligands.[85,86] The typical reaction mechanism is depicted in Scheme 1.11. The substrate coordinates to the electron-rich palladium(0) centre to give complex **A**. The leaving group is located in the *anti* position relative to the metal. The oxidative addition to the η^3-allylpalladium complex **B** is rate determining. Thus, electron

donating phosphines are necessary to enrich the palladium atom and allow the reaction to take place. The electrophilicity of **B** is thereby reduced, but the following nucleophilic substitution to **D** is irreversible and therefore is the driving force of the reaction.

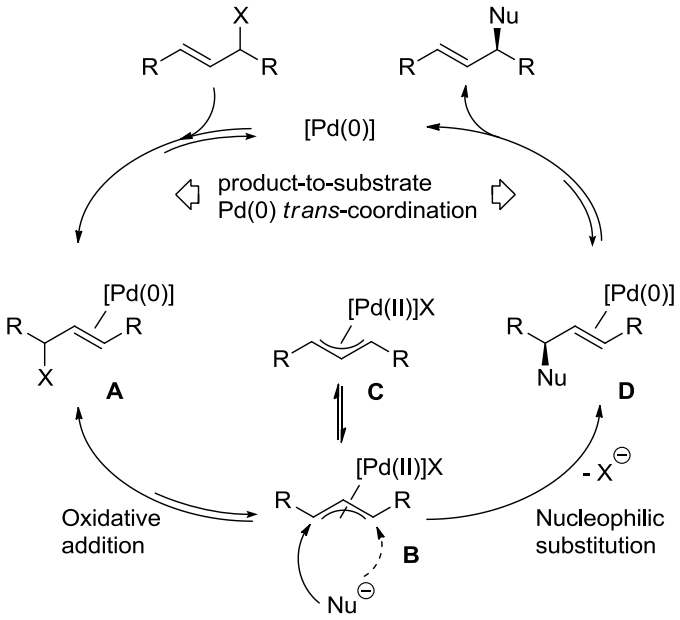

Scheme 1.11 Representative catalytic cycle for the palladium catalysed allylic alkylation.

The nucleophilic attack occurs in the *anti* position to the metal. Its regioselectivity determines the enantioselectivity of the product if prochiral substrates with identical substituents at the terminal allyl carbons are used. The dashed arrow in Scheme 1.11 marks the alternative position of the attack leading to the opposite enantiomer. The allyl fragment can also undergo isomerisation to **C** before being attacked by the nucleophile, and thus influencing the enantioselectivity of the reaction.

Dynamic equilibria of allylpalladium complexes have been studied in the absence of a nucleophile and different mechanisms for the allyl rotation have been described.[87] The herein discussed processes are known as (i) *syn*/*anti* exchange and (ii) apparent allyl rotation. The observed dynamics depend on the steric and electronic nature of the complex. For monodentate phosphine ligands the allyl rotation is typically the result of a η^3–η^1–η^3 equilibrium, leading to a *syn*/*anti* exchange (i) through C–C bond rotation in the η^1-bonded mode (Scheme 1.12).[88] Due to the strong *trans* influence of the phosphine ligand, the *syn*/*anti* displacement is normally observed in *cis* position to the phosphine (R^1 and R^2), following the selective η^3–η^1 opening of the allyl ligand and rotation around the *cis* terminus.[89] The *syn*/*anti* dynamics of the MOP complex [PdCl(allyl)(OMe-MOP)] were measured by NOESY NMR yielding an exchange rate of 2.2 s^{-1} at 0 °C.[76]

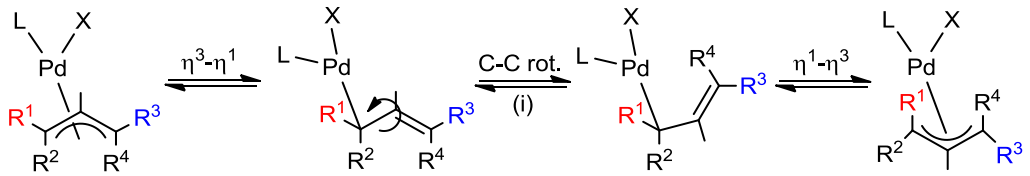

Scheme 1.12 *Syn-anti* exchange (i) *via* η^3–η^1–η^3 mechanism for a generic allylpalladium complex.

Another dynamic equilibrium can be caused by the apparent allyl rotation (ii), a formal rotation of the allyl group around the Pd-allyl axis. Three possible pathways have been proposed (Scheme 1.13): (ii a) A dissociative mechanism which leads to the formation of a coordinatively unsaturated three-coordinated complex; this is followed by the rotation around the L–Pd bond.[76,90] (ii b) A η^3–η^1–η^3 coordination equilibrium with a rotation around the C–Pd bond in the η^1-mode.[64b,91] (ii c) An associative mechanism that involves the coordination of an additional ligand (coordination of a solvent molecule or an anion) forming a five-membered coordination sphere to allow for pseudorotation.[92]

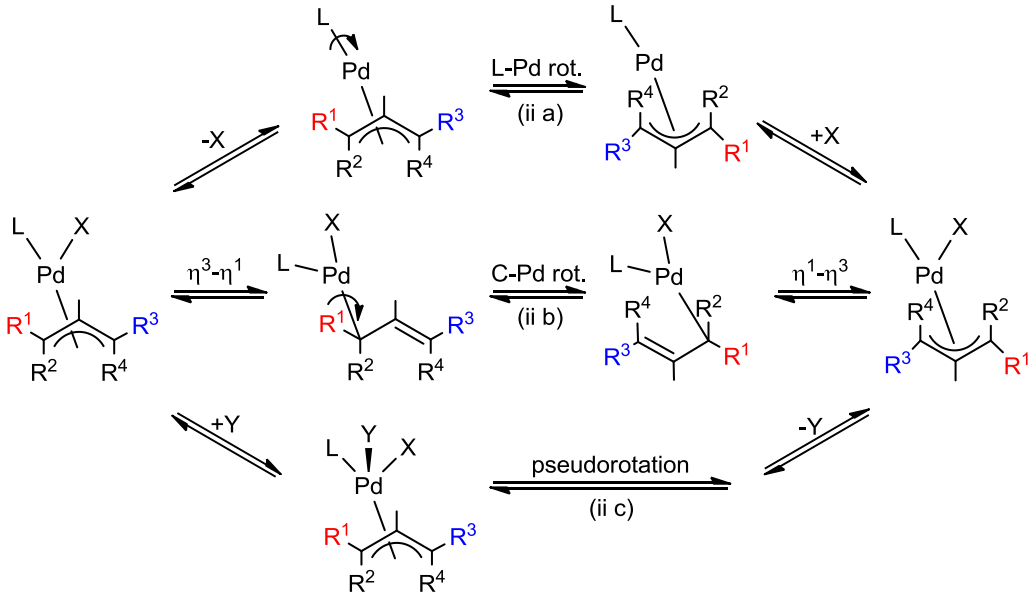

Scheme 1.13 Possible pathways for the apparent allyl rotation in allylpalladium complexes: (ii a) dissociative mechanism with L–Pd bond rotation; (ii b) η^3–η^1–η^3 exchange mechanism with C–Pd bond rotation; (ii c) associative mechanism with Berry pseudorotation.

The apparent allyl rotation is the dominant exchange process in complexes with bidentate nitrogen ligands.[92,93] However, an apparent allyl rotation has been observed for the MOP complex [Pd(allyl)(OMe-MOP)]OTf as the minor mode of interconversion, which occurred in addition to a *syn*/*anti* interchange in a relative ratio of 4:6 at 24.8 °C; none of the two exchange mechanisms were detected at lower temperature (–25 °C).[94]

Monophosphine ligands based on the atropisomeric binaphthyl backbone successfully alkylated allylic substrates in palladium catalysed reactions as illustrated in Figure 1.12. The results are summarised in Table 1.3. The symmetrically substituted (*E*)-1,3-diphenylallyl acetate (**XXXII**) was converted in up to 99% *ee* using ligands **XXXV** or **XXXVI**.[95,96]

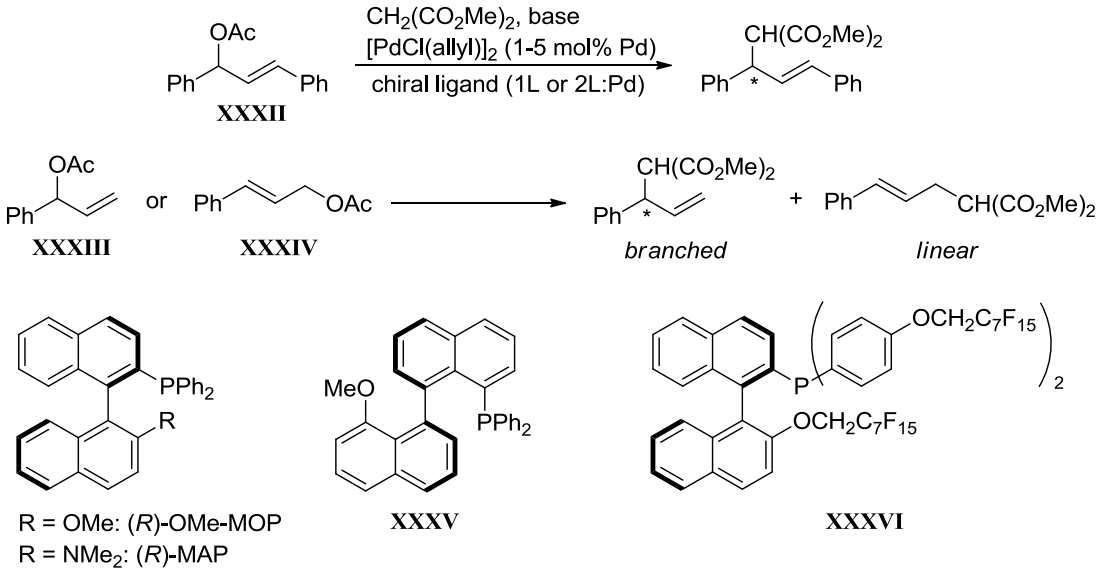

Figure 1.12 Examples of the allylic alkylation catalysed by chiral monophosphine-palladium complexes.

Table 1.3 Palladium catalysed asymmetric allylic alkylation of substrates **XXXII**, **XXXIII** and **XXXIV**.

entry	ligand	substrate	base	solvent	*T*/°C	*t*/h.	Yield	b:l[a]	*ee*	ref.
1	**XXXV**	**XXXII**	BSA	CH_2Cl_2	0	16	82%	—	86%	95
2	**XXXV**	**XXXII**	BSA	toluene	0	48	95%	—	99%	95
3	**XXXVI**	**XXXII**	BSA	toluene	0	48	95%	—	99%	96
4	MAP	**XXXII**	BSA	CH_2Cl_2	rt	24	87%	—	64%	97
5	MAP	**XXXIII**	BSA	CH_2Cl_2	rt	24	91%	3:97	n.d.	97
6	MAP	**XXXIV**	BSA	CH_2Cl_2	rt	24	94%	1:200	n.d.	97
7	OMe-MOP	**XXXIII**	NaH	THF	–30	6	97%	82:18	86%	98
8	OMe-MOP	**XXXIV**	NaH	THF	20	12	97%	21:79	n.d.	99

[a] Ratio of branched to linear product formation.

For the alkylation of the pure regioisomers of linear (**XXXIII**) or branched (**XXXIV**) phenylpropenyl acetate the selective formation of the linear product was observed when MAP was employed as ligand in the reaction.[97] In the case of OMe-MOP a regiochemical memory effect was noted; the linear substrate reacted predominantly to the linear product while the branched isomer gave the branched product as major compound.[98,99] The regioselectivity and memory effect of the allylic alkylation have been subjected to further investigations.[94,100,101]

1.3.5 Palladium Catalysed Hydrosilylation

The asymmetric hydrosilylation of alkenes has been recognised as an important reaction for the preparation of chiral alcohols *via* their respective silanes.[102] It was first reported by Hayashi *et al.* who were utilising their OMe-MOP ligand in this palladium catalysed transformation in order to obtain 2-alkanols from terminal alkenes.[103] The branched regioisomers were formed in ratios of about 9:1 compared to the linear products and high enantioselectivities of up to 95% were achieved.

The hydrosilylation of styrene derivatives gave complete regioselectivity forming the branched products exclusively (Figure 1.13).[104] Major improvements to the observed enantioselectivities in this reaction were made when the 2'-substituent of the MOP ligand was modified; selected results are listed in Table 1.4 (entries 1-5). The most successful derivative was the H-MOP ligand which was used to convert styrene to the branched silane product in 93% *ee*.[105]

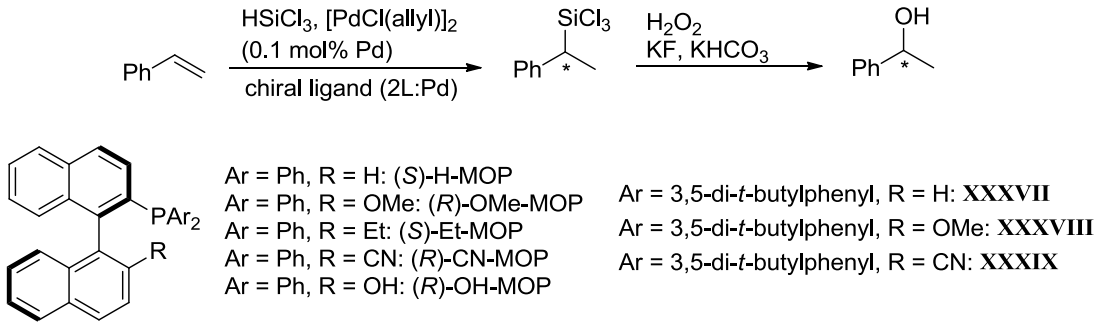

Figure 1.13 Examples of MOP-type ligands that were used in the hydrosilylation of styrene.

Table 1.4 Palladium catalysed asymmetric hydrosilylation of styrene.

entry	ligand[a]	*T*/°C	*t*/h.	Yield	*ee*	ref.
1	(*S*)-H-MOP	0	12	100%	93% (*R*)	105
2	(*R*)-OMe-MOP	0	24	100%	14% (*R*)	105
3	(*S*)-Et-MOP	0	12	100%	18% (*R*)	105
4	(*R*)-CN-MOP	0	24	100%	26% (*R*)	105
5	(*R*)-OH-MOP	0	22	84%	34% (*S*)	105
6	**XXXVII**	5	16	100%	88% (*R*)	106
7	**XXXVIII**	5	43	100%	57% (*R*)	106
8	**XXXIX**	5	2	100%	81% (*S*)	106

[a] Catalysts were prepared *in situ*; reactions were conducted in solvent free conditions.

The H-MOP ligand was modified by introducing different aryl-substituents onto its phenyl groups.[64a] As a result, the selectivity of the hydrosilylation reaction could be further enhanced to 97% *ee* at 0 °C using a H-MOP ligand derivative with 3,5-$(CF_3)_2C_6H_3$ aryl groups on the phosphine. Modification of the P-aryl substituents also improved the selectivity of the OMe and CN substituted MOP ligands; the utilisation of 3,5-di-*t*-butylphenyl derivatives **XXXVIII** and **XXXIX** led to major selectivity improvements compared to the use of their respective MOP counterparts (Table 1.4, entries 7-8).[106] The introduction of aryl-substituents in the 2'-position of the binaphthyl group gave ligands that were successfully used in the asymmetric hydrosilylation of cyclic dienes.[107]

The proposed catalytic cycles for the asymmetric hydrosilylation of styrene are depicted in Scheme 1.14.[108] In the presence of a 2:1 ratio of monophosphine (L_P) to palladium the reaction is believed to proceed *via* cycle A. The oxidative addition of trichlorosilane to the $Pd(L_P)_2$ species affords complex **a**. The following ligand exchange reaction allows for coordination of the alkene to give **b**; the equilibrium is expected to be on the side of the substrate because of the much higher metal affinity of the phosphine ligand. Hence, bidentate phosphorus ligands were found to be poor ligands in this transformation, due to their reluctance to liberate a coordination space for the incoming alkene. Subsequent migratory insertion and ligand coordination proceed to **c** and **d**. The cycle is closed after reductive elimination of the silane product and reformation of the $Pd(L_P)_2$ complex.

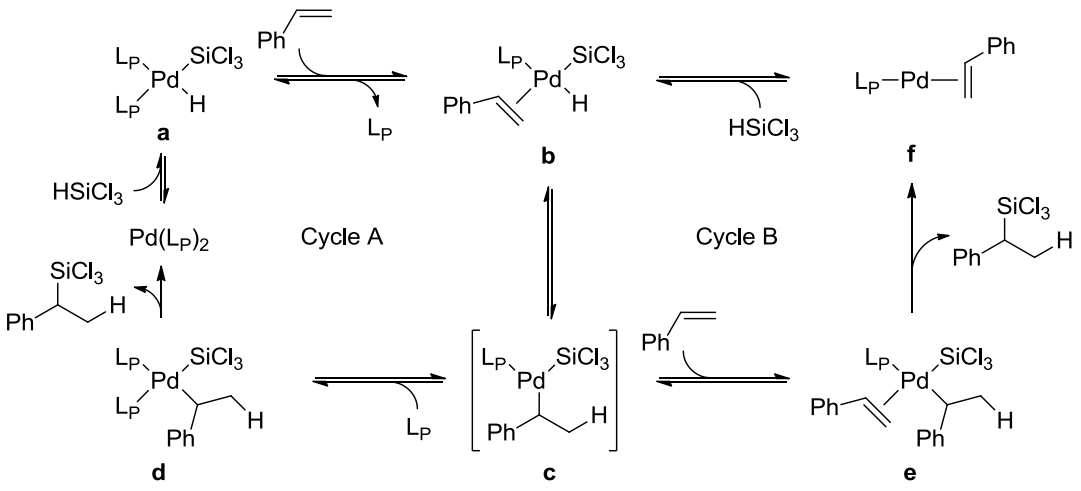

Scheme 1.14 Proposed catalytic cycles for the palladium catalysed hydrosilylation of styrene at higher (cycle A) and lower (cycle B) phosphine loading.

Low loadings of P-ligand facilitate the formation of complex **e** in which the palladium atom is stabilised by coordination of an additional alkene molecule. Reductive elimination of the silane product gives the two-coordinate complex **f**. Cycle B is completed after the oxidative

addition of trichlorosilane and formation of **b**. Cycle B is expected to proceed at a faster rate than cycle A as it does not require the displacement of a phosphine ligand. The possibility for side-on aryl coordination of MOP-type ligands (see Chapter 1.3.2) suggests that such arene interactions may arise to stabilise the low coordinated intermediates (*i.e.* **c** and **f**).[102a]

1.3.6 Asymmetric Hydrogenation of Alkenes

The asymmetric hydrogenation of alkenes is arguably one of the most studied reactions in homogeneous catalysis (*cf.* Chapter 1.1). In recent years monodentate binaphthyl based ligands with phosphonite,[28] phosphite[29a] and phosphoramidite[30] functionalities have received much attention in this area of research.[34,109] Their straightforward synthesis allows for the creation of large ligand libraries and subsequent combinatorial screening with any given substrate.[110] For example, the MonoPhos ligand (**XLIV**) is synthesised in one step from BINOL-PCl, Et_2NH and Et_3N; the same reaction parameters have been used with a wide variety of secondary and primary amines to create hundreds of differently substituted MonoPhos derived phosphoramidite ligands.[110,111]

The asymmetric hydrogenations of methyl 2-acetamidoacrylate (**XL**) and (*Z*)-2-acetamido-cinnamate (**XLI**) are common benchmark reactions for this type of catalysis (Figure 1.14). BINOL-based phosphonite ligands **XLII** and **XLIII** gave up to 92% *ee* in the rhodium catalysed hydrogenation of **XL** and **XLI** (Table 1.5, entries 1-4).

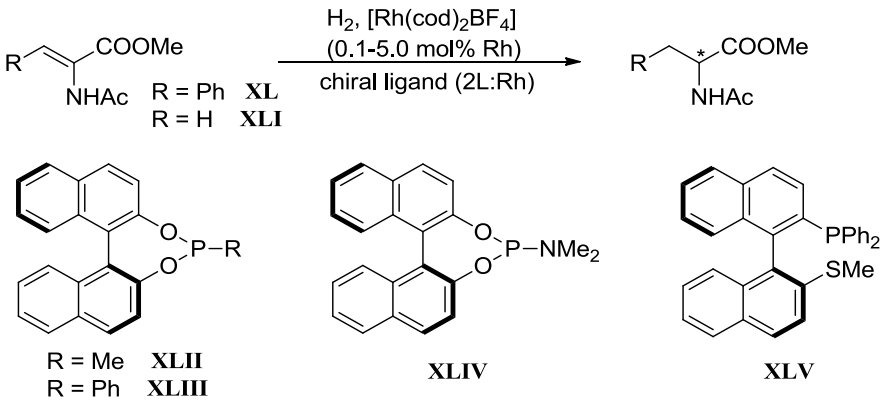

Figure 1.14 Examples of monodentate binaphthyl based phosphorus ligands that were employed in catalytic asymmetric hydrogenations.

MonoPhos (**XLIV**) is one of the most successful ligands for asymmetric hydrogenations as it gives excellent enantioselectivities of up to 99% *ee* depending on the substrate (entries 5-6). Complete conversion of the starting material is normally achieved after a few hours at atmospheric pressure of hydrogen gas.[30]

MOP-type ligands have scarcely been used in asymmetric hydrogenation reactions and ligand **XLV** is one rare example. The reactivity of the catalyst was found to be considerably lower than MonoPhos yielding only 13% in the hydrogenation of **XLI** after 16 hours with a moderate selectivity of 60% *ee* (entry 7).[112] In a different study the same reaction was tested with a H-MOP ligated rhodium complex (**XXIX**, Scheme 1.10 on page 15), but only 6% of product and no significant enantioselection were detected after 40 hours reaction time.[81]

Table 1.5 Rhodium catalysed asymmetric hydrogenation of alkenes.

entry	ligand[a]	substrate	solvent	$p(H_2)$/bar	T/°C	t/h	Yield	*ee*	ref.
1	**XLII**	**XL**	CH_2Cl_2	1.5	25	20	100%	80% (*R*)	28
2	**XLIII**	**XL**	CH_2Cl_2	1.5	25	20	100%	63% (*R*)	28
3	**XLII**[b]	**XLI**	CH_2Cl_2	1.3	rt	20	100%	92% (*S*)	29b
4	**XLIII**[b]	**XLI**	CH_2Cl_2	1.3	rt	20	100%	73% (*S*)	29b
5	**XLIV**	**XL**	CH_2Cl_2	1	25	20	100%	95% (*R*)	30
6	**XLIV**	**XLI**	CH_2Cl_2	1	25	20	100%	99% (*R*)	30
7	**XLV**	**XLI**	benzene/ methanol[c]	2.6	25	16	13%	60% (*R*)	112

[a] Catalysts were prepared *in situ*. [b] The (*R*)-configured enantiomer was employed. [c] Used in a 1:1 ratio.

1.4 Primary Phosphines as Ligand Precursors

1.4.1 Air-stability of (Primary) Phosphines

Primary phosphines have a reputation as unstable hazardous compounds due to their commonly observed high reactivity towards oxygen. Certain alkyl mono- (*e.g.* CH_3PH_2) and di- (*e.g.* $H_2P(CH_2)_2PH_2$) primary phosphines have been found to spontaneously ignite in air.[113] They also possess a characteristic pungent odour. For instance, King *et al.* reported that *"...the odors emanating from the hood exhausts were so strong that they invalidated experiments on the olfactory sense of snakes in a neighbouring building. Phenylphosphine was the worst offender followed by phenyldivinylphosphine and 1,2-diphosphinoethane."*[114] However, a few examples of user-friendly air-stable primary phosphines have been described.[115] The introduction of steric encumbrance around the phosphorus usually leads to increased stability. As such, supermesitylphosphine (**XLVI**, Figure 1.15) is reasonably air-stable and only oxidised very slowly over a few months in air.[116] Sterics have also been used to rationalise the air-stability observed for (9,10-dihydro-9,10-ethenoanthracen-9-yl)phosphine (**XLVII**).[117]

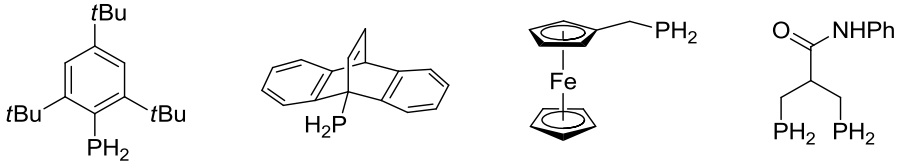

XLVI **XLVII** **XLVIII** **XLIX**

Figure 1.15: Primary phosphines with a high degree of air stability.

More unexpected was the air-stability reported for ferrocenylphosphine **XLVIII**; its X-ray crystallographic analysis indicated that the PH_2-unit is orientated away from the ferrocenyl group, and thus cannot offer steric protection at least in the solid-state.[118] The authors proposed that the stability is caused by kinetics due to the presence of the redox-active ferrocene. Furthermore, the alkyl spacer seemed to play a key role in providing air-stability as the derivative without the spacer group was found to be sensitive to oxidation.[119] The primary bisphosphine **XLIX** is also stable in air; the authors attributed the stabilisation to the remote electronegative heteroatoms which might confer stability through negative hyperconjugation to the P(III) centre.[120] The first air-stable chiral primary phosphines **1a**,**b** were reported by our group (Figure 1.16).[73] Crystallographic analysis of **1b** revealed that the environment around the phosphino group is exposed without any direct steric shielding, and an interaction between the P atom and O atom can be ruled out.

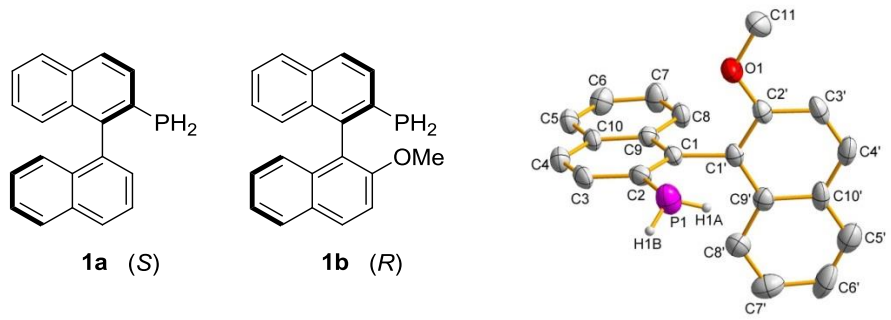

1a (*S*) **1b** (*R*)

Figure 1.16 Air-stable chiral primary phosphines **1a**,**b** (left) and the solid-state structure of OMe-MOP-H_2 (**1b**, right) showing the exposed phosphino group.

Decreasing the amount of conjugation on the aryl backbone had a noticeable effect on the air-stability. Primary phosphines with varied aryl substituents were exposed to air over 7 days at room temperature either neat or in chloroform solution. The relative amounts of primary phosphines remaining after this timeframe are shown in the diagram of Figure 1.17. The solution samples show a clear trend from the highly conjugated stable MOP-H_2 phosphines **1a**,**b** (100% respectively), to the reasonably stable naphthylphosphines (72/74% respectively), to the even less conjugated and less stable 5,6,7,8-tetrahydro(2-naphthyl)phosphine (59%) and

phenylphosphine (42%). The observed variations for the values in the neat state were attributed to the fact that **1a**,**b** and 2-naphthylphosphine are solids under ambient conditions while 1-naphthylphosphine, tetrahydro(2-naphtyl)phosphine and phenylphosphine are oils.

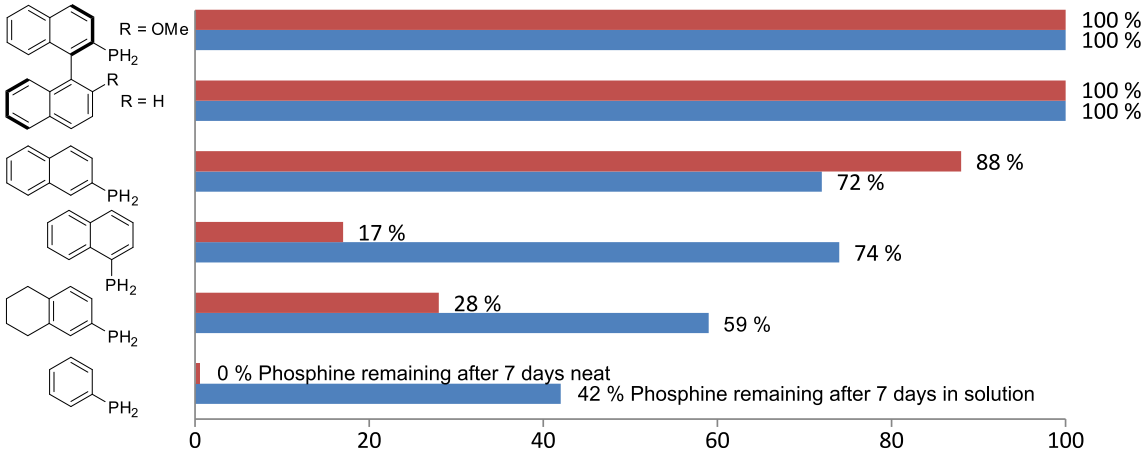

Figure 1.17 Stability of primary phosphines with a different extend of aromatic conjugation.

As sterics are apparently an insignificant factor for the stabilisation of **1a**,**b** towards air-oxidation, the electronic nature of the compounds was investigated by the means of quantum chemical calculations. Remarkably few mechanistic studies on the air oxidation of phosphines have been published.[121] From one of the more recent investigations there is spectroscopic evidence that the photolytic formation of the radical cation of triphenylphosphine leads to its oxidation in air *via* a radical mechanism.[121d] The proposed mechanism is shown in Scheme 1.15; the radical cation is formed and reacts with dioxygen to give a peroxy radical that ultimately leads to the phosphine oxide after reaction with a second equivalent of phosphine.

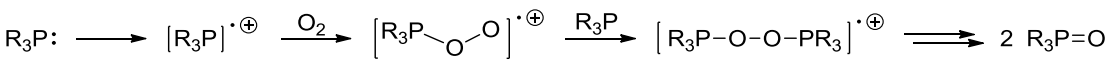

Scheme 1.15 Proposed mechanism for the oxidation of phosphines to phosphine oxides.

The SOMO energy levels of the radical cations of **1a**,**b** were modelled and compared to those phosphines with less conjugated aryl-backbones (Figure 1.18) and a threshold value of –10 eV was postulated; phosphines with values above this level were found to be air-stable.[122] The model therefore allows for a universal prediction of the air stability/sensitivity of phosphine functionalised compounds. One must keep in mind however, that the oxidation of air-stable phosphines may still occur in specific environments such as in the presence of peroxides in aged ether solvents or by certain transition metal complexes.

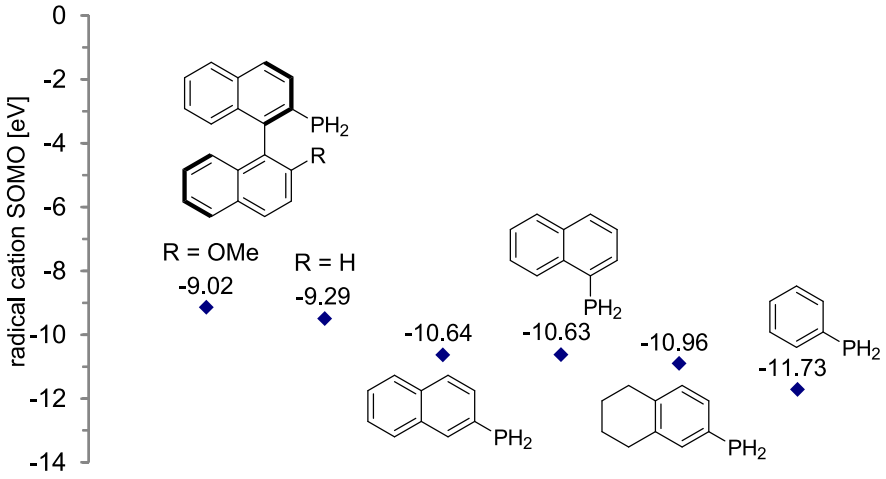

Figure 1.18 Radical cation SOMO energies (in eV) for different primary phosphines. Phosphines above -10 eV are found to be air-stable.

1.4.2 Reactivity of Primary Phosphines as Ligand Precursors

The high reactivity of the PH_2 group and its consequently easy functionalisation makes primary phosphines an ideal class of precursor compound for other phosphorus ligands, which can be used in a variety of applications.[113,123] Representative examples of synthetic transformations for primary phosphines are shown in Scheme 1.16.

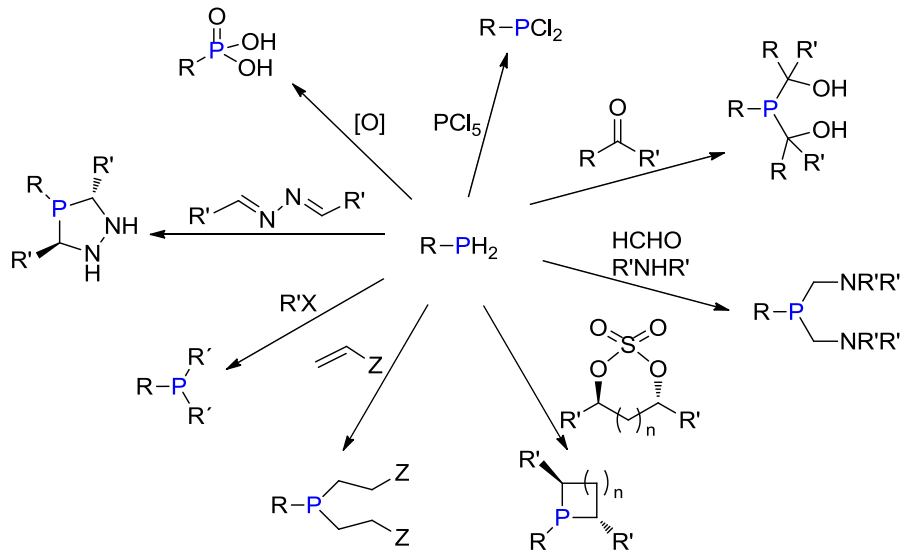

Scheme 1.16 Primary phosphines as versatile precursors to a variety of phosphorus compounds.

The formation of dichlorophosphines was achieved using PCl_5,[124] triphosgene,[125] phosgene[126] or *N*-chlorosuccinimide[127] as chlorinating reagent. The PCl_2 group can function as an electrophile to give access to P–C, P–O, and P–N derivatives that are potentially useful ligands in homogeneous catalysis (see Chapters 4.2 and 5.2).[125]

Water soluble (hydroxymethyl)phosphine derivatives have potential applications in biphasic catalysis and biomedicine. They are synthesised from the reaction of primary phosphines with aldehydes or ketones.[128] The products form stable amine linkages with amino acids or peptides.[128a,129]

Burk's DuPHOS ligand family are very effective catalysts in rhodium catalysed asymmetric hydrogenations (*q.v.* Chapter 1.1).[19] The five-membered phosphine heterocycles (phospholanes), as well as the four membered counterparts (phosphetanes), are obtained from primary phosphines and the corresponding cyclic sulfates.[72,130]

The hydrophosphination of the PH_2 group has been carried out to get access to tripodal P-ligand motifs (for example with Z=PPh_2 or P(O)$(OEt)_2$).[131] Highly fluorescent derivatives of this type, which can potentially act as imaging agents in analytical biomedicine, have recently been synthesised in our group.[132]

Further transformations from primary phosphines include the syntheses of dialkylphosphines (see Chapters 3.2 and 4.2),[133] or diazaphospholanes[134].

1.5 Objectives

This thesis aims to exploit new chiral ligand systems based on the MOP-type architecture. Primary phosphines **1a**,**b** are the first air-stable chiral primary phosphines and ideal precursors for the purpose of accessing a variety of P-ligand functionalities (Chapter 1.4). Firstly, we describe the optimisation of the synthetic route to the valuable precursors **1a**,**b**, in order to prepare these compounds on a multigram scale (Chapter 2). Secondly, the functionalisation of the PH_2 group was undertaken, generally relying on two different synthetic strategies: (a) deprotonation of the primary phosphines enabled the reaction with electrophiles which gave access to novel phosphiranes (**14a**,**b**; Chapter 3), and (b) the transformation of primary phosphines to the corresponding dichlorophosphines made the phosphorus atom electrophilic, which then reacted with nucleophiles and facilitated the synthesis of dimethylphosphines (**16a**,**b**; Chapter 4), bis(dimethylamino)phosphines (**18a**,**b**; Chapter 4), phosphonites (**19a**,**b**, **33a**,**b**, **34a**,**b**; Chapters 4-5) and phosphonodichalcogenoites (**51a**,**b**, **52a**,**b**, **53b**; Chapter 6). Thirdly, the coordination chemistry of these ligands was investigated on catalytically relevant transition-metals. The ligand-effects were described by their individual steric and electronic parameters, and a number of spectroscopic and crystallographic analyses were carried out to get a more detailed insight into the nature of the ligand-metal bonds. Aryl side-on coordination of MOP-type ligands *via* their binaphthyl backbone was found for selected

compounds in their palladium and rhodium complexes. Fourthly, we looked at the application of our ligands in asymmetric catalytic processes. The hydrosilylation of styrene and the allylic alkylation of (*rac*)-(*E*)-1,3-diphenylallyl acetate are common benchmark reactions to test the asymmetric induction of MOP-type ligands. These catalytic reactions were carried out (amongst others) in comparative studies to evaluate the potential of our ligands.

1.6 References

1 (a) J. F. Young, J. A. Osborn, F. H. Jardine, G. Wilkinson, *Chem. Commun. (London)* **1965**, 131; (b) F. H. Jardine, J. A. Osborn, G. Wilkinson, *J. Chem. Soc. A* **1967**, 1574.

2 A. Behr, P. Neubert, *Applied Homogeneous Catalysis*, Wiley-VCH, Weinheim, 2012, pp. 5–7.

3 "The Nobel Prize in Chemistry 1973", www.nobelprize.org (22/01/2013).

4 L. Vaska, R. E. Rhodes, *J. Am. Chem. Soc.* **1965**, *87*, 4970.

5 L. Horner, H. Winkler, A. Rapp, A. Mentrup, H. Hoffmann, P. Beck, *Tetrahedron Lett.* **1961**, *2*, 161.

6 L. Horner, H. Büthe, H. Siegel, *Tetrahedron Lett.* **1968**, *9*, 4023.

7 W. S. Knowles, M. J. Sabacky, *Chem. Commun. (London)* **1968**, 1445.

8 L. Horner, *Pure Appl. Chem.* **1964**, *9*, 225.

9 L. Horner, H. Siegel, H. Büthe, *Angew. Chem. Int. Ed. Engl.* **1968**, *7*, 942.

10 J. D. Morrison, W. F. Masler, *J. Org. Chem.* **1974**, *39*, 270.

11 J. D. Morrison, R. E. Burnett, A. M. Aguiar, C. J. Morrow, C. Phillips, *J. Am. Chem. Soc.* **1971**, *93*, 1301.

12 W. S. Knowles, M. J. Sabacky, B. D. Vineyard, *J. Chem. Soc., Chem. Commun.* **1972**, 10.

13 T. P. Dang, H. B. Kagan, *J. Chem. Soc. D: Chem. Commun.* **1971**, 481.

14 W. S. Knowles, M. J. Sabacky, B. D. Vineyard, D. J. Weinkauff, *J. Am. Chem. Soc.* **1975**, *97*, 2567.

15 (a) W. S. Knowles, *J. Chem. Educ.* **1986**, *63*, 222; (b) W. S. Knowles, M. J. Sabacky, B. D. Vineyard, Monsanto Company, U.S. Patent 4005127, **1977**.

16 W. S. Knowles, *Angew. Chem. Int. Ed.* **2002**, *41*, 1998.

17 A. Miyashita, A. Yasuda, H. Takaya, K. Toriumi, T. Ito, T. Souchi, R. Noyori, *J. Am. Chem. Soc.* **1980**, *102*, 7932.

18 Noyori's Nobel Lecture: R. Noyori, *Angew. Chem. Int. Ed.* **2002**, *41*, 2008.

19 M. J. Burk, *Acc. Chem. Res.* **2000**, *33*, 363.

20 M. J. Burk, *J. Am. Chem. Soc.* **1991**, *113*, 8518.

21 H.-U. Blaser, W. Brieden, B. Pugin, F. Spindler, M. Studer, A. Togni, *Top. Catal.* **2002**, *19*, 3.

22 T. Hayashi, M. Konishi, M. Fukushima, T. Mise, M. Kagotani, M. Tajika, M. Kumada, *J. Am. Chem. Soc.* **1982**, *104*, 180.

23 T. Hayashi, Y. Uozumi, *Pure Appl. Chem.* **1992**, *64*, 1911.

24 T. Hayashi, *Acc. Chem. Res.* **2000**, *33*, 354.

25 For further reading on "Black Swan events" in organic synthesis: W. A. Nugent, *Angew. Chem. Int. Ed.* **2012**, *51*, 8936.

26 J.-C. Fiaud, J.-Y. Legros, *Tetrahedron Lett.* **1991**, *32*, 5089.

27 F. Guillen, J.-C. Fiaud, *Tetrahedron Lett.* **1999**, *40*, 2939.

28 C. Claver, E. Fernandez, A. Gillon, K. Heslop, D. J. Hyett, A. Martorell, A. G. Orpen, P. G. Pringle, *Chem. Commun.* **2000**, 961.

29 (a) M. T. Reetz, G. Mehler, *Angew. Chem. Int. Ed.* **2000**, *39*, 3889; (b) M. T. Reetz, T. Sell, *Tetrahedron Lett.* **2000**, *41*, 6333.

30 M. van den Berg, A. J. Minnaard, E. P. Schudde, J. van Esch, A. H. M. de Vries, J. G. de Vries, B. L. Feringa, *J. Am. Chem. Soc.* **2000**, *122*, 11539.

31 I. V. Komarov, A. Börner, *Angew. Chem. Int. Ed.* **2001**, *40*, 1197.

32 F. Lagasse, H. B. Kagan, *Chem. Pharm. Bull.* **2000**, *48*, 315.

33 (a) J. F. Teichert, B. L. Feringa, *Angew. Chem. Int. Ed.* **2010**, *49*, 2486; (b) B. L. Feringa, *Acc. Chem. Res.* **2000**, *33*, 346.

34 Selected review articles and accounts on chiral monophosphorus ligands: (a) G. Hongchao, D. Kuiling, D. Lixin, *Chin. Sci. Bull.* **2004**, *49*, 2003; (b) T. Jerphagnon, J.-L. Renaud, C. Bruneau, *Tetrahedron: Asymmetry* **2004**, *15*, 2101; (c) G. Erre, S. Enthaler, K. Junge, S. Gladiali, M. Beller, *Coord. Chem. Rev.* **2008**, *252*, 471; (d) M. T.

Reetz, *Angew. Chem. Int. Ed.* **2008**, *47*, 2556; (e) J.-H. Xie, Q.-L. Zhou, *Acc. Chem. Res.* **2008**, *41*, 581.

35 P. B. Dias, M. E. Minas de Piedade, J. A. Martinho Simões, *Coord. Chem. Rev.* **1994**, *135/136*, 737.

36 C. A. Tolman, *Chem. Rev.* **1977**, *77*, 313.

37 For an overview of steric and electronic descriptors in general see: N. Fey, *Dalton Trans.* **2010**, *39*, 296.

38 For a review on the "percent buried volume" descriptor for phosphine and *N*-heterocyclic carbene ligands see: H. Clavier, S. P. Nolan, *Chem. Commun.* **2010**, *46*, 841–841.

39 C. A. Tolman, *J. Am. Chem. Soc.* **1970**, *92*, 2956.

40 T. L. Brown, K. J. Lee, *Coord. Chem. Rev.* **1993**, *128*, 89.

41 J. M. Smith, N. J. Coville, *Organometallics* **2001**, *20*, 1210.

42 T. E. Müller, D. M. P. Mingos, *Transition Met. Chem.* **1995**, *20*, 533.

43 H. M. Senn, D. V. Deubel, P. E. Blöchl, A. Togni, G. Frenking, *J. Mol. Struct. Theochem* **2000**, *506*, 233.

44 B. J. Dunne, R. B. Morris, A. G. Orpen, *J. Chem. Soc., Dalton Trans.* **1991**, 653.

45 J. Mathew, T. Thomas, C. H. Suresh, *Inorg. Chem.* **2007**, *46*, 10800.

46 (a) N. Fey, A. C. Tsipis, S. E. Harris, J. N. Harvey, A. G. Orpen, R. A. Mansson, *Chem. Eur. J.* **2006**, *12*, 291; (b) N. Fey, A. G. Orpen, J. N. Harvey, *Coord. Chem. Rev.* **2009**, *253*, 704; (c) J. Jover, N. Fey, J. N. Harvey, G. C. Lloyd-Jones, A. G. Orpen, G. J. J. Owen-Smith, P. Murray, D. R. J. Hose, R. Osborne, M. Purdie, *Organometallics* **2010**, *29*, 6245.

47 For a review on experimental and theoretical methods see: O. Kühl, *Coord. Chem. Rev.* **2005**, *249*, 693.

48 (a) A. Roodt, S. Otto, G. Steyl, *Coord. Chem. Rev.* **2003**, *245*, 121; (b) S. Otto, A. Roodt, *Inorg. Chim. Acta* **2004**, *357*, 1.

49 (a) D. W. Allen, B. F. Taylor, *J. Chem. Soc., Dalton Trans.* **1982**, 51; (b) R. P. Pinnell, C. A. Megerle, S. L. Manatt, P. A. Kroon, *J. Am. Chem. Soc.* **1973**, *95*, 977.

50 (a) W. McFarlane, D. S. Rycroft, *J. Chem. Soc., Dalton Trans.* **1973**, 2162; (b) W. McFarlane, D. S. Rycroft, *J. Chem. Soc., Chem. Commun.* **1972**, 902.

51 H. A. Bent, *Chem. Rev.* **1961**, *61*, 275.

52 A. Muller, S. Otto, A. Roodt, *Dalton Trans.* **2008**, 650.

53 J. M. Brunel, *Chem. Rev.* **2005**, *105*, 857.

54 Reviews: (a) P. S: Pregosin, *Chem. Commun.* **2008**, 4875; (b) P. S. Pregosin, *Coord. Chem. Rev.* **2008**, *252*, 2156.

55 G. P. Moss, *Pure Appl. Chem.* **1996**, *68*, 2193.

56 (a) L. C. Cross, W. Klyne, *Pure Appl. Chem.* **1976**, *45*, 11; (b) R. S. Cahn, C. K. Ingold, V. Prelog, *Angew. Chem. Int. Ed. Eng.* **1966**, *5*, 385.

57 For the nomenclature of the respective organometallic compounds see: A. Salzer, *Pure Appl. Chem.* **1999**, *71*, 1557.

58 Y. Uozumi, N. Suzuki, A. Ogiwara, T. Hayashi, *Tetrahedron* **1994**, *50*, 4293.

59 (a) H. Sasaki, R. Irie, T. Katsuki, *Synlett* **1993**, 300; (b) N. Hosoya, A. Hatayama, R. Irie, H. Sasaki, T. Katsuki, *Tetrahedron* **1994**, *50*, 4311.

60 Y. Uozumi, A. Tanahashi, S.-Y. Lee, T. Hayashi, *J. Org. Chem.* **1993**, *58*, 1945.

61 L. Kurz, G. Lee, D. Morgans Jr., M. J. Waldyke, T. Ward, *Tetrahedron Lett.* **1990**, *44*, 6321.

62 T. Hayashi, H. Iwamura, Y. Uozumi, Y. Matsumoto, F. Ozawa, *Synthesis* **1994**, 526.

63 T. Hayashi, S. Niizuma, T. Kamikawa, N. Suzuki, Y. Uozumi, *J. Am. Chem. Soc.* **1995**, *117*, 9101.

64 (a) T. Hayashi, S. Hirate, K. Kitayama, H. Tsuji, A. Torii, Y. Uozumi, *J. Org. Chem.* **2001**, *66*, 1441; (b) M. Kawatsura, Y. Uozumi, M. Ogasawara, T. Hayashi, *Tetrahedron* **2000**, *56*, 2247.

65 T. V. RajanBabu, N. Nomura, J. Jin, M. Nandi, H. Park, X. Sun, *J. Org. Chem.* **2003**, *68*, 8431.

66 T. Hamada, A. Chieffi, J. Åhman, S. L. Buchwald, *J. Am. Chem. Soc.* **2002**, *124*, 1261.

67 (a) M. Shi, L.-H. Chen, C.-Q. Li, *J. Am. Chem. Soc.* **2005**, *127*, 3790; (b) M. Shi, C.-Q. Li, *Tetrahedron: Asymmetry* **2005**, *16*, 1385; (c) M. Shi, X.-G. Liu, Y.-W. Guo, W. Zhang, *Tetrahedron* **2007**, *63*, 12731.

68 X. Xie, T. Y. Zhang, Z. Zhang, *J. Org. Chem.* **2006**, *71*, 6522.

69 (a) E. F. Clarke, E. Rafter, H. Müller-Bunz, L. J. Higham, D. G. Gilheany, *J. Organomet. Chem.* **2011**, *696*, 3608; (b) L. J. Higham, E. F. Clarke, H. Müller-Bunz, D. G. Gilheany, *J. Organomet. Chem.* **2005**, *690*, 211; (c) N. J. Kerrigan, E. C. Dunne, D. Cunningham, P. McArdle, K. Gilligan, D. G. Gilheany, *Tetrahedron Lett.* **2003**, *44*, 8461.

70 See also: (a) M. Jahjah, R. Jahjah, S. Pellet-Rostaing, M. Lemaire, *Tetrahedron: Asymmetry* **2007**, *18*, 1224; (b) M.-C. Duclos, Y. Singjunla, C. Petit, A. Favre-Réguillon, E. Jeanneau, F. Popowycz, E. Métay, M. Lemaire, *Tetrahedron Lett.* **2012**, *53*, 5984.

71 D. Cai, J. F. Payack, D. R. Bender, D. L. Hughes, T. R. Verhoeven, P. J. Reider, *J. Org. Chem.* **1994**, *59*, 7180.

72 B. Saha, T. V. RajanBabu, *J. Org. Chem.* **2007**, *72*, 2357.

73 R. M. Hiney, L. J. Higham, H. Müller-Bunz, D. G. Gilheany, *Angew. Chem. Int. Ed.* **2006**, *45*, 7248.

74 P. Dotta, P. G. A. Kumar, P. S. Pregosin, A. Albinati, S. Rizzato, *Organometallics* **2004**, *23*, 4247.

75 P. Dotta, P. G. A. Kumar, P. S. Pregosin, A. Albinati, S. Rizzato, *Organometallics* **2003**, *22*, 5345.

76 P. G. A. Kumar, P. Dotta, R. Hermatschweiler, P. S. Pregosin, *Organometallics* **2005**, *24*, 1306.

77 P. Kočovský, Š. Vyskočil, I. Císařová, J. Sejbal, I. Tišlerová, M. Smrčina, G. C. Lloyd-Jones, S. C. Stephen, C. P. Butts, M. Murray, V. Langer, *J. Am. Chem. Soc.* **1999**, *121*, 7714.

78 T.-K. Zhang, D.-L. Mo, L.-X. Dai, X.-L. Hou, *Org. Lett.* **2008**, *10*, 3689.

79 L. M. Alcazar-Roman, J. F. Hartwig, A. L. Rheingold, L. M. Liable-Sands, I. A. Guzei, *J. Am. Chem. Soc.* **2000**, *122*, 4618.

80 (a) T. J. Geldbach, P. S. Pregosin, S. Rizzato, A. Albinati, *Inorg. Chim. Acta* **2006**, *359*, 962; (b) T. J. Geldbach, F. Breher, V. Gramlich, P. G. A. Kumar, P. S. Pregosin, *Inorg. Chem.* **2004**, *43*, 1920; (c) T. J. Geldbach, P. S. Pregosin, A. Albinati, *Organometallics* **2003**, *22*, 1443; (d) T. J. Geldbach, D. Drago, P. S. Pregosin, *J. Organomet. Chem.*

2002, *643-644*, 214; (e) T. J. Geldbach, P. S. Pregosin, A. Albinati, F. Rominger, *Organometallics* **2001**, *20*, 1932; (f) T. J. Geldbach, D. Drago, P. S. Pregosin, *Chem. Commun.* **2000**, 1629.

81 M. Soleilhavoup, L. Viau, G. Commenges, C. Lepetit, R. Chauvin, *Eur. J. Inorg. Chem.* **2003**, 207.

82 P. Pérez-Galán, N. Delpont, E. Herrero-Gómez, F. Maseras, A. Echavarren, *Chem. Eur. J.* **2010**, *16*, 5324.

83 A. Velian, S. Lin, A. J. M. Miller, M. W. Day, T. Agapie, *J. Am. Chem. Soc.* **2010**, *132*, 6296.

84 B. M. Trost, M. L. Crawley, *Chem. Rev.* **2003**, *103*, 2921.

85 P. R. Auburn, P. B. Mackenzie, B. Bosnich, *J. Am. Chem. Soc.* **1985**, *107*, 2033.

86 For extensive reviews on the topic see: (a) G. Poli, G. Prestat, F. Liron, C. Kammerer-Pentier, *Top. Organomet. Chem.* **2012**, *38*, 1; (b) I. G. Rios, A. Rosas-Hernandez, E. Martin, *Molecules* **2011**, *16*, 970; (c) Z. Lu, S. Ma, *Angew. Chem. Int. Ed.* **2008**, *47*, 258.

87 P. S. Pregosin, R. Salzmann, *Coord. Chem. Rev.* **1996**, *155*, 35.

88 N. Solin, K. J. Szabó, *Organometallics* **2001**, *20*, 5464.

89 For selected examples see: (a) S. Filipuzzi, P. S. Pregosin, M. J. Calhorda, P. J. Costa, *Organometallics* **2008**, *27*, 2949; (b) S. Filipuzzi, P. S. Pregosin, A. Albinati, S. Rizzato, *Organometallics* **2008**, *27*, 437; (c) C. Breutel, P. S. Pregosin, R. Salzmann, A. Togni, *J. Am. Chem. Soc.* **1994**, *116*, 4067; (d) U. J. Scheele, M. John, S. Dechert, F. Meyer, *Eur. J. Inorg. Chem.* **2008**, 373; (e) B. E. Ketz, A. P. Cole, R. M. Waymouth, *Organometallics* **2004**, *23*, 2835; (f) H. M. Peng, G. Song, Y. Li, X. Li, *Inorg. Chem.* **2008**, *47*, 8031.

90 (a) A. Gogoll, H. Grennberg, A. Axén, *Organometallics* **1997**, *16*, 1167; (b) J. W. Faller, H. L. Stokes-Huby, M. A. Albrizzio, *Helv. Chim. Acta* **2001**, *84*, 3031.

91 J.-M. Camus, J. Andrieu, P. Richard, R. Poli, *Eur. J. Inorg. Chem.* **2004**, 1081.

92 (a) A. Guerrero, F. A. Jalon, B. R. Manzano, A. Rodriguez, R. M. Claramunt, P. Cornago, V. Milata, J. Elguero, *Eur. J. Inorg. Chem.* **2004**, 549; (b) F. A. Jalón, B. R. Manzano, B. Moreno-Lara, *Eur. J. Inorg. Chem.* **2005**, 100; (c) V. Montoya, J. Pons, J. Garcia-Antón, X. Solans, M. Font-Bardía, J. Ros, *Organometallics* **2007**, *26*, 3183.

93 See for example: A. Ficks, C. Sibbald, M. John, S. Dechert, F. Meyer, *Organometallics* **2010**, *29*, 1117.

94 G. C. Lloyd-Jones, S. C. Stephen, M. Murray, C. P. Butts, Š. Vyskočil, P. Kočovský, *Chem. Eur. J.* **2000**, *6*, 4348.

95 K. Fuji, H. Ohnishi, S. Moriyama, K. Tanaka, T. Kawabata, K. Tsubaki, *Synlett* **2000**, *3*, 351.

96 M. Cavazzini, G. Pozzi, S. Quici, D. Maillard, D. Sinou, *Chem. Commun.* **2001**, 1220.

97 Š. Vyskočil, M. Smrčina, V. Hanuš, M. Polášek, P. Kočovský, *J. Org. Chem.* **1998**, *63*, 7738.

98 T. Hayashi, M. Kawatsura, Y. Uozumi, *Chem. Commun.* **1997**, 561.

99 T. Hayashi, M. Kawatsura, Y. Uozumi, *J. Am. Chem. Soc.* **1998**, *120*, 1681.

100 T. Hayashi, *J. Organomet. Chem.* **1999**, *576*, 195.

101 (a) I. J. S. Fairlamb, G. C. Lloyd-Jones, Š. Vyskočil, P. Kočovský, *Chem. Eur. J.* **2002**, *8*, 4443; (b) L. Gouriou, G. C. Lloyd-Jones, Š. Vyskočil, P. Kočovský, *J. Organomet. Chem.* **2003**, *687*, 525.

102 For review articles see: (a) S. E. Gibson, M. Rudd, *Adv. Synth. Catal.* **2007**, *349*, 781; (b) L. Tietze, H. Ito, H. P. Bell, *Chem. Rev.* **2004**, *104*, 3453.

103 Y. Uozumi, T. Hayashi, *J. Am. Chem. Soc.* **1991**, *113*, 9887.

104 Y. Uozumi, K. Kitayama, T. Hayashi, *Tetrahedron: Asymmetry* **1993**, *4*, 2419.

105 K. Kitayama, Y. Uozumi, T. Hayashi, *J. Chem. Soc., Chem Commun.* **1995**, 1533.

106 P. Dotta, P. G. A. Kumar, P. S. Pregosin, A. Albinati, S. Rizzato, *Organometallics* **2004**, *23*, 2295.

107 (a) T. Hayashi, J. W. Han, A. Takeda, J. Tang, K. Nohmi, K. Mukaide, H. Tsuji, Y. Uozumi, *Adv. Synth. Catal.* **2001**, *343*, 279; (b) J. W. Han, T. Hayashi, *Tetrahedron: Asymmetry* **2010**, *21*, 2193.

108 H. L. Pedersen, M. Johannsen, *J. Org. Chem.* **2002**, *67*, 7982.

109 For mechanistic studies see for example: (a) I. D. Gridnev, T. Imamoto, *Chem. Commun.* **2009**, 7447; (b) E. Alberico, W. Baumann, J. G. de Vries, H.-J. Drexler, S. Gladiali, D. Heller, H. J. W. Henderickx, L. Lefort, *Chem. Eur. J.* **2011**, *17*, 12683; (c) I. D. Gridnev, C. Fan, P. G. Pringle, *Chem. Commun.* **2007**, 1319; (d) M. van den Berg,

A. J. Minnaard, R. M. Haak, M. Leeman, E. P. Schudde, A. Meetsma, B. L. Feringa, A. H. M. de Vries, C. E. P. Maljaars, C. E. Willans, D. Hyett, J. A. F. Boogers, H. J. W. Henderickx, J. G. de Vries, *Adv. Synth. Catal.* **2003**, *345*, 308.

110 A. J. Minnaard, B. L. Feringa, L. Lefort, J. G. de Vries, *Acc. Chem. Res.* **2007**, *40*, 1267.

111 L. Eberhardt, D. Armspach, J. Harrowfield, D. Matt, *Chem. Soc. Rev.* **2008**, *37*, 839.

112 S. Gladiali, F. Grepioni, S. Medici, A. Zucca, Z. Berente, L. Kollár, *Eur. J. Inorg. Chem.* **2003**, 556.

113 K. V. Katti, N. Pillarsetty, K. Raghuraman, *Top. Curr. Chem.* **2003**, *229*, 121.

114 R. B. King, P. N. Kapoor, *J. Am. Chem. Soc.* **1971**, *93*, 4158.

115 M. Brynda, *Coord. Chem. Rev.* **2005**, *249*, 2013.

116 (a) M. Yoshifuji, K. Shibayama, N. Inamoto, T. Matsushita, K. Nishimoto, *J. Am. Chem. Soc.* **1983**, *105*, 2495; (b) M. Yoshifuji, K. Shibayama, K. Toyota, N. Inamoto, *Tetrahedron Lett.* **1983**, *24*, 4227.

117 (a) M. Brynda, M. Geoffroy, G. Bernardinelli, *Chem. Commun.* **1999**, 961; (b) G. Ramakrishnan, A. Jouaiti, M. Geoffroy, G. Bernardinelli, *J. Phys. Chem.* **1996**, *100*, 10861.

118 (a) N. J. Goodwin, W. Henderson, B. K. Nicholson, *Chem. Commun.* **1997**, 31; (b) N. J. Goodwin, W. Henderson, B. K. Nicholson, J. Fawcett, D. R. Russell, *J. Chem. Soc., Dalton Trans.* **1999**, 1785.

119 W. Henderson, S. R. Alley, *J. Organomet. Chem.* **2002**, *656*, 120.

120 (a) N. Pillarsetty, K. Raghuraman, C. L. Barnes, K. V. Katti, *J. Am. Chem. Soc.* **2005**, *127*, 331; (b) H. Gali, S. R. Karra, V. S. Reddy, K. V. Katti, *Angew. Chem. Int. Ed.* **1999**, *38*, 2020.

121 (a) T. E. Barder, S. L. Buchwald, *J. Am. Chem. Soc.* **2007**, *129*, 5096; (b) S. A. Buckler, *J. Am. Chem. Soc.* **1962**, *84*, 3093; (c) M. M. Rauhut, H. A. Currier, *J. Org. Chem.* **1961**, *26*, 4626; (d) S. Yasui, S. Tojo, T. Majima, *Org. Biomol. Chem.* **2006**, *4*, 2969; (e) Z. B. Alfassi, P. Neta, B. Beaver, *J. Phys. Chem. A* **1997**, *101*, 2153.

122 (a) B. Stewart, A. Harriman, L. J. Higham, *Organometallics* **2011**, *30*, 5338; (b) B. Stewart, A. Harriman, L. J. Higham, in *Specialist Periodical Reports - Organometallic Chemistry* (Eds.: I. J. S. Fairlamb, J. M. Lynam), RSC, 2012, *38*, pp. 36–47.

123 L. J. Higham, in *Phosphorus Compounds - Advanced Tools in Catalysis and Material Sciences* (Eds.: M. Peruzzini, L. Gonsalvi), Springer, 2011, pp. 1–19, and references therein.

124 N. Z. Weferling, *Z. Anorg. Allg. Chem.* **1987**, *548*, 55.

125 L. Dahlenburg, A. Kaunert, *Eur. J. Inorg. Chem.* **1998**, 885.

126 W. A. Henderson Jr., S. A. Buckler, N. E. Day, M. Grayson, *J. Org. Chem.* **1961**, *26*, 4770.

127 H. Kischkel, G.-V. Röschenthaler, *Chem. Ber.* **1985**, *118*, 4842.

128 (a) K. V. Katti, H. Gali, C. J. Smith, D. E. Berning, *Acc. Chem. Res.* **1999**, *32*, 9; (b) V. S. Reddy, K. V. Katti, C. L. Barnes, *J. Chem. Soc. Dalton Trans.* **1996**, 1301; (c) R. M. Hiney, A. Ficks, H. Müller-Bunz, D. G. Gilheany, L. J. Higham, in *Specialist Periodical Reports - Organometallic Chemistry* (Eds.: I. J. S. Fairlamb, J. M. Lynam), RSC, 2011, *37*, pp. 27–45.

129 D. E. Berning, K. V. Katti, C. L. Barnes, W. A. Volkert, *J. Am. Chem. Soc.* **1999**, *121*, 1658.

130 (a) A. Marinetti, V. Kruger, F.-X. Buzin, *Tetrahedron Lett.* **1997**, *38*, 2947; (b) C. Sibbald, L. J. Higham, unpublished results.

131 (a) R. B. King, P. N. Kapoor, *J. Am. Chem. Soc.* **1969**, *91*, 5191; (b) R. B. King, J. C. Cloyd, P. N. Kapoor, *J. Chem. Soc., Perkin Trans. 1* **1973**, 2226

132 L. H. Davies, B. Stewart, R. W. Harrington, W. Clegg, L. J. Higham, *Angew. Chem. Int. Ed.* **2012**, *51*, 4921.

133 (a) F. Yang, P. E. Fanwick, C. P. Kubiak, *Organometallics* **1999**, *18*, 4222; (b) F. Yang, P. E. Fanwick, C. P. Kubiak, *Inorg. Chem.* **2002**, *41*, 4805.

134 C. R. Landis, W. Jin, J. S. Owen, T. P. Clark, *Angew. Chem. Int. Ed.* **2001**, *40*, 3432.

Chapter 2 — Multigram Synthesis of Primary Phosphines

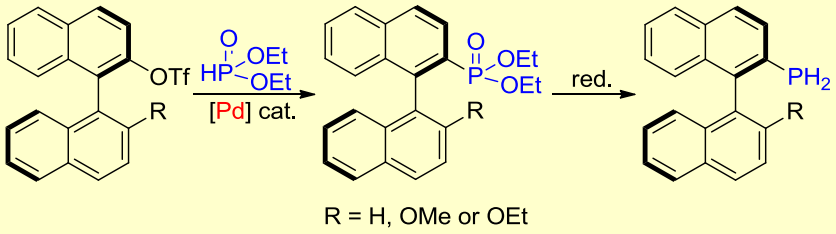

Air-stable, chiral primary phosphines have been synthesised on a multigram scale. The key synthetic step is an optimised palladium catalysed phosphonylation reaction of aryltriflates, which opens up a valuable synthetic route to a chiral scaffold that is easily derivatised into novel phosphines.[135]

2.1 Introduction

Primary phosphines are largely neglected from the perspective of synthetic methodology, owing to their reputation as highly air-sensitive, toxic and pyrophoric compounds.[136] In recent years a very limited number of "user-friendly" primary phosphines have been reported,[137] some of which take advantage of steric encumbrance in order to afford kinetic stability towards air oxidation;[138] by definition this impacts on subsequent opportunities for further functionalisation. A handful of other primary phosphines whose unexplained and surprising air stability cannot be accounted for on steric grounds have also appeared in the literature (*cf.* Chapter 1.4.1).[139]

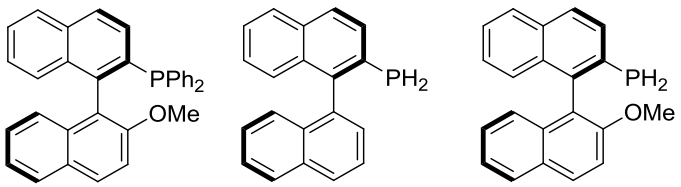

Figure 2.1 (*R*)-OMe-MOP and the primary phosphines **1a** and **1b**.

We discovered the first air-stable chiral primary phosphines **1a**,**b** (Figure 2.1);[140] according to our density functional theory-based model their air stability is attributable to the high level of conjugation in the binaphthyl backbone (Chapter 1.4.1).[141] We have since shown that, despite this resistance to air oxidation (in air, no oxidation in the solid state or in chloroform solution was observed after seven days[140,142]), the phosphino group remains readily transformable to

yield diverse, previously inaccessible derivatives of the hemilabile phosphine MOP, an effective yet expensive ligand used in asymmetric catalysis.[143,144] The potential of **1a**,**b** as ligand precursors was demonstrated by the synthesis, *inter alia*, of novel phosphiranes and phosphonites which were then employed in asymmetric catalysis (Chapters 3-6).[145]

After our earlier discovery, we therefore sought an efficient large-scale synthesis of **1a**,**b**. The described synthetic approach was re-evaluated and the most problematic key step identified as the carbon-phosphorus coupling reaction which yields the diethyl phosphonates **6** and **9** (Scheme 2.1). Typical yields for this transformation were moderate and reaction times of 3–4 days were rather long. We also found that this reaction was somewhat temperamental and did not always provide us with the reported yields. Herein we report a new synthetic method which affords both these and previously unreported synthons in multigram quantities *via* a simplified and improved approach, with the focus on the phosphonylation step.

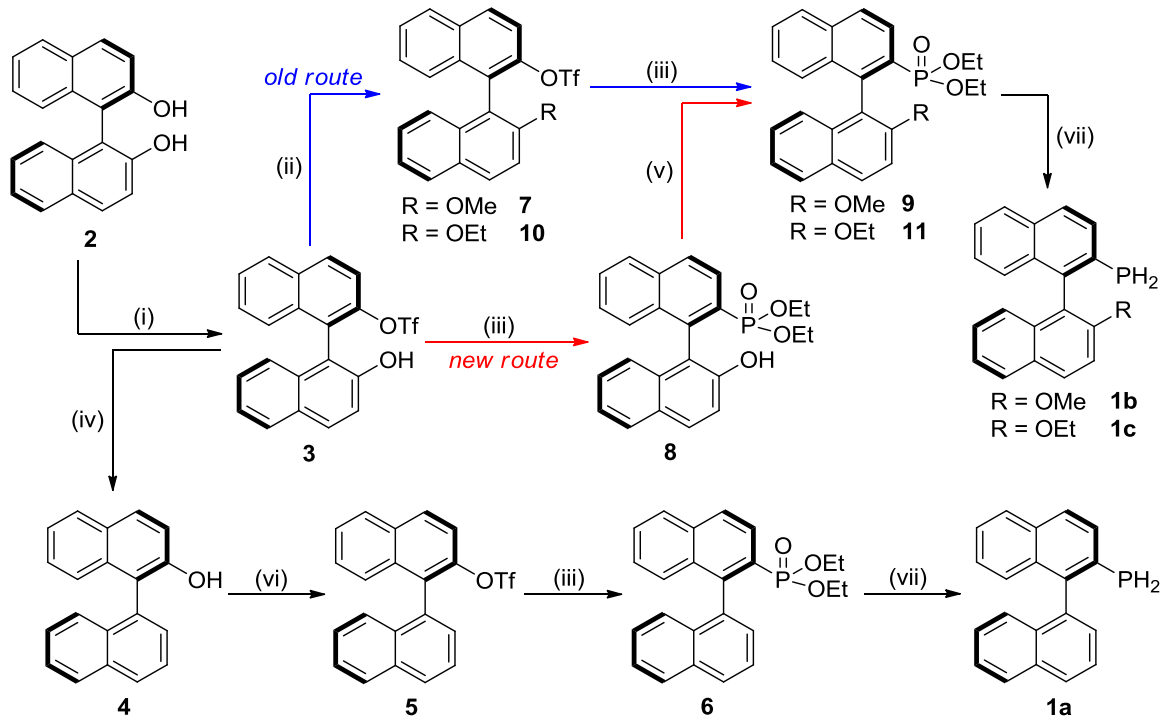

Scheme 2.1 Synthesis of **1a**, **1b** and **1c**: (i) Tf_2O, $(iPr)_2NEt$, DCM, 0 °C; (ii) Alkyl iodide, K_2CO_3, acetone; (iii) NEt_3, $HP(O)(OEt)_2$, $Pd(OAc)_2$, DPPP, DMSO, H_2O, 90 °C, or μ-wave, THF, 120 °C; (iv) H_2, NEt_3, Pd/C, EtOH; (v) Alkyl iodide, KOH, acetone; (vi) Tf_2O, pyridine, DCM; (vii) $LiAlH_4$, TMSCl, THF, –78 °C to rt.

2.2 Results and Discussion

The synthesis of **1a** and **1b** both started from commercially available (*R*)-BINOL (**2**; Scheme 2.1). The slow addition of one equivalent of triflic anhydride at 0 °C in the presence of *N*,*N*-diisopropylethylamine selectively afforded the monotriflated hydroxy binaphthalene **3** in an

excellent yield of 97%. The hydrogen atom as substituent in the 2'-position was introduced *via* hydrogenation on palladium/charcoal to give **4** in 84% yield; subsequent triflation of the remaining hydroxyl group led to **5** in 92% yield. All of these reactions proceeded quantitatively and yielded sufficiently clean products that could be used for subsequent reactions without the need for purification by column chromatography.

Originally, access to the MeO-MOP derivative **1b** was *via* the methoxy triflate **7**. This was prepared by reacting **2** with the mild yet costly triflating reagent *N*-phenyl trifluoromethanesulfonimide[146] to give monotriflate **3**, followed by subsequent addition of methyl iodide.[147] The transformation of **7** into the phosphonate **9** caused us some difficulties due to its unpredictable nature, erratic yields and small scale. A number of protocols describing the transition-metal catalysed phosphonylation and mechanistic studies of phosphorus-carbon bond formation have been published.[148,149] However, reports about the preparation of arylphosphonates from aryltriflates remain relatively scarce.[150]

Table 2.1 Screening of reaction conditions for the palladium catalysed phosphonylation.[a]

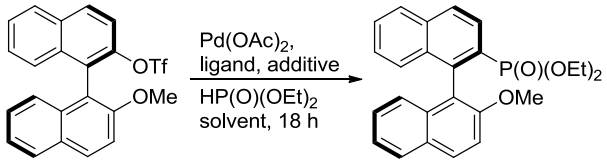

7 **9**

entry	ligand	solvent	additive	yield (%)[b]
1	DPPP	DMSO	–	0
2	DPPP	DMSO	KOAc (4.5 mg)	0
3	DPPP	DMSO	H_2O (0.01 mL)	43
4	DPPP	DMSO	H_2O (0.1 mL)	47
5	DPPP	EtOH	–	0
6	DPPP	THF	–	0
7	DPPP	THF	H_2O (0.01 mL)	12
8	DPPP	THF	H_2O (0.1 mL)	8
9	DPPP	Toluene	–	0
10	DPPB	DMSO	H_2O (0.1 mL)	32
11	DPPF	DMSO	H_2O (0.1 mL)	0
12	PPh_3	DMSO	H_2O (0.1 mL)	0
13	(*S*)-BINAP	DMSO	H_2O (0.1 mL)	0

[a] Conditions: 200 mg (0.46 mmol) **7**, 0.10 mL NEt_3, 0.07 mL diethyl phosphite, 5.2 mg (23 µmol) $Pd(OAc)_2$, 35 µmol bidentate ligand or 70 µmol PPh_3, 2 mL solvent, reflux or max. 90 °C, 18 h. [b] Isolated yields after column chromatographic work-up.

Following on from our earlier investigations, optimisation of the reaction conditions was carried out by screening the phosphonylation of **7** to obtain **9** (Table 2.1). The active species in the catalytic cycle is palladium(0); when using palladium(II) acetate as catalyst precursor, an excess of phosphine is used as the reducing agent.[151] The amount of starting material, the relative ratio of substrates, and the reaction time were kept constant throughout the screening. The quantity of diethyl phosphite was reduced to 1.2 equivalents as it has been reported that a significant excess of this compound can deactivate the palladium catalyst.[149]

The reaction was first attempted in dry dimethylsulfoxide and by employing the ligand 1,3-bis(diphenylphosphinopropane), but no product could be isolated either in this case (entry 1), or when potassium acetate was used as an additive (entry 2). Interestingly, the addition of small amounts of water did lead to product formation (entries 3-4). The positive effect of added water on phosphonylation reactions has been described before, and was found to improve reproducibility of results.[152] The exact role of the water in the original report and in our reaction has not yet been elucidated; however, it quickly became apparent that its presence appears crucial for product formation. The reaction could also be performed with tetrahydrofuran as solvent, again with added water, but this significantly lowered the yields (entries 6–8). Other phosphorus ligands tested were found to be inactive or inferior compared to the use of bis(diphenylphosphinopropane) (entries 10–13).

Table 2.2 Substrate screening for the palladium catalysed phosphonylation.[a]

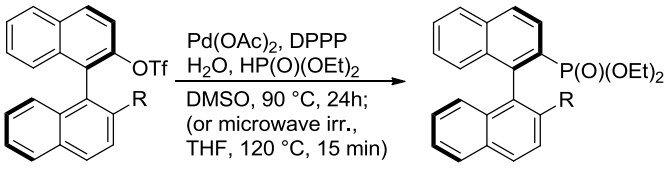

entry	substrate	product	yield (%)[b]
1	**7** (R = OMe)	**9**	42 (33[d])
2	**5** (R = H)	**6**	70 (14[d])
3	**3** (R = OH)	**8**	74 (84[d])
4	**12** (R = OTf)	**13**[c]	42
5	**10** (R = OEt)	**11**	38

[a] Conditions: 0.46 mmol aryltriflate, 0.10 mL NEt_3, 0.07 mL diethyl phosphite, 5.2 mg $Pd(OAc)_2$, 14.2 mg DPPP, 2 mL DMSO, 0.1 mL H_2O, 90 °C, 24 h. [b] Isolated yields after column chromatographic work-up. [c] Crude product also contained **6** which was isolated in 3% yield. [d] μ-wave, closed vessel: 2 mL THF, 0.1 mL H_2O, 120 °C, 15 min.

Having established viable reaction parameters for the conversion of triflate **7** to phosphonate **9**, we varied the aryltriflate using the optimised conditions. The procedure was carried out with the 2'-substituted binaphthyl triflates **3**, **5**, **7**, **10** and **12**, and the results are listed in Table

2.2. The reaction gave moderate to good yields, depending on the nature of the substituent. The best yields were achieved with the hydroxy derivative **3** and the H-substituted triflate **5**. The yields decreased for the more sterically demanding triflates **7** and **10**. The use of bis(triflate) **12** gave a moderate yield of the monophosphonate derivative **13**; however, trace amounts of **6** in the reaction mixture made the purification of the crude material extremely difficult.

We were also interested in the effect of using microwave irradiation for our phosphonylation reactions; the conversion of phenyltriflate to diethyl phenylphosphonate has been shown to be accelerated considerably by using a microwave power source.[153] We chose to use the same reaction parameters that we had found from our initial screening (*vide supra*), but using closed microwave vessels. The employment of dimethylsulfoxide as solvent, however, led to an instant increase in pressure due to its degradation, a phenomenon that has been observed before.[154] As a result, the solvent was changed to tetrahydrofuran and the temperature increased to 120 °C for 15 minutes. Although for the starting triflates **5** and **7** worse yields were attained from microwave irradiation, for the transformation of the hydroxy derivative **3** into phosphonate **8**, the yield increased to 84%, which successfully decreased the reaction time from 24 hours. This product crystallised as a dichloromethane solvate of a hydrogen-bonded dimer, exhibiting pairwise interactions between the phenolic H atom and terminal O atom of the phosphonate group, with distances O1–H1···O6 of 0.83(5) Å and 1.83(5) Å, and O5–H5···O2 of 0.74(7) Å and 1.98(7) Å (Figure 2.2).

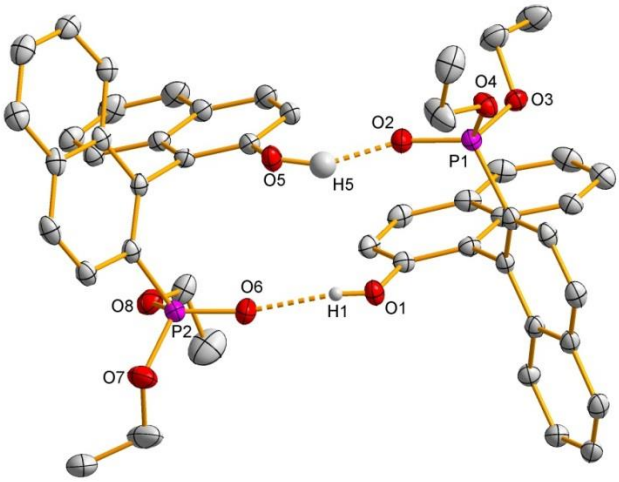

Figure 2.2 View of the structure of the hydrogen-bonded dimer of **8** (25% probability displacement ellipsoids for non H-atoms, 10% for H atoms). All hydrogen atoms except H1 and H5 are omitted for clarity, together with the disordered solvent and minor disorder components of ethyl groups. The main conformational differences between the two halves of the dimer are in the orientations of the ethyl groups.

Having established high-yielding access to phosphonate **8** by both conventional heating and microwave irradiation, we reacted this derivative with methyl or ethyl iodide to give the corresponding alkoxy derivatives **9** and **11** respectively, using potassium hydroxide as base. It should be noted that, due to the lower solubility of **8** compared to its alkoxy-substituted counterparts in non-chlorinated organic solvents such as diethyl ether and ethyl acetate, it is convenient to directly alkylate the crude product of **8** and only then purify the resulting alkoxy compounds **9** and **11** by column chromatography; this gave higher overall yields (68–79%). The X-ray crystal structure of phosphonate **9** is shown in Figure 2.3.

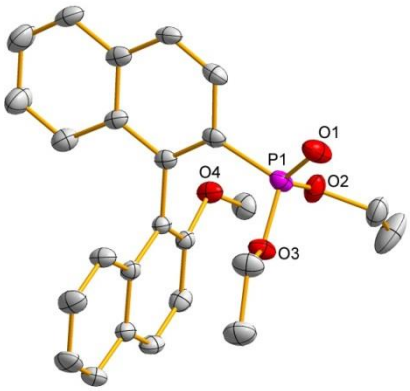

Figure 2.3 View of the structure of one of the two crystallographically independent molecules of **9** in the asymmetric unit (50% probability displacement ellipsoids). Hydrogen atoms are omitted for clarity. The two molecules show only minor conformational differences.

The phosphonates **6**, **9** and **11** were subsequently reduced to give the corresponding primary phosphines **1a**, **1b** and **1c** using lithium aluminium hydride and trimethylsilyl chloride as co-reductants. This combination of reducing agents is important, as it allows for essentially quantitative conversion; in the absence of trimethylsilyl chloride the reduction of **9** to **1b** was limited to just 16%.[155] The use of peroxide-free solvents is crucial to achieve a clean reaction process as the products are prone to oxidation by this species. The remarkable air-stability of the primary phosphines allowed for their straightforward purification on silica media, a procedure seldom considered or indeed applicable for this family of compound, with good yields of 81–85% recorded.

2.3 Conclusion

In summary we have now optimised an economical and more versatile synthetic route to valuable chiral primary phosphines. All reactions have been carried out on a multigram scale without reductions in yields. Hydroxy phosphonate **8** is functionalised readily to give new

alkoxy-substituted phosphonates and primary phosphines, as has been shown by the synthesis of the ethoxy derivatives **11** and **1c**.

2.4 Experimental Section

2.4.1 General Considerations

Table 2.3 Selected crystallographic data for compounds **8** and **9**.

	8	**9**
formula	$2C_{24}H_{23}O_4P \cdot CH_2Cl_2$	$C_{25}H_{25}O_4P$
formula wt	897.71	420.42
cryst syst	orthorhombic	monoclinic
space group	$P222_1$	$P2_1$
a, Å; α, deg	11.29130(10); 90	8.1104(12); 90
b, Å; β, deg	23.1203(3); 90	18.188(5); 100.908(13)
c, Å; γ, deg	33.9256(4); 90	14.941(4); 90
V, Å^3	8856.56(17)	2164.2(8)
Z	8	4
ρ_{calc}, g cm^{-3}	1.347	1.290
μ, mm^{-1}	2.449	0.156
$F(000)$	3760	888
T_{min}/T_{max}	0.5472/0.7577	0.9374/0.9547
hkl range	–13 to 11, –25 to 27, –40 to 40	–10 to 10, –22 to 23, –18 to 19
θ range, deg	4.0 to 67.1	4.1 to 27.5
no. of measd rflns	13362	17135
no. of unique rflns (R_{int})	7134 (0.0265)	9417 (0.0238)
no. of obsd rflns, $I > 2\sigma(I)$	6550	7443
refined params/restraints	608/34	541/1
goodness of fit	1.038	1.043
Abs. structure param.	0.06(2)	0.01(7)
R1/wR2 ($I > 2\sigma(I)$)	0.0576/0.1597	0.0434/0.0845
R1/wR2 (all data)	0.0622/0.1653	0.0687/0.0945
resid electron dens, e Å^{-3}	0.39/–0.67	0.26/–0.40

All air- and/or water-sensitive reactions were performed under a nitrogen atmosphere using standard Schlenk line techniques. Tetrahydrofuran (sodium/benzophenone ketyl), toluene (sodium), ethanol (calcium hydride) and dichloromethane (calcium hydride) were dried and distilled prior to use. DMSO (Aldrich) was purchased in an anhydrous state and stored over molecular sieves. All other chemicals were used as received without further purification. Microwave-assisted reactions were performed in 10 mL closed vessels on a CEM Discover apparatus under automated power control based on temperature feedback. Flash

chromatography was performed on silica gel from Fluorochem (silica gel, 40-63u, 60A, LC301). Thin-layer chromatography was performed on Merck aluminium-based plates with silica gel and fluorescent indicator 254 nm. ^{1}H NMR, ^{13}C{^{1}H} NMR, ^{19}F NMR, and ^{31}P{^{1}H} NMR spectra were recorded on a JEOL Lambda 500 (^{1}H 500.16 MHz) or JEOL ECS-400 (^{1}H 399.78 MHz) spectrometer at room temperature (21°C) using the indicated solvent as internal reference. Optical rotation values were determined on an Optical Activity Polaar 2001 device. Mass spectrometry was carried out by the EPSRC National Mass Spectrometry Service Centre at Swansea. Compounds **7**[147] and **12**[156] have been prepared according to literature procedures. Analytical data for **1a**,**b**,[140] **3**,[157] **4** and **5**,[158] **6** and **9**,[140] and **13**[159] were consistent with the previously published values. Key crystallographic data are given in Table 2.3; the labelling scheme is given in Figure 2.4.

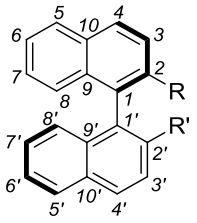

Figure 2.4 Labelling scheme used for binaphthyl compounds (R has a higher priority than R').

2.4.2 (*R*)-2'-Hydroxy-[1,1'-binaphthalen]-2-yl trifluoromethanesulfonate (**3**)

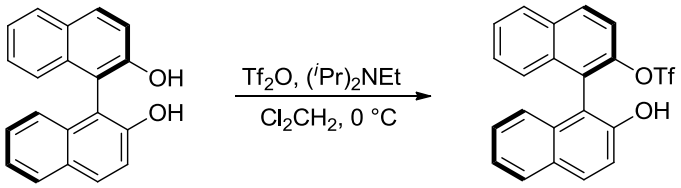

(*R*)-BINOL (**2**, 8.00 g, 27.9 mmol) was dissolved in CH_2Cl_2 (500 mL). The solution was cooled to 0 °C and DIPEA (4.9 mL, 27.9 mmol) was added followed by the dropwise addition of Tf_2O (4.7 mL, 27.9 mmol). The reaction mixture was stirred at room temperature overnight, after which time the solution was concentrated to half of its volume. The organic phase was washed with H_2O (100 mL), 1M aqueous HCl (100 mL), and brine (100 mL), and dried over $MgSO_4$. The fairly pure product was isolated as pale yellow oil (11.3 g, 27.0 mmol, 97%).[157]

^{1}H NMR (400 MHz, $CDCl_3$): δ = 8.12 (d, $^{3}J_{HH}$ = 8.2 Hz, 1H, Ar*H*), 8.02 (d, $^{3}J_{HH}$ = 8.2 Hz, 1H, Ar*H*), 7.97 (d, $^{3}J_{HH}$ = 8.2 Hz, 1H, Ar*H*), 7.88 (d, $^{3}J_{HH}$ = 8.2 Hz, 1H, Ar*H*), 7.60 (m, 2H, 2 Ar*H*), 7.44 (m, 2H, 2 Ar*H*), 7.37-7.24 (m, 3H, 3 Ar*H*), 7.01 (d, $^{3}J_{HH}$ = 8.2 Hz, 1H, Ar*H*),

4.90 (br s, 1H, O*H*) ppm. **^{19}F NMR** (376 MHz, $CDCl_3$): $\delta = -74.3$ ppm. **TLC** (silica gel; toluene): $R_f = 0.25$.

2.4.3 (*S*)-[1,1'-Binaphthalen]-2-ol (**4**)

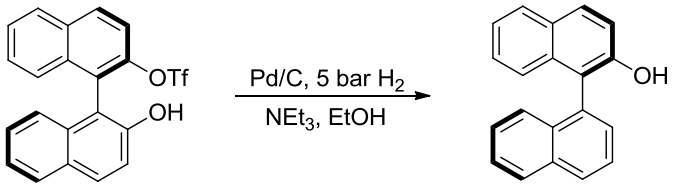

To a solution of **3** (8.25 g, 19.7 mmol) in EtOH (40 mL) was added NEt_3 (8.24 mL, 59.2 mmol) and 5% Pd on charcoal (419 mg, 0.20 mmol Pd). The suspension was stirred for 2 days under 5 bar H_2 gas pressure in a miniclave system, after which time TLC analysis showed complete consumption of the starting material. The reaction mixture was filtered and the residue washed with CH_2Cl_2. More CH_2Cl_2 (100 mL) was added to the filtrate and the organic phase was washed with H_2O (80 mL), 1 M aqueous HCl (80 mL), 0.1 M aqueous $NaHCO_3$ (80 mL), and brine (80 mL). After drying over $MgSO_4$ the fairly pure product was obtained as a white solid (4.46 g, 16.5 mmol, 84%).[158]

^{1}H NMR (400 MHz, $CDCl_3$): $\delta = 8.03$ (d, $^3J_{HH} = 8.2$ Hz, 1H, Ar*H*), 7.98 (d, $^3J_{HH} = 8.2$ Hz, 1H, Ar*H*), 7.91 (d, $^3J_{HH} = 8.7$ Hz, 1H, Ar*H*), 7.86 (d, $^3J_{HH} = 7.8$ Hz, 1H, Ar*H*), 7.65 (m, $J_{HH} = 8.2$ Hz, 1H, Ar*H*), 7.53 (m, 2H, 2 Ar*H*), 7.41-7.21 (m, 5H, 5 Ar*H*), 7.01 (d, $^3J_{HH} = 8.2$ Hz, 1H, Ar*H*), 4.91 (s, 1H, O*H*) ppm. **TLC** (silica gel; toluene): $R_f = 0.5$.

2.4.4 (*S*)-[1,1'-Binaphthalen]-2-yl trifluoromethanesulfonate (**5**)

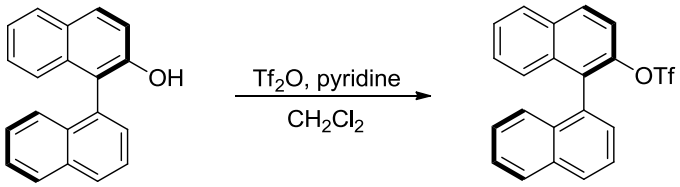

To a solution of **4** (9.30 g, 34.4 mmol) in CH_2Cl_2 (125 mL) and pyridine (4.20 mL, 51.6 mmol) was slowly added Tf_2O (8.70 mL, 51.6 mmol) at 0 °C. The resulting yellow suspension was allowed to warm up to ambient temperature and stirred for 2 hours. The organic phase was washed with H_2O (70 mL), 1M aqueous HCl (70 mL), 0.1 M aqueous $NaHCO_3$ (70 mL) and brine (70 mL), dried over $MgSO_4$, filtered and concentrated to give the title product as a pale orange solid (12.7 g, 31.6 mmol, 92%).[158]

^{1}H NMR (400 MHz, $CDCl_3$): δ = 8.06-7.95 (m, 4H, 4 Ar*H*), 7.64 (t, 1H, Ar*H*), 7.58-7.47 (m, 4H, 4 Ar*H*), 7.42-7.29 (m, 3H, 3 Ar*H*), 7.21 (d, $^{3}J_{HH}$ = 7.8 Hz, 1H, Ar*H*). **^{19}F NMR** (376 MHz, $CDCl_3$): δ = –74.4 ppm. **TLC** (silica gel; toluene): R_f = 0.9.

2.4.5 (*R*)-2'-Ethoxy-[1,1'-binaphthalen]-2-yl trifluoromethanesulfonate (**10**)

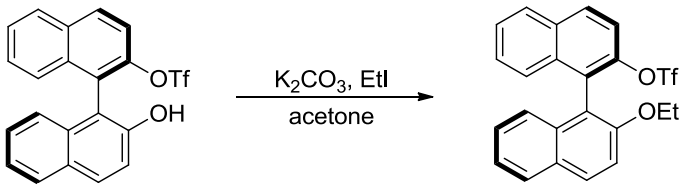

To a solution of **3** (1.14 g, 2.72 mmol) in acetone (100 mL) were added K_2CO_3 (1.51 g, 10.90 mmol) and EtI (0.87 mL, 10.90 mmol). The mixture was stirred for 3 days, during which time the reaction was monitored by TLC analysis. After complete consumption of the starting materials, the volatiles were removed *in vacuo* and the residue was dissolved in CH_2Cl_2 (30 mL). The organic phase was washed with H_2O (30 mL) and dried over $MgSO_4$. The crude product was purified by column chromatography through silica media using hexane to remove the impurities, then toluene to obtain the title product as an off-white solid (967 mg, 2.16 mmol, 79%).

^{1}H NMR (500 MHz, $CDCl_3$): δ = 8.03 (d, $^{3}J_{HH}$ = 9.1 Hz, 1H, *H*4), 8.03 (d, $^{3}J_{HH}$ = 9.1 Hz, 1H, *H*4'), 7.97 (d, $^{3}J_{HH}$ = 8.2 Hz, 1H, *H*5), 7.88 (d, $^{3}J_{HH}$ = 8.2 Hz, 1H, *H*5'), 7.58 (d, $^{3}J_{HH}$ = 9.1 Hz, 1H, *H*3), 7.54 (m, 1H, *H*6), 7.43 (d, $^{3}J_{HH}$ = 9.1 Hz, 1H, *H*3'), 7.37-7.32 (m, 3H, *H*6'+*H*7+*H*8), 7.26-7.23 (m, 1H, *H*7'), 7.02 (d, $^{3}J_{HH}$ = 8.2 Hz, 1H, *H*8'), 4.15-4.10 (m, 2H, CH_2), 1.15 (t, $^{3}J_{HH}$ = 7.0 Hz, 3H, CH_3) ppm. **^{13}C{^{1}H} NMR** (126 MHz, $CDCl_3$): δ = 154.7 (*C*2'), 145.7 (*C*2), 133.8 (*C*9'+*C*1), 132.6 (*C*9), 131.0 (*C*4'), 130.2 (*C*4), 128.9 (*C*10'), 128.3 (*C*5), 128.1 (*C*5'), 127.5 (*C*10), 127.3 (*C*7), 127.1 (*C*8), 126.8 (*C*7'+*C*6), 125.0 (*C*8'), 123.7 (*C*6'), 119.6 (*C*3), 115.6 (*C*1'), 114.2 (*C*3'), 64.6 (*C*H_2), 14.8 (*C*H_3) ppm. **^{19}F NMR** (376 MHz, $CDCl_3$): δ = –74.8 ppm. **HRMS** (NSI^+, MeOH): Found: *m*/*z* = 447.0879. Calculated for $[M + H]^+$: *m*/*z* = 447.0872. **OR** ($CHCl_3$, *c* = 1.0 mg/ml): $[\alpha]_D^{20}$ = –78°. **TLC** (silica gel; toluene): R_f = 0.9.

2.4.6 General Procedure for the Phosphonylation of Aryltriflates

Method A: $Pd(OAc)_2$ (193 mg, 0.86 mmol), DPPP (532 mg, 1.29 mmol) and the appropriate trifluoromethanesulfonate (17.2 mmol) were dissolved in DMSO (60 mL) and H_2O (0.1 mL) and purged with nitrogen for 10 minutes. NEt_3 (3.60 mL, 25.8 mmol) and diethyl phosphite (2.66 mL, 20.6 mmol) were added subsequently and the solution was heated to 90 °C

overnight. H_2O (30 mL) was added to the reaction mixture and the suspension was extracted with CH_2Cl_2 (100 mL). The organic layer was washed with brine (3 x 50 mL) and dried over $MgSO_4$ to give the crude product, which was usually used without further purification for its alkylation.

Method B: $Pd(OAc)_2$ (5.2 mg, 23 μmol), DPPP (14.2 mg, 35 μmol) and the appropriate trifluoromethanesulfonate (0.46 mmol) were placed in a microwave vessel and dissolved in THF (2 mL) and H_2O (0.01 mL). The solution was stirred for 15 minutes, after which time NEt_3 (0.10 mL, 0.67 mmol) and diethyl phosphite (0.07 mL, 0.56 mmol) were added. The closed vessel was irradiated with microwaves at 120 °C for 15 minutes. The volatiles were evaporated to give the crude product.

2.4.7 (*S*)-Diethyl [1,1'-binaphthalen]-2-ylphosphonate (**6**)

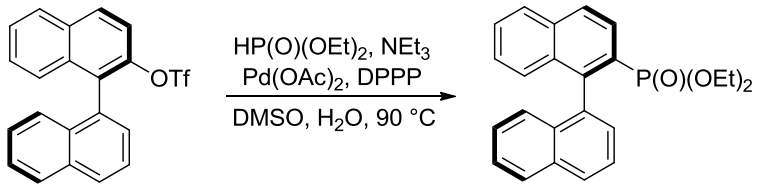

The crude product was further purified by column chromatography (EtOAc/hexane, 2:1) on silica media (h = 16 cm, d = 4 cm) to give the title product as a white solid (4.34 g, 11.1 mmol, 65%).[140]

^{1}H NMR (400 MHz, $CDCl_3$): δ = 8.20 (dd, $^3J_{HP}$ = 12.4 Hz, $^3J_{HH}$ = 8.7 Hz, 1H, *H*3), 8.01 (dd, $^3J_{HH}$ = 8.7 Hz, $^4J_{HP}$ = 3.7 Hz, 1H, *H*4), 7.97-7.90 (m, 3H, 3 Ar*H*), 7.59 (d, $^3J_{HH}$ = 7.8 Hz, 1H, Ar*H*), 7.54-7.47 (m, 2H, 2 Ar*H*), 7.42 (m, 1H, Ar*H*), 7.27-7.15 (m, 3H, 3 Ar*H*), 7.07 (d, $^3J_{HH}$ = 8.2 Hz, 1H, Ar*H*), 3.81-3.50 (m, 4H, 2 OCH_2CH$_3$), 0.96 (t, $^3J_{HH}$ = 6.9 Hz, 3H, OCH$_2$CH_3), 0.69 (t, $^3J_{HH}$ = 6.9 Hz, 3H, OCH$_2$CH_3) ppm. **^{31}P{^{1}H} NMR** (162 MHz, $CDCl_3$): δ = 18.6 ppm. **TLC** (silica gel; EtOAc/hexane, 2:1): R_f = 0.3.

2.4.8 (*R*)-Diethyl (2'-hydroxy-[1,1'-binaphthalen]-2-yl)phosphonate (**8**)

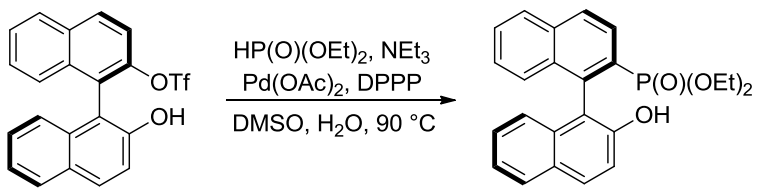

The crude product was usually used without further purification for its methylation (next synthetic step, *vide infra*) but further cleaning was possible by column chromatography

(CH_2Cl_2/MeOH, 50:1) on silica media (h = 26 cm, d = 4 cm) to give the title product as a white solid (5.50 g, 13.5 mmol, 79%).

^{1}H NMR (400 MHz, $CDCl_3$): δ = 8.08 (ddd, $^3J_{HP}$ = 11.8 Hz, $^3J_{HH}$ = 8.5 Hz, J_{HH} = 1.0 Hz, 1H, *H*3), 8.01 (dd, $^3J_{HH}$ = 8.5 Hz, $^4J_{HP}$ = 4.3 Hz, 1H, *H*4), 7.92 (d, $^3J_{HH}$ = 8.2 Hz, 1H, *H*5), 7.87 (d, $^3J_{HH}$ = 8.9 Hz, 1H, *H*4'), 7.83 (d, $^3J_{HH}$ = 8.9 Hz, 1H, *H*5'), 7.53 (m, 1H, *H*6), 7.35 (dd, $^3J_{HH}$ = 8.9 Hz, J_{HH} = 1.2 Hz, 1H, *H*3'), 7.29-7.23 (m, 2H, *H*6'+*H*7), 7.19 (d, $^3J_{HH}$ = 8.5 Hz, 1H, *H*8), 7.14 (m, 1H, *H*7'), 6.77 (d, $^3J_{HH}$ = 8.5 Hz, 1H, *H*8'), 6.52 (s, 1H, O*H*), 3.99-3.85 (m, 2H, OCH_2CH$_3$), 3.58 (m, 1H, OCH_2CH$_3$), 3.22 (m, 1H, OCH_2CH$_3$), 1.05 (t, $^3J_{HH}$ = 6.9 Hz, 3H, OCH$_2$CH_3), 0.69 (t, $^3J_{HH}$ = 6.9 Hz, 3H, OCH$_2$CH_3) ppm. **^{13}C{^{1}H} NMR** (101 MHz, $CDCl_3$): δ = 152.4 (*C*2'), 139.5 (d, $^2J_{CP}$ = 10.0 Hz, *C*1), 135.5 (d, $^4J_{CP}$ = 2.6 Hz, *C*10), 134.6 (*C*9'), 133.3 (d, $^1J_{CP}$ = 16.2 Hz, *C*2), 130.1 (*C*4'), 129.0 (*C*10'), 128.5 (*C*9), 128.4 (*C*6), 128.4 (*C*4), 128.2 (*C*5), 127.9 (*C*3), 127.9 (*C*5'), 127.3 (*C*7), 127.3 (*C*8), 126.3 (*C*7'), 125.5 (*C*8'), 123.4 (*C*6'), 120.2 (*C*3'), 119.6 (d, $^3J_{CP}$ = 5.3 Hz, *C*1'), 62.5 (d, $^2J_{CP}$ = 6.0 Hz, *C*H$_2$), 62.4 (d, $^2J_{CP}$ = 6.0 Hz, *C*H$_2$), 16.0 (d, $^3J_{CP}$ = 6.7 Hz, *C*H$_3$), 15.6 (d, $^3J_{CP}$ = 6.7 Hz, *C*H$_3$) ppm. **^{31}P{^{1}H} NMR** (162 MHz, $CDCl_3$): δ = 18.6 ppm. **HRMS** (NSI^+, MeOH): Found: *m*/*z* = 407.1404. Calculated for $[M + H]^+$: *m*/*z* = 407.1407. **OR** ($CHCl_3$, *c* = 1.0 mg/ml): $[\alpha]_D^{20}$ = –98°. **TLC** (silica gel; CH_2Cl_2/MeOH, 50:1): R_f = 0.35.

2.4.9 General Procedure for 2'-Alkoxy-[1,1'-binaphthalen]-2-ylphosphonates from **8**

Phosphonate **8** (27.7 mmol) was dissolved in acetone (500 mL). KOH (6.22 g, 111 mmol) and alkyl iodide (111 mmol) were added to the solution. The reaction mixture was stirred overnight, after which time TLC analysis showed complete consumption of the starting material. The volatiles were removed *in vacuo* and the residue was dissolved in diethyl ether (150 mL). The organic phase was washed with H_2O (80 mL), 1 M aqueous HCl (80 mL), 0.1 M aqueous $NaHCO_3$ (80 mL), and brine (80 mL) and dried over $MgSO_4$ to give the crude product.

2.4.10 (*R*)-Diethyl (2'-methoxy-[1,1'-binaphthalen]-2-yl)phosphonate (**9**)

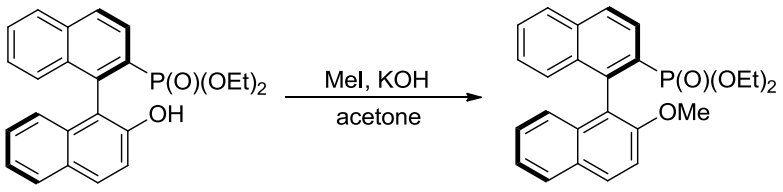

The crude was purified by column chromatography on silica media (EtOAc/hexane, 3:1) or recrystallised from acetone to yield the intended product as a white solid (9.15 g, 21.8 mmol, 79%).[140]

^{1}H NMR (400 MHz, $CDCl_3$): δ = 8.20 (dd, $^{3}J_{HH}$ = 8.2 Hz, $^{3}J_{HH}$ = 11.9 Hz, 1H, Ar*H*), 8.00 (m, 2H, 2 Ar*H*), 7.93 (d, $^{3}J_{HH}$ = 8.2 Hz, 1H, Ar*H*), 7.83 (d, $^{3}J_{HH}$ = 8.2 Hz, 1H, Ar*H*), 7.52 (m, $^{3}J_{HH}$ = 8.2 Hz, 1H, Ar*H*), 7.41 (d, $^{3}J_{HH}$ = 9.2 Hz, 1H, Ar*H*), 7.25 (m, 3H, 3 Ar*H*), 7.15 (m, 1H, Ar*H*), 6.86 (d, $^{3}J_{HH}$ = 8.7 Hz, 1H, Ar*H*), 3.80-3.48 (m, 4H, 2OCH_2CH$_3$), 3.76 (s, 3H, OCH_3), 0.96 (t, $^{3}J_{HH}$ = 7.3 Hz, 3H, OCH$_2$CH_3), 0.76 (t, $^{3}J_{HH}$ = 7.3 Hz, 3H, OCH$_2$CH_3) ppm. **^{31}P{^{1}H} NMR** (162 MHz, $CDCl_3$): δ = 18.6 ppm. **TLC** (silica gel; EtOAc/hexane, 3:1): R_f = 0.25.

2.4.11 (*R*)-Diethyl (2'-ethoxy-[1,1'-binaphthalen]-2-yl)phosphonate (**11**)

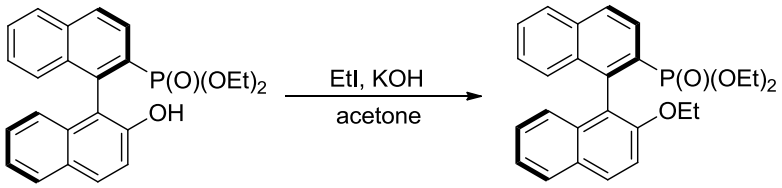

Further purification by column chromatography (EtOAc/hexane, 3:1) on silica media gave the intended product as a white solid (7.72 g, 18.4 mmol, 68%).

^{1}H NMR (500 MHz, $CDCl_3$): δ = 8.20 (dd, $^{3}J_{HP}$ = 12.1 Hz, $^{3}J_{HH}$ = 8.6 Hz, 1H, *H*3), 8.00 (dd, $^{3}J_{HH}$ = 8.6 Hz, $^{4}J_{HP}$ = 3.8 Hz, 1H, *H*4), 7.96 (d, $^{3}J_{HH}$ = 9.0 Hz, 1H, *H*4'), 7.92 (d, $^{3}J_{HH}$ = 8.3 Hz, 1H, *H*5), 7.83 (d, $^{3}J_{HH}$ = 8.3 Hz, 1H, *H*5'), 7.50 (m, 1H, *H*6), 7.39 (d, $^{3}J_{HH}$ = 9.0 Hz, 1H, *H*3'), 7.27-7.24 (m, 3H, *H*6'+*H*7+*H*8), 7.15 (m, 1H, *H*7'), 6.90 (d, 1H, $^{3}J_{HH}$ = 8.6 Hz, *H*8'), 4.09-3.99 (m, 2H, ArOCH_2CH$_3$), 3.83-3.75 (m, 1H, P(O)OCH_2CH$_3$), 3.70-3.55 (m, 3H, P(O)OCH_2CH$_3$), 1.01 (t, $^{3}J_{HH}$ = 6.9 Hz, 3H, ArOCH$_2$CH_3), 1.00 (t, $^{3}J_{HH}$ = 7.0 Hz, 3H, P(O)OCH$_2$CH_3), 0.77 (t, $^{3}J_{HH}$ = 7.0 Hz, 3H, P(O)OCH$_2$CH_3) ppm. **^{13}C{^{1}H} NMR** (126 MHz, $CDCl_3$): δ = 154.5 (*C*2'), 140.9 (d, $^{2}J_{CP}$ = 9.3 Hz, *C*1), 135.2 (*C*10), 134.7 (*C*9'), 133.2 (d, $^{1}J_{CP}$ = 16.3 Hz, *C*2), 129.9 (*C*4'), 129.1 (d, $^{2}J_{CP}$ = 10.5 Hz, *C*3), 128.7 (*C*10'), 128.0 (*C*5), 127.8 (*C*6), 127.7 (*C*5'), 127.5 (*C*9), 127.4 (*C*4), 127.3 (*C*7), 126.6 (*C*8), 126.1 (*C*7'), 125.9 (*C*8'), 123.4 (*C*6'), 121.5 (*C*1'), 114.5 (*C*3'), 64.6 (ArO*C*H$_2$CH$_3$), 61.7 (d, $^{2}J_{CP}$ = 17.3 Hz, P(O)O*C*H$_2$-CH$_3$), 61.6 (d, $^{2}J_{CP}$ = 17.3 Hz, P(O)O*C*H$_2$CH$_3$), 16.1 (d, $^{3}J_{CP}$ = 6.7 Hz, P(O)OCH$_2$*C*H$_3$), 15.7 (d, $^{3}J_{CP}$ = 6.7 Hz, P(O)OCH$_2$*C*H$_3$), 15.0 (ArOCH$_2$*C*H$_3$) ppm. **^{31}P{^{1}H} NMR** (202 MHz, $CDCl_3$): δ = 18.7 ppm. **HRMS** (APCI^{+}, MeCN): Found:

m/z = 435.1719. Calculated for $[M + H]^+$: m/z = 435.1720. **OR** ($CHCl_3$, c = 1.0 mg/ml): $[\alpha]_D^{20}$ = +46°. **TLC** (silica gel; EtOAc/hexane, 3:1): R_f = 0.4.

2.4.12 General Procedure for the Reduction of Phosphonates

$LiAlH_4$ (2.20 g, 57.6 mmol) was dissolved in THF (60 mL) and cooled to −78 °C. Me_3SiCl (7.3 mL, 57.6 mmol) was added and the reaction mixture was warmed up to room temperature over 30 min. The solution was cooled to −78 °C and the appropriate phosphonate (19.2 mmol) in THF (60 mL) was added slowly to the reaction mixture. The solution was allowed to warm up to room temperature and stirred overnight. The reaction was quenched with H_2O (20 mL) and extracted with Et_2O (3 x 30 mL). The organic phase was washed with H_2O (20mL) and dried over $MgSO_4$. Purification was performed by column chromatography (CH_2Cl_2/hexane, 1:1) on silica media to give the intended product.

2.4.13 (*S*)-[1,1'-Binaphthalen]-2-ylphosphine (**1a**)

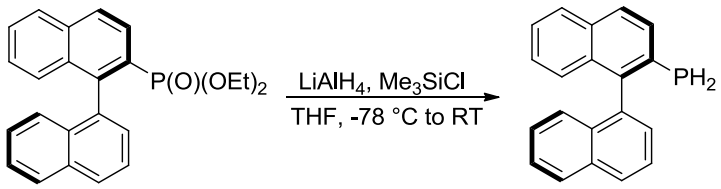

The product was obtained as a white solid (4.66 g, 16.4 mmol, 85%).[140]

^{1}H NMR (400 MHz, $CDCl_3$): δ = 7.98 (m, 2H, 2 Ar*H*), 7.90 (d, $^3J_{HH}$ = 8.2 Hz, 1H, Ar*H*), 7.86 (d, $^3J_{HH}$ = 8.2 Hz, 1H, Ar*H*), 7.72 (dd, $^3J_{HH}$ = 8.7 Hz, $^3J_{HH}$ = 5.5 Hz, 1H, Ar*H*), 7.72 (dd, $^3J_{HH}$ = 8.2 Hz, $^3J_{HH}$ = 6.9 Hz, 1H, Ar*H*), 7.51-7.40 (m, 3H, 3 Ar*H*), 7.32-7.15 (m, 4H, 4 Ar*H*), 3.67 (AB quartet, $^1J_{PHa}$ = 204.7 Hz, $^1J_{PHb}$ = 206.5 Hz, $^2J_{HH}$ = 11.9 Hz, 2H, PH_2) ppm. **^{31}P{^{1}H} NMR** (162 MHz, $CDCl_3$): δ = –124.8 ppm. **TLC** (silica gel, hexane/CH_2Cl_2, 2:1): R_f = 0.55.

2.4.14 (*R*)-(2'-Methoxy-[1,1'-binaphthalen]-2-yl)phosphine (**1b**)

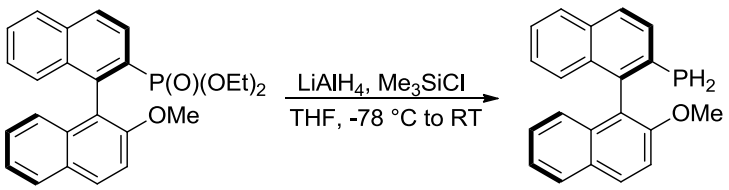

The product was obtained as a white solid (4.66 g, 14.7 mmol, 83%).[140]

^{1}H NMR (500 MHz, $CDCl_3$): δ = 8.03 (d, $^3J_{HH}$ = 9.2 Hz, 1H, Ar*H*), 7.89 (d, $^3J_{HH}$ = 8.3 Hz, 2H, 2 Ar*H*), 7.86 (d, $^3J_{HH}$ = 8.7 Hz, 1H, Ar*H*), 7.75 (dd, $^3J_{HH}$ = 8.3 Hz, $^3J_{HH}$ = 5.5 Hz, 1H, Ar*H*), 7.44 (m, 2H, 2 Ar*H*), 7.34 (t, $^3J_{HH}$ = 6.9 Hz, 1H, Ar*H*), 7.24 (m, 2H, 2 Ar*H*), 7.16 (d, $^3J_{HH}$ = 8.3 Hz, 1H, Ar*H*), 6.97 (d, $^3J_{HH}$ = 8.3 Hz, 1H, Ar*H*), 3.80 (s, 3H, OCH_3), 3.64 (AB quartet, $^1J_{PHa}$ = 203.9 Hz, $^1J_{PHb}$ = 204.8 Hz, $^2J_{HH}$ = 12.4 Hz, 2H, PH_2) ppm. **^{31}P{^{1}H} NMR** (202 MHz, $CDCl_3$): δ = –125.7 ppm. **TLC** (silica gel, hexane/CH_2Cl_2, 2:1): R_f = 0.5.

2.4.15 (*R*)-(2'-Ethoxy-[1,1'-binaphthalen]-2-yl)phosphine (**1c**)

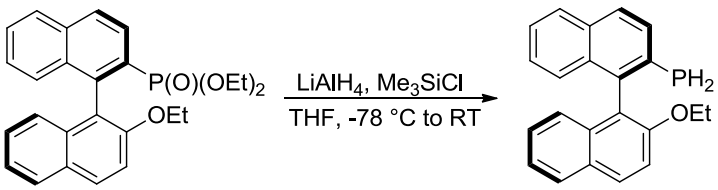

The product was obtained as a white solid (268 mg, 0.81 mmol, 81%).

^{1}H NMR (500 MHz, $CDCl_3$): δ = 8.05 (d, $^3J_{HH}$ = 9.2 Hz, 1H, *H*4'), 7.96 (m, 2H, *H*5+*H*5'), 7.91 (d, $^3J_{HH}$ = 8.5 Hz, 1H, *H*4), 7.82 (dd, $^3J_{HH}$ = 8.5 Hz, $^3J_{HP}$ = 5.4 Hz, 1H, *H*3), 7.50 (d, $^3J_{HH}$ = 9.2 Hz, 1H, *H*3'), 7.50 (m, 1H, *H*6), 7.40 (m, 1H, *H*6'), 7.30 (m, 3H, *H*7+*H*7'+*H*8), 7.09 (d, $^3J_{HH}$ = 8.5 Hz, 1H, *H*8'), 4.20-4.09 (m, 2H, OCH_2CH$_3$), 4.05-3.44 (AB quartet, $^1J_{PHa}$ = 203.9 Hz, $^1J_{PHb}$ = 204.8 Hz, $^2J_{HH}$ = 12.3 Hz, 2H, PH_2), 1.17 (t, $^3J_{HH}$ = 7.0 Hz, 3H, OCH$_2$CH_3) ppm. **^{13}C{^{1}H} NMR** (126 MHz, $CDCl_3$): δ = 154.0 (C2'), 139.2 (d, $^2J_{CP}$ = 16.4 Hz, C1), 133.7(d, $^4J_{CP}$ = 1.3 Hz, C9'), 133.5 (C10), 133.4 (d, $^1J_{CP}$ = 3.6 Hz, C2), 133.8 (d, $^2J_{CP}$ = 8.2 Hz, C3), 130.2 (C4'), 129.4 (C10'), 129.0 (d, $^3J_{CP}$ = 8.2 Hz, C9), 128.3 (C5), 128.3 (C5'), 127.5 (d, $^3J_{CP}$ = 3.9 Hz, C4), 127.0 (C7'), 126.5 (C7), 126.1 (C8), 126.0 (C6), 125.0 (C8'), 124.0 (C6'), 123.0 (C1'), 115.3 (C3'), 65.0 (O*C*H$_2$CH$_3$), 15.3 (OCH$_2$*C*H$_3$) ppm. **^{31}P{^{1}H} NMR** (162 MHz, $CDCl_3$): δ = –125.4 ppm. **HRMS** (NSI$^+$, MeOH): Found: *m*/*z* = 331.1252. Calculated for [M + H]$^+$: *m*/*z* = 331.1246. **OR** ($CHCl_3$, *c* = 1.0 mg/ml): $[\alpha]_D^{20}$ = +14°. **TLC** (silica gel, hexane/CH_2Cl_2, 1:1): R_f = 0.7.

2.5 References

135 The content of this chapter has been published in the following peer-reviewed scientific journal: A. Ficks, C. Sibbald, S. Ojo, R. W. Harrington, W. Clegg, L. J. Higham, *Synthesis* **2013**, *45*, 265.

136 (a) L. Maier, in *Organic Phosphorus Compounds, Vol. 1* (Eds.: G. M. Kosolapoff, L. Maier), Wiley-Interscience, New York, 1972, pp. 4–16; (b) L. J. Higham, in

Phosphorus Compounds: Advanced Tools in Catalysis and Material Sciences, Catalysis by Metal Complexes, Vol. 37 (Eds.: M. Peruzzini, L. Gonsalvi), Springer, Germany, **2011**, pp. 1–19.

137 (a) M. Brynda, *Coord. Chem. Rev.* **2005**, *249*, 2013; (b) K. V. Katti, N. Pillarsetty, K. Raghuraman, *Top. Curr. Chem.* **2003**, *229*, 121.

138 (a) M. Yoshifuji, K. Shibayama, N. Inamoto, T. Matsushita, K. Nishimoto, *J. Am. Chem. Soc.* **1983**, *105*, 2495; (b) M. Yoshifuji, K. Shibayama, K. Toyota, N. Inamoto, *Tetrahedron Lett.* **1983**, *24*, 4227.

139 (a) W. Henderson, S. R. Alley, *J. Organomet. Chem.* **2002**, *656*, 120; (b) N. Pillarsetty, K. Raghuraman, C. L. Barnes, K. V. Katti, *J. Am. Chem. Soc.* **2005**, *127*, 331.

140 R. M. Hiney, L. J. Higham, H. Müller-Bunz, D. G. Gilheany, *Angew. Chem. Int. Ed.* **2006**, *45*, 7248.

141 B. Stewart, A. Harriman, L. J. Higham, *Organometallics* **2011**, *30*, 5338.

142 Note the presence of peroxides *will* oxidise the phosphines and thus the presence of these should be avoided (aged ether solvents, sunlight etc).

143 (*R*)-MOP currently retails at £116.00 for 100 mg at www.sigmaaldrich.com (07/07/2012).

144 T. Hayashi, *Acc. Chem. Res*. **2000**, 33, 354.

145 (a) A. Ficks, I. Martinez-Botella, B. Stewart, R. W. Harrington, W. Clegg, L. J. Higham, *Chem. Commun.* **2011**, *47*, 8274; (b) A. Ficks, R. M. Hiney, R. W. Harrington, D. G. Gilheany, L. J. Higham, *Dalton Trans.* **2012**, *41*, 3515.

146 H. Sasaki, R. Irie, T. Katsuki, *Synlett* **1993**, 300.

147 L. J. Higham, E. F. Clarke, H. Müller-Bunz, D. G. Gilheany, *J. Organomet. Chem.* **2005**, *690*, 211.

148 For comprehensive reviews see: (a) F. M. J. Tappe, V. T. Trepohl, M. Oestreich, *Synthesis* **2010**, 3037; (b) I. P. Beletskaya, M. A. Kazankova, *Russ. J. Org. Chem.* **2002**, *38*, 1391; (c) S. Van der Jeught, C. V. Stevens, *Chem. Rev.* **2009**, *109*, 2672.

149 (a) M. Kalek, J. Stawinski, *Organometallics* **2007**, *26*, 5840; (b) M. Kalek, J Stawinski, *Organometallics* **2008**, *27*, 5876; (c) M. C. Kohler, T. V. Grimes, X. Wang, T. R. Cundari, R. A. Stockland Jr., *Organometallics* **2009**, *28*, 1193.

150 (a) L. Kurz, G. Lee, D. Morgans Jr., M. J. Waldyke, T. Ward, *Tetrahedron Lett.* **1990**, *44*, 6321; (b) K. S. Petrakis, T. L. Nagabhushan, *J. Am. Chem. Soc.* **1987**, *109*, 2831.

151 (a) C. Amatore, A. Jutand, A. Thuilliez, *Organometallics* **2001**, *20*, 3241; (b) C. Amatore, E. Carré, A. Jutand, M. A. M'Barki, *Organometallics* **1995**, *14*, 1818; (c) C. Amatore, A. Jutand, M. A. M'Barki, *Organometallics* **1992**, *11*, 3009.

152 G. Lavén, J. Stawinski, *Synlett* **2009**, 225.

153 M. Kalek, A. Ziadi, J. Stawinski, *Org. Lett.* **2008**, *10*, 4637.

154 C. Mésangeau, S. Yous, B. Pérès, D. Lesieur, T. Besson, *Tetrahedron Lett.* **2005**, *46*, 2465.

155 B. Saha, T. V. RajanBabu, *J. Org. Chem.* **2007**, *72*, 2357.

156 Y. Uozumi, A. Tanahashi, S. Y. Lee, T. Hayashi, *J. Org. Chem.* **1993**, *58*, 1945.

157 N. Hosoya, A. Hatayama, R. Irie, H. Sasaki, T. Katsuki, *Tetrahedron* **1994**, *50*, 4311.

158 Y. Uozumi, N. Suzuki, A. Ogiwara, T. Hayashi, *Tetrahedron* **1994**, *50*, 4293.

159 N. Armanino, R. Koller, A. Togni, *Organometallics* **2010**, *29*, 1771.

Chapter 3 — Easy-to-handle Chiral Phosphiranes

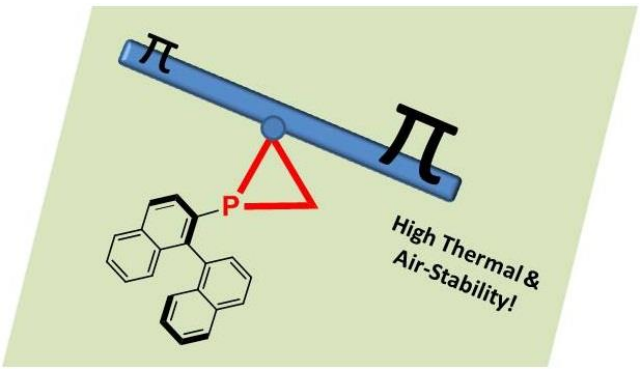

Enantiopure chiral phosphiranes possessing a binaphthyl backbone demonstrate remarkable thermal stability, are highly resistant to air-oxidation and are effective ligands in catalytic asymmetric hydrosilylations.[160]

3.1 Introduction

The phosphiranes are heterocycles which possess a three-membered phosphorus-containing ring which is highly strained as a result of the small sum of bond angles at the phosphorus atom (Σ(P) <260°).[161] The resultant greater *s*-character in the pyramidalised structure is considered to manifest itself in the form of lowered HOMO and LUMO energy levels (Figure 3.1), conferring upon the ligand a poorer σ-donor, but better π-acceptor electronic profile. Such characteristics are desirable because they offer the opportunity to synthesise ligand libraries for catalysis with a different window of activity from that offered by the more typical PR_3 reagents. For instance, if one assumes that the reductive elimination is the rate determining step in a catalytic conversion, the stabilisation of the lower oxidation state of the metal would increase the overall efficiency of the process. This can be achieved by the introduction of electronegative substituents or electron accepting ligands (*e.g.* phosphiranes) to reduce the electron density on the metal.

However, these intriguing molecules are still overlooked because of their tendency to be unstable:[161b] The synthesis of the parent phosphirane $HP(C_2H_4)$ was confirmed in 1967 by Wagner *et al.* and the product was reported to decompose completely within 24 h at 25°C.[162] About two decades later the more stable phosphirene complex **L** (Figure 3.2) was prepared by Mathey and co-workers and unambiguously characterised by X-ray crystallography.[163] Bulky substituents around the phosphorus lend stability to the ring; thus phenylphosphirane **LI** is

stable at 0 °C for a month but undergoes decomposition at higher temperatures,[164,165] **LII** is a distillable liquid[166] and **LIII** is a colourless crystalline solid.[167] The other strategy one can employ to stabilise a phosphirane (apart from metal coordination) is to incorporate the three-membered ring into an elaborate polycyclic structure. This niche approach was used to prepare the elegant BABAR-Phos (**LIV**) series of phosphiranes which resist decomposition.[168] Phosphirano-[1,2]-thiaphospholes **LV** have [*a*]-annelated bicyclic structures, isomerising in their tungsten complexes over the temperature range 25–80 °C.[169]

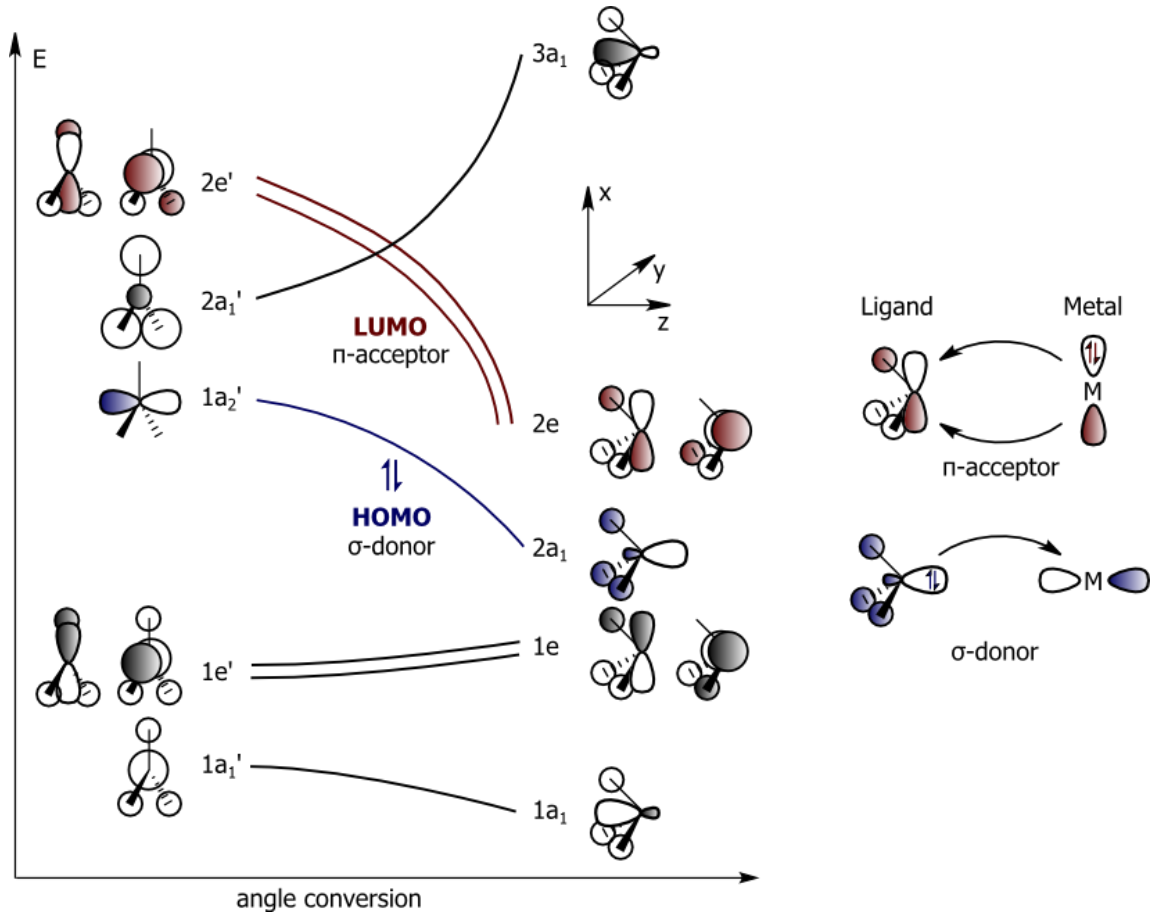

Figure 3.1 (Left) Walsh diagram showing the relative orbital energies of a molecule with trigonal planar (D_{3h}) symmetry converting into pyramidal (C_{3v}) symmetry.[168b] (Right) Ligand orbital interaction with metal centred orbitals.

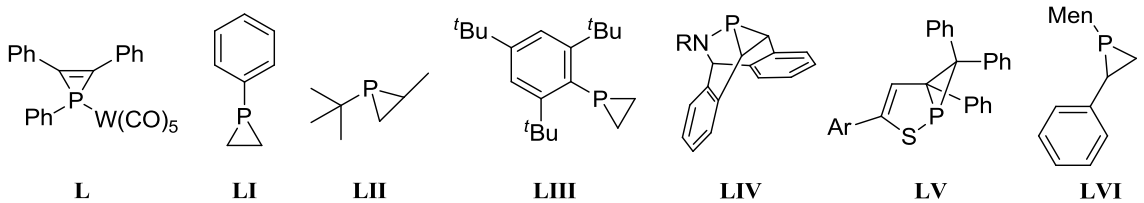

L **LI** **LII** **LIII** **LIV** **LV** **LVI**

Figure 3.2 Phosphirene **L** and phosphiranes of varying thermal stability. Phenylphosphine (**LI**) is unstable above RT; steric protection (**LII**, **LIII**) and ring fusion aid stability (**LIV**, **LV**). The chiral derivative **LVI** (Men ≡ menthyl) has been used as a ligand in asymmetric catalysis.

Phosphiranes can be synthesised from oxiranes if the substrates are coordinated to group 6 transition metal complexes (Scheme 3.1, *a*).[170] Alternatively primary phosphines provide a suitable platform as phosphirane precursors. Gaspar and co-workers reacted primary phosphines with diol ditosylates to obtain molecules with a stereocentre located on the phosphirane ring (Scheme 3.1, *b*).[171] Similarly, chiral phosphiranes **LVI** (Men ≡ menthyl) were synthesised and tested on their catalytic behaviour in the rhodium catalysed hydrogenation of alkenes.[170b] 1-(9-Anthracenyl)phosphirane has been synthesised from the parent anthracenyl primary phosphine and 1,2-dichloroethane, and its coordination chemistry on platinum has been studied in some detail.[172] Furthermore, a number of theoretical studies about the reactivity of phosphiranes were carried out investigating the possible ring-opening polymerisation of the small phosphorus heterocycle,[173] and 1-trimethylsilylphosphirane has been reported as a stable masked reagent for phosphirane.[174]

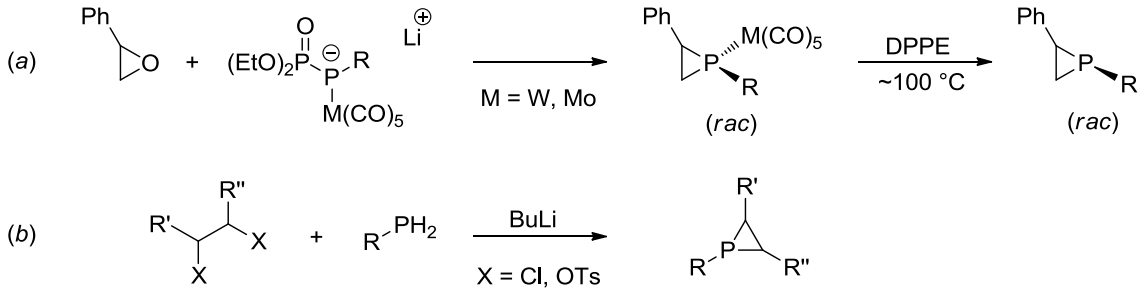

Scheme 3.1 Available synthetic strategies to obtain phosphiranes.

In Chapter 1.4.1 we discussed an electronic stabilising effect whereby increasing the amount of π-conjugation on the backbone of primary phosphines allowed us to prepare the novel air-stable, chiral derivatives **1a**,**b**.[175] These primary phosphines have since been efficiently synthesised on a multigram scale (Chapter 2) and therefore we were keen to use these precursors to prepare chiral phosphiranes to examine their properties, structure and reactivity. According to our predictions the resulting binaphthyl phosphirane compounds should exhibit similar resistance to air-oxidation as the parent primary phosphines.

3.2 Results and Discussion

Following the synthetic method of Kubiak and co-workers,[176] **1a**,**b** were treated with two equivalents of methyllithium followed by dichloroethane, and thus we were able to prepare the asymmetric compounds **14a**,**b** in high yields (Scheme 3.2).

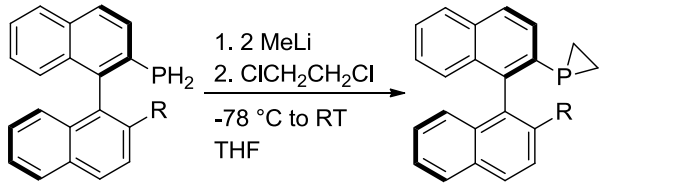

1a (*S*) R = H
1b (*R*) R = OMe

14a (*S*) R = H 87%
14b (*R*) R = OMe 89%

Scheme 3.2 Synthetic procedure for **14a** (R = H) and **14b** (R = OMe).

The $^{31}P\{^{1}H\}$ NMR spectroscopic data for the two phosphiranes are consistent with those found for other members of this class, showing a characteristic resonance at very high field (δ = –235.0 ppm for **14a**, and –235.4 ppm for **14b**). The ^{1}H NMR spectrum shows four distinctive peaks for the protons on the heterocycle, with a complicated fine-structure arising from coupling to each other and coupling to the phosphorus nucleus (Figure 3.3). Simulation of the four heterocyclic proton resonances in **14b** with gNMR[177] gave an accurate match to experimental data when homonuclear coupling constants of 10.6 Hz (for *endo*1-*endo*2 and *exo*1-*exo*2), 8.3Hz (*endo*1-*exo*2 and *endo*2-*exo*1) and 6.5 Hz (*endo*1-*exo*1 and *endo*2-*exo*2) were used.[178] The coupling of the phosphorus nucleus to the two *exo* protons is significantly larger ($^{2}J_{HP}$ = 18.7 Hz respectively) than its coupling to the *endo* protons ($^{2}J_{HP}$ = 1.7 Hz respectively). The latter smaller coupling was thereby not fully resolvable in the proton undecoupled ^{31}P NMR spectrum which has the shape of an apparent triplet. The $^{13}C\{^{1}H\}$ NMR spectra also demonstrate the diastereotopic nature of the phosphirane-ring carbon atoms; two individual resonances are observed although the phosphorus-carbon coupling constants within the phosphirane ring are equivalent ($^{1}J_{PC}$ = 40.3 Hz for **14a**; $^{1}J_{PC}$ = 40.1 Hz for **14b**).

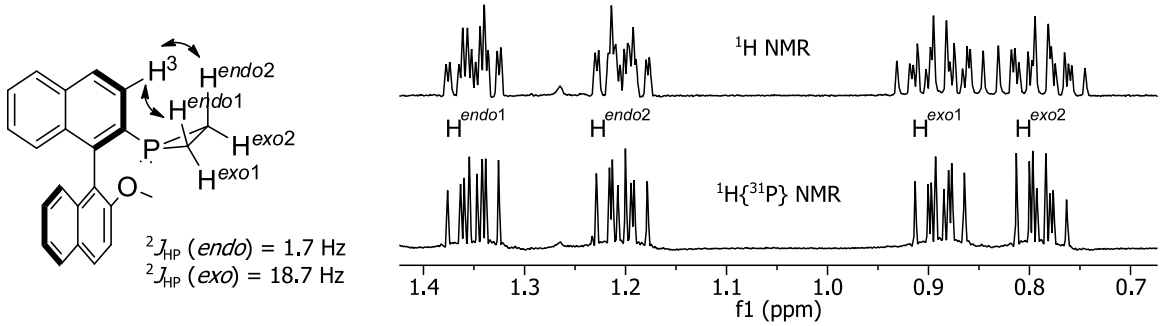

Figure 3.3 Observed nOe correlations (arrows) and aliphatic sections of the ^{1}H and $^{1}H\{^{31}P\}$ NMR spectra of **14b** (J_{HH} ≈ 10.6 Hz, 8.3Hz, 6.5 Hz). Comparable nOe contacts and coupling constants are also found for **14a**.

The two proton signals at lower field (*endo* protons) both show nOe correlations to the aromatic proton in the 3-position. Quantum chemical calculations at the B3LYP/6-31G* level

of theory indicated that the phosphirane unit might be rotating in solution. To elucidate the likelihood of different rotamers, the torsion angle of the heterocycle relative to the binaphthyl backbone was constrained, and rotated stepwise to give the relative energies of the molecules (Figure 3.4).

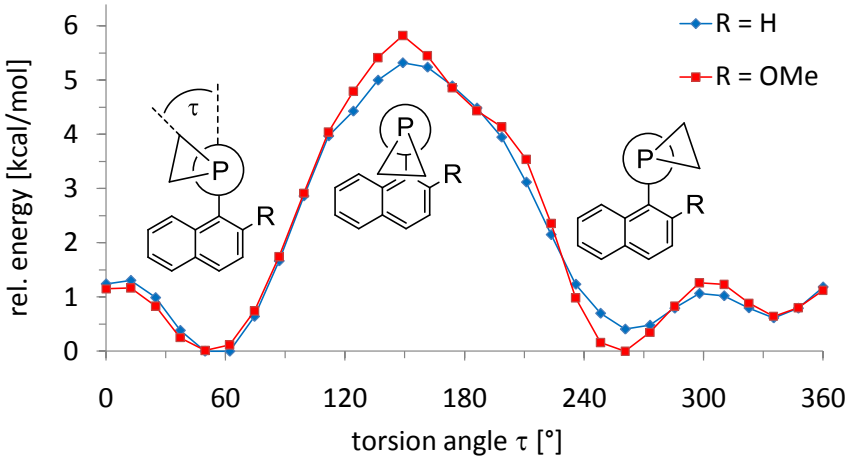

Figure 3.4 The effect of changing the phosphirane torsion angle in **14a** and **14b** on the relative optimised energy (B3LYP/6-31G*) of the molecules. The phosphirane is shown in the Newman projection.

The conformer in which the heterocycle is pointing over the aromatic backbone is disfavoured ($\tau \approx 150°$), being approximately 5.5 kcal/mol higher in energy than the lowest energy conformer. Both derivatives show the presence of three rotamers with relative energies of under 0.7 kcal/mol ($\tau \approx 50°, 260°, 340°$), which can interconvert *via* an activation barrier smaller than 1.5 kcal/mol.

Two important features of our novel phosphiranes lie in their high thermal stability and their excellent resistance to air-oxidation. Remarkably **14a**,**b** showed no sign of decomposition when heated overnight in refluxing toluene (under nitrogen). Nor was there any evidence of decomposition when the compounds were left open to the atmosphere in chloroform solution for seven days. In fact, in the solid state they can be stored in air over several months without problems. Treatment of the phosphiranes by peroxides in reagent-grade tetrahydrofuran does oxidise the compounds, but this process takes place *via* a different mechanistic process than the oxidation by air.[179] A larger study on the air-stability or otherwise of the phosphine class of compounds in general has been provided elsewhere,[180] and has also been introduced in Chapter 1.4.1.

This remarkable behaviour led us to further investigate the reactivity of the phosphiranes. It has previously been reported that 2,6-dimethoxyphenylphosphirane reacts readily with sulfur at room temperature;[181] **14a**,**b** gave no reaction under these conditions, nor were any

differences observed when the samples were heated at 50 °C in toluene for two hours. However, **14a**,**b** reacted with the strong methylating agent methyl trifluoromethanesulfonate which led to **15a**,**b** in a quantitative conversion (Scheme 3.3). The same reactivity pattern was reported for 1-phenylphosphirane,[182] while the stabilised $^{i\text{Pr}}$BABARphos phosphirane ligand was found to be unreactive in this conversion,[168a] further highlighting reactivity differences within the phosphirane class. The ^{31}P NMR spectra showed single peaks at –101.2 ppm for **15a** and –102.0 ppm for **15b**, whilst in the ^{1}H NMR spectrum, the newly introduced methyl group appears as a doublet for both compounds at 1.60 ppm for **15a** ($^{2}J_{PH}$ = 17.9 Hz) and at 1.63 ppm for **15b** ($^{2}J_{PH}$ = 18.3 Hz).

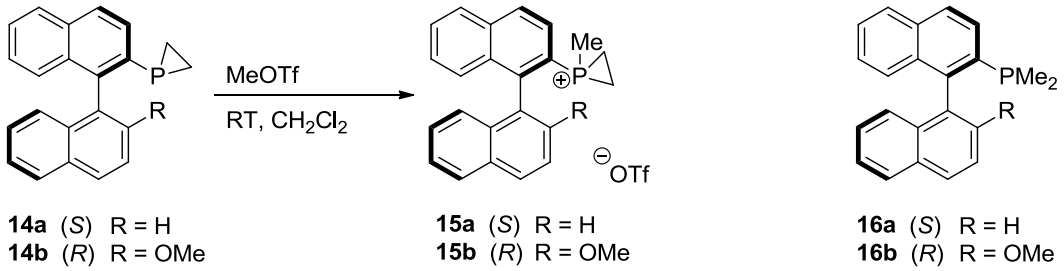

Scheme 3.3 Left: Synthetic procedure for the methylphosphiranium triflates **15a** and **15b**. Right: Unstrained MOP-dimethylphosphine derivatives **16a**,**b**.

In order to gain further insights into the geometry and electronic nature of the phosphirane group, we undertook a number of quantum chemical calculations of **14a**,**b** at the B3LYP/6-31G* level of theory. The HOMO and LUMO energy levels of **14a**,**b** were calculated and compared to their unstrained dimethylphosphine MOP derivatives **16a**,**b** (Scheme 3.3). For each pair, introduction of the phosphorus heterocycle lowers the energy of both the HOMO and LUMO (Figure 3.5). Thus we anticipate the phosphiranes **14a**,**b** to be poorer σ-donors but better π-acceptors than their corresponding unstrained dimethylphosphines **16a**,**b** (*cf.* Figure 3.1 on page 54). Furthermore, the HOMO and LUMO energies for both H-MOP derivatives **14a** and **16a** were lower than their respective OMe-MOP counterparts, indicating that one has to consider not just the presence of the strained heterocycle but the backbone as a whole when ascertaining the relative energy levels of these compounds (a more detailed comparison is given in Chapter 4.2.2). Calculated bond angles around the phosphorus show a similar degree of pyramidalisation for **14a** and **14b** (Σ(P) 250/251°).

We were keen to study the coordination chemistry of these binaphthyl-based phosphiranes with late transition metals as these are highly relevant for contemporary catalysis, but to date few examples have been reported.[169a,176] Reaction of two equivalents of **14a**,**b** with *cis*-[Pt(η^4-cod)Cl_2] resulted in the rapid, quantitative formation of *cis*-[Pt(**14a**,**b**)$_2Cl_2$] (**17a**,**b**) complexes

respectively, as shown by HRMS, NMR, and X-ray crystallographic analyses. In the ^{31}P NMR spectra of both complexes the ^{195}Pt satellites accompanying the central peak show large $^{1}J_{PPt}$ coupling constants (**17a**: –149.2 ppm, $^{1}J_{PtP}$ = 4170 Hz; **17b**: –149.3 ppm, $^{1}J_{PtP}$ = 4160 Hz). This is a much larger coupling than those observed for the more conventional *cis*-[Pt(PR$_3$)$_2$Cl$_2$] complexes ($^{1}J_{PtP}$ = 3400–3700 Hz),[183] but it relates well to that found for the only bisphosphirane platinum dichloride complex previously isolated ($^{1}J_{PtP}$ = 4133 Hz).[176b] The 10 Hz larger coupling for **17a** could be interpreted as a result of the ligand's higher π-acceptor strength in comparison to **17b**,[183,184] which would also be in agreement with our calculated LUMO energy levels for these phosphirane ligands.

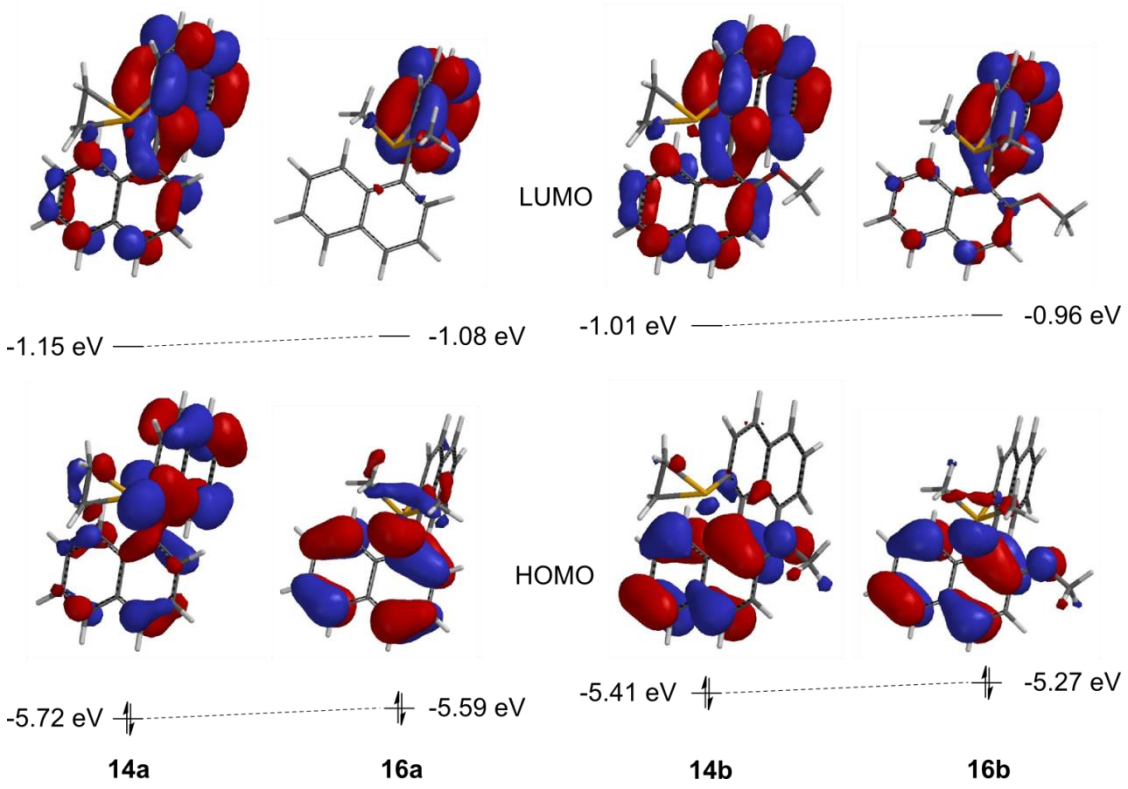

Figure 3.5 HOMO and LUMO energies of **14a**, **16a** and **14b**, **16b** calculated at the B3LYP/6-31G* level of theory.

Crystals suitable for X-ray analysis were grown from concentrated dichloromethane (**17a**, Figure 3.6) or chloroform (**17b**, Figure 3.7) solutions, and both compounds were obtained as the respective solvates. Selected bond lengths and angles are given in the figure captions. Complex **17b** has a crystallographic two-fold rotational symmetry, with the two phosphirane ligands equivalent, while **17a** has no imposed symmetry. The complexes each show a distorted square planar platinum(II) coordination geometry with typical bond lengths and angles about the platinum centre. The high degree of strain in the phosphirane ring is shown by the small C-P-C angles of 50.2(4) and 50.8(4)° for **17a** and 50.9(3)° for **17b**. The

heterocycles point over the aromatic rings of the second coordinated ligand (closest inter-ligand C···C distances: 3.5-3.7 Å). The steric demand of the methoxy group in **17b** appears responsible for the increased torsion angle of the binaphthyl backbone, the value of –94.7(8)° being significantly larger than those in **17a** of –81.8(10) and –88.5(9)°. These values compare well with the related complex *cis*-dichlorobis[1-(9-anthracene)phosphirane]platinum(II)[176b] which exhibits slightly longer Pt-P bond lengths of 2.235(4) and 2.256(4) Å. This anthracenylphosphirane derivative has a slightly higher strain within its heterocyclic ring and is more pyramidalised at phosphorus (C-P-C bond angles: 49.7(8)–49.8(8)°) than **17a** or **17b**.

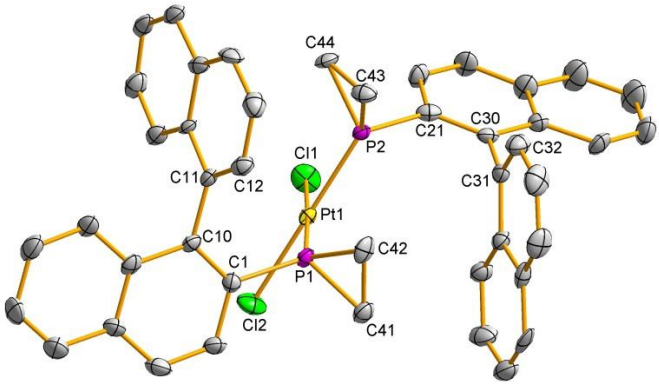

Figure 3.6 View of the molecular structure of *cis*-[Pt(**14a**)$_2$Cl$_2$] (**17a**) with 50% probability displacement ellipsoids. Hydrogen atoms have been omitted for clarity. Selected bond distances [Å] and angles [°]: Pt–Cl1 2.337(2), Pt–Cl2 2.334(2), Pt–P1 2.212(2), Pt–P2 2.209(2), P1–C41 1.802(3), P1–C42 1.816(8), P1–C1 1.814(7), C41–C42 1.534(11), P2–C43 1.786(8), P2–C44 1.782(7), P2–C21 1.794(8), C43–C44 1.529(11); Cl1-Pt-Cl2 90.52(8), Cl1-Pt-P2 87.06(10), Cl2-Pt-P1 85.40(9), P1-Pt-P2 97.02(8), Pt-P1-C1 118.8(2), C1-P1-C41 107.6(4), C1-P1-C42 111.7(4), C41-P1-C42 50.2(4), Pt-P2-C21 119.1(3), C21-P2-C43 109.8(4), C21-P2-C44 106.4(4), C43-P2-C44 50.8(4); C1-C10-C11-C12 –81.8(10), C21-C30-C31-C32 –88.5(9).

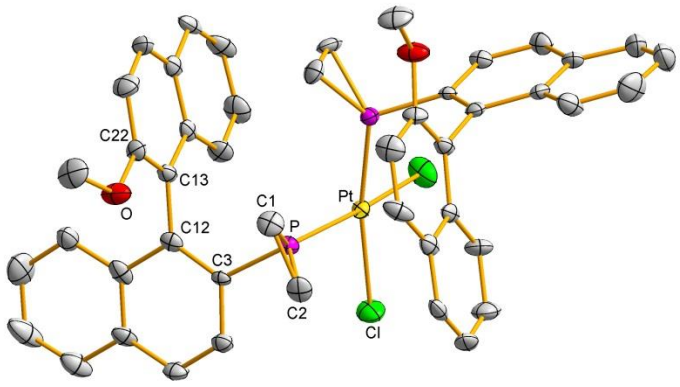

Figure 3.7 View of the molecular structure of *cis*-[Pt(**14b**)$_2$Cl$_2$] (**17b**) with 50% probability displacement ellipsoids. Hydrogen atoms have been omitted for clarity. Selected average bond distances [Å] and angles [°]:Pt–Cl 2.338(3), Pt–P 2.204(3), P–C1 1.799(7), P–C2 1.811(7), P–C3 1.802(7), C1–C2 1.550(10); Cl-Pt-Cl′ 90.42(15), Cl-Pt-P 87.28(7), P-Pt-P′ 96.92(14), Pt-P-C3 115.3(2), C1-P-C3 110.6(3), C2-P-C3 106.0(3), C1-P-C2 50.9(3); C3-C12-C13-C22 –94.7(8). A prime indicates a symmetry-equivalent atom.

Having established that the thermal and air-stability of our phosphiranes does not infringe on their ability to coordinate to a late transition metal, we sought to extend the research to include a pilot study of the potential of these ligands for asymmetric catalysis. A field of major importance in asymmetric catalysis is the hydrogenation of C=C double bonds, as it allows access to a variety of substituted chiral compounds.[185] As a first test of chiral induction, phosphirane ligands **14a**,**b** were evaluated in the asymmetric hydrogenation of (*Z*)-methyl-2-acetamido cinnamate (*cf.* Chapter 1.3.6). The reaction was examined on a 1.0 mmol scale using 7.5 bar hydrogen pressure and 2 mol% of *in situ* generated catalyst (from ligand and $[Rh(\eta^4\text{-cod})_2]PF_6$ in a 2:1 ratio) in methanol (Scheme 3.4).

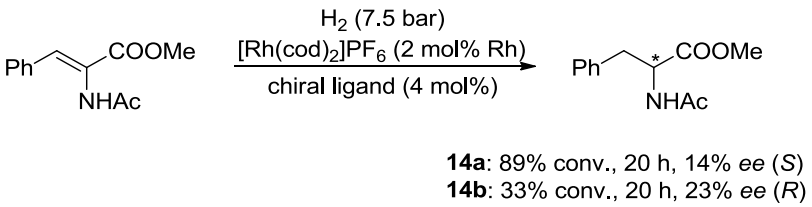

Scheme 3.4 Rhodium catalysed hydrogenation of (*Z*)-methyl-2-acetamido cinnamate.

The catalytic activity was effective in particular for **14a** with 89% conversion of the starting material after an overnight reaction (20 h). For **14b** the conversion over the same time frame was low, at 33%. Only low enantioselectivities were observed for both ligands, which was as expected for MOP-type ligands (see Chapter 1.3.6). *In situ* generated catalysts from ligands **14a**,**b** gave an enantiomeric excess of 14% (*S*) and 23% (*R*) respectively. Interestingly the excess enantiomer of the product has the opposite stereochemistry depending on the substituent in the 2'-position of the phosphorus ligand.

As an additional benchmark, the asymmetric induction capabilities of **14a**,**b** were investigated in the catalytic hydrosilylation of styrene (Scheme 3.5; see also Chapter 1.3.5).[186] The reaction is required to be both highly regio- and enantioselective; oxidation of the initially formed trichlorosilane proceeds with retention of configuration and chiral 1-phenylethanol is produced. Our catalysts were prepared *in situ* by reacting the chiral phosphirane ligand with $[PdCl(\eta^3\text{-}C_3H_5)]_2$.

The results obtained with the two ligands differ significantly. The hydrogen substituent in the 2′-position of the binaphthyl backbone seems to promote the activity as well as the enantioselectivity of the catalyst. A similar trend was found for the related parent MOP ligands when used in this transformation (*cf.* Chapter 1.3.5).[187] The full conversion obtained with **14a**, coupled with attaining an enantiomeric excess of 80% indicates the potential

applications of this neglected class of ligand. To the best of our knowledge this is the first time that phosphiranes with the chirality located solely on the ligand backbone have been utilised in asymmetric catalysis.[188] Note that these reaction conditions are not optimised and the results represent only a first glance at the catalytic potential of these ligands.

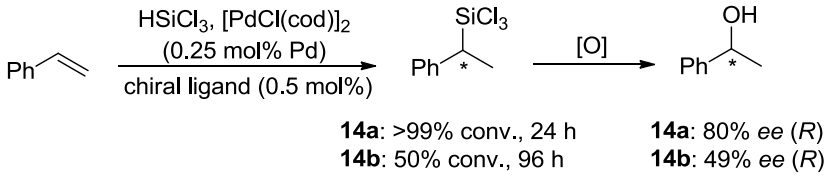

Scheme 3.5 The asymmetric hydrosilylation of styrene gives the chiral trichlorosilane, subsequent oxidation of which gives 1-phenylethanol.

3.3 Conclusion

In summary, we have synthesised the chiral phosphiranes **14a**,**b** and their corresponding platinum(II) complexes **17a**,**b**. The phosphiranes themselves possess remarkable thermal stability and resistance to air-oxidation. Importantly, these properties do not impinge on the typical reactivity associated with phosphines; they still behave as nucleophiles with methyl trifluoromethanesulfonate to generate the novel chiral phosphiranium salts **15a**,**b** and they also react in a classic fashion with transition metal precursors to yield novel platinum and palladium complexes. The latter have demonstrated here their intriguing potential as ligands in asymmetric catalytic transformations, which indicate that chiral phosphiranes in general may play a more prominent role in the future.

3.4 Experimental Section

3.4.1 General Considerations

All air- and/or water-sensitive reactions were performed under a nitrogen atmosphere using standard Schlenk line techniques. Tetrahydrofuran and dichloromethane were dried over sodium/benzophenone and calcium hydride respectively, and distilled prior to use. Toluene (Acros) was purchased in an anhydrous state. Flash chromatography was performed on silica gel from Fluorochem (silica gel, 40-63u, 60A, LC301). Procedures for the preparation of **1a**,**b** are given in the Experimental Section of Chapter 2. (*Z*)-Methyl-2-acetamido cinnamate was synthesised according to a literature procedure.[189] All other chemicals were used as purchased without further purification.

All calculations were carried out using the Spartan 10 software.[190] Full geometry optimisations of the studied compounds were performed using density functional theory with a B3LYP/6-31G* basis set. A vibrational frequency analysis was performed at the same level to characterise calculated structures as minima.

Table 3.1 Selected crystallographic data for the platinum complexes **17a** and **17b**.

	17a	**17b**
formula	$C_{44}H_{34}Cl_2P_2Pt \cdot 0.5CH_2Cl_2$	$C_{46}H_{38}Cl_2O_2P_2Pt \cdot CHCl_3$
formula wt	933.10	1070.06
cryst syst	monoclinic	monoclinic
space group	$P12_11$	P121
a, Å; α, deg	14.8961(3); 90	19.9049(8); 90
b, Å; β, deg	8.09270(10); 105.640(2)	8.3739(2); 122.417(6)
c, Å; γ, deg	16.9803(3)	14.7846(6); 90
V, Å^3	1971.18(6)	2080.30(13)
Z	2	2
ρ_{calc}, g cm^{-3}	1.572	1.708
μ, mm^{-1}	3.875	3.811
F(000)	922	1060
T_{min}/T_{max}	0.4442/0.6980	0.7502/0.9277
hkl range	–17 to 16, –9 to 9, –20 to 20	–23 to 23, –9 to 9, –16 to 17
θ range, deg	2.8 to 25.0	2.8 to 25.0
no. of measd rflns	11728	8694
no. of unique rflns (R_{int})	6013 (0.0343)	3631 (0.0521)
no. of obsd rflns, $I > 2\sigma(I)$	5534	3587
refined params/restraints	470/1	235/1
goodness of fit	1.036	1.048
Abs. structure param.	–0.003(8)	0.010(9)
R1/wR2 ($I > 2\sigma(I)$)	0.0337/0.0905	0.0337/0.0766
R1/wR2 (all data)	0.0370/0.0913	0.0341/0.0767
resid electron dens, e Å^{-3}	2.00/–0.82	1.62/–0.82

Melting points were determined in open glass capillary tubes on a Stuart SMP3 melting point apparatus. ^{1}H, ^{13}C{^{1}H}, ^{19}F, and ^{31}P{^{1}H} NMR spectra were recorded on a JEOL Lambda 500 (^{1}H 500.16 MHz) or JEOL ECS-400 (^{1}H 399.78 MHz) spectrometer at room temperature (21°C) if not otherwise stated using the indicated solvent as internal reference. The labelling scheme is given in Figure 3.8; if necessary, the assignment of signals was carried out by using two-dimensional NMR experiments (COSY, NOESY, HSQC, HMBC). The absolute assignment of the spin system on the phosphirane heterocycle (1"/2" signals) relative to the spin-system on the binaphthyl group was unavailable due to absence of conclusive nOe contacts. Infrared spectra were recorded on a Varian 800 FT-IR spectrometer. Mass

spectrometry was carried out by the EPSRC National Mass Spectrometry Service Centre, Swansea. Optical rotation values were determined on an Optical Activity Polaar 2001 device. Thin layer chromatography was performed on Merck aluminium-based plates with silica gel and fluorescent indicator (254 nm). For indicating, UV light (λ = 254 nm/366 nm) or potassium permanganate solution (1.0 g $KMnO_4$, 6.7 g K_2CO_3, 0.1 g NaOH, 100 ml H_2O) was used. Analytical high performance liquid chromatography (HPLC) was performed on a Varian Pro Star HPLC equipped with a variable wavelength detector using a Daicel Chiralcel OD or Chiralpak AD-H column, or on a Shimadzu Prominence HPLC equipped with diode-array detector using a Lux 5u Cellulose-1 column. Key crystallographic data are given in Table 3.1.

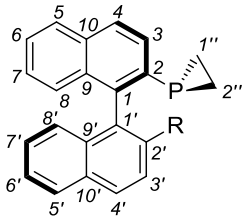

Figure 3.8 Labelling scheme used for binaphthyl phosphirane compounds.

3.4.2 (*S*)-1-([1,1'-Binaphthalen]-2-yl)phosphirane (**14a**)

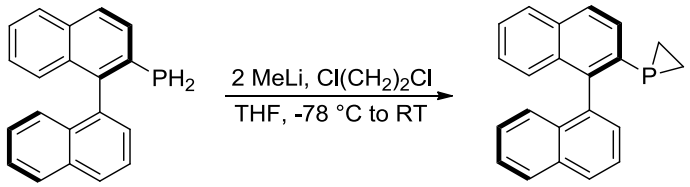

Primary phosphine **1a** (500 mg, 1.75 mmol) was dissolved in THF (10 mL) and cooled to –78 °C. Methyllithium (2.40 mL, 1.6 M in Et_2O, 3.84 mmol) was added and the orange-red solution was stirred at –78 °C for 30 minutes. 1,2-Dichloroethane (0.17 mL, 2.10 mmol) was added, the solution was allowed to warm-up to ambient temperature and stirred for 2 hours to give a yellow-brown solution. The reaction was slowly quenched with H_2O (10 mL) and extracted with Et_2O (2x 30 mL). The organic phase was dried over $MgSO_4$ to give the fairly pure crude product as a pale-yellow solid (513 mg). Purification was performed by column chromatography (cyclohexane/CH_2Cl_2, 1:1) on silica media (w = 2 cm, h = 10 cm), to yield the intended product as a white solid (473 mg, 1.51 mmol, 87%).

MP (uncorrected): 92 °C. **^{1}H NMR** (500 MHz, $CDCl_3$): δ = 8.04 (d, $^3J_{HH}$ = 8.2 Hz, 1H, *H*4'), 8.00 (d, $^3J_{HH}$ = 8.5 Hz, 1H, *H*5'), 7.88 (d, $^3J_{HH}$ = 8.2 Hz, 1H, *H*5), 7.86 (d, $^3J_{HH}$ = 8.2 Hz, 1H, *H*4), 7.69 (dd, $^3J_{HH}$ = 8.2 Hz, $^3J_{HH}$ = 6.9 Hz, 1H, *H*3'), 7.54 (d, $^3J_{HH}$ = 6.9 Hz, 1H, *H*2'), 7.51

(ddd, $^3J_{HH}$ = 8.5 Hz, $^3J_{HH}$ = 6.7 Hz, $^4J_{HH}$ = 1.2 Hz, 1H, *H*6'), 7.47-7.43 (m, 2H, *H*6+*H*3), 7.32 (ddd, $^3J_{HH}$ = 8.3 Hz, $^3J_{HH}$ = 6.7 Hz, $^4J_{HH}$ = 1.2 Hz, 1H, *H*7'), 7.25 (ddd, $^3J_{HH}$ = 8.3 Hz, $^3J_{HH}$ = 6.7 Hz, $^4J_{HH}$ = 1.2 Hz, 1H, *H*7), 7.22 (d, $^3J_{HH}$ = 8.3 Hz, 1H, *H*8'), 7.18 (d, $^3J_{HH}$ = 8.3 Hz, 1H, *H*8), 1.31 (m, 1H, *endo-H*1''), 1.22 (m, 1H, *endo-H*2''), 1.01 (m, 1H, *exo-H*1''), 0.82 (m, 1H, *exo-H*2'') ppm. **^{13}C{^{1}H} NMR** (101 MHz, $CDCl_3$): δ = 144.9 (d, $^2J_{CP}$ = 23.0 Hz, *C*1), 137.4 (d, $^3J_{CP}$ = 8.2 Hz, *C*1'), 137.4 (d, $^1J_{CP}$ = 40.1 Hz, *C*2), 133.8, 133.3, 133.1, 132.9, 129.2 (d, $^4J_{CP}$ = 1.9 Hz, *C*2'), 128.5 (*C*5'), 128.4 (*C*4'), 127.9 (*C*4+*C*5), 127.0 (d, $^2J_{CP}$ = 2.9 Hz, *C*3), 126.5 (*C*7), 126.5 (*C*8), 126.4 (*C*7'+*C*8'), 126.2 (*C*6), 126.1 (*C*6'), 125.6 (*C*3'), 10.7 (d, $^1J_{CP}$ = 40.3 Hz, *C*1''), 10.0 (d, $^1J_{CP}$ = 40.3 Hz, *C*2'') ppm. **^{31}P NMR** (202 MHz, $CDCl_3$): δ = –235.4 (pseudo-t, average $^2J_{PH}$ = 18.6 Hz) ppm. **IR** (neat): ν = 3048.3 (w), 2922.8 (w), 1587.2 (w), 1553.3 (w), 1501.5 (m), 1358.7 (m), 1255.9 (w), 1047.5 (w), 1014.9 (w), 968.6 (w), 867.5 (w), 801.6 (s), 779.5 (s), 744.9 (s), 686.5 (m), 628.3 (m), 561.2 (w) cm^{-1}. **HRMS** (ESI$^+$, acetone): Found: *m*/*z* = 313.1146. Calculated for [M + H]$^+$: *m*/*z* = 313.1146. **OR** ($CHCl_3$, *c* = 1.0 mg/ml): $[\alpha]_D^{20}$ = +74°. **TLC** (silica gel; cyclohexane/ CH_2Cl_2, 1:1): R_f = 0.7.

3.4.3 (*R*)-1-(2'-Methoxy-[1,1'-binaphthalen]-2-yl)phosphirane (**14b**)

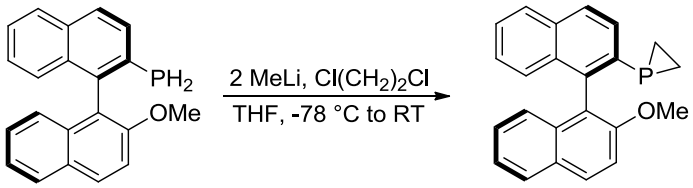

Primary phosphine **1b** (500 mg, 1.58 mmol) was dissolved in THF (10 mL) and cooled to –78 °C. Methyllithium (2.17 mL, 1.6 M in Et_2O, 3.48 mmol) was added and the orange-red solution was stirred at –78 °C for 30 minutes. 1,2-Dichloroethane (0.15 mL, 1.90 mmol) was added, the solution was allowed to warm-up to ambient temperature and stirred for 2 hours to give an orange solution. The reaction was slowly quenched with H_2O (10 mL) and extracted with Et_2O (2x 30 mL). The organic phase was dried over $MgSO_4$ to give the fairly pure crude product (530 mg). Purification was performed by column chromatography (cyclohexane/ CH_2Cl_2, 1:1) on silica media (w = 4 cm, h = 7 cm), to yield the intended product as a white solid (482 mg, 1.41 mmol, 89%).

MP (uncorrected): 142 °C. **^{1}H NMR** (400 MHz, $CDCl_3$): δ = 8.06 (d, $^3J_{HH}$ = 9.1 Hz, 1H, *H*4'), 7.91 (d, $^3J_{HH}$ = 8.2 Hz, 1H, *H*5'), 7.86 (d, $^3J_{HH}$ = 8.4 Hz, 1H, *H*4), 7.84 (d, $^3J_{HH}$ = 8.2 Hz, 1H, *H*5), 7.50 (d, $^3J_{HH}$ = 9.1 Hz, 1H, *H*3'), 7.44 (dd, $^3J_{HH}$ = 8.4 Hz, $^3J_{PH}$ = 3.6 Hz, 1H, *H*3), 7.42 (ddd, $^3J_{HH}$ = 8.2 Hz, $^3J_{HH}$ = 6.7 Hz, $^4J_{HH}$ = 1.2 Hz, 1H, *H*6), 7.34 (ddd, $^3J_{HH}$ = 8.2 Hz,

$^{3}J_{HH}$ = 6.7 Hz, $^{4}J_{HH}$ = 1.2 Hz, 1H, *H*6'), 7.27 (m, 2H, *H*7+*H*7'), 7.16 (d, $^{3}J_{HH}$ = 8.2 Hz, 1H, *H*8'), 6.96 (d, $^{3}J_{HH}$ = 8.2 Hz, 1H, *H*8), 3.85 (s, 3H, OCH_3), 1.35 (m, 1H, *endo-H*1"), 1.21 (m, 1H, *endo-H*2"), 0.89 (m, 1H, *exo-H*1"), 0.79 (m, 1H, *exo-H*2") ppm. **^{13}C{^{1}H} NMR** (101 MHz, $CDCl_3$): δ = 155.0 (*C*2'), 141.2 (d, $^{2}J_{CP}$ = 24.5 Hz, *C*1), 137.7 (d, $^{1}J_{CP}$ = 38.8 Hz, *C*2), 134.1, 133.2, 132.6, 130.0 (*C*4'), 129.0, 128.0 (*C*5'), 127.9 (*C*4), 127.6 (*C*5), 127.1 (*C*3), 126.7 (*C*7'), 126.3 (*C*7), 126.0 (*C*6), 125.8 (*C*8), 125.1 (*C*8'), 123.6 (*C*6'), 122.0 (d, $^{3}J_{CP}$ = 6.7 Hz, *C*1'), 113.4 (*C*3'), 56.6 (s, O*C*H_3), 9.1 (d, $^{1}J_{CP}$ = 40.1 Hz, *C*2"), 8.7 (d, $^{1}J_{CP}$ = 40.1 Hz, *C*1") ppm. **^{31}P NMR** (202 MHz, $CDCl_3$): δ = –235.0 (pseudo-t, average $^{2}J_{PH}$ = 18.6 Hz) ppm. **IR** (neat): ν = 3051.6 (w), 2930.0 (w), 1620.7 (w), 1592.4 (m), 1507.5 (m), 1460.7 (w), 1338.9 (w), 1249.3 (s), 1147.1 (w), 1079.1 (m), 1050.6 (m), 1019.6 (w), 907.2 (w), 866.2 (w), 806.2 (s), 774.1 (w), 745.2 (s), 686.1 (w), 627.5 (w) cm^{-1}. **HRMS** (ESI^+, acetone): Found: *m*/*z* = 343.1246. Calculated for $[M + H]^+$: *m*/*z* = 343.1252. **OR** ($CHCl_3$, *c* = 1.1 mg/ml): $[\alpha]_D^{20}$ = +60°. **TLC** (silica gel; cyclohexane/CH_2Cl_2, 1:1): R_f = 0.5.

3.4.4 (*S*)-1-([1,1'-Binaphthalen]-2-yl)-1-methylphosphiranium triflate (**15a**)

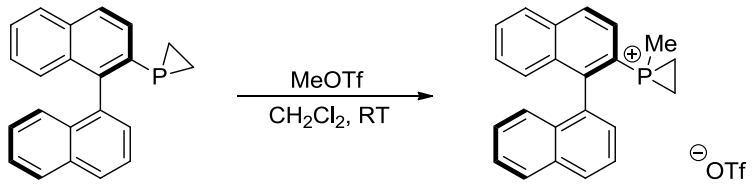

Phosphirane **14a** (31.2 mg, 0.10 mmol) was dissolved in CH_2Cl_2 (7 mL) and MeOTf (32.8 mg, 0.02 mL, 0.05 mmol) was added. The reaction mixture was stirred at room temperature for 2 hours. The volatiles were removed *in vacuo* to give the intended product as a colourless solid (quantitative conversion).

^{1}H NMR (400 MHz, $CDCl_3$): δ = 8.18 (dd, $^{4}J_{HP}$ = 4.0 Hz, $^{3}J_{HH}$ = 8.7 Hz, 1H, *H*4), 8.15 (d, $^{3}J_{HH}$ = 8.7 Hz, 1H, *H*4'), 8.06 (dd, $^{3}J_{HH}$ = 8.7 Hz, $^{3}J_{HP}$ = 13.9 Hz, 1H, *H*3), 8.03 (m, $^{3}J_{HH}$ = 8.7 Hz, 2H, *H*5+*H*5'), 7.72 (dd, $^{3}J_{HH}$ = 7.8 Hz, $^{3}J_{HH}$ = 8.7 Hz, 1H, *H*3'), 7.70 (m, 1H, *H*6), 7.57 (m, 1H, *H*6'), 7.55 (d, $^{3}J_{HH}$ = 7.8 Hz, 1H, *H*2'), 7.44 (m, 1H, *H*7), 7.37 (m, 1H, *H*7'), 7.34 (d, $^{3}J_{HH}$ = 8.7 Hz, 1H, *H*8), 7.00 (d, $^{3}J_{HH}$ = 8.7 Hz, 1H, *H*8'), 2.31 (m, 1H, *endo-H*1"), 2.06 (m, 2H, *endo-H*2"+*exo-H*1"), 1.91 (m, 1H, *exo-H*2"), 1.60 (d, $^{2}J_{HP}$ = 17.9 Hz, 3H, CH_3) ppm. **^{13}C{^{1}H} NMR** (101 MHz, $CDCl_3$): δ = 149.0 (d, $^{2}J_{CP}$ = 10.1 Hz, *C*1), 136.2, 133.6, 132.7, 132.5, 132.3, 131.1 (*C*4'), 130.6, 130.4, 129.2, 129.1, 128.7, 128.6, 128.0, 127.9, 127.8, 127.4 (*C*6'), 127.3 (*C*8), 125.6 (*C*3'), 125.1 (*C*8'), 9.5 (d, $^{1}J_{CP}$ = 5.5 Hz, *C*1"), 7.8 (d, $^{1}J_{CP}$ = 5.5 Hz, *C*2"), 6.3 (d, $^{1}J_{CP}$ = 50.5 Hz, *C*H_3) ppm. **^{19}F NMR** (376 MHz, $CDCl_3$): δ = –78.3 ppm. **^{31}P{^{1}H} NMR** (202 MHz, $CDCl_3$): δ = –101.2 ppm. **IR** (neat): ν = 3062.0 (w),

3001.7 (w), 2921.4 (w), 1586.9 (w), 1558.1 (w), 1506.0 (w), 1370.0 (w), 1275.8 (m), 1222.7 (s), 1162.8 (s), 1027.2 (m), 969.8 (m), 911.1 (m), 806.8 (m), 782.9 (m), 728.9 (s), 688.8 (w), 634.3 (s) cm^{-1}. **HRMS** (ESI^+, MeCN): Found: $m/z = 327.1301$. Calculated for $[M - CF_3SO_3]^+$: $m/z = 327.1297$.

3.4.5 (*R*)-1-(2'-Methoxy-[1,1'-binaphthalen]-2-yl)-1-methylphosphiranium triflate (**15b**)

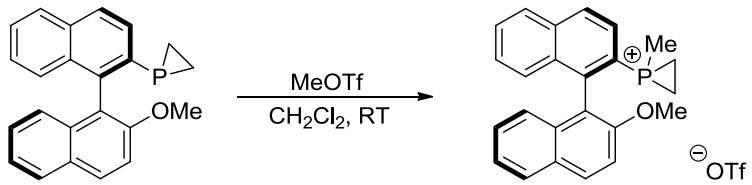

Phosphirane **14b** (34.2 mg, 0.10 mmol) was dissolved in CH_2Cl_2 (7 mL) and MeOTf (32.8 mg, 0.02 mL, 0.05 mmol) was added. The reaction mixture was stirred at room temperature for 2 hours. The volatiles were removed *in vacuo* to give the intended product as a colourless solid (quantitative conversion).

^{1}H NMR (400 MHz, $CDCl_3$): $\delta = 8.18$ (d, $^3J_{HH} = 9.2$ Hz, 1H, *H*4'), 8.15 (dd, $^3J_{HH} = 8.2$ Hz, $^4J_{HP} = 4.1$ Hz, 1H, *H*4), 8.05 (dd, $^3J_{HH} = 8.2$ Hz, $^3J_{HP} = 13.7$ Hz, 1H, *H*3), 8.02 (d, $^3J_{HH} = 8.2$ Hz, 1H, *H*5), 7.94 (d, $^3J_{HH} = 8.7$ Hz, 1H, *H*5'), 7.68 (m, 1H, *H*6), 7.52 (d, $^3J_{HH} = 9.2$ Hz, 1H, *H*3'), 7.41 (m, 1H, *H*7), 7.39 (m, 1H, *H*6'), 7.29 (d, $^3J_{HH} = 8.2$ Hz, 1H, *H*8), 7.28 (m, 1H, *H*7'), 6.71 (d, $^3J_{HH} = 8.7$ Hz, 1H, *H*8'), 3.81 (s, 3H, OCH_3), 2.28 (m, 1H, *endo*-*H*1''), 2.16 (m, 1H, *endo*-*H*2''), 2.03 (m, 1H, *exo*-*H*1''), 1.84 (m, 1H, *exo*-*H*2''), 1.63 (d, $^2J_{HP} = 18.3$ Hz, 3H, CH_3) ppm. **^{13}C{^{1}H} NMR** (101 MHz, $CDCl_3$): $\delta = 154.9$ (*C*2'), 146.1 (d, $^2J_{CP} = 10.5$ Hz, *C*1), 136.5, 133.2 (*C*4'), 132.5 (d, $^1J_{CP} = 15.3$ Hz, *C*2), 128.0 (d, $^3J_{CP} = 14.4$ Hz, *C*4), 130.2 (*C*6), 128.9, 128.8 (*C*5+*C*5'), 128.5 (*C*7+*C*7'), 128.1 (d, $^2J_{CP} = 13.4$ Hz, *C*3), 126.7 (*C*8), 124.9 (*C*6'), 123.6 (*C*8'), 117.7 (d, $^3J_{CP} = 6.7$ Hz, *C*1'), 113.0 (*C*3'), 56.3 (s, OCH_3), 7.6 (d, $^1J_{CP} = 4.8$ Hz, *C*1''), 7.0 (d, $^1J_{CP} = 4.8$ Hz, *C*2''), 5.3 (d, $^1J_{CP} = 50.8$ Hz, CH_3) ppm. **^{19}F NMR** (376 MHz, $CDCl_3$): $\delta = -78.3$ ppm. **^{31}P{^{1}H} NMR** (202 MHz, $CDCl_3$): $\delta = -102.0$ ppm. **IR** (neat): $\nu = 3087.4$ (w), 3002.5 (w), 2922.1 (w), 2846.5 (w), 1621.5 (w), 1592.9 (w), 1508.8 (w), 1464.6 (w), 1251.3 (s), 1223.0 (s), 1026.9 (s), 969.2 (w), 906.2 (m), 872.7 (w), 813.1 (m), 775.3 (w), 728.8 (s), 688.2 (w), 634.9 (s), 572.6 (w) cm^{-1}. **HRMS** (ESI^+, MeCN): Found: $m/z = 357.1408$. Calculated for $[M - CF_3SO_3]^+$: $m/z = 357.1403$.

3.4.6 *cis*-Bis((*S*)-1-([1,1'-binaphthalen]-2-yl)phosphirane)dichloroplatin (**17a**)

14a (31.2 mg, 0.10 mmol) and *cis*-[Pt(η^4-cod)Cl_2] (19.2 mg, 0.05 mmol) were dissolved in CH_2Cl_2 (7 mL) and stirred at room temperature for 2 hours. The volatiles were removed *in vacuo* to give the intended product as a colourless solid (quantitative conversion). Crystals suitable for X-ray analysis were obtained by slow diffusion of Et_2O into a solution of $CHCl_3$ at ambient temperature.

^{1}H NMR (500 MHz, CD_2Cl_2): δ = 8.07 (d, $^3J_{HH}$ = 8.2 Hz, 2H, *H*4'), 8.00 (d, $^3J_{HH}$ = 8.2 Hz, 2H, *H*5), 7.89 (d, $^3J_{HH}$ = 8.2 Hz, 2H, *H*5'), 7.81 (d, $^3J_{HH}$ = 8.6 Hz, 2H, *H*4), 7.69 (m, 2H, *H*3), 7.66 (dd, $^3J_{HH}$ = 8.2 Hz, $^3J_{HH}$ = 7.0 Hz, 2H, *H*3'), 7.54 (ddd, $^3J_{HH}$ = 8.2 Hz, $^3J_{HH}$ = 6.8 Hz, $^4J_{HH}$ = 1.2 Hz, 2H, *H*6), 7.50 (ddd, $^3J_{HH}$ = 8.2 Hz, $^3J_{HH}$ = 6.8 Hz, $^4J_{HH}$ = 1.2 Hz, 2H, *H*6'), 7.32 (d, $^3J_{HH}$ = 7.0 Hz, 2H, *H*2'), 7.30 (ddd, $^3J_{HH}$ = 8.6 Hz, $^3J_{HH}$ = 6.8 Hz, $^4J_{HH}$ = 1.2 Hz, 2H, *H*7), 7.21 (ddd, $^3J_{HH}$ = 8.6 Hz, $^3J_{HH}$ = 6.8 Hz, $^4J_{HH}$ = 1.2 Hz, 2H, *H*7'), 7.00 (d, $^3J_{HH}$ = 8.6 Hz, 2H, *H*8), 6.80 (d, $^3J_{HH}$ = 8.6 Hz, 2H, *H*8'), 1.21 (m, 2H, *endo-H*), 0.99 (m, 2H, *endo-H*), 0.50 (m, 2H, *exo-H*), 0.23 (m, 2H, *exo-H*) ppm. **^{13}C{^{1}H} NMR** (125 MHz, CD_2Cl_2): δ = 144.2 (*C*1), 135.4, 134.3, 133.8, 132.8, 132.5, 131.3, 129.4, 129.1, 129.1, 128.5, 128.0, 127.6, 127.2, 127.0, 126.8, 126.5, 126.4, 125.5, 10.5 (*C*1"), 8.3 (*C*2") ppm. **^{31}P{^{1}H} NMR** (202 MHz, CD_2Cl_2): δ = –149.2 (s with ^{195}Pt satellites, $^1J_{PPt}$ = 4170 Hz) ppm. **IR** (neat): ν = 3060.3 (w), 2991.3 (w), 1586.0 (w), 1557.2 (w), 1501.3 (w), 1376.1 (w), 1313.6 (w), 1258.0 (w), 1013.5 (w), 946.7 (w), 913.6 (s), 782.3 (s), 739.2 (s), 707.4 (m), 672.6 (m) cm^{-1}. **HRMS** (ESI$^+$, MeCN): Found: *m*/*z* = 913.1054. Calculated for [M + Na]$^+$: *m*/*z* = 913.1048.

3.4.7 *cis*-Bis((*R*)-1-(2'-methoxy-[1,1'-binaphthalen]-2-yl)phosphirane)dichloroplatin (**17b**)

14b (34.2 mg, 0.10 mmol) and *cis*-[Pt(η^4-cod)Cl_2] (19.2 mg, 0.05 mmol) were dissolved in CH_2Cl_2 (7 mL) and stirred at room temperature for 2 hours. The volatiles were removed *in vacuo* to give the intended product as a colourless solid (quantitative conversion). Crystals suitable for X-ray analysis were obtained by slow evaporation of $CHCl_3$ at ambient temperature.

^{1}H NMR (500 MHz, $CDCl_3$): δ = 8.10 (d, $^3J_{HH}$ = 9.2 Hz, 2H, *H*4'), 7.91 (d, $^3J_{HH}$ = 8.3 Hz, 2H, *H*5'), 7.84 (d, $^3J_{HH}$ = 8.3 Hz, 2H, *H*5), 7.78 (m, 4H, *H*3+*H*4), 7.45 (m, 4H, *H*3'+*H*6), 7.39 (m, 2H, *H*6'), 7.30 (m, 2H, *H*7'), 7.18 (m, 2H, *H*7), 6.90 (d, $^3J_{HH}$ = 8.3 Hz, 2H, *H*8'), 6.84 (d, $^3J_{HH}$ = 8.4 Hz, 2H, *H*8), 3.74 (s, 6H, OCH_3), 1.22 (m, 2H, *endo-H*1"), 1.02 (m, 2H, *endo-H*2"), 0.32 (m, 2H, *exo-H*2"), –0.07 (m, 2H, *exo-H*1") ppm. **^{13}C{^{1}H} NMR** (125 MHz,

$CDCl_3$): δ = 154.7 (*C*2'), 141.1 (*C*1), 134.5, 133.7, 132.5, 131.7 (*C*3), 131.3 (*C*4'), 129.2, 128.1 (*C*5+*C*5'), 128.0 (*C*7'), 127.9 (*C*6), 127.5 (*C*4), 127.0 (*C*7), 126.3 (*C*8), 125.7 (*C*8'), 124.6 (*C*6'), 120.0 (*C*1'), 113.1 (*C*3'), 56.4 (s, OCH_3), 7.8 (*C*2''), 7.2 (*C*1'') ppm. **$^{31}P\{^1H\}$ NMR** (202 MHz, $CDCl_3$): δ = –149.3 (s with ^{195}Pt satellites, $^1J_{PtP}$ = 4160 Hz) ppm. **IR** (neat): ν = 3058.4 (w), 2986.2 (w), 2937.1 (w), 1620.7 (w), 1592.3 (w), 1506.8 (m), 1473.8 (w), 1429.7 (w), 1383.6 (w), 1333.1 (w), 1271.5 (s), 1252.8 (s), 1215.8 (w), 1181.3 (w), 1149.6 (w), 1117.8 (w), 1076.9 (m), 1046.5 (m), 1018.8 (w), 951.0 (w), 916.3 (s), 871.4 (w), 808.1 (s), 774.6 (w), 738.3 (s), 708.9 (m), 680.7 (m), 628.8 (m) cm^{-1}. **HRMS** (ESI^+, MeCN): Found: *m*/*z* = 971.1237. Calculated for $[M + Na]^+$: *m*/*z* = 971.1242.

3.4.8 Rhodium Catalysed Hydrogenation of (*Z*)-Methyl-2-acetamido cinnamate

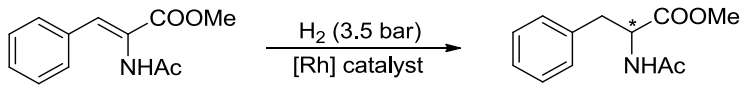

$[Rh(\eta^4\text{-cod})_2]PF_6$ (9.3 mg, 0.02 mmol) and ligand (0.04 mmol) were dissolved in MeOH (20 mL) and left to stir for 2 hours. (*Z*)-Methyl-2-acetamido cinnamate (219 mg, 1.00 mmol) was added and the autoclave was filled with 3.5 bar H_2 gas. The reaction mixture was stirred for 20 hours, the solvent was evaporated and the conversion was determined by ^{1}H NMR spectroscopy. The crude product was purified by column chromatography (EtOAc/hexane, 3:1) on silica media (h = 10 cm, d = 2 cm). The enantiomeric excess was measured by chiral HPLC (Column Daicel Chiralpak AD-H; flow rate: 0.8 mL/min; hexane/2-propanol, 90:10; retention times: (*R*) t_1 = 9.8 min, (*S*) t_2 = 13.1 min).[191]

3.4.9 Palladium Catalysed Hydrosilylation of Styrene

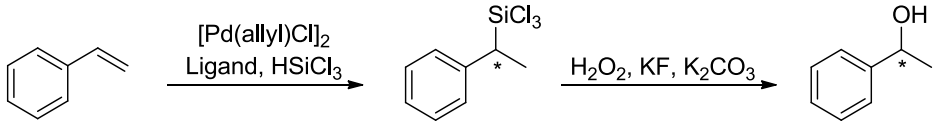

$[Pd(\eta^3\text{-}C_3H_5)Cl]_2$ (4.6 mg, 0.0125 mmol), ligand (0.050 mmol) and styrene (1.2 mL, 1.0 g, 10.0 mmol) were stirred at room temperature for 20 minutes. Trichlorosilane (1.2 mL, 1.6 g, 12.0 mmol) was added and the reaction was stirred at room temperature for the appropriate time (24-96 h). The conversion of the reaction was followed by ^{1}H NMR spectroscopy, and the product was purified by Kugelrohr distillation (reduced pressure, 150 °C).

Trichloro(1-phenylethyl)silane (400 mg, 1.67 mmol) was dissolved in MeOH (30 mL) and THF (30 mL). K_2CO_3 (1.40 g, 10.1 mmol), KF (600 mg, 10.3 mmol) and 35% H_2O_2 (1.8mL)

were added subsequently and left to stir overnight. The solution was filtered, H_2O was added and it was extracted with Et_2O (3x). The combined organic washings were dried over $MgSO_4$. The crude product was purified by column chromatography (hexane/EtOAc, 4:1, $R_f = 0.20$) on silica media to obtain the desired product. The enantiomeric excess was measured by chiral HPLC on the Varian (Column Daicel Chiralcel OD; flow rate: 0.5 mL/min; hexane/2-propanol, 95:5; retention times: (*R*) t_1 = 19.3 min, (*S*) t_2 = 22.3 min), or Shimadzu device (Lux 5u Cellulose-1 Column, 250 x 4.6 mm; flow rate: 1.0 mL/min; hexane/2-propanol, 95:5; retention times: (*R*) t_1 = 8.9 min, (*S*) t_2 = 10.2 min).[192]

3.5 References

160 The content of this chapter has partly been published in the following peer-reviewed scientific journal: A. Ficks, I. Martinez-Botella, B. Stewart, R. W. Harrington, W. Clegg, L. J. Higham, *Chem. Commun.* **2011**, *47*, 8274.

161 Reviews: (a) F. Mathey, *Chem. Rev.* **1990**, *90*, 997; (b) L. D. Quin, in *A Guide to Organophosphorus Chemistry* (Ed.: L. D. Quin), John Wiley Sons, New York, 2000, pp. 234–241; (c) F. Mathey, M. Regitz, in *Phosphorus-Carbon Heterocyclic Chemistry: The Rise of a New Domain* (Ed.: F. Mathey), Elsevier Science, Amsterdam, 2001, pp. 17–55.

162 R. I. Wagner, L. D. Freeman, H. Goldwhite, D. G. Rowsell, *J. Am. Chem. Soc.* **1967**, *89*, 1102.

163 A. Marinetti, F. Mathey, J. Fischer, A. Mitschler, *J. Am. Chem. Soc.* **1982**, *104*, 4484.

164 (a) Y. B. Kang, M. Pabel, A. C. Willis, S. B. Wild, *J. Chem. Soc., Chem. Commun.* **1994**, 475; (b) D. C. R. Hockless, Y. B. Kang, M. A. McDonald, M. Pabel, A. C. Willis, S. B. Wild, *Organometallics* **1996**, *15*, 1301.

165 X. Li, K. D. Robinson, P. P. Gaspar, *J. Org. Chem.* **1996**, *61*, 7702.

166 M. Baudler, J. Germeshausen, *Chem. Ber.* **1985**, *118*, 4285.

167 T. Oshikawa, M. Yamashita, *Synthesis* **1985**, 290.

168 (a) J. Liedtke, S. Loss, G. Alcaraz, V. Gramlich, H. Grützmacher, *Angew. Chem. Int. Ed.* **1999**, *38*, 1623; (b) J. Liedtke, S. Loss, C. Widauer, H. Grützmacher, *Tetrahedron* **2000**, *56*, 143; (c) J. Liedtke, H. Rüegger, S. Loss, H. Grützmacher, *Angew. Chem. Int. Ed.* **2000**, *39*, 2478; (d) C. Laporte, G. Frison, H. Grützmacher, A. C. Hillier, W. Sommer, S. P. Nolan, *Organometallics* **2003**, *22*, 2202.

169 (a) S. Maurer, C. Burkhart, G. Maas, *Eur. J. Org. Chem*. **2010**, 2504; (b) T. Jikyo, G. Maas, *Chem. Commun*. **2003**, 2794.

170 (a) A. Marinetti, L. Ricard, F. Mathey, *Synthesis* **1992**, 157; (b) A. Marinetti, F. Mathey, L. Ricard, *Organometallics* **1993**, *12*, 1207.

171 X. Li, K. D. Robinson, P. P. Gaspar, *J. Org. Chem.* **1996**, *61*, 7702.

172 (a) F. Yang, P. E. Fanwick, C. P. Kubiak, *Organometallics* **1999**, *18*, 4222; (b) F. Yang, P. E. Fanwick, C. P. Kubiak, *Inorg. Chem.* **2002**, *41*, 4805.

173 (a) D. B. Chesnut, L. D. Quin, S. B. Wild, *Heteroatom Chem.* **1997**, *8*, 451; (b) T. I. Sølling, M. A. McDonald, S. B. Wild, L. Radom, *J. Am. Chem. Soc.* **1998**, *120*, 7063; (c) T. I. Sølling, S. B. Wild, L. Radom, *J. Organomet. Chem.* **1999**, *580*, 320; (d) J. L. Hodgson, M. L. Coote, *Macromolecules* **2005**, *38*, 8902; (e) M. L. Coote, J. L. Hodgson, E. H. Krenske, S. B. Wild, *Heteroatom Chem.* **2007**, *18*, 118; (f) M. L. Coote, E. H. Krenske, I. Maulana, J. Steinbach, S. B. Wild *Heteroatom Chem.* **2008**, *19*, 178.

174 H. A. Tallis, P. D. Newman, P. G. Edwards, L. Ooi, A. Stasch, *Dalton Trans.* **2008**, 47.

175 R. M. Hiney, L. J. Higham, H. Müller-Bunz, D. G. Gilheany, *Angew. Chem. Int. Ed.* **2006**, *45*, 7248.

176 (a) N. Mézailles, P. E. Fanwick, C. P. Kubiak, *Organometallics* **1997**, *16*, 1526; (b) F. Yang, P. E. Fanwick, C. P. Kubiak, *Organometallics* **1999**, *18*, 4222.

177 P. H. M. Budzelaar, *gNMR 5.0.6.0*; IvorySoft, 2006.

178 For the NMR data of phosphirane see: (a) H. Goldwhite, D. Rowsell, L. E. Vertal, M. T. Bowers, M. A. Cooper, S. L. Manatt, *Org. Magn. Reson.* **1983**, *21*, 494; (b) E. Díez, J. Casanueva, J. San Fabián, A. L. Esteban, M. P. Galache, V. Barone, J. E. Peralta, R. H. Contreras, *Mol. Phys.* **2005**, *103*, 1307.

179 H. R. Hudson, in *The Chemistry of Organophosphorus Compounds, Vol. 1* (Ed.: F. R. Hartley), Wiley, New York, 1990, pp. 438–439 and references therein.

180 B. Stewart, A. Harriman, L. J. Higham, *Organometallics* **2011**, *30*, 5338.

181 P. P. Gaspar, H. Qian, A. M. Beatty, D. André d'Avignon, J. L.-F. Kao, J. C. Watt, N. P. Rath, *Tetrahedron* **2000**, *56*, 105.

182 (a) D. C. R. Hockless, M. A. McDonald, M. Pabel, S. B. Wild, *J. Chem. Soc., Chem. Commun.* **1995**, 257; (b) D. C. R. Hockless, M. A. McDonald, M. Pabel, S. B. Wild, *J. Organomet. Chem.* **1997**, *529*, 189.

183 P. S. Pregosin, *Annu. Rep. NMR Spectrosc.* **1986**, *17*, 285.

184 C. M. Haar, S. P. Nolan, W. J. Marshal, K. G. Moloy, A. Prock, W. P. Giering, *Organometallics* **1999**, *18*, 474.

185 (a) G. Erre, S. Enthaler, K. Junge, S. Gladiali, M. Beller, *Coord. Chem. Rev.* **2008**, *252*, 471; (b) Y.-M. Li, F.-Y. Kwong, W.-Y. Yu, A. S. C. Chan, *Coord. Chem. Rev.* **2007**, *251*, 2119; (c) W. Zhang, Y. Chi, X. Zhang, *Acc. Chem. Res.* **2007**, *40*, 1278; (d) W. Tang, X. Zhang, *Chem. Rev.* **2003**, *103*, 3029.

186 (a) Y. Uozumi, T. Hayashi, *J. Am. Chem. Soc.* **1991**, *113*, 9887; (b) K. Kitayama, Y. Uozumi, T. Hayashi, *J. Chem. Soc., Chem Commun.* **1995**, 1533; (c) J. W. Han, T. Hayashi, *Tetrahedron: Asymmetry* **2010**, *21*, 2193 and references therein.

187 K. Kitayama, Y. Uozumi, T. Hayashi, *J. Chem. Soc., Chem Commun.* **1995**, 1533; at 0°C (*S*)-H-MOP gave full conversion in 12 h with 93% ee, (*R*)-MOP required 24 h for full conversion (14% ee).

188 Phosphiranes with chirality on the heterocycles have been used in asymmetric hydrogenations: See A. Marinetti, F. Mathey, L. Ricard, *Organometallics* **1993**, *12*, 1207 and references therein.

189 M. Kitamura, M. Tsukamoto, Y. Bessho, M. Yoshimura, U. Kobs, M. Widhalm, R. Noyori, *J. Am. Chem. Soc*. **2002**, *124*, 6649.

190 *Spartan 10*; Wavefunction Inc., Irvine, CA, 2011.

191 Absolute stereochemical assignment according to literature data: A. Zanotti-Gerosa, C. Malan, D. Herzberg, *Org. Lett.* **2001**, *3*, 3687.

192 Absolute stereochemical assignment according to literature data: M. Ito, Y. Endo, N. Tejima, T. Ikariya, *Organometallics* **2010**, *29*, 2397.

Chapter 4 — MOP-Type Ligands: Structural and Electronic Design

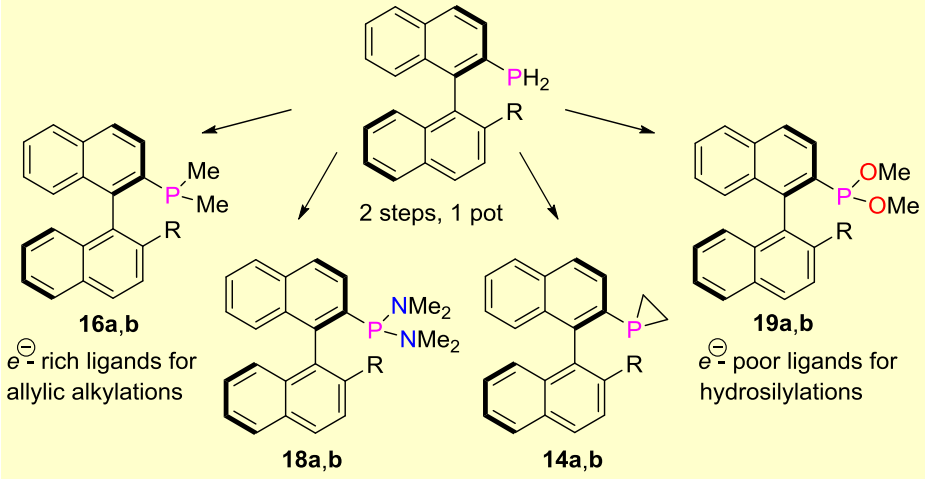

The synthesis of chiral MOP-type ligands **14a**,**b**, **16a**,**b**, **18a**,**b** and **19a**,**b** is reported, accessible in one-pot reactions from stable primary phosphines **1a**,**b**. They offer a range of structural and electronic parameters that have been determined by a number of experimental and theoretical studies. Dimethylphosphines **16a**,**b** and bis(dimethylamino)phosphines **18a**,**b** are good electron donors, while phosphiranes **14a**,**b** and phosphonites **19a**,**b** are electron poor compounds. The ligands were coordinated to platinum(II) and the weak *trans*-influence of the highly strained phosphiranes **14a**,**b** was revealed both in solution and the solid-state. Methallylpalladium(II) complexes were analysed for their allyl rotation showing subtle differences in exchange rates that were mainly attributed to steric effects. Aryl side-on coordination of the MOP-backbone to palladium(II) was observed for complexes with a non-coordinating counter-ion and structurally analysed in the case of ligand **18b**. The asymmetric induction and catalytic activity of **14a**,**b**, **16a**,**b**, **18a**,**b** and **19a**,**b** were tested in the hydrosilylation of styrene as well as the allylic alkylation of (*rac*)-(*E*)-1,3-diphenylallyl acetate. Major differences in reactivities were related back to the electronic parameters of the ligands.[193]

4.1 Introduction

In transition-metal catalysed reactions the design of the chiral ligand is crucial for transferring the stereochemical information effectively onto the substrate.[194] A fine balance of steric and electronic properties is often necessary to achieve high asymmetric induction while ensuring good catalytic activity. It is therefore desirable to obtain characteristic values for each ligand that describe their steric and electronic effects. The separation of electronic and steric

parameters of phosphorus(III) ligands was most profoundly influenced by Tolman,[195] and his study was used as the foundation for numerous experimental and theoretical investigations thereafter (*cf.* Chapter 1.2).[196]

An important class of chiral mono-phosphines are Hayashi's MOP ligands (Figure 4.1, top left).[197,198] They are based on a binaphthyl-derived skeleton exhibiting axial chirality and are capable of catalysing a number of asymmetric transformations.[199] Different substituents have been employed in the 2'-position (most commonly H or OMe) which causes major changes in their catalytic behaviour.[197] The aryl-substituents on the phosphorus atom (phenyl in the case of MOP) have been modified in order to tweak the electronics of the donor and thereby increase the catalytic performance.[200] Note that changes in the electronic properties of a ligand can have equally dramatic consequences on catalyst activity and selectivity as modifications on the ligand's spatial demand.[196c] More drastically changed P-substituents (*e.g.* alkyl- instead of aryl-substituents) have seldom been introduced,[201] presumably as a result of synthetic restraints or the need to access these derivatives *via* their respective primary phosphines (*cf.* Chapter 1.3.2).

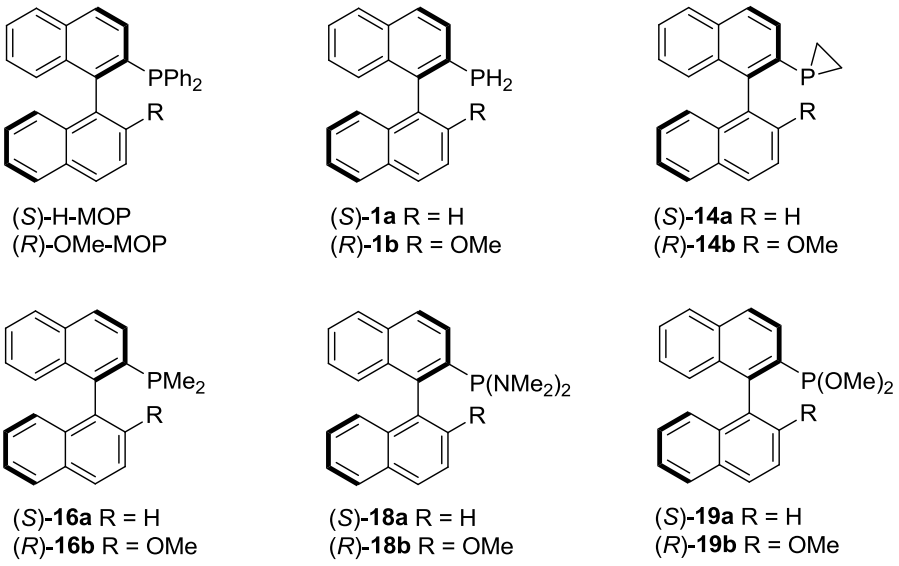

Figure 4.1 MOP-type ligands with different functionalities that are investigated in this chapter.

Primary phosphines are readily functionalised by substitution of their P-bound hydrogen atoms; however their reputation as highly air-sensitive, toxic and pyrophoric compounds has somewhat inhibited their use in synthetic methodology.[202] More recently there has been an increased amount of interest in the synthesis of air-stable primary phosphines, whose stability is owed to steric encumbrance,[203] or is as of yet unexplained (*cf.* Chapter 1.4.1).[204] In this context we reported the first air-stable, chiral primary phosphines **1a**,**b** (Figure 4.1; see

Chapter 2 for their multigram synthesis) which were subsequently utilised to access chiral MOP-type ligands (*e.g.* see Chapter 3 for the synthesis of MOP-phosphiranes).[205] The full exploration of **1a**,**b** as ligand precursors is still ongoing. Here, we investigate four fundamentally different P-donor ligands that were accessible from these primary phosphines in one-pot reaction procedures, for the purpose of examining their different structural and electronic parameters.

In our recent communication about phosphirane ligands **14a**,**b** (Figure 4.1) we described some of the unusual donor properties caused by the strain of the small P-heterocycle (Chapter 3.2).[206] We therefore sought experimental data to compare these intriguing molecules to their corresponding unstrained dimethylphosphines **16a**,**b**. Furthermore we wanted to include bis(dimethylamino)phosphines **18a**,**b** and dimethyl phosphonites **19a**,**b** into the comparative study in order to evaluate the unique properties of a range of P-ligand motifs. The structural and electronic impact of the ligands is shown in a number of experimental and theoretical analyses, most notably their palladium(II) and platinum(II) complexes, which have been studied in detail in solution and in the solid-state. Their application as catalysts was tested in the palladium catalysed asymmetric hydrosilylation of styrene as well as in the asymmetric allylic alkylation of (*rac*)-(*E*)-1,3-diphenylallyl acetate.

4.2 Results and Discussion

4.2.1 Ligand Synthesis and Stability

We recently reported chiral phosphirane ligands **14a**,**b** bearing a highly strained three-membered heterocycle around the phosphorus. These were prepared from their parent primary phosphines **1a**,**b** in a straightforward one-step reaction procedure (Chapter 3.2).[206] Phosphiranes **14a**,**b** possess unusual electronic properties caused by the strain of the small P-heterocycle resulting in greater s-character of the donor orbital. This ultimately leads to weaker σ-donor but better π-acceptor properties compared to their unstrained counterparts.[207]

Dimethylphosphine ligands **16a**,**b** were first reported by Stryker and co-workers,[201f] and further studied by Shi *et al.* mainly for their application as catalysts in the aza-Baylis-Hillman reaction.[208] We became interested in evaluating these ligands for their steric and electronic properties, especially in view with comparing them to other MOP-type entities like our phosphiranes **14a**,**b**; synthetic pathways to obtain enantiomerically pure **16a**,**b** are known from earlier reports.[208] However, we were also keen to develop an efficient one-pot synthesis starting from our primary phosphines **1a**,**b** which have been proven as valuable synthons in

the preparation of phosphorus ligands and have since been prepared efficiently by us on a large scale (Chapter 2).[209] In a synthetic methodology we had originally adapted from Weferling,[210] and which we have used to prepare chiral MOP-phosphonite ligands (Chapter 5.2.1),[211] we reacted **1a**,**b** with phosphorus pentachloride in toluene to generate the respective dichlorophosphine derivatives *in situ* (Scheme 4.1, path i). After removing the volatiles *in vacuo* further reactions were performed in the same reaction vessel. Initially we attempted the methylation by adding a solution of methyllithium in diethyl ether, but this resulted in the formation of compound mixtures. Instead we found that a much cleaner reaction was achieved when methylmagnesium chloride in tetrahydrofuran was used as the methylating agent (Scheme 4.1, path ii). Analysis of the crude reaction mixtures by ^{31}P NMR showed complete conversions to the desired products (–54.0 ppm for **16a**,**b**). Thus, dimethylphosphines **16a**,**b** were obtained in good yields (76%/73% respectively) after purification on silica media. The ligands were found to be air-stable after leaving the compounds open to the atmosphere for 7 days neat or in chloroform solution. This observation differs from an earlier report in which the authors stated that the compounds were air-sensitive but without giving further details on their reactivity.[201f] The remarkable air-stability of primary phosphines **1a**,**b** and MOP-type ligands in general has been attributed to the high conjugation in their extended aromatic backbone.[205] We have developed a DFT model in order to predict the air-stability of phosphines (Chapter 1.4.1),[212] and calculations according to this model suggested that **16a**,**b** would be air-stable (SOMO energies of the radical cations are –9.05 eV (**16a**) and –8.83 eV (**16b**) respectively).

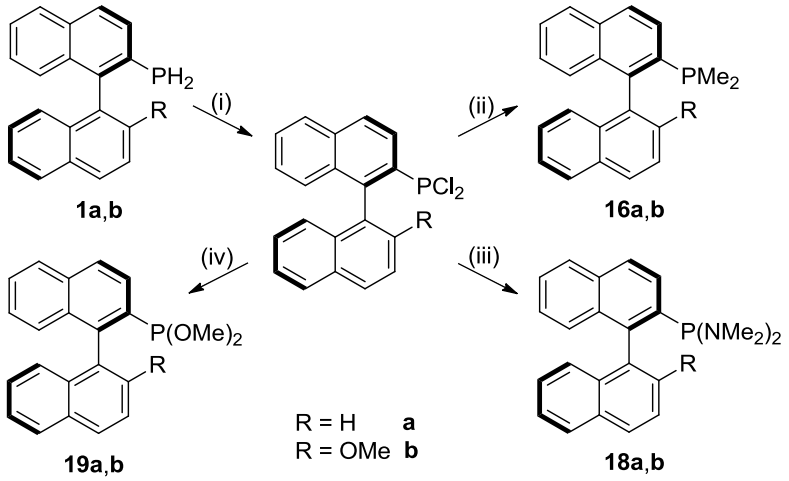

Scheme 4.1 Reaction conditions: (i) PCl_5, toluene; (ii) MeMgCl, THF, –78 °C to rt; (iii) Me_2NH, NEt_3, THF; (iv) MeOH, NEt_3, CH_2Cl_2.

As another target we aimed to synthesise bis(dimethylamino)phosphines **18a**,**b**. In contrast to phosphiranes **14a**,**b** and dimethylphosphines **16a**,**b** these compounds possess two P–N bonds resulting in a different electronic environment around the phosphorus. The amino-substituents are known to lend σ-donor strength to the phosphorus arising from electron donation of the nitrogen lone pairs.[213] Aminophosphines are commonly prepared by condensation reaction of phosphorus(III) halides with secondary amines.[214] Hence, we were able to use our primary phosphines **1a**,**b** as starting materials to generate the respective dichlorophosphines *in situ* (*vide supra*); these were then treated with dimethylamine under basic conditions to give **18a**,**b** (Scheme 4.1, path iii) in very good yields (93%/89% respectively after purification). The ^{31}P NMR spectra show typical resonances for bis-heteroatom substituted 3-coordinated phosphines at 99.9 ppm (**18a**) or 101.0 ppm (**18b**). Ligands **18a**,**b** are moderately sensitive towards moisture and protic solvents such as alcohols. Purification on alumina media with reagent grate solvents was possible and no evidence for oxidation of these ligands in air was found. Generally **18a**,**b** can be handled in air without the need of an inert atmosphere but they should be stored in closed vials to avoid hydrolysis after prolonged exposure to moisture.

Finally, we decided to assess the effect of incorporating electronegative methoxy groups at the phosphorus. Dimethyl phosphonite ligands **19a**,**b** were synthesised in an analogous reaction from primary phosphines **1a**,**b** *via* methanolysis of the respective dichlorophosphine intermediates in the presence of triethylamine (Scheme 4.1, path iv). The crude products were found to decompose on silica and alumina media. The generated amine-salt impurity was therefore separated by filtration of a toluene solution of the ligand through a pad of celite. Ligands **19a**,**b** were usually obtained with >90% purity by ^{31}P NMR and no further purification was performed (P(V)-species were observed as the only remaining side-products). Their resonances in the ^{31}P NMR spectra are located at lower field relative to the other ligands in this study (157.5 ppm for **19a**, 155.8 ppm for **19b**), caused by the electronegative methoxy substituents on the phosphorus atom. Ligands **19a**,**b** are prone to hydrolysis and should therefore be stored and handled under the exclusion of moisture.

4.2.2 Assessment of Structural and Electronic Properties

The $^{1}J_{PSe}$ coupling in $R_3P(Se)$ compounds can be used to determine the effective electronegativity of the substituents on the phosphorus atom.[215] The $^{1}J_{PSe}$ magnitude is inversely correlated to the σ-donor strength of a R_3P ligand; electron-donating substituents cause the coupling constant to decrease (*cf.* Chapter 1.2.2). Sterically demanding substituents can indirectly influence the coupling if the intervalence angles on the phosphorus are

widened; the s-character of the phosphorus lone pair is thereby reduced resulting in increased Lewis basicity.[216] Furthermore, it should be noted that the presence of π-back donation may also affect the σ-donation due to synergic effects in phosphorus-metal bonds.[217]

The respective $ArP(Se)R_2$ derivatives were prepared by the reaction of ligands **16a**,**b**, **18a**,**b** or **19a**,**b** with potassium selenocyanide.[218] In our initial study on phosphiranes we had found that the reactivity of **14a**,**b** towards sulfur is somewhat reduced (Chapter 3.2);[206] similarly we were unable to observe any selenide product formation for these substrates even at elevated temperatures and prolonged reaction times. For the $ArP(Se)R_2$ derivatives of dimethylphosphines **16a**,**b** we found lower coupling constant values than for the respective derivatives of ligands **18a**,**b** and **19a**,**b**, corresponding to a better σ-donor character (Table 4.1). This is in accord with the expectation as the electronegative nitrogen atoms in **18a**,**b**, and to a greater extent the oxygen atoms in **19a**,**b** reduce the σ-donor strength of the phosphorus atom.

Table 4.1 Structural and electronic parameters of phosphorus ligands **14a**,**b**, **16a**,**b**, **18a**,**b** and **19a**,**b**.

ligand	$^1J_{PSe}$ [a]	ν (CO_{Rh}) [b]	E_{HOMO} [c]	PA [d]	S4 [e]
14a	—	1983	–5.72	228.0	130.1°
14b	—	1985	–5.41	231.4	127.5°
16a	685	1965	–5.59	247.3	53.5°
16b	683	1963	–5.27	250.4	53.7°
18a	770	1972	–5.11	254.6	52.1°
18b	765	1969	–5.01	257.5	51.7°
19a	858	1999	–5.69	243.0	59.5°
19b	860	1996	–5.38	246.9	62.2°

[a] Coupling from the $ArP(Se)R_2$ derivative in Hertz. [b] CO-stretch of *trans*-$[RhCl(CO)(ArPR_2)_2]$ in CH_2Cl_2 in cm^{-1}. [c] Calculated HOMO energies in eV of the optimised structures of the free ligand. [d] Calculated proton affinity in kcal/mol of the free ligand. [e] Calculated from the optimised structure of the free ligand.

In order to include phosphiranes **14a**,**b** into the comparative study of electronic properties, we synthesised *trans*-$[Rh(L_P)_2(CO)Cl]$ complexes (L_P = phosphorus ligand) and measured the symmetric carbonyl stretching frequencies in the IR spectrum. A higher wavenumber of the vibration indicates a lower net-donor property of L_P as the reduced electron density on the metal allows for less back-bonding into the antibonding π*-orbitals of the carbonyl groups.[219] The IR spectra were recorded from dichloromethane solutions, since packing effects in the solid state may have significant influence on the observed values.[220] We found that dimethylphosphines **16a**,**b** are the strongest net-donors (1965, 1963 cm^{-1}), subsequently followed by bis(dimethylamino)phosphines **18a**,**b** (1972, 1969 cm^{-1}), phosphiranes **14a**,**b** (1983, 1985 cm^{-1}) and dimethyl phosphonites **19a**,**b** (1999, 1996 cm^{-1}). The weak donating

properties of phosphiranes **14a**,**b** compared to their dimethylphosphine counterparts **16a**,**b** have been attributed to their pyramidalised structures which result in increased s-character of the donor orbitals. In fact, phosphiranes **14a**,**b** show weaker net-donation than PPh_3 (1979 cm^{-1}), but are better donors than the strongly pyramidalised $^{i\text{Pr}}$BABAR-Phos[221] phosphirane ligand (1991 cm^{-1}, for the structural formula of this ligand see **LIV** in Figure 3.2 on page 54).[219a]

Electronic descriptors measuring the donor abilities of our ligands were calculated in their HOMO orbital energy levels and proton affinity (PA) in a series of DFT calculations (calculated at the B3LYP/6-31G* level of theory). The energy of the HOMO usually corresponds to the lone pair of the phosphorus and PA is a measure of its σ-basicity; the two values have been found to correlate fairly well for a range of phosphorus ligands.[222]

The HOMO energies were calculated from the optimised structures of the free ligands and the values are listed in Table 4.1. We observed higher E_{HOMO} values in the direct comparison of H-MOP derivatives (**a**) to their respective OMe-MOP counterparts (**b**). The spatial representations of the HOMO orbitals (Figure 4.2) reveal their distribution on the binaphthyl backbone, and also on the methoxy-group in the case of the OMe-MOP derivatives (**b**). Arguably, the differences in energies are amplified by the subtle distinction in HOMO-delocalisation on the ligand's backbone.

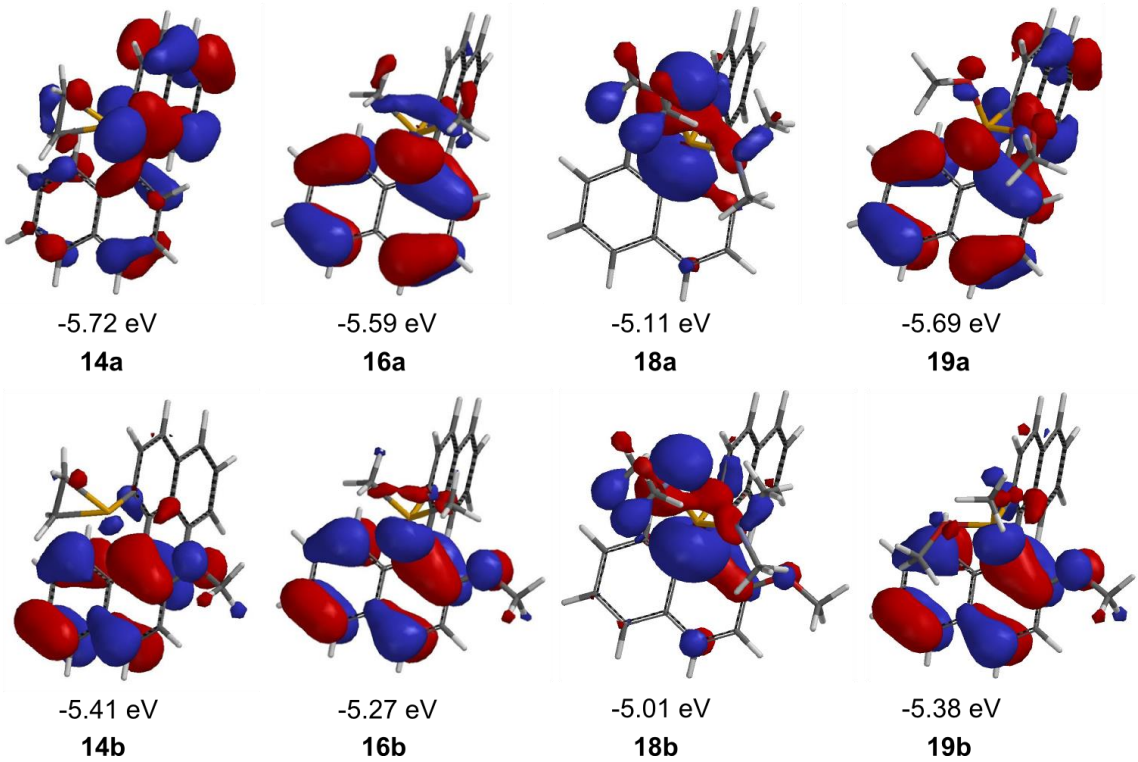

Figure 4.2 HOMO energies of **14a**,**b**, **16a**,**b**, **18a**,**b** and **19a**,**b** calculated at the B3LYP/6-31G* level of theory.

The PA values show much less deviation in this respect (Table 4.1). Their energy was calculated from the differential in molecular energies of the DFT-optimised structure of the free ligand, and the optimised structure of the protonated ligand (protonated on the phosphorus atom).[222,223] Their magnitude increases (indicating an increasing σ-basicity) in the order **14a**,**b** < **19a**,**b** < **16a**,**b** < **18a**,**b**. In comparison to the relative trend of the net-donor properties from the experimentally determined values ν (CO_{Rh}) it is noticeable that the calculated σ-basicity is somewhat overestimated for the heteroatom-substituted derivatives **18a**,**b** and **19a**,**b**.

To get an insight into the structural properties of the phosphorus ligands we calculated the symmetric deformation coordinate from their DFT-optimised geometries. The S4' parameter was first introduced by Orpen *et al.*[224] as an alternative to Tolman's cone angle (θ_T).[195,225] Its use is appropriate for MOP-type compounds in particular since the θ_T parameter would be dominated by the bulky binaphthyl substituent (*cf.* Chapter 1.2.1).[226] As a measure of flattening or pyramidality around the phosphorus, S4' is defined as the sum of Z-P-R angles (α_i) minus the sum of R-P-R angles (β_i), with Z describing the coordinated atom of the PR_3 ligand (Figure 4.3). A modified descriptor coined S4 is given for free ligands, where Z is a perpendicular vector to the plane containing the three substituents of the phosphorus atom.[227] The S4 values were determined from the optimised minimal energy geometries of each ligand at the B3LYP/6-31G* level (Table 4.1). The pyramidalisation of phosphiranes **14a**,**b** is recognised in unusually large values for S4 (130.1° and 127.5° respectively). In contrast, **16a**,**b** and **18a**,**b** exhibit much smaller S4 values of similar magnitudes (51.7°-53.7°) which is unsurprising in the absence of ring-strain. The values are slightly increased for **19a**,**b** (59.5° and 62.2° respectively) in comparison to the other unstrained derivatives, presumably as a result of the lesser steric hindrance around the phosphorus.

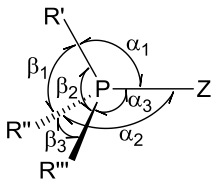

Figure 4.3 Definition of angles for the calculation of S4' = ($\alpha_1 + \alpha_2 + \alpha_3$) – ($\beta_1 + \beta_2 + \beta_3$).

4.2.3 Platinum(II) Coordination Properties

To investigate the structural and electronic behaviour of our ligands upon coordination to a metal centre, we prepared a series of square planar platinum(II) complexes. Solution studies

of these compounds can give an insight into the nature of the phosphorus-platinum bonds by the $^{1}J_{PtP}$ coupling constants in their NMR spectra.[228] It has been suggested that the main contributor to the one-bond coupling is the Fermi interaction of the two involved nuclei.[229] This means that the s-component of the P–Pt bond has a direct influence on the coupling constant, yielding larger values with increasing s-orbital overlap. However, p- and d-components will indirectly affect the s-orbital interaction by changing the bond order, and previous reports have shown that there is a good correlation between the $^{1}J_{PtP}$ magnitude and the Pt–P bond length.[230] This relationship allows for the determination of *cis* and *trans* influences in platinum complexes, *i.e.* the ability of a ligand to weaken the bond to a substituent in the *cis*/*trans* position,[231] which then helps in rationalising the σ-donor and π-acceptor properties of the ligands.[232,233] Complementary studies, using X-ray crystallographic analysis to determine bond lengths, are available to supplement the results in solution.

Platinum(II) dichloride complexes with the general formula $[Pt(L_P)_2Cl_2]$ (L_P = phosphorus ligand) were synthesised from the reaction of *cis*-$[Pt(\eta^4\text{-cod})Cl_2]$ with the appropriate ligand (Figure 4.4). In solution as well as in the solid state the selective formation of *cis*-**17a**,**b** (the crystal structures of *cis*-**17a**,**b** are depicted in Figure 3.6 and Figure 3.7 on page 60)[206] or *cis*-**20b** (Figure 4.5) was observed when phosphiranes **14a**,**b** or dimethylphosphine **16b** were used as ligands respectively. Under the same reaction conditions the more sterically demanding ligand **18b** gave the *trans*-**21b** (Figure 4.6) isomer with complete selectivity. The ^{31}P NMR spectra show the expected singlet resonance with a doublet of ^{195}Pt satellites. For the *cis* complexes the $^{1}J_{PtP}$ coupling is larger in *cis*-**17a**,**b** (4170, 4160 Hz) compared to *cis*-**20b** (3647 Hz) as a result of the higher s-character of the phosphirane donor orbitals. The $^{1}J_{PtP}$ coupling in *trans*-**21b** (2955 Hz) is significantly smaller compared to the *cis* complexes because of the stronger reciprocal *trans* influence of the phosphine ligands compared to the *trans* influence of a chloride ligand.

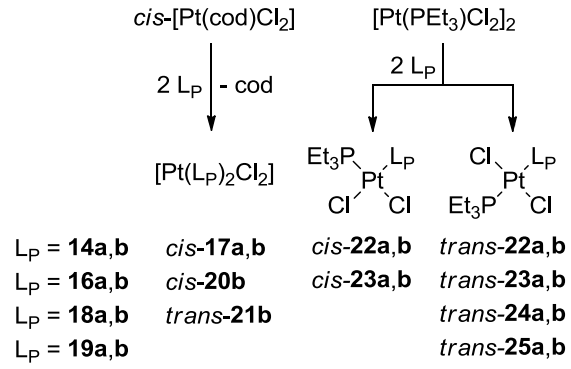

Figure 4.4 Numbering of the platinum complexes used in this study (L_P = phosphorus ligand).

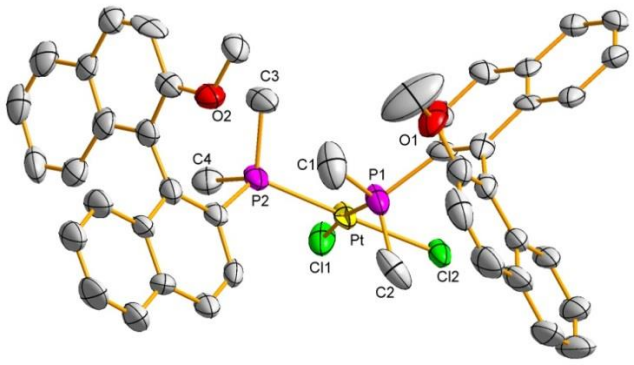

Figure 4.5 View of the molecular structure of *cis*-[Pt(**16b**)$_2$Cl$_2$] (*cis*-**20b**) with 50% probability displacement ellipsoids. Hydrogen atoms and co-crystallised solvent (2 Et$_2$O) have been omitted for clarity.

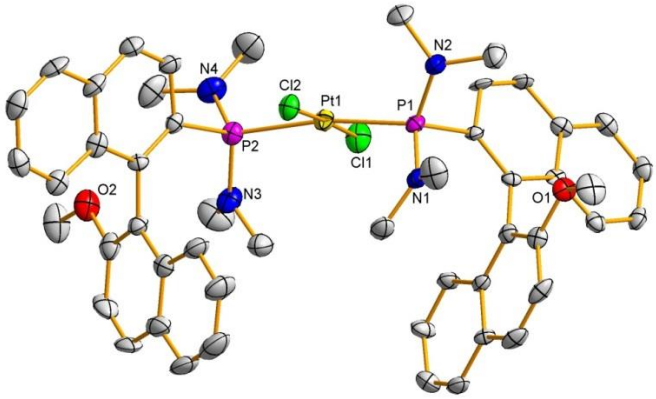

Figure 4.6 View of the molecular structure of *trans*-[Pt(**18b**)$_2$Cl$_2$] (*trans*-**21b**) with 50% probability displacement ellipsoids. Hydrogen atoms have been omitted for clarity.

Table 4.2 Selected bond distances [Å], angles [°] and S4' data from X-ray crystallographic analysis.

	cis-**17a**	*cis*-**17b**[a]	*cis*-**20b**	*trans*-**21b**	*trans*-**22b**	*trans*-**24a**
Pt–P1	2.212(2)	2.204(3)	2.244(3)	2.308(2)	2.3044(18)	2.3395(11)
Pt–P2	2.209(2)	—	2.243(2)	2.314(2)	2.2835(19)	2.3050(11)
Pt–Cl1	2.337(2)	2.338(3)	2.338(2)	2.292(2)	2.2925(18)	2.3001(10)
Pt–Cl2	2.334(2)	—	2.368(2)	2.3023(19)	2.3072(17)	2.3080(10)
P1-Pt-P2	97.02(8)	96.92(14)	96.60(10)	170.37(7)	178.76(9)	176.90(4)
P1-Pt-Cl1	175.90(10)	169.05(10)	172.58(9)	92.00(7)	90.86(6)	92.34(4)
P1-Pt-Cl2	85.40(9)	—	83.37(9)	87.97(7)	88.32(6)	91.41(4)
P2-Pt-Cl1	87.06(10)	87.28(7)	90.77(9)	87.79(7)	88.06(7)	85.15(4)
P2-Pt-Cl2	177.57(10)	—	178.37(9)	91.82(7)	92.78(7)	91.25(4)
Cl1-Pt-Cl2	90.52(8)	90.42(15)	89.29(8)	177.54(8)	178.24(11)	173.86(5)
S4' (P1)	98.0	105.4	24.3	21.3	105.7	18.7
S4' (P2)	103.6	—	17.9	21.5	24.0	27.8

[a] Two-fold rotational symmetry

Selected bond lengths and angles for the solid-state structures of *cis*-**17a**,**b**, *cis*-**20b** and *trans*-**21b** are given in Table 4.2. Phosphirane complexes *cis*-**17a**,**b** form shorter Pt–P bonds (2.209(2)-2.212(2) Å) than the dimethylphosphine ligated derivative *cis*-**20b** (2.243(2) Å, 2.244(3) Å), which is attributed to the better π-acceptor character of the phosphirane ligands in *cis*-**17a**,**b**. The Pt–P bond lengths are further elongated in *trans*-**21b** (2.308(2) Å, 2.314(2) Å) due to the relatively strong reciprocal *trans* influence in agreement with the NMR data as described above. The strong pyramidalisation of the phosphirane group is retained when bound to platinum and manifests itself in large S4' values for *cis*-**17a**,**b** (98.0-103.6°; calculated from X-ray structural data). For *cis*-**20b** and *trans*-**21b** the adjacent groups around the phosphorus are only slightly tilted out of the plane, resulting in much smaller S4' values (17.9-21.5°).

For further evaluation of the relative *cis* and *trans* influences of the different phosphorus donor ligands we synthesised unsymmetrical platinum(II) complexes with the general formula $[Pt(L_P)(PEt_3)Cl_2]$ (selected NMR spectral data is given in Table 4.3).[223] The reaction of two equivalents of phosphorus ligand (L_P) with $[Pt(PEt_3)Cl_2]_2$ proceeded quantitatively in all instances (Figure 4.4). In the case of phosphiranes **14a**,**b** and dimethylphosphines **16a**,**b** we observed the formation of both *cis* and *trans* isomers of the corresponding platinum complexes **22a**,**b** and **23a**,**b** in solution. The two respective isomers can be easily distinguished by their $^2J_{PP}$ coupling constants in the ^{31}P NMR spectrum. The *trans* complexes show a characteristic large $^2J_{PP}$ coupling (482-575 Hz) while the equivalent coupling for the corresponding *cis* isomers is much smaller (18-23 Hz, Figure 4.7). The obtained ratios of *cis* and *trans* isomers varied from 2:1 to 1:2 depending on the ligand. EXSY experiments showed no exchange of the two isomers on the NMR timescale and additional NMR spectra that were recorded after leaving the complexes in solution for 24 hours yielded unchanged *cis*/*trans* ratios. In previous reports about related platinum(II) complexes the *trans* products have been found to convert to their *cis* isomers over time.[234] When bis(dimethylamino)phosphines **18a**,**b** or dimethyl phosphonites **19a**,**b** were used as ligands the *trans*-**24a**,**b** or *trans*-**25a**,**b** isomers were formed exclusively, displaying the typical $^2J_{PP}$ coupling constants of 543-604 Hz in the ^{31}P NMR (Figure 4.7).

The fast relaxation time of the platinum nucleus in the studied compounds allowed for a rapid collection of their ^{195}Pt NMR spectra (Figure 4.7). The resonances for the *trans* complexes are observed downfield (–3839 to –3941 ppm) to their corresponding *cis* isomers (–4362 to –4501 ppm, Table 4.3). The phosphirane ligands in **22a**,**b** generally induce stronger shielding to the platinum nucleus. The effect is most pronounced for *cis*-**22a**,**b** which show an upfield

shift of about 100 ppm compared to *cis*-**23a**,**b**. The strongest de-shielding effects were found for complexes of the heteroatom substituted ligands in *trans*-**24a**,**b** and *trans*-**25a**,**b** (–3839 to –3881 ppm).

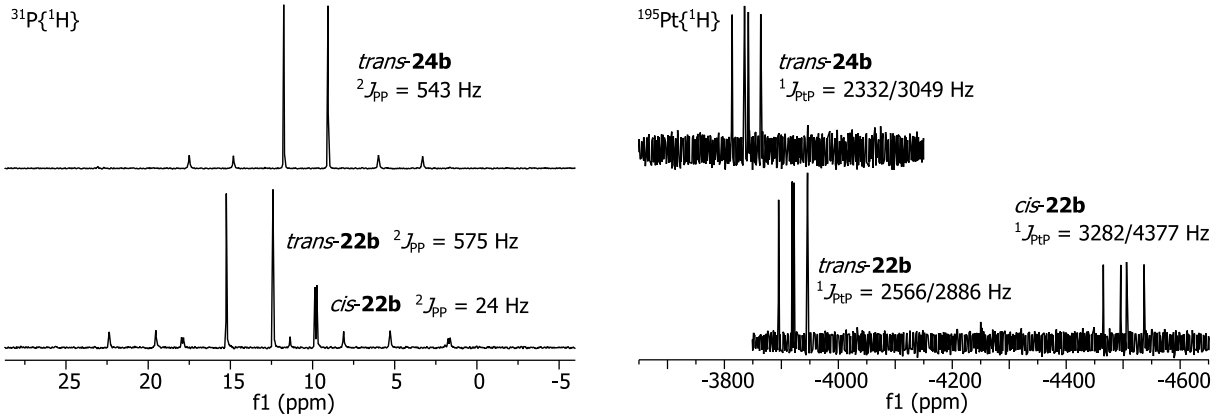

Figure 4.7 Left: $^{31}P\{^{1}H\}$ NMR (202 MHz) spectra of the PEt_3 resonances in **22b** (*cis* and *trans* isomers present) and *trans*-**24b**. The satellite peaks are caused by coupling to the ^{195}Pt nucleus. Right: $^{195}Pt\{^{1}H\}$ NMR (108 MHz) spectra of **22b** (*cis* and *trans* isomers present) and *trans*-**24b**.

Table 4.3 Selected NMR data of the platinum complexes prepared in this study.

complex	$\delta(Pt)^a$	$\delta(L_P)^b$	$^1J_{PtP}(L_P)^c$	$\delta(PEt_3)^d$	$^1J_{PtP}(PEt_3)^e$
cis-**17a**	n.d.	–149.2	4170	—	—
cis-**17b**	n.d.	–149.3	4160	—	—
cis-**20b**	–4362	–6.1	3647	—	—
trans-**21b**	–3747	87.8	2955	—	—
cis-**22a**	–4493	–144.1	4381	10.4	3281
trans-**22a**	–3941	–149.6	2570	15.5	2871
cis-**22b**	–4501	–144.1	4377	9.8	3282
trans-**22b**	–3921	–151.9	2566	13.8	2886
cis-**23a**	–4401	–5.1	3725	7.1	3412
trans-**23a**	–3914	–4.5	2364	12.5	2479
cis-**23b**	–4412	–2.9	3737	7.2	3404
trans-**23b**	–3917	–1.3	2402	12.0	2464
trans-**24a**	–3869	90.4	3030	10.7	2365
trans-**24b**	–3839	90.4	3049	10.4	2332
trans-**25a**	–3881	119.8	3428	10.4	2402
trans-**25b**	–3859	117.3	3454	8.9	2407

[a] Chemical shift in ppm. [b] Resonance of the $ArPR_2$-ligand in ppm. [c] Coupling of the $ArPR_2$-ligand in Hertz. [d] Resonance of the PEt_3-ligand in ppm. [e] Coupling of the PEt_3-ligand in Hertz.

The $^1J_{PtP}$ magnitude of the PEt_3 ligand in $[Pt(L_P)(PEt_3)Cl_2]$ corresponds well to the Pt–PEt_3 bond length (*vide supra*) and can therefore be used as a probe to determine the relative *cis*/*trans* influences of various phosphorus ligands (L_P); a smaller coupling is indicative of a

larger *cis*/*trans* influence. The *trans* influence for the phosphirane ligands in *trans*-**22a**,**b** is comparatively weak in relation to the dimethylphosphine ligands in *trans*-**23a**,**b** (2871/2886 Hz versus 2479/2464 Hz). The situation is reversed for the *cis* influence which is stronger for the phosphiranes in *cis*-**22a**,**b** compared to *cis*-**23a**,**b** (3281/3282 Hz versus 3412/3404 Hz). The *trans* influence observed in *trans*-**25a**,**b** (2402/2407 Hz) and *trans*-**24a**,**b** (2365/2332 Hz) is subsequently further strengthened; data accounting for the *cis* influence in these compounds is unavailable due to the selective formation of the *trans* isomer only.

The rationale for the unusually strong *cis* influence in **22a**,**b** lies in the higher s-character of the phosphirane donor orbital caused by its stronger pyramidalised structure (Figure 4.8). The interaction of the donor orbital with a symmetric metal centred s-orbital results in weakened bonds to both *cis* and *trans* ligands in **22a**,**b**. In contrast, the *trans* effect is stronger in **23a**,**b** without causing much *cis* effect because the increased p-character of the ligand donor orbital predominantly interacts with p- or d-orbitals on the metal. These mainly weaken the bond to the ligand in *trans* position while there is small overlap to orbitals of ligands in the *cis* position. The further increased *trans* effect in **24a**,**b** and **25a**,**b** is an indication for the predominantly p-character of the respective phosphorus donor orbitals in **18a**,**b** and **19a**,**b**.

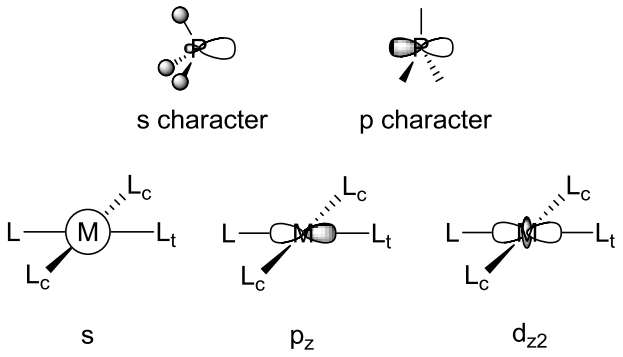

Figure 4.8 Model of P-ligand and metal centred orbitals. Ligands with higher s-character donor orbitals will interact with metal centred s-orbitals weakening *cis* and *trans* substituents. P-donors with p-character interact with p- and d-orbitals on the metal and show predominantly *trans* influence.

Slow evaporation from dichloromethane solutions of *trans*-**22b** (Figure 4.9) and *trans*-**24a** (Figure 4.10) yielded crystals suitable for X-ray analysis (selected structural parameters are given in Table 4.2 on page 82). The large S4' value of the phosphirane ligand in *trans*-**22b** (105.7°) indicates the strain caused by the heterocycle; the S4' value of the unstrained bis(dimethylamino)phosphine ligand in *trans*-**24a** accounts to only 18.7°. The Pt–P bond length of the PEt_3 ligand is shorter in *trans*-**22b** (2.2835(19) Å) compared to *trans*-**24a** (2.3050(11) Å) which is in agreement with the solution NMR data and confirms the weak *trans* influence of the phosphirane ligand. The Pt–Cl bond lengths in *cis* position are almost

equidistant in both complexes. The phosphirane ligand in *trans*-**22b** has a shorter distance to the platinum compared to the bis(dimethylamino)phosphine ligand in *trans*-**24a** (2.3044(18) versus 2.3395(11) Å), which is a result of the strong π-acceptor character of the phosphirane ligand.

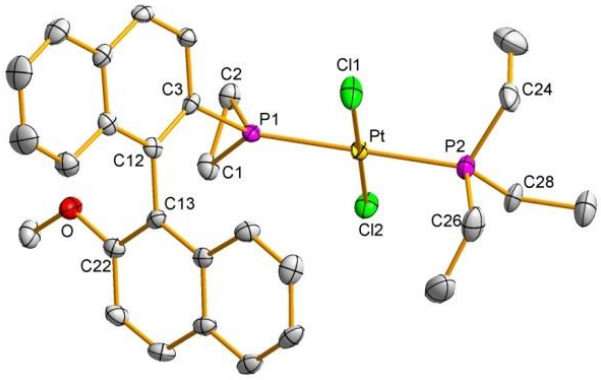

Figure 4.9 View of the molecular structure of *trans*-[Pt(**14b**)(PEt_3)Cl_2] (*trans*-**22b**) with 50% probability displacement ellipsoids. Hydrogen atoms have been omitted for clarity.

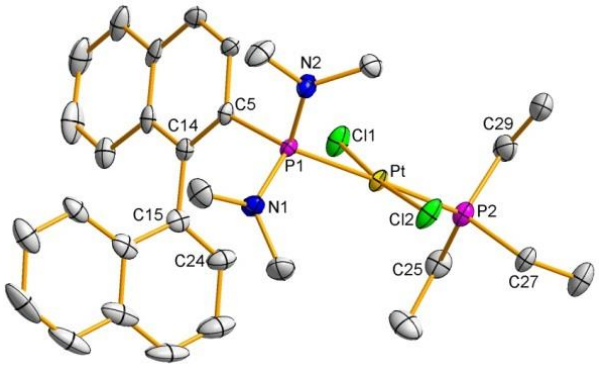

Figure 4.10 View of the molecular structure of *trans*-[Pt(**18a**)(PEt_3)Cl_2] (*trans*-**24a**) with 50% probability displacement ellipsoids. Hydrogen atoms have been omitted for clarity.

4.2.4 Palladium(II) Coordination Properties

We next studied the coordination chemistry of ligands **14b**, **16b**, **18b** and **19b** on palladium(II); the reaction of the appropriate ligand with chloro(2-methallyl)palladium dimer gave the respective palladium chloride complexes **26b**, **27b**, **28b** and **29b** (Scheme 4.2). For all these complexes the formation of two different isomers was indicated by the appearance of two independent resonances in the ^{31}P NMR spectra, as a consequence of the selective orientation of the methallyl group.

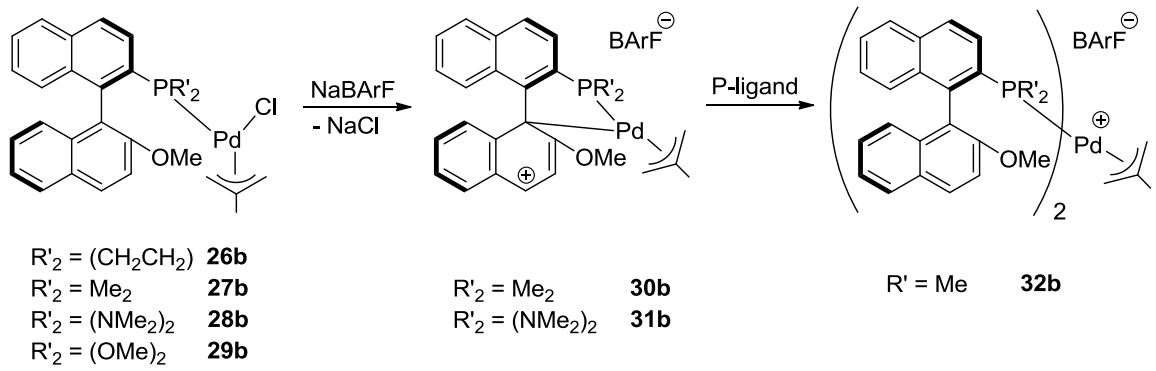

Scheme 4.2 Synthesised palladium(II) complexes of ligands **14b**, **16b**, **18b** and **19b**.

In the NOESY spectra we identified a rapid exchange process caused by the selective η^3–η^1–η^3 interchange mechanism of the methallyl fragment that resulted in broadened peaks at room temperature. During that process the protons in the *cis* position exchange in a *syn*/*anti* fashion while a *syn*/*syn* and *anti*/*anti* exchange is observed for the protons in the *trans* position (Scheme 4.3).[211,235] The selective opening of the allyl ligand in the *trans* position is due to the stronger *trans* effect of the P-donor ligand compared to the chloride ligand.

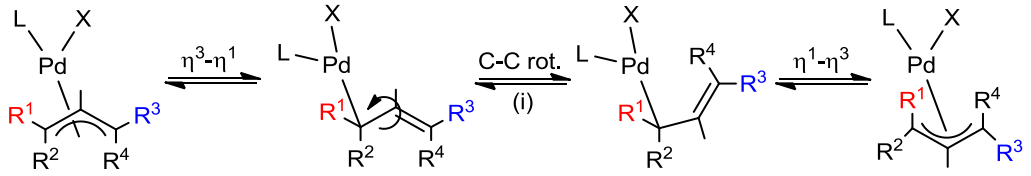

Scheme 4.3 *Syn*/*anti* exchange (R^1/R^2) in *cis* position to L *via* a selective η^3–η^1–η^3 mechanism.

Cooling to –25 °C gave rise to sharpened resonances which allowed for the assignment of the two isomers appearing in ~2:1 (**26b**, **27b**), ~3:2 (**28b**) and ~9:1 (**29b**) ratios. Quantitative analysis of the peaks integrals in the NOESY at –25 °C yielded exchange rate constants of k_{AB} ≈ 0.8 s^{-1} and k_{BA} ≈ 1.3 s^{-1} for **26b**, k_{AB} ≈ 0.4 s^{-1} and k_{BA} ≈ 0.7 s^{-1} for **27b**, k_{AB} ≈ 0.1 s^{-1} and k_{BA} ≈ 0.2 s^{-1} for **28b**, and k_{AB} ≈ 0.3 s^{-1} and k_{BA} ≈ 3.1 s^{-1} for **29b**. The same experiment at –50 °C showed no evidence of exchange. We believe that the relative ratio of isomers as well as the rate of exchange in solution mainly originates from steric effects. For a bulkier MOP-phosphonite ligand with more pronounced binding pockets and steric encumbrance (see complex **36b** in Chapter 5.2.3) exchange rate constants have been observed at a significantly smaller magnitude (k_{AB} ≈ 0.1 s^{-1} and k_{BA} ≈ 1.5 s^{-1} at room temperature).[211]

In the case of **26b**, slow diffusion of diethyl ether into a dichloromethane solution yielded crystals suitable for X-ray crystallographic analysis (Figure 4.11). The structure contains two independent molecules which have the (2-methallyl)palladium moiety coordinated in different

geometric angles. The palladium atom is located at a distance of 3.328(3) Å or 3.590(4) Å from the nearest carbon on the naphthyl group. Pd–P bond lengths are found at 2.2970(8) and 2.2688(9) Å which is shorter than for the two MOP-phosphine allylpalladium complexes previously reported (2.3098(9) and 2.3279(9) Å).[236]

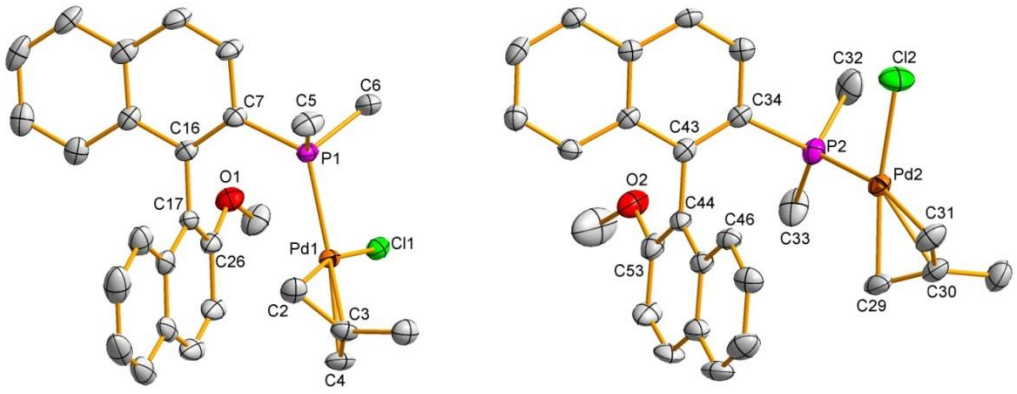

Figure 4.11 View of the molecular structure of [Pd(**16b**)(η^3-C_4H_7)Cl] (**26b**) with 50% probability displacement ellipsoids. Hydrogen atoms have been omitted for clarity. Selected bond distances [Å] and angles [°]: Pd1–P1 2.2970(8), Pd1–Cl1 2.3720(9), Pd1–C2 2.106(3), Pd1–C3 2.183(3), Pd1–C4 2.196(3), Pd1···C17 3.3283(1), Pd2–P2 2.2688(9), Pd2–Cl2 2.3548(10), Pd2–C29 2.090(4), Pd2–C30 2.154(3), Pd2–C31 2.199(4), Pd2···C46 3.5904(1); P1-Pd1-Cl1 99.77(3), P1-Pd1-C2 99.97(11), Cl1-Pd1-C4 66.88(15), P2-Pd2-Cl2 91.25(3), P2-Pd2-C29 100.91(12), Cl2-Pd2-C31 100.21(12), C7-C16-C17-C26 –91.4(4), C34-C43-C44-C53 –100.9(4).

MOP ligands are able to utilise their aromatic backbone to coordinate to a vacant metal site in a chelating P,C-σ-donor or P,C-π-arene bidentate fashion (*cf.* Chapter 1.3.3).[237,238] The reaction of **27b** and **28b** with NaBArF was carried out to exchange the coordinated chloride with the non-coordinating BArF-anion giving complexes **30b** and **31b** (Scheme 4.2 on page 87). This frees up a binding site and allows for coordination of the naphthyl moiety. We were able to obtain the crystal structure of the bis(dimethylamine) derivative **31b** which clearly illustrates the P,C coordination mode in the solid-state. The distance between the palladium atom and the bonded carbon C11 on the naphthyl ring is 2.302(3) Å (Figure 4.12). The position of the palladium above the naphthyl is moved slightly towards C20 to which the distance is 2.553(3) Å; in comparison, the distance to C12 is longer at 2.856(3) Å. The coordinated naphthyl heterocycle is tilted backwards out of its usual plane. The Pd–P distance was found at 2.2546(9) Å and relates well to other MOP-type complexes as described above. Interestingly the two Pd–N bond lengths and angles are inequivalent and show a peculiar pattern. The phosphorus atom carries a shorter bonded planer N-atom (N2–P distance at 1.655(3) Å, sum of angles around N-atom: 358°) and a longer bonded N-atom that shows a pyramidal distorted geometry (N1–P distance at 1.683(3) Å, sum of angles: 343°). The pattern is much less pronounced in the platinum structures *trans*-**21b** (Figure 4.6 on page 82) and

trans-**24a** (Figure 4.10 on page 86) which show only minor distortions around the N atom (sum of angles: 356° to 360°). It is assumed that the planarity of the nitrogen arises from electron donation of its lone pair towards the phosphorus.[213]

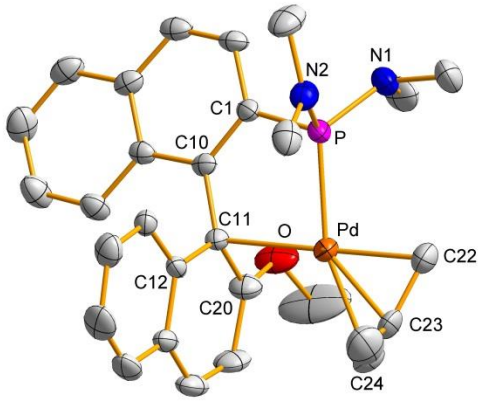

Figure 4.12 View of the molecular structure of [Pd(**18b**)(η^3-C_4H_7)]BArF (**31b**) with 50% probability displacement ellipsoids. Hydrogen atoms and the BArF-anion have been omitted for clarity. Selected bond distances [Å] and angles [°]: Pd–P 2.2546(9), Pd–C11 2.302(3), Pd···C12 2.856(3), Pd···C20 2.553(3), Pd···O 3.154(3), Pd–C22 2.109(4), Pd–C23 2.193(4), Pd–C24 2.228(4), N1–P 1.683(3), N2–P 1.655(3), C11–C20 1.402(4), C22–C23 1.434(6), C23–C44 1.378(7); P-Pd-C11 82.16(8), P-Pd-C20 104.03(9), P-Pd-C22 97.26(11), C11-Pd-C24 114.13(14), C20-Pd-C24 87.95(15), C1-C10-C11-C20 –101.3(4).

In solution we observed the formation of two isomers in a 1:1 ratio for both **30b** and **31b** caused by rotation of the methallyl group (Scheme 4.2 on page 87). As the coordination sphere of the palladium atom is filled by side-on bonding to the C1'-carbon (labelled as C11 in the X-ray structure of **31b**), we consequently found an upfield shift of C1' by about 20 ppm in the ^{13}C NMR spectra compared to the free ligands **16b** and **18b** and the palladium chloride complexes **27b** and **28b**. The NOESY spectrum of **30b** showed exchange of the two isomers at room temperature. Interestingly, we detected *syn*/*anti* exchange (Scheme 4.3 on page 87) as well as an apparent allyl rotation (Scheme 4.4) in a relative ratio of 2:3 (*cf.* Chapter 1.3.4).

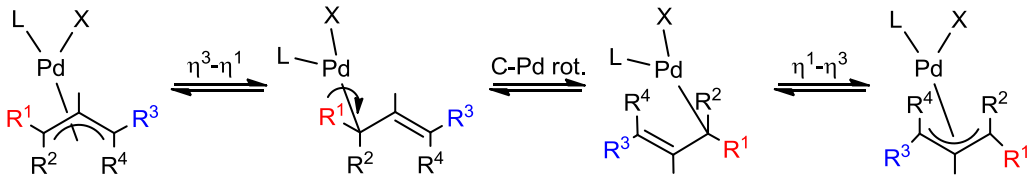

Scheme 4.4 Apparent allyl rotation in allylpalladium complexes (only one possible pathway is shown; for more details see Chapter 1.3.4).

Quantitative analysis of the methoxy resonances in the NOESY spectrum yielded a combined total exchange rate of $k_{AB} \approx k_{BA} \approx 0.2\ s^{-1}$. The exchange rate is therefore smaller than for the related allylpalladium chloride complexes **27b**, which gave exchange rates of that magnitude

at much lower temperature (–25 °C, *vide supra*). The NOESY spectrum of **31b** showed no exchange at room temperature.

We were interested in coordinating two phosphorus ligands to the palladium centre, since these species may form as intermediates in catalytic reaction cycles (*cf.* Chapter 1.3.5).[239,240] The addition of one equivalent of dimethylphosphine ligand **16b** to complex **30b** resulted in the quantitative formation of **32b** (Scheme 4.2 on page 87). The product was analysed by NMR spectroscopy and HRMS; unfortunately we were unable to obtain crystals for X-ray diffraction. The $^{13}C\{^{1}H\}$ NMR spectrum gave no further evidence of aryl coordination; the vacated coordination-site from the dissociated C1'-carbon of **30b** was filled by the added phosphorus donor. One single isomer was observed in the ^{31}P NMR in the form of two doublet resonances (–2.1 ppm and –7.6 ppm) with a reciprocal coupling of $^{2}J_{PP}$ = 43 Hz; we suspect that the induced symmetry by coordination of two equivalent phosphorus ligands leads to identical structures upon allyl rotation. We detected no dynamic behaviour in the NOESY NMR spectrum at room temperature, presumably because of the crowded coordination sphere around the metal. We were unable to isolate equivalent products using ligands **14b**, **18b** or **19b**. The preferred coordination of either one or two ligands per palladium atom will depend on the steric demand around the phosphorus; more bulky groups on the phosphorus as in bis(dimethylamino)phosphine **18b** allow for the straightforward isolation of the 1:1 species (**31b**) while the smaller methyl groups in dimethylphosphine **16b** facilitate the formation of the 2:1 species (**32b**).

4.2.5 Asymmetric Hydrosilylation

For testing the catalytic activity of our ligands we performed the asymmetric hydrosilylation of styrene (Table 4.4).[200,240] Johannsen and co-workers have proposed the competitive action of two cycles for the catalytic hydrosilylation of alkenes (see Chapter 1.3.5).[239] According to their model either one or two coordination sites can be occupied by phosphine ligands. In the case of a one-coordinate phosphine complex, the vacant site is filled with a π-coordinated substrate alkene, or alternatively by utilising the aromatic backbone of the MOP-type compound, which can act as a hemilabile binding site.[240] Conversely, when a ligand to palladium ratio of 2:1 is employed, the formation of an active catalytic species with two coordinated phosphorus ligands may be favoured.[239]

The catalysts were generated *in situ* by the reaction of the ligand with allylpalladium dimer. A ligand to palladium ratio of 1:1 or 2:1 was chosen to account for both possible catalytic pathways as described above, and to selectively promote one pathway over the other.

However, it should be noted that the complex formation is also dependent on the nature of the ligand as we have seen from our coordination studies on palladium(II) (*vide supra*).

Table 4.4 Palladium catalysed hydrosilylation of styrene.

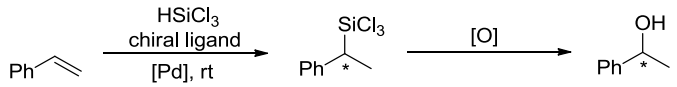

entry	ligand	L:Pd ratio[a]	reaction time	conversion[b]	*ee*[c]
1	**14a**	1:1	6 h	>99%	70% (*R*)
2	**14a**	2:1	24 h	>99%	80% (*R*)
3	**14b**	1:1	48 h	65%	17% (*R*)
4	**14b**	2:1	96 h	50%	49% (*R*)
5	**16a**	1:1	48 h	11%	17% (*R*)
6	**16a**	2:1	48 h	88%	86% (*R*)
7	**16b**	1:1	48 h	15%	73% (*R*)
8	**16b**	2:1	48 h	15%	5% (*S*)
9	**18a**	1:1	6 h	86%	28% (*R*)
10	**18a**	2:1	6 h	>99%	20% (*R*)
11	**18b**	1:1	6 h	84%	37% (*R*)
12	**18b**	2:1	6 h	>99%	43% (*R*)
13	**19a**	1:1	16 h	>99%	82% (*R*)
14	**19a**	2:1	16 h	>99%	84% (*R*)
15	**19b**	1:1	16 h	>99%	7% (*R*)
16	**19b**	2:1	16 h	>99%	2% (*R*)
17	(*S*)-H-MOP[d]	2:1	12 h (0 °C)	100%	93% (*R*)
18	(*R*)-OMe-MOP[d]	2:1	24 h (0 °C)	100%	14% (*R*)

[a] Catalyst was generated *in situ* from ligand (0.25 mol% or 0.50 mol%) and $[Pd(allyl)Cl]_2$ (0.125 mol%) and reacted with styrene (10.0 mmol) and trichlorosilane (12.0 mmol). [b] Determined by ^1H NMR spectroscopy. [c] Determined by chiral HPLC (Lux 5u Cellulose-1 Column). [d] Taken from ref. 242.

The catalytic hydrosilylation reaction of styrene was carried out without additional solvent. Subsequent oxidation of the silane afforded 1-phenylethanol, the absolute configuration of which was determined. Notably ligands **14a**, **18a**,**b** and **19a**,**b** (entries 1-2, 9-16) all showed complete consumption of the starting material in less than 24 hours reaction time, whereas the OMe-substituted phosphirane **14b** (entries 3-4) and dimethylphosphine derivatives **16a**,**b** (entries 5-8) are significantly less reactive in this transformation. Calculations on the reaction mechanism of the hydrosilylation suggest that the rate determining step in the catalytic cycle is the reductive elimination.[241] Therefore one would expect that the good donor ligands **16a**,**b** are less active catalysts as they favour the high oxidation state on the metal. More surprising was the high activity that we observed for the electron rich bis(dimethylamino)phosphine

ligands **18a**,**b** and the reduced activity of the poor donor ligand **14b**, which we are unable to rationalise as yet. With the enantioselectivities of the reactions being taken into account, the best results were obtained with phosphirane **14a** and phosphonite **19a** (entries 1-2, 13-14). Both derivatives show good activity as well as good selectivity of 70-84% enantiomeric excess. Their respective OMe-substituted derivatives **14b** and **19b** (entries 3-4, 15-16) gave inferior selectivities in agreement with the reported values for OMe- and other 2'-substituted MOP ligands (entries 17-18).[242] The bis(dimethylamino)phosphines **18a**,**b** (entries 9-12) gave low *ee* values (20-43%) despite being amongst the most catalytically active catalysts tested. The effect of the L:Pd ratio on the reaction was found to be limited and only in the case of **16a**,**b** (entries 5-8) did we find more pronounced derivations. The inconsistencies may be caused by the overall low activity for **16a**,**b** as no complete substrate conversions were achieved, but curiously in our coordination studies dimethylphosphine ligand **16b** was the only derivative that we could utilise to make the related palladium complex **32b** with a L:Pd ratio of 2:1 (*vide supra*). Arguably, ligand derivatives **14a**,**b**, **18a**,**b** and **19a**,**b** might favour the formation of complexes in a 1:1 ratio of L:Pd, even if an excess of ligand is used.

4.2.6 Asymmetric Allylic Alkylation

As another common benchmark reaction to test the efficiency of chiral ligands in catalysis, we investigated the asymmetric allylic alkylation of (*rac*)-(*E*)-1,3-diphenylallyl acetate (Table 4.5).[243] The nucleophile was generated from dimethyl malonate and bis(trimethylsilyl)acetamide (BSA). This reaction follows a different mechanism than the hydrosilylation one, and hence is expected to show an alternative outcome for the investigated ligands. The oxidative addition is regarded as a possible rate determining step and thus a donor ligand is necessary to enrich the palladium centre with electrons. The following nucleophilic substitution furnishes an energetic barrier that is favoured for electron-withdrawing ligands, but in contrast to the oxidative addition the reaction step is irreversible (*cf.* Chapter 1.3.4).[244]

The activity of the catalysts correlates with the net-donor strength of the ligands (Table 4.1 on page 78). Consequently the fastest catalysts were found in **16a**,**b** ligated compounds giving complete conversions within less than 4 hours (Table 4.5, entries 3-4). Good catalytic activities were also found for **18a**,**b** (completed after 6 hours, entries 5-8) and to a lesser extent for **14a**,**b** (22 hours, entries 1-2). Reactions with phosphonite ligands **19a**,**b** were incomplete even after prolonged reaction time (entries 9-10), most likely as a result of their poor σ-donor character. The best selectivities were achieved with ligands **16a** (41% *ee* (*R*))

and **18a** (66-67% *ee* (*S*)), interestingly yielding their major enantiomers in opposed absolute configurations. In the case of **18a**,**b** we checked for the influence of the L:Pd ratio (2:1 versus 1:1, entries 5-8) but the reaction gave virtually the same outcome.

Table 4.5 Palladium catalysed asymmetric allylic alkylation of (*rac*)-(*E*)-1,3-diphenylallyl acetate.

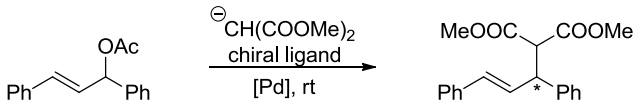

entry	ligand	L:Pd ratio[a]	reaction time[b]	yield[c]	*ee*[d]
1	**14a**	2:1	22 h	91%	17% (*R*)
2	**14b**	2:1	22 h	93%	1% (*S*)
3	**16a**	2:1	3 h	91%	41% (*R*)
4	**16b**	2:1	4 h	98%	14% (*R*)
5	**18a**	2:1	5 h	89%	66% (*S*)
6	**18a**	1:1	6 h	86%	67% (*S*)
7	**18b**	2:1	5 h	88%	13% (*S*)
8	**18b**	1:1	6 h	95%	12% (*S*)
9	**19a**	2:1	48 h	20%	15% (*R*)
10	**19b**	2:1	48 h	2%	29% (*R*)

[a] Catalyst was generated *in situ* from ligand (8.0 mol% or 4.0 mol%) and $[Pd(allyl)Cl]_2$ (2.0 mol%) and reacted with (*rac*)-(*E*)-1,3-diphenylallyl acetate (0.5 mmol), dimethyl malonate (1.0 mmol), BSA (1.0 mmol) and KOAc (0.05 mmol). [b] Reaction progress was monitored by TLC analysis. [c] Isolated yield after column chromatographic workup. [d] Determined by chiral HPLC (Daicel Chiralpak AD-H Column).

4.3 Conclusion

Primary phosphines are versatile ligand precursors that can give rise to a variety of phosphorus compounds. In an earlier communication (see Chapter 3) we have shown the synthesis of phosphiranes **14a**,**b**, their remarkable thermal stability, resistance to air-oxidation and their intriguing potential as ligands in asymmetric catalytic transformations.[206] Here, we reported the preparation of novel ligands **18a**,**b** and **19a**,**b** as well as a simplified synthesis of **16a**,**b** which were achieved in straightforward two-step, one-pot reaction approaches.

We have discussed the unique electronic and steric properties of these different P-ligand functionalities, how they compare with each other and how they manifest themselves in platinum(II) and palladium(II) metal complexes. The highly strained phosphiranes **14a**,**b** show remarkably low *trans* influence but equally enhanced *cis* influence in their platinum(II) complexes as a result of the high s-character of their donor orbital. Their poor donor but good acceptor characteristics compare best to phosphonite ligands **19a**,**b**. These ligands are best

employed in catalytic reactions such as hydrosilylations where the reductive elimination is the rate determining step. Interestingly, the small size of the P-substituents adding to the MOP-backbone seems to have little effect on the enantioselectivities. The steric burden of the phosphirane moiety is minimal, yet up to 80% *ee* were obtained when using **14a** in this transformation. Equally good results were obtained with phosphonite **19a** yielding up to 84% *ee*. It should be noted that more bulky P-substituents have been found to alter the position of the palladium atom relative to the MOP-fragment in our BINOL-derived phosphonites, and they can thereby influence the outcome of the catalytic reaction (*cf.* Chapter 5.2.3).[211]

Different electronic characteristics are present in dimethylphosphines **16a**,**b** and bis(dimethylamino)phosphines **18a**,**b** which are electron-rich σ-donor ligands. The strongest donors were found in **16a**,**b** while the donor properties of **18a**,**b** seem adaptable to some extend by transferring electron-density from either one or two of their nitrogen lone pairs onto the phosphorus (indicated by the degree of distortion around the nitrogen atom). It may be for this reason that, although usually being good donor ligands, **18a**,**b** show high activity in the hydrosilylation reaction. Together with **16a**,**b** they are also suitable catalysts for the allylic alkylation reaction for which we observed enantioselectivities of up to 67% *ee*. Notably, the absolute configuration of the major product was reversed when bis(dimethylamino)-phosphines **18a**,**b** were used as asymmetric ligands in this transformation.

MOP-type ligands can act as hemilabile ligands *via* coordination of their aryl backbone, which we have unambiguously shown by crystallographic analysis of **31b**. However, hemilabile binding to saturate the coordination sphere of the metal centre may be disfavoured when a second P-donor ligand is available. The prominent active species in each of the catalytic transformations is still somewhat speculative and further investigations regarding its disclosure are underway.

4.4 Experimental Section

4.4.1 General Considerations

All air and/or water sensitive reactions were performed under a nitrogen atmosphere using standard Schlenk line techniques. THF (Na/benzophenone ketyl), toluene (Na) and CH_2Cl_2 (CaH) were dried and distilled prior to use. Flash chromatography was performed on silica gel from Fluorochem (silica gel, 40-63 μm, 60A, LC301) or alumina media from Acros (aluminium oxide, neutral, Brockmann I, 50-200 μm, 60A). Thin-layer-chromatography was performed on Merck aluminium-based plates with silica gel and fluorescent indicator 254 nm.

^{1}H, ^{11}B, ^{13}C{^{1}H}, ^{19}F, and ^{31}P{^{1}H} and ^{195}Pt{^{1}H} NMR spectra were recorded on a JEOL Lambda 500 (^{1}H 500.16 MHz) or JEOL ECS-400 (^{1}H 399.78 MHz) spectrometer at room temperature (21°C) if not otherwise stated using the indicated solvent as internal reference. ^{195}Pt chemical shifts are given relative to Ξ(^{195}Pt) = 21.49689 MHz. If necessary the assignment of signals was done by using two-dimensional NMR experiments (COSY, NOESY, HSQC, HMBC).

Table 4.6 Summary of X-ray crystallographic data for *cis*-**20b**, *trans*-**21b** and *trans*-**22b**.

	cis-**20b**	*trans*-**21b**	*trans*-**22b**
formula	$C_{46}H_{42}Cl_2O_2P_2Pt\cdot$ 2 $C_4H_{10}O$	$C_{50}H_{54}Cl_2N_4O_2P_2Pt$	$C_{29}H_{34}Cl_2OP_2Pt$
formula wt	1092.89	1070.90	726.49
cryst syst	orthorhombic	orthorhombic	triclinic
space group	$P2_12_12_1$	$P2_12_12_1$	P1
a, Å; *α*, deg	11.1244(5)	8.3469(4)	8.3743(3); 65.118(3)
b, Å; *β*, deg	20.0436(7)	18.7004(9)	9.5312(3); 71.277(3)
c, Å; *γ*, deg	23.8540(12)	29.0688(16)	10.9589(4); 69.349(3)
V, Å^3	5318.8(4)	4537.4(4)	727.02(4)
Z	4	4	1
ρ_{calc}, g cm^{-3}	1.365	1.568	1.659
μ, mm^{-1}	2.840	3.326	5.139
F(000)	2200	2160	358
T_{min}/T_{max}	0.3963/0.4829	0.58086/1.00000	0.5125/0.6275
hkl range	–9 to 13, –21 to 23, –24 to 28	–11 to 10, –25 to 24, –38 to 37	–10 to 11, –12 to 12, –13 to 14
θ range, deg	2.9 to 25.0	3.0 to 28.6	3.0 to 28.6
no. of measd rflns	24393	29323	11179
no. of unique rflns (R_{int})	9364 (0.0392)	9858 (0.0419)	5954 (0.0236)
no. of obsd rflns, $I > 2\sigma(I)$	7935	8759	5952
refined params/restraints	484/0	560/276	320/3
goodness of fit	1.089	1.180	1.028
Abs. structure param.	–0.008(9)	0.012(8)	–0.001(3)
R1/wR2 ($I > 2\sigma(I)$)	0.0526/0.1146	0.0590/0.0971	0.0185/0.0412
R1/wR2 (all data)	0.0653/0.1202	0.0695/0.1010	0.0185/0.0413
resid electron dens, e Å^{-3}	2.77/–1.50	4.23/–3.68	0.76/–0.80

Table 4.7 Summary of X-ray crystallographic data for *trans*-**24a**, **26b** and **31b**.

	trans-**24a**	**26b**	**31b**
formula	$C_{30}H_{40}Cl_2N_2P_2Pt$	$C_{27}H_{28}ClOPPd$	$C_{29}H_{34}N_2OPPd^{+\cdot}$ $C_{32}H_{12}BF_{24}^{-}$
formula wt	756.57	541.31	1427.18
cryst syst	orthorhombic	monoclinic	orthorhombic
space group	$P2_12_12_1$	$P12_11$	$P2_12_12_1$
a, Å; α, deg	7.8976(3); 90	10.5937(4); 90	12.5151(3); 90
b, Å; β, deg	12.9784(4); 90	14.2040(5); 14.2040(5)	13.7875(4); 90
c, Å; γ, deg	29.8031(10); 90	18.3113(8); 90	37.1072(15); 90
V, Å^3	3054.76(18)	2710.22(18)	6402.9(4)
Z	4	4	4
ρ_{calc}, g cm^{-3}	1.645	1.327	1.481
μ, mm^{-1}	4.895	0.857	0.426
F(000)	1504	1104	2864
T_{min}/T_{max}	0.3214/0.3214	0.7255/0.9584	0.8482/0.8829
hkl range	–10 to 10, –17 to 13, –37 to 38	–14 to 13, –18 to 18, –24 to 19	–16 to 16, –17 to 18, –37 to 50
θ range, deg	2.9 to 28.6	3.1 to 28.6	3.0 to 28.6
no. of measd rflns	15460	26914	34951
no. of unique rflns (R_{int})	6419 (0.0391)	11398 (0.0305)	13678 (0.0295)
no. of obsd rflns, $I > 2\sigma(I)$	6158	10533	12550
refined params/restraints	342/0	567/1	883/72
goodness of fit	1.034	1.055	1.074
Abs. structure param.	–0.010(5)	–0.035(16)	–0.005(18)
R1/wR2 ($I > 2\sigma(I)$)	0.0296/0.0506	0.0316/0.0702	0.0439/0.0995
R1/wR2 (all data)	0.0323/0.0520	0.0369/0.0729	0.0492/0.1024
resid electron dens, e Å^{-3}	1.31/–1.08	0.44/–0.36	0.56/–0.52

Infrared spectra were recorded on a Varian 800 FT-IR spectrometer. Mass spectrometry was carried out by the EPSRC National Mass Spectrometry Service Centre Swansea. Analytical high performance liquid chromatography (HPLC) was performed on a Varian Pro Star HPLC or a Shimadzu Prominence HPLC equipped with diode-array detectors. The preparations of **1a**,**b** and **2a**,**b** are described in the experimental section of Chapter 2 (**1a**,**b**) or Chapter 3 (**2a**,**b**). The experimental procedure for the palladium catalysed asymmetric hydrosilylation of styrene is described in Chapter 3.4.9. Literature procedures were followed for the synthesis of *trans*-$[Pt(PEt_3)Cl_2]_2$.[245] All other chemicals were used as purchased without further purification. Key crystallographic data are given in Table 4.6 and Table 4.7.

4.4.2 (*S*)-[1,1'-Binaphthalen]-2-yldimethylphosphine (**16a**)

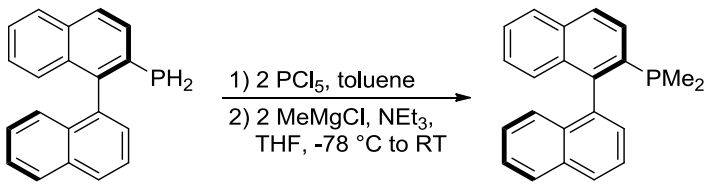

PCl_5 (458 mg, 2.20 mmol) was dissolved in toluene (8 mL). **1a** (286 mg, 1.00 mmol) was added and the reaction mixture was left to stir for 45 minutes. The volatiles were removed *in vacuo*, THF (8 mL) was added and the resulting solution was cooled to –78 °C. MeMgCl (0.70 mL, 3.0 M in THF, 2.10 mmol) was added and stirred at –78 °C for 30 minutes. The solution was allowed to warm up to ambient temperature and stirred for 1.5 hours. The reaction was slowly quenched with H_2O (10 mL) and extracted with Et_2O (2x 30 mL). The organic phase was dried over $MgSO_4$ to give the fairly pure crude product as a pale-yellow solid. Purification was performed by column chromatography (hexane/EtOAc, 10:1, $R_f = 0.4$.) on a silica media (w = 2 cm, h = 10 cm) to yield the intended product as a white solid (238 mg, 0.36 mmol, 76%).

MP (uncorrected): 112 °C. **^{1}H NMR** (400 MHz, $CDCl_3$): $\delta = 7.99$ (d, $^3J_{HH} = 8.5$ Hz, 1H, *H*4), 7.98 (d, $^3J_{HH} = 8.2$ Hz, 1H, *H*4'), 7.94 (d, $^3J_{HH} = 8.2$ Hz, 1H, *H*5), 7.91 (d, $^3J_{HH} = 8.2$ Hz, 1H, *H*5'), 7.78 (dd, $^3J_{HH} = 8.5$ Hz, $^3J_{HP} = 2.9$ Hz, 1H, *H*3), 7.62 (dd, $^3J_{HH} = 8.2$ Hz, $^3J_{HH} = 7.0$ Hz, 1H, *H*3'), 7.48-7.43 (m, 3H, *H*6+*H*6'+*H*2'), 7.28-7.22 (m, 2H, *H*7'+*H*7), 7.19-7.14 (m, 2H, *H*8+*H*8'), 1.22 (d, $^2J_{HP} = 3.9$ Hz, 3H, CH_3), 1.02 (d, $^2J_{HP} = 3.9$ Hz, 3H, CH_3') ppm. **^{13}C{^{1}H} NMR** (101 MHz, $CDCl_3$): $\delta = 143.4$ (d, $^2J_{CP} = 29.7$ Hz, *C*1), 138.8 (d, $^1J_{CP} = 14.4$ Hz, *C*2), 137.7 (d, $^3J_{CP} = 7.8$ Hz, *C*1'), 133.5 (*C*10), 133.4 (d, $^4J_{CP} = 2.4$ Hz, *C*9'), 133.3 (*C*10'), 133.1 (d, $^3J_{CP} = 5.7$ Hz, *C*9), 128.7 (d, $^4J_{CP} = 3.3$ Hz, *C*2'), 128.4 (*C*5), 128.2 (*C*4), 128.2 (*C*4'), 127.9 (*C*5'), 127.0 (d, $^4J_{CP} = 2.3$ Hz, *C*8), 126.5 (*C*8'), 126.4 (*C*7'), 126.3 (*C*7), 126.1 (*C*6'), 125.9 (*C*6), 125.7 (d, $^2J_{CP} = 1.4$ Hz, *C*3), 125.3 (*C*3'), 15.0 (d, $^1J_{CP} = 14.0$ Hz, *C*H$_3$), 14.4 (d, $^1J_{CP} = 14.0$ Hz, *C*H$_3$') ppm. **^{31}P{^{1}H} NMR** (202 MHz, $CDCl_3$): $\delta = -54.0$ ppm. **IR** (neat): $\nu = 3052.2$ (w), 2893.6 (w), 1591.9 (w), 1501.4 (w), 1428.8 (w), 1360.6 (w), 1154.7 (w), 1013.4 (w), 938.9 (m), 894.3 (m), 869.4 (w), 781.6 (s), 749.5 (s), 708.0 (m), 685.7 (w), 627.5 (w) 578.5 (w) cm^{-1}. **HRMS** (ESI$^+$): Found: $m/z = 315.1294$. Calculated for $[M + H]^+$: $m/z = 315.1297$. **OR** ($CHCl_3$, $c = 1.0$ mg/ml): $[\alpha]_D^{20} = -44°$. **TLC** (silica gel; hexane/EtOAc, 10:1): $R_f = 0.4$.

4.4.3 (*R*)-(2'-Methoxy-[1,1'-binaphthalen]-2-yl)dimethylphosphine (**16b**)

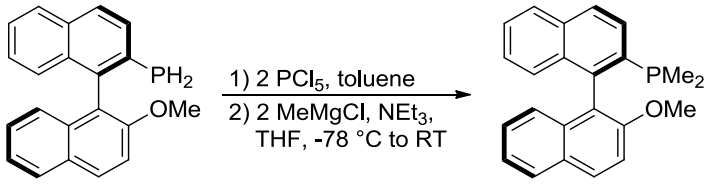

The same procedure was followed as for **16a**, except for using **1b** as the substrate. Purification was performed by column chromatography (hexane/EtOAc, 10:1, $R_f = 0.4$) on a silica media (w = 2 cm, h = 10 cm) to yield the intended product as a white solid (125 mg, 0.36 mmol, 73%).

MP (uncorrected): 128 °C. **^{1}H NMR** (500 MHz, $CDCl_3$): δ = 8.03 (d, $^3J_{HH}$ = 9.0 Hz, 1H, *H*4'), 8.00 (d, $^3J_{HH}$ = 8.5 Hz, 1H, *H*4), 7.91 (d, $^3J_{HH}$ = 8.3 Hz, 1H, *H*5), 7.87 (d, $^3J_{HH}$ = 8.3 Hz, 1H, *H*5'), 7.81 (dd, $^3J_{HH}$ = 8.5 Hz, $^3J_{HP}$ = 2.9 Hz, 1H, *H*3), 7.45 (ddd, $^3J_{HH}$ = 8.3 Hz, $^3J_{HH}$ = 6.5 Hz, $^4J_{HH}$ = 1.3 Hz, 1H, *H*6), 7.45 (d, $^3J_{HH}$ = 9.0 Hz, 1H, *H*3'), 7.31 (ddd, $^3J_{HH}$ = 8.3 Hz, $^3J_{HH}$ = 6.5 Hz, $^4J_{HH}$ = 1.3 Hz, 1H, *H*6'), 7.24 (ddd, $^3J_{HH}$ = 8.3 Hz, $^3J_{HH}$ = 6.5 Hz, $^4J_{HH}$ = 1.3 Hz, 1H, *H*7), 7.20 (d, $^3J_{HH}$ = 8.3 Hz, 1H, *H*8), 7.19 (ddd, $^3J_{HH}$ = 8.3 Hz, $^3J_{HH}$ = 6.5 Hz, $^4J_{HH}$ = 1.3 Hz, 1H, *H*7'), 6.93 (d, $^3J_{HH}$ = 8.3 Hz, 1H, *H*8'), 3.78 (s, 3H, OCH_3), 1.21 (d, $^2J_{HP}$ = 3.9 Hz, 3H, CH_3), 1.05 (d, $^2J_{HP}$ = 4.0 Hz, 3H, CH_3') ppm. **^{13}C{^{1}H} NMR** (126 MHz, $CDCl_3$): δ = 154.8 (d, $^4J_{CP}$ = 1.9 Hz, *C*2'), 140.1 (d, $^2J_{CP}$ = 31.7 Hz, *C*1), 139.1 (d, $^1J_{CP}$ = 13.1 Hz, *C*2), 134.4 (d, $^4J_{CP}$ = 1.9 Hz, *C*9'), 133.6 (*C*10), 132.9 (d, $^3J_{CP}$ = 6.8 Hz, *C*9), 129.9 (*C*4'), 128.9 (*C*10'), 128.1 (C4), 128.0 (*C*5+*C*5'), 126.5 (*C*8+*C*7'), 126.3 (*C*6+*C*7), 125.7 (d, $^2J_{CP}$ = 1.9 Hz, *C*3), 125.4 (*C*8'), 123.6 (*C*6'), 122.4 (d, $^3J_{CP}$ = 8.7 Hz, *C*1'), 113.3 (*C*3'), 56.4 (O*C*H_3), 14.7 (d, $^1J_{CP}$ = 14.4 Hz, *C*H_3), 14.6 (d, $^1J_{CP}$ = 13.9 Hz, *C*H_3') ppm. **^{31}P{^{1}H} NMR** (202 MHz, $CDCl_3$): δ = –54.0 ppm. **IR** (neat): ν = 3060.9 (w), 1620.3 (m), 1592.8 (m), 1505.0 (m), 1457.8 (w), 1428.1 (w), 1344.2 (m), 1251.4 (s), 1178.1 (w), 1147.4 (w), 1119.2 (w), 1077.7 (s), 1051.3 (m), 1020.7 (m), 937.9 (m), 895.5 (m), 870.5 (w), 810.3 (s), 746.9 (s), 709.1 (m), 679.9 (m), 627.9 (w) cm^{-1}. **HRMS** (ESI$^+$): Found: *m*/*z* = 345.1404. Calculated for [M + H]$^+$: *m*/*z* = 345.1403. **OR** ($CHCl_3$, *c* = 1.0 mg/ml): $[\alpha]_D^{20} = -14°$. **TLC** (silica gel; hexane/EtOAc, 10:1): $R_f = 0.4$.

4.4.4 (*S*)-*N*,*N*,*N*',*N*'-Tetramethyl-1-(1,1'-binaphthalen-2-yl)phosphinediamine (**18a**)

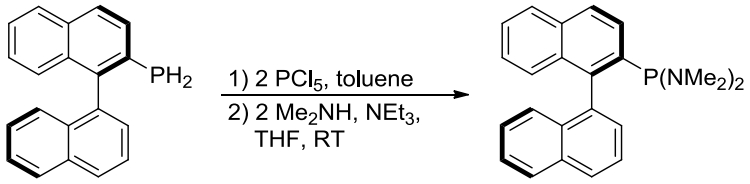

PCl_5 (687 mg, 3.30 mmol) was dissolved in toluene (12 mL). **1a** (429 mg, 1.50 mmol) was added and the reaction mixture was left to stir for 45 minutes after which time the volatiles were removed *in vacuo*. The resulting solid was dissolved in THF (12 mL). NEt_3 (0.92 mL, 6.60 mmol) and $HNMe_2$ (1.60 mL, 2.0 M in THF, 3.15 mmol) were added subsequently and the solution was left to stir overnight. The volatiles were removed *in vacuo* and the crude product was filtered through a small plug of alumina media in a 1:1 mixture of cyclohexane and Et_2O ($R_f = 0.8$). The title product was obtained after removal of the solvent, as a white solid (519 mg, 0.93 mmol, 93%).

MP (uncorrected): 105 °C. **^{1}H NMR** (500 MHz, CD_2Cl_2): $\delta = 7.97$ (d, $^3J_{HH} = 8.5$ Hz, 1H, *H*4), 7.94 (d, $^3J_{HH} = 8.3$ Hz, 1H, *H*5), 7.93-7.89 (m, 3H, *H*5'+*H*4'+*H*3), 7.60 (dd, $^3J_{HH} = 8.3$ Hz, $^3J_{HH} = 7.0$ Hz, 1H, *H*3'), 7.46-7.42 (m, 2H, *H*6'+*H*6), 7.41 (d, $^3J_{HH} = 7.0$ Hz, 1H, *H*2'), 7.25-7.19 (m, 3H, *H*7'+*H*7+*H*8'), 7.16 (d, $^3J_{HH} = 8.5$ Hz, 1H, *H*8), 2.42 (d, $^3J_{HP} = 9.0$ Hz, 6H, N(CH_3)$_2$), 2.26 (d, $^3J_{HP} = 9.3$ Hz, 6H, N(CH_3)$_2$') ppm. **^{13}C{^{1}H} NMR** (126 MHz, CD_2Cl_2): $\delta = 141.5$ (d, $^2J_{CP} = 26.0$ Hz, *C*1), 138.8 (d, $^1J_{CP} = 11.0$ Hz, *C*2), 137.5 (d, $^3J_{CP} = 4.7$ Hz, *C*1'), 133.7 (d, $^3J_{CP} = 3.8$ Hz, *C*9), 133.7 (*C*10), 133.5 (*C*10'), 132.6 (d, $^4J_{CP} = 1.4$ Hz, *C*9'), 128.1 (*C*5), 128.0 (*C*2'), 128.0 (*C*3), 127.8 (*C*4'), 127.5 (*C*5'), 127.1 (d, $^4J_{CP} = 1.3$ Hz, *C*4), 127.0 (d, $^5J_{CP} = 1.3$ Hz, *C*7), 126.4 (d, $^4J_{CP} = 2.5$ Hz, *C*8), 126.0 (*C*7), 125.8 (*C*6+*C*6'), 125.6 (*C*8'), 125.4 (*C*7'), 125.2 (*C*3'), 41.0 (d, $^2J_{CP} = 18.0$ Hz, N(*C*H_3)$_2$), 40.9 (d, $^2J_{CP} = 18.6$ Hz, N(*C*H_3)$_2$') ppm. **^{31}P{^{1}H} NMR** (202 MHz, CD_2Cl_2): $\delta = 99.9$ ppm. **IR** (neat): $\nu = 3059.0$ (w), 2979.2 (w), 2872.0 (w), 2827.9 (w), 2783.3 (w), 1497.3 (w), 1355.6 (w), 1261.8 (w), 1189.7 (m), 1061.4 (w), 1022.2 (w), 949.1 (s), 869.2 (w), 824.0 (m), 804.6 (m), 781.5 (s), 748.2 (s), 667.4 (s), 640.9 (m) cm^{-1}. **HRMS** (ESI$^+$): Found: $m/z = 373.1827$. Calculated for $[M + H]^+$: $m/z = 373.1828$. **OR** ($CHCl_3$, $c = 1.0$ mg/ml): $[\alpha]_D^{20} = -32°$. **TLC** (alumina; cyclohexane/Et_2O, 1:1): $R_f = 0.8$.

4.4.5 (*R*)-*N*,*N*,*N*',*N*'-Tetramethyl-1-(2'-methoxy-[1,1'-binaphthalen]-2-yl)phosphinediamine (**18b**)

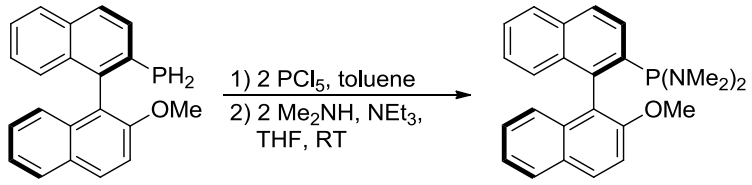

The same procedure was followed as for **18a**, except for using **1b** as the substrate. The title product was obtained as a white solid (536 mg, 1.33 mmol, 89%).

MP (uncorrected): 122 °C. **^{1}H NMR** (500 MHz, CD_2Cl_2): δ = 7.97 (d, $^3J_{HH}$ = 9.1 Hz, 1H, *H*4'), 7.96 (d, $^{3,4}J_{HP}$ = 2.0 Hz, 2H, *H*3+*H*4), 7.92 (d, $^3J_{HH}$ = 8.2 Hz, 1H, *H*5), 7.86 (d, $^3J_{HH}$ = 8.2 Hz, 1H, *H*5'), 7.47-7.43 (m, 2H, *H*3'+*H*6), 7.29 (ddd, $^3J_{HH}$ = 8.1 Hz, $^3J_{HH}$ = 6.7 Hz, $^4J_{HH}$ = 1.3 Hz, 1H, *H*6'), 7.21 (ddd, $^3J_{HH}$ = 8.5 Hz, $^3J_{HH}$ = 6.5 Hz, $^4J_{HH}$ = 1.3 Hz, 1H, *H*7), 7.18-7.14 (m, 2H, *H*8+*H*7'), 6.93 (d, $^3J_{HH}$ = 8.5 Hz, 1H, *H*8'), 3.78 (s, 3H, OCH_3), 2.36 (d, $^3J_{HP}$ = 9.5 Hz, 6H, N(CH_3)$_2$), 2.21 (d, $^3J_{HP}$ = 9.2 Hz, 6H, N(CH_3)$_2$') ppm. **^{13}C{^{1}H} NMR** (126 MHz, CD_2Cl_2): δ = 154.4 (d, $^4J_{CP}$ = 1.6 Hz, *C*2'), 139.1 (d, $^2J_{CP}$ = 13.9 Hz, *C*1), 139.0 (d, $^1J_{CP}$ = 29.0 Hz, *C*2), 134.0 (d, $^4J_{CP}$ = 1.9 Hz, *C*10), 133.7 (*C*9'), 133.4 (d, $^3J_{CP}$ = 4.8 Hz, *C*9), 129.2 (*C*4'), 128.9 (*C*10'), 127.9 (*C*5), 127.8 (d, $^2J_{CP}$ = 4.2 Hz, *C*3), 127.7 (*C*5'), 126.8 (d, $^3J_{CP}$ = 1.2 Hz, *C*4), 126.1 (*C*6), 126.0 (d, $^5J_{CP}$ = 2.5 Hz, *C*7), 125.9 (*C*7'), 125.8 (*C*8'), 125.8 (d, $^4J_{CP}$ = 1.3 Hz, *C*8), 123.2 (*C*6'), 121.9 (d, $^3J_{CP}$ = 6.1 Hz, *C*1'), 113.0 (*C*3'), 56.0 (O*C*H$_3$), 40.5 (d, $^2J_{CP}$ = 19.2 Hz, N(*C*H$_3$)$_2$), 40.4 (d, $^2J_{CP}$ = 19.2 Hz, N(*C*H$_3$)$_2$') ppm. **^{31}P{^{1}H} NMR** (202 MHz, CD_2Cl_2): δ = 101.0 ppm. **IR** (neat): ν = 3060.3 (w), 2965.9 (w), 2825.5 (w), 2780.6 (w), 1621.8 (w), 1593.3 (w), 1510.4 (m), 1461.1 (m), 1340.5 (w), 1263.7 (s), 1194.5 (m), 1078.1 (m), 1053.4 (w), 1021.3 (w), 978.2 (m), 955.4 (s), 910.2 (w), 822.3 (w), 802.7 (s), 742.1 (s), 674.2 (m), 638.3 (m) cm^{-1}. **HRMS** (ESI$^+$): Found: *m*/*z* = 403.1939. Calculated for [M + H]$^+$: *m*/*z* = 403.1934. **OR** ($CHCl_3$, *c* = 1.0 mg/ml): $[\alpha]_D^{20}$ = –60°. **TLC** (alumina; cyclohexane/Et_2O, 1:1): R_f = 0.8.

4.4.6 Dimethyl [1,1'-binaphthalen]-2-ylphosphonite (**19a**)

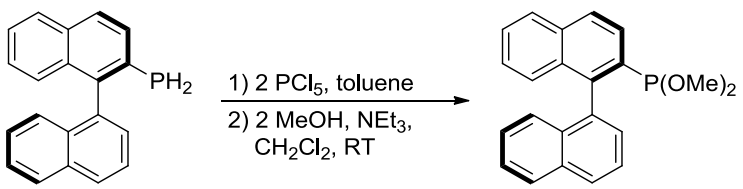

PCl_5 (458 mg, 2.20 mmol) was dissolved in toluene (5 mL). **1a** (286 mg, 1.00 mmol) was added and the reaction mixture was left to stir for 45 minutes after which time the volatiles were removed *in vacuo*. The resulting solid was dissolved in CH_2Cl_2 (5 mL). NEt_3 (0.61 mL, 4.40 mmol) and MeOH (0.09 mL, 2.20 mmol) were added subsequently and the solution was left for 2 hours. The volatiles were removed *in vacuo* and a toluene suspension of the crude product was filtered through a small plug of celite. The title product was obtained after removal of the solvent, as a pale yellow oil.

^{1}H NMR (400 MHz, CD_2Cl_2): δ = 8.04 (dd, $^3J_{HH}$ = 8.5 Hz, $^3J_{HP}$ = 1.9 Hz, 1H, *H*3), 8.02-8.00 (m, 2H, *H*4+*H*4'), 7.98-7.94 (m, 2H, *H*5+*H*5'), 7.62 (dd, $^3J_{HH}$ = 8.5 Hz, $^3J_{HH}$ = 7.0 Hz, 1H, *H*3'), 7.52-7.46 (m, 3H, *H*6+*H*6'+*H*2'), 7.29-7.24 (m, 2H, *H*7+*H*7'), 7.19-7.13 (m, 2H, *H*8+*H*8'), 3.45 (d, $^3J_{HP}$ = 10.8 Hz, 3H, POCH_3), 3.00 (d, $^3J_{HP}$ = 11.7 Hz, 3H, POCH_3') ppm. **^{13}C{^{1}H} NMR** (101 MHz, CD_2Cl_2): δ = 142.8 (d, $^2J_{CP}$ = 32.6 Hz, *C*1), 137.7 (d, $^1J_{CP}$ = 21.4 Hz, *C*2), 135.6 (d, $^3J_{CP}$ = 7.8 Hz, *C*1'), 134.3 (*C*10), 133.5 (d, $^4J_{CP}$ = 1.9 Hz, *C*9'), 133.3 (*C*10'), 132.1 (d, $^3J_{CP}$ = 5.0 Hz, *C*9), 129.6 (d, $^4J_{CP}$ = 3.4 Hz, *C*2'), 128.4 (*C*5), 128.2 (*C*5'), 128.0 (*C*4'), 127.3 (d, $^3J_{CP}$ = 1.4 Hz, *C*4), 127.0 (*C*6'), 126.6 (*C*8'), 126.6 (*C*8), 126.2 (*C*7'), 126.1 (*C*7), 125.9 (*C*6), 125.3 (d, $^2J_{CP}$ = 3.4 Hz, *C*3), 125.0 (*C*3'), 53.8 (d, $^2J_{CP}$ = 15.8 Hz, POCH_3'), 53.2 (d, $^2J_{CP}$ = 10.0 Hz, POCH_3) ppm. **^{31}P{^{1}H} NMR** (202 MHz, CD_2Cl_2): δ = 157.5 ppm. **IR** (neat): ν = 3052.1 (w), 2933.4 (w), 2831.1 (w), 1591.7 (w), 1557.6 (w), 1505.7 (w), 1454.6 (w), 1361.8 (w), 1231.7 (w), 1163.4 (w), 1037.0 (s), 1015.7 (s), 879.9 (w), 828.9 (m) cm^{-1}. **HRMS** (APCI$^+$): Found: *m*/*z* = 347.1193. Calculated for [M + H]$^+$: *m*/*z* = 347.1195. **OR** ($CHCl_3$, *c* = 1.0 mg/ml): $[\alpha]_D^{20}$ = –44°.

4.4.7 Dimethyl (2'-methoxy-[1,1'-binaphthalen]-2-yl)phosphonite (**19b**)

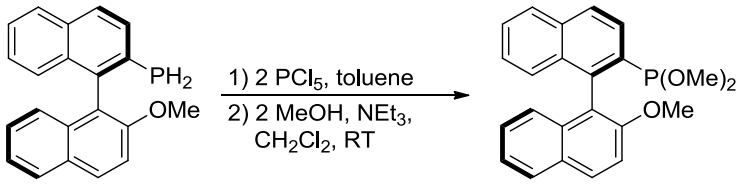

The same procedure was followed as for **19a**, except for using **1b** as the substrate. The title product was obtained as a pale yellow oil.

^{1}H NMR (500 MHz, CD_2Cl_2): δ = 8.05 (d, $^3J_{HH}$ = 9.1 Hz, 1H, *H*4'), 8.04 (d, $^3J_{HH}$ = 8.5 Hz, $^3J_{HP}$ = 1.9 Hz, 1H, *H*3), 7.99 (d, $^3J_{HH}$ = 8.5 Hz, 1H, *H*4), 7.95 (d, $^3J_{HH}$ = 8.1 Hz, 1H, *H*5), 7.89 (d, $^3J_{HH}$ = 8.2 Hz, 1H, *H*5'), 7.51 (ddd, $^3J_{HH}$ = 8.1 Hz, $^3J_{HH}$ = 6.7 Hz, $^4J_{HH}$ = 1.3 Hz, 1H, *H*6), 7.47 (d, $^3J_{HH}$ = 9.1 Hz, 1H, *H*3'), 7.32 (ddd, $^3J_{HH}$ = 8.2 Hz, $^3J_{HH}$ = 6.7 Hz, $^4J_{HH}$ = 1.2 Hz, 1H, *H*6'), 7.28-7.18 (m, 3H, *H*7+*H*7'+*H*8), 6.91 (d, $^3J_{HH}$ = 8.5 Hz, 1H, *H*8'), 3.79 (s, 3H, OCH_3),

3.43 (d, $^{3}J_{HP}$ = 10.3 Hz, 3H, POCH_3), 3.32 (d, $^{3}J_{HP}$ = 11.5 Hz, 3H, POCH_3') ppm. **^{13}C{^{1}H} NMR** (126 MHz, CD_2Cl_2): δ = 155.6 (d, $^{4}J_{CP}$ = 2.0 Hz, *C*2'), 139.6 (d, $^{2}J_{CP}$ = 33.8 Hz, *C*1), 137.8 (d, $^{1}J_{CP}$ = 21.7 Hz, *C*2), 134.6 (*C*9'), 134.5 (d, $^{4}J_{CP}$ = 2.2 Hz, *C*10), 132.9 (d, $^{3}J_{CP}$ = 5.2 Hz, *C*9), 130.2 (*C*4'), 128.6 (*C*10'), 128.1 (*C*5), 127.9 (*C*5'), 127.1 (*C*4), 127.0 (*C*6), 126.5 (*C*7'), 126.2 (*C*7), 126.0 (d, $^{4}J_{CP}$ = 2.4 Hz, *C*8), 125.7 (d, $^{2}J_{CP}$ = 3.3 Hz, *C*3), 125.3 (*C*8'), 123.5 (*C*6'), 119.9 (d, $^{3}J_{CP}$ = 8.1 Hz, *C*1'), 112.9 (*C*3'), 56.1 (OCH_3), 53.6 (d, $^{2}J_{CP}$ = 15.1 Hz, POCH_3'), 52.6 (d, $^{2}J_{CP}$ = 8.5 Hz, POCH_3) ppm. **^{31}P{^{1}H} NMR** (202 MHz, CD_2Cl_2): δ = 155.8 ppm. **IR** (neat): ν = 3053.8 (w), 2933.5 (w), 2828.0 (w), 1621.2 (w), 1592.6 (w), 1507.8 (m), 1461.7 (w), 1332.7 (w), 1268.9 (s), 1248.9 (s), 1147.3 (w), 1079.4 (m), 1035.7 (s), 1011.6 (s), 907.8 (w), 868.1 (w) cm^{-1}. **HRMS** (APCI^{+}): Found: *m*/*z* = 376.1218. Calculated for [M]$^{+}$: *m*/*z* = 376.1223. **OR** ($CHCl_3$, *c* = 1.0 mg/ml): $[\alpha]_D^{20}$ = –20°.

4.4.8 *cis*-Bis((*R*)-(2'-methoxy-[1,1'-binaphthalen]-2-yl)dimethylphosphine)-dichloroplatin (*cis*-**20b**)

[Pt(η^4-cod)Cl_2] (6.7 mg, 17.5 μmol) and **16b** (11.0 mg, 35.0 μmol) were dissolved in CH_2Cl_2 (2 mL) and stirred at room temperature for 15 minutes. The volatiles were removed *in vacuo* to give the intended product as a colourless solid (quantitative conversion). Slow diffusion of Et_2O into the reaction mixture yielded colourless crystals overnight which were suitable for X-ray diffraction analysis.

^{1}H NMR (400 MHz, $CDCl_3$): δ = 8.66 (dd, $^{3}J_{HP}$ = 13.9 Hz, $^{3}J_{HH}$ = 8.7 Hz, 2H, *H*3), 7.98 (d, $^{3}J_{HH}$ = 9.2 Hz, 2H, *H*4'), 7.87-7.81 (m, 6H, *H*5+*H*4+*H*5'), 7.48 (ddd, $^{3}J_{HH}$ = 8.3 Hz, $^{3}J_{HH}$ = 6.8 Hz, $^{4}J_{HH}$ = 1.3 Hz, 2H, *H*6), 7.35-7.28 (m, 4H, *H*3'+*H*6'), 7.20 (ddd, $^{3}J_{HH}$ = 8.3 Hz, $^{3}J_{HH}$ = 6.8 Hz, $^{4}J_{HH}$ = 1.3 Hz, 2H, *H*7), 7.03 (ddd, $^{3}J_{HH}$ = 8.3 Hz, $^{3}J_{HH}$ = 6.8 Hz, $^{4}J_{HH}$ = 1.3 Hz, 2H, *H*7'), 6.96 (d, $^{3}J_{HH}$ = 8.3 Hz, 2H, *H*8), 6.72 (d, $^{3}J_{HH}$ = 8.3 Hz, 2H, *H*8'), 3.57 (s, 6H, OCH_3), 1.26 (d, $^{2}J_{HP}$ = 10.6 Hz, 6H, PCH_3), 1.11 (d, $^{2}J_{HP}$ = 10.6 Hz, 6H, PCH_3) ppm. **^{13}C{^{1}H} NMR** (101 MHz, $CDCl_3$): δ = 154.9 (*C*2'), 138.5 (*C*1), 134.5 (*C*10), 134.5 (*C*9'), 133.2 (*C*9), 132.3 (m, *C*3), 131.2 (*C*4'), 128.8 (*C*5'), 128.7 (*C*10'), 128.1 (*C*4), 128.1 (*C*5), 127.8 (*C*6), 127.3 (*C*7'), 127.1 (*C*7), 126.5 (*C*8), 125.7 (*C*8'), 124.1 (*C*6'), 119.6 (*C*1'), 112.8 (*C*3'), 55.8 (s, OCH_3), 7.8 (d, $^{1}J_{CP}$ = 44.6 Hz, *C*H_3), 7.2 (d, $^{1}J_{CP}$ = 43.1 Hz, *C*H_3) ppm. **^{31}P{^{1}H} NMR** (162 MHz, $CDCl_3$): δ = –6.1 (s with ^{195}Pt satellites, $^{1}J_{PtP}$ = 3647 Hz) ppm. **^{195}Pt{^{1}H} NMR** (108 MHz, CD_2Cl_2): δ = –4362 (t, $^{1}J_{PtP}$ = 3647 Hz) ppm. **HRMS** (ESI^{+}, MeOH): Found: *m*/*z* = 917.1960. Calculated for [M – Cl]$^{+}$: *m*/*z* = 917.1975.

4.4.9 *trans*-Bis((*R*)-*N*,*N*,*N*',*N*'-tetramethyl-1-(2'-methoxy-[1,1'-binaphthalen]-2-yl)-phosphinediamine)dichloroplatin (*trans*-**21b**)

[Pt(η^4-cod)Cl_2] (6.7 mg, 17.5 µmol) and **18b** (11.0 mg, 35.0 µmol) were dissolved in CH_2Cl_2 (2 mL) and stirred at room temperature for 15 minutes. The volatiles were removed *in vacuo* to give the intended product as a colourless solid (quantitative conversion). Slow diffusion of Et_2O into the reaction mixture yielded colourless crystals overnight which were suitable for X-ray diffraction analysis.

^{1}H NMR (500 MHz, CD_2Cl_2): δ = 8.02 (m, $^3J_{HH}$ = 8.8 Hz, $^3J_{HP} \approx$ 12.9 Hz, 2H, *H*3), 7.96 (d, $^3J_{HH}$ = 9.1 Hz, 2H, *H*4'), 7.85 (m, 6H, *H*5'+*H*5+*H*4), 7.44 (d, $^3J_{HH}$ = 9.1 Hz, 2H, *H*3'), 7.41 (ddd, $^3J_{HH}$ = 8.2 Hz, $^3J_{HH}$ = 6.8 Hz, $^4J_{HH}$ = 0.9 Hz, 2H, *H*6), 7.39 (d, $^3J_{HH}$ = 8.5 Hz, 2H, *H*8'), 7.27 (ddd, $^3J_{HH}$ = 8.2 Hz, $^3J_{HH}$ = 6.8 Hz, $^4J_{HH}$ = 0.9 Hz, 2H, *H*6'), 7.11 (ddd, $^3J_{HH}$ = 8.5 Hz, $^3J_{HH}$ = 6.8 Hz, $^4J_{HH}$ = 1.2 Hz, 2H, *H*7), 7.05 (ddd, $^3J_{HH}$ = 8.5 Hz, $^3J_{HH}$ = 6.8 Hz, $^4J_{HH}$ = 1.2 Hz, 2H, *H*7'), 6.79 (d, $^3J_{HH}$ = 8.5 Hz, 2H, *H*8) 3.72 (s, 6H, OCH_3), 2.77 (pt, $^3J_{HP} \approx$ 9.3 Hz, 12H, N(CH_3)$_2$), 1.84 (pt, $^3J_{HP} \approx$ 10.0 Hz, 12H, N(CH_3)$_2$') ppm. **^{13}C{^{1}H} NMR** (126 MHz, CD_2Cl_2): δ = 154.2 (*C*2'), 137.6 (pt, $^2J_{CP}$+$^4J_{CP} \approx$ 6.3 Hz, *C*1), 134.6 (*C*9'), 134.3 (pt, $^1J_{CP}$+$^3J_{CP} \approx$ 74.0 Hz, *C*2), 133.9 (*C*10), 133.2 (pt, $^3J_{CP} \approx$ 9.3 Hz, *C*9), 131.9 (pt, $^2J_{CP}$+$^4J_{CP} \approx$ 20.8 Hz, *C*3), 129.0 (*C*4'), 128.9 (*C*10'), 127.7 (*C*5), 127.4 (*C*5'), 126.9 (*C*6), 126.7 (*C*8'), 126.4 (*C*7'), 126.3 (*C*8), 125.8 (*C*7), 125.0 (pt, $^2J_{CP}$+$^4J_{CP} \approx$ 13.7 Hz, *C*4), 123.6 (*C*6'), 122.0 (*C*1'), 112.5 (*C*3'), 55.7 (O*C*H$_3$), 41.8 (pt, $^2J_{CP}$+$^4J_{CP} \approx$ 6.7 Hz, N(*C*H$_3$)$_2$), 39.6 (pt, $^2J_{CP}$+$^4J_{CP} \approx$ 8.6 Hz, N(*C*H$_3$)$_2$') ppm. **^{31}P{^{1}H} NMR** (202 MHz, CD_2Cl_2): δ = 87.8 (s with ^{195}Pt satellites, $^1J_{PtP}$ = 2955 Hz) ppm. **^{195}Pt{^{1}H} NMR** (108 MHz, CD_2Cl_2): δ = –3747 (t, $^1J_{PtP}$ = 2955 Hz) ppm. **HRMS** (ESI$^+$, MeOH): Found: *m*/*z* = 1093.2626. Calculated for [M + Na]$^+$: *m*/*z* = 1093.2636.

4.4.10 General Procedure for the Preparation of L_P(Se)

The appropriate phosphorus ligand (L_P, 50.0 µmol) and KSeCN (14.4 mg, 100 µmol) were dissolved in THF (1 mL) and heated to 50 °C for 2 hours. The solvent was removed and the residue dissolved in $CDCl_3$. After filtration through celite the product was analysed by ^{31}P{^{1}H} NMR.

^{31}P{^{1}H} NMR (202 MHz, $CDCl_3$): δ = **16a**(Se): 19.6 ($^1J_{PSe}$ = 685 Hz); **16b**(Se): 22.0 ($^1J_{PSe}$ = 683 Hz); **18a**(Se): 80.1 ($^1J_{PSe}$ = 770 Hz); **18b**(Se): 79.8 ($^1J_{PSe}$ = 765 Hz); **19a**(Se): 95.8 ($^1J_{PSe}$ = 858 Hz); **19b**(Se): 97.4 ($^1J_{PSe}$ = 860 Hz) ppm.

4.4.11 General Procedure for the Preparation of *trans*-[Rh(L$_P$)$_2$(CO)Cl]

$[Rh(CO)_2Cl]_2$ (1.2 mg, 3.125 μmol) and phosphorus ligand (L_P, 12.5 μmol) were dissolved in CH_2Cl_2 (0.5 mL) and left to react for 10 minutes. The solvent was removed *in vacuo* and the product analysed by IR spectroscopy.

IR (CH_2Cl_2): ν [Rh(**14a**)$_2$(CO)Cl]: 1983; [Rh(**14b**)$_2$(CO)Cl]: 1985; [Rh(**16a**)$_2$(CO)Cl]: 1965; [Rh(**16b**)$_2$(CO)Cl]: 1963; [Rh(**18a**)$_2$(CO)Cl]: 1972; [Rh(**18b**)$_2$(CO)Cl]: 1969; [Rh(**19a**)$_2$(CO)Cl]: 1999; [Rh(**19b**)$_2$(CO)Cl]: 1996 cm^{-1}.

4.4.12 General Procedure for the Preparation of *trans*-[Pt(L$_P$)(PEt$_3$)Cl$_2$]

$[Pt(PEt_3)Cl_2]_2$ (19.2 mg, 25.0 μmol) and phosphorus ligand (L_P, 50.0 μmol) were dissolved in CD_2Cl_2 (0.55 mL) and left to react for 30 minutes. The products were analysed by $^{31}P\{^1H\}$ and $^{195}Pt\{^1H\}$ NMR spectroscopy.

$^{31}P\{^1H\}$ NMR (202 MHz, CD_2Cl_2): δ = **22a** (*trans*, 51%): 15.5 ($^1J_{PPt}$ = 2871 Hz, $^2J_{PP}$ = 573 Hz, PEt_3), –149.6 ($^1J_{PPt}$ = 2570 Hz, $^2J_{PP}$ = 573 Hz, **14a**); (*cis*, 49%): 10.4 ($^1J_{PPt}$ = 3281 Hz, $^2J_{PP}$ = 23 Hz, PEt_3), –144.1 ($^1J_{PPt}$ = 4381 Hz, $^2J_{PP}$ = 23 Hz, **14a**); **22b** (*trans*, 65%): 13.8 ($^1J_{PPt}$ = 2886 Hz, $^2J_{PP}$ = 575 Hz, PEt_3), –151.9 ($^1J_{PPt}$ = 2566 Hz, $^2J_{PP}$ = 575 Hz, **14b**); (*cis*, 35%): 9.8 ($^1J_{PPt}$ = 3282 Hz, $^2J_{PP}$ = 24 Hz, PEt_3), –144.1 ($^1J_{PPt}$ = 4377 Hz, $^2J_{PP}$ = 24 Hz, **14b**); **23a** (*trans*, 32%): 12.5 ($^1J_{PPt}$ = 2479 Hz, $^2J_{PP}$ = 484 Hz, PEt_3), –4.5 ($^1J_{PPt}$ = 2364 Hz, $^2J_{PP}$ = 484 Hz, **16a**); (*cis*, 68%): 7.1 ($^1J_{PPt}$ = 3412 Hz, $^2J_{PP}$ = 18 Hz, PEt_3), –5.1 ($^1J_{PPt}$ = 3725 Hz, $^2J_{PP}$ = 18 Hz, **16a**); **23b** (*trans*, 36%): 12.0 ($^1J_{PPt}$ = 2464 Hz, $^2J_{PP}$ = 482 Hz, PEt_3), –1.3 ($^1J_{PPt}$ = 2402 Hz, $^2J_{PP}$ = 482 Hz, **16b**); (*cis*, 64%): 7.2 ($^1J_{PPt}$ = 3404 Hz, $^2J_{PP}$ = 18 Hz, PEt_3), –2.9 ($^1J_{PPt}$ = 3737 Hz, $^2J_{PP}$ = 18 Hz, **16b**); **24a** (*trans*, 100%): 90.4 ($^1J_{PPt}$ = 3030 Hz, $^2J_{PP}$ = 545 Hz, **18a**), 10.7 ($^1J_{PPt}$ = 2365 Hz, $^2J_{PP}$ = 545 Hz, PEt_3); **24b** (*trans*, 100%): 90.4 ($^1J_{PPt}$ = 3049 Hz, $^2J_{PP}$ = 543 Hz, **18b**), 10.4 ($^1J_{PPt}$ = 2332 Hz, $^2J_{PP}$ = 543 Hz, PEt_3); **25a** (*trans*, 100%): 119.8 ($^1J_{PPt}$ = 3428 Hz, $^2J_{PP}$ = 604 Hz, **19a**), 10.4 ($^1J_{PPt}$ = 2402 Hz, $^2J_{PP}$ = 604 Hz, PEt_3); **25b** (*trans*, 100%): 117.3 ($^1J_{PPt}$ = 3454 Hz, $^2J_{PP}$ = 604 Hz, **19b**), 8.9 ($^1J_{PPt}$ = 2407 Hz, $^2J_{PP}$ = 604 Hz, PEt_3) ppm. **$^{195}Pt\{^1H\}$ NMR** (108 MHz, CD_2Cl_2): δ = **22a**: –3941 (dd, $^1J_{PtP}$ = 2871 Hz, $^1J_{PtP}$ = 2570 Hz, *trans*), –4493 (dd, $^1J_{PtP}$ = 4381 Hz, $^1J_{PtP}$ = 3281 Hz, *cis*); **22b**: –3921 (dd, $^1J_{PtP}$ = 2886 Hz, $^1J_{PtP}$ = 2566 Hz, *trans*), –4501 (dd, $^1J_{PtP}$ = 4377 Hz, $^1J_{PtP}$ = 3282 Hz, *cis*); **23a**: –3914 (dd, $^1J_{PtP}$ = 2479 Hz, $^1J_{PtP}$ = 2364 Hz, *trans*), –4401 (dd, $^1J_{PtP}$ = 3412 Hz, $^1J_{PtP}$ = 3725 Hz, *cis*); **23b**: –3917 (dd, $^1J_{PtP}$ = 2464 Hz, $^1J_{PtP}$ = 2402 Hz, *trans*), –4412 (dd, $^1J_{PtP}$ = 3404 Hz, $^1J_{PtP}$ = 3737 Hz, *cis*); **24a**: –3869 (dd, $^1J_{PtP}$ = 3030 Hz, $^1J_{PtP}$ = 2365 Hz, *trans*); **24b**: –3839 (dd, $^1J_{PtP}$ = 3049 Hz,

$^{1}J_{PtP}$ = 2332 Hz, *trans*); **25a**: –3881 (dd, $^{1}J_{PtP}$ = 3428 Hz, $^{1}J_{PtP}$ = 2402 Hz, *trans*); **25b**: –3859 (dd, $^{1}J_{PtP}$ = 3454 Hz, $^{1}J_{PtP}$ = 2407 Hz, *trans*).

4.4.13 Chloro((*R*)-1-(2'-methoxy-[1,1'-binaphthalen]-2-yl)phosphirane)(η³-2-methylallyl)palladium (**26b**)

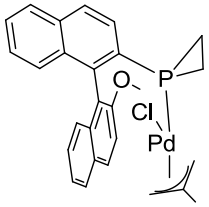

$[Pd(\eta^3\text{-}C_4H_7)Cl]_2$ (19.7 mg, 50 µmol) and **14b** (34.2 mg, 100 µmol) were dissolved in CH_2Cl_2 (2 mL) and stirred for 15 minutes. The intended complex was formed quantitatively.

^{1}H NMR (500 MHz, CD_2Cl_2, –25 °C): δ = isomer **A**,**B** 8.14-8.10 (m, 2H, $H4'^{B}$+$H4'^{A}$), 7.99-7.92 (m, 5H, $H4^{A}$+$H4^{B}$+$H5^{AB}$+$H5'^{B}$), 7.92-7.86 (m, 2H, $H5'^{A}$+$H3^{A}$), 7.84 (dd, $^{3}J_{HH}$ = 8.5 Hz, $^{3}J_{HP}$ = 8.5 Hz, 1H, $H3^{B}$), 7.56-7.49 (m, 4H, $H3'^{AB}$+$H6^{AB}$), 7.33-7.23 (m, 5H, $H6'^{AB}$+$H7^{AB}$+$H7'^{A}$), 7.19-7.09 (m, 3H, $H7'^{B}$+$H8^{A}$+$H8^{B}$), 6.98 (d, $^{3}J_{HH}$ = 8.5 Hz, 1H, $H8'^{A}$), 6.83 (d, $^{3}J_{HH}$ = 8.5 Hz, 1H, $H8'^{B}$), 4.19 (dd, $^{3}J_{HP}$ = 7.4 Hz, $^{4}J_{HH}$ = 2.3 Hz, 1H, allyl-$Ht_{syn}{}^{B}$), 4.12 (dd, $^{3}J_{HP}$ = 7.4 Hz, $^{4}J_{HH}$ = 2.3 Hz, 1H, allyl-$Ht_{syn}{}^{A}$), 3.83 (s, 3H, $OCH_3{}^{B}$), 3.82 (s, 3H, $OCH_3{}^{A}$), 3.14 (s, 1H, allyl-$Hc_{syn}{}^{B}$), 2.90 (d, $^{3}J_{HP}$ = 12.8 Hz, 1H, allyl-$Ht_{anti}{}^{B}$), 2.47 (s, 1H, allyl-$Hc_{syn}{}^{A}$), 2.75 (d, $^{3}J_{HP}$ = 12.8 Hz, 1H, allyl-$Ht_{anti}{}^{A}$), 2.14 (s, 1H, allyl-$Hc_{anti}{}^{B}$), 1.71 (s, 3H, allyl-$CH_3{}^{B}$), 1.61 (s, 3H, allyl-$CH_3{}^{A}$), 1.59 (s, 1H, allyl-$Hc_{anti}{}^{A}$), 1.55-1.05 (m, 8H, $P(CH_2CH_2)^{AB}$) ppm. **^{13}C{^{1}H} NMR** (126 MHz, CD_2Cl_2, –25 °C): δ = isomer **A**,**B** 154.7 ($C2'^{B}$), 154.6 ($C2'^{A}$), 140.8 (d, $^{2}J_{CP}$ = 10.9 Hz, $C1^{AB}$), 134.1 ($C9'^{A}$), 134.0 ($C9'^{A}$), 133.6, 133.5, 132.6-132.4 (m), 132.0-131.7, (m) 131.4 (d, J_{CP} = 5.9 Hz), 130.9 ($C4'^{B}$), 130.8 ($C4'^{A}$), 130.2 (d, $^{2}J_{CP}$ = 10.2 Hz, $C3^{A}$), 129.7 (d, $^{2}J_{CP}$ = 11.1 Hz, $C3^{B}$), 129.0 ($C10'^{B}$), 128.9 ($C10'^{A}$), 128.4 ($C5^{B}$), 128.3 ($C5^{A}$), 128.3 ($C5'^{B}$), 128.3 ($C5'^{A}$), 128.2 (d, $^{3}J_{CP}$ = 9.0 Hz, $C4^{B}$), 128.0 (d, $^{3}J_{CP}$ = 8.5 Hz, $C4^{A}$), 127.6 ($C7'^{A}$), 127.5 ($C6^{AB}$), 127.2 ($C7^{B}$), 127.1 ($C7^{A}$), 127.0 ($C7'^{B}$), 126.2 ($C8^{B}$), 126.1 ($C8^{A}$), 125.6 ($C8'^{A}$), 125.2 ($C8'^{B}$), 124.0 ($C6'^{B}$), 123.8 ($C6'^{A}$), 119.9 (m, $C1'^{AB}$), 113.2 ($C3'^{B}$), 113.0 ($C3'^{A}$), 75.9 (d, $^{2}J_{CP}$ = 40.6 Hz, allyl-Ct^{B}), 75.6 (d, $^{2}J_{CP}$ = 40.6 Hz, allyl-Ct^{A}), 57.7 (allyl-Cc^{A}), 57.6 (allyl-Cc^{B}), 56.2 ($OCH_3{}^{B}$), 56.0 ($OCH_3{}^{A}$), 23.3 (allyl-$CH_3{}^{B}$), 23.2 (allyl-$CH_3{}^{A}$), 18.5 (d, $^{1}J_{CP}$ = 17.5 Hz, $P(CH_2CH_2)^{B}$), 7.7 (d, $^{1}J_{CP}$ = 16.5 Hz, $P(CH_2CH_2)^{A}$), 7.6 (d, $^{1}J_{CP}$ = 16.5 Hz, $P(CH_2CH_2)^{B}$), 7.4 (d, $^{1}J_{CP}$ = 17.1 Hz, $P(CH_2CH_2)^{A}$) ppm. **^{31}P{^{1}H} NMR** (202 MHz, CD_2Cl_2, –25 °C): δ = isomer **A** (63%) –164.9; isomer **B** (37%) –165.8 ppm. **HRMS** (ESI^+): Found: *m*/*z* = 503.0744. Calculated for $[M - Cl]^+$: *m*/*z* = 503.0751.

4.4.14 Chloro((*R*)-(2'-methoxy-[1,1'-binaphthalen]-2-yl)dimethylphosphine)(η³-2-methylallyl)palladium (**27b**)

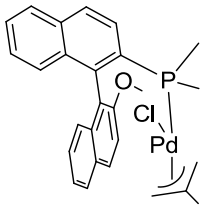

$[Pd(\eta^3\text{-}C_4H_7)Cl]_2$ (19.7 mg, 50 µmol) and **16b** (34.4 mg, 100 µmol) were dissolved in CH_2Cl_2 (2 mL) and stirred for 15 minutes. The intended complex was formed quantitatively. Slow diffusion of Et_2O into the reaction mixture yielded colourless crystals overnight, which were suitable for X-ray diffraction analysis.

^{1}H NMR (500 MHz, CD_2Cl_2, –25 °C): δ = isomer **A**,**B** 8.07-8.03 (m, 4H, *H*4'^{A}+*H*4^A+*H*4^B+*H*4'^{B}), 7.96-7.93 (m, 2H, *H*5^{AB}), 7.91 (dd, $^3J_{HH}$ = 8.8 Hz, $^3J_{HP}$ = 8.8 Hz, 1H, *H*3^B), 7.85 (d, $^3J_{HH}$ = 8.2 Hz, 1H, *H*5'^{B}), 7.83 (dd, $^3J_{HH}$ = 8.8 Hz, $^3J_{HP}$ = 8.8 Hz, 1H, *H*3^A), 7.81 (d, $^3J_{HH}$ = 8.1 Hz, 1H, *H*5'^{A}), 7.52-7.48 (m, 3H, *H*3'^{B}+*H*6^{AB}), 7.47 (d, $^3J_{HH}$ = 9.1 Hz, 1H, *H*3'^{A}), 7.29-7.18 (m, 5H, *H*6'^{A}+*H*7^{AB}+*H*6'^{B}+*H*7'^{A}), 7.15 (ddd, $^3J_{HH}$ = 8.4 Hz, $^3J_{HH}$ = 6.8 Hz, $^4J_{HH}$ = 1.3 Hz, 1H, *H*7'^{B}), 7.12 (d, $^3J_{HH}$ = 8.5 Hz, 1H, *H*8'^{A}), 7.03-6.99 (m, 2H, *H*8^{AB}), 6.79 (d, $^3J_{HH}$ = 8.3 Hz, 1H, *H*8'^{B}), 3.92 (dd, $^3J_{HP}$ = 7.1 Hz, $^4J_{HH}$ = 2.9 Hz, 1H, allyl-*H*t$_{syn}$^{B}), 3.88 (s, 3H, OC*H*$_3$^{B}), 3.82 (dd, $^3J_{HP}$ = 7.1 Hz, $^4J_{HH}$ = 2.6 Hz, 1H, allyl-*H*t$_{syn}$^{A}), 3.79 (s, 3H, OC*H*$_3$^{A}), 2.61 (m, 1H, allyl-*H*c$_{syn}$^{B}), 2.47 (m, 1H, allyl-*H*c$_{syn}$^{A}), 2.14 (d, $^3J_{HP}$ = 10.6 Hz, 1H, allyl-*H*t$_{anti}$^{B}), 2.03 (d, $^3J_{HP}$ = 10.4 Hz, 1H, allyl-*H*t$_{anti}$^{A}), 1.72 (d, $^2J_{HP}$ = 8.7 Hz, 3H, PC*H*$_3$^{A}), 1.65 (s, 3H, allyl-C*H*$_3$^{A}), 1.63 (s, 3H, allyl-C*H*$_3$^{B}), 1.53 (d, $^2J_{HP}$ = 7.7 Hz, 3H, PC*H*$_3$^{B}), 1.50 (d, $^2J_{HP}$ = 9.6 Hz, 3H, PC*H*$_3$^{B}), 1.26 (d, $^2J_{HP}$ = 9.1 Hz, 3H, PC*H*$_3$^{A}), 0.91 (s, 1H, allyl-*H*c$_{anti}$^{B}), 0.53 (s, 1H, allyl-*H*c$_{anti}$^{A}) ppm. **^{13}C{^{1}H} NMR** (126 MHz, CD_2Cl_2, –25 °C): δ = isomer **A**,**B** 155.5 (*C*2'^{B}), 155.1 (*C*2'^{A}), 139.5 (d, $^2J_{CP}$ = 14.5 Hz, *C*1^B), 138.7 (d, $^2J_{CP}$ = 11.3 Hz, *C*1^A), 134.4, 134.0, 133.8, 133.8, 133.1 (d, $^1J_{CP}$ = 56.2 Hz, *C*2^B), 133.0 (d, J_{CP} = 8.4 Hz), 132.8 (d, J_{CP} = 8.4 Hz), 132.6 (d, $^1J_{CP}$ = 56.2 Hz, *C*2^A), 131.9 (d, J_{CP} = 5.4 Hz, allyl-*C*^{B}), 131.2 (d, $^2J_{CP}$ = 5.4 Hz, allyl-*C*^{A}), 130.9, 129.9, 128.8, 128.4, 128.3, 128.2, 128.2, 128.1, 127.8, 127.7, 127.7, 127.5, 127.3 (*C*6^{AB}), 127.2, 127.1, 127.0 (*C*3^A), 126.9 (*C*3^B), 126.9 (*C*8'^{B}), 126.8 (*C*7^{AB}), 126.7 (*C*7'^{B}), 125.7 (*C*8^A), 123.4 (*C*8'^{B}), 119.8 (d, $^3J_{CP}$ = 5.7 Hz, *C*1'^{A}), 119.5 (d, $^3J_{CP}$ = 6.7 Hz, *C*1'^{B}), 113.8 (*C*3'^{B}), 112.6 (*C*3'^{A}), 76.8 (d, $^2J_{CP}$ = 35.4 Hz, allyl-*C*t^B), 75.1 (d, $^2J_{CP}$ = 35.1 Hz, allyl-*C*t^A), 55.8 (O*C*H$_3$^{A}), 55.8 (O*C*H$_3$^{B}), 55.1 (allyl-*C*c^B), 53.6 (d, $^2J_{CP}$ = 1.8 Hz, allyl-*C*c^A), 23.6 (allyl-*C*H$_3$^{B}), 23.6 (allyl-*C*H$_3$^{A}), 17.6 (d, $^1J_{CP}$ = 26.2 Hz, P*C*H$_3$^{B}), 16.3 (d, $^1J_{CP}$ = 25.8 Hz, P*C*H$_3$^{A}), 15.4 (d, $^1J_{CP}$ = 26.4 Hz, P*C*H$_3$^{B}), 14.4 (d,

$^{1}J_{CP}$ = 28.7 Hz, P*C*H$_3$^{A}) ppm. **^{31}P{^{1}H} NMR** (202 MHz, CD_2Cl_2, –25 °C): δ = isomer **A** (67%) –6.1; isomer **B** (33%) –8.7 ppm. **HRMS** (NSI$^+$, MeOH): Found: *m*/*z* = 505.0906. Calculated for [M – Cl]$^+$: *m*/*z* = 505.0918.

4.4.15 Chloro(η^3-2-methylallyl)((*R*)-*N*,*N*,*N*',*N*'-tetramethyl-1-(2'-methoxy-[1,1'-binaphthalen]-2-yl)phosphinediamine)palladium (**28b**)

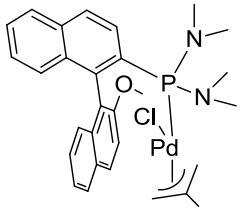

[Pd(η^3-C_4H_7)Cl]$_2$ (19.7 mg, 50 μmol) and **18b** (34.4 mg, 100 μmol) were dissolved in CH_2Cl_2 (2 mL) and stirred for 15 minutes. The intended complex was formed quantitatively.

^{1}H NMR (500 MHz, CD_2Cl_2, –25 °C): δ = isomer **A**,**B** 7.99-7.95 (m, 4H, *H*4'^{AB}+*H*4^{AB}), 7.90-7.87 (m, 4H, *H*5^{AB}+*H*5'^{AB}), 7.68 (dd, $^{3}J_{HP}$ = 12.9 Hz, $^{3}J_{HH}$ = 8.8 Hz, 1H, *H*3^{B}), 7.68 (dd, $^{3}J_{HP}$ = 12.6 Hz, $^{3}J_{HH}$ = 8.8 Hz, 1H, *H*3^{A}), 7.50-7.45 (m, 4H, *H*3'^{AB}+*H*6^{AB}), 7.31-7.26 (m, 2H, *H*6'^{AB}), 7.20-7.15 (m, 4H, *H*7^{AB}+*H*7'^{AB}), 7.00 (d, $^{3}J_{HH}$ = 8.4 Hz, 1H, *H*8'^{B}), 6.99 (d, $^{3}J_{HH}$ = 8.4 Hz, 1H, *H*8'^{A}), 6.91 (d, $^{3}J_{HH}$ = 8.5 Hz, 1H, *H*8^{B}), 6.88 (d, $^{3}J_{HH}$ = 8.5 Hz, 1H, *H*8^{A}), 4.20 (dd, $^{3}J_{HP}$ = 8.1 Hz, $^{4}J_{HH}$ = 3.2 Hz, 1H, allyl-*H*t$_{syn}$^{B}), 4.18 (dd, $^{3}J_{HP}$ = 8.0 Hz, $^{4}J_{HH}$ = 3.1 Hz, 1H, allyl-*H*t$_{syn}$^{A}), 3.76 (s, 3H, OC*H*$_3$^{B}), 3.74 (s, 3H, OC*H*$_3$^{A}), 3.32 (d, $^{3}J_{HP}$ = 11.2 Hz, 1H, allyl-*H*t$_{anti}$^{B}), 3.30 (d, $^{3}J_{HP}$ = 11.2 Hz, 1H, allyl-*H*t$_{anti}$^{A}), 2.78 (s, 1H, allyl-*H*c$_{syn}$^{B}), 2.59 (s, 1H, allyl-*H*c$_{syn}$^{A}), 2.49 (d, $^{3}J_{HP}$ = 9.4 Hz, 6H, N(C*H*$_3$)$_2$^{A}), 2.44 (s, 2H, allyl-*H*c$_{anti}$^{AB}), 2.30 (d, $^{3}J_{HP}$ = 9.4 Hz, 6H, N(C*H*$_3$)$_2$^{B}), 2.16 (d, $^{3}J_{HP}$ = 10.0 Hz, 6H, N(C*H*$_3$)$_2$^{B}), 2.04 (d, $^{3}J_{HP}$ = 9.4 Hz, 6H, N(C*H*$_3$)$_2$^{A}), 1.88 (s, 3H, allyl-C*H*$_3$^{B}), 1.85 (s, 3H, allyl-C*H*$_3$^{A}) ppm. **^{13}C{^{1}H} NMR** (126 MHz, CD_2Cl_2, –25 °C): δ = isomer **A**,**B** 153.9 (*C*2'^{A}), 153.9 (*C*2'^{B}), 138.6 (d, $^{1}J_{CP}$ = 20.3 Hz, *C*2^{A}), 138.3 (d, $^{1}J_{CP}$ = 22.3 Hz, *C*2^{B}), 135.6 (d, $^{2}J_{CP}$ = 6.6 Hz, *C*1^{A}), 135.5 (d, $^{2}J_{CP}$ = 6.2 Hz, *C*1^{B}), 134.0 (*C*9'^{B}), 133.9 (*C*9'^{A}), 133.5 (d, $^{4}J_{CP}$ = 1.5 Hz, *C*10^{A}), 133.5 (d, $^{4}J_{CP}$ = 1.5 Hz, *C*10^{B}), 133.0 (d, $^{3}J_{CP}$ = 8.1 Hz, *C*9^{A}), 132.9 (d, $^{3}J_{CP}$ = 8.1 Hz, *C*9^{B}), 132.7 (d, J_{CP} = 5.7 Hz, allyl-*C*^{A}), 132.6 (d, J_{CP} = 5.7 Hz, allyl-*C*^{B}), 129.6 (d, $^{2}J_{CP}$ = 23.0 Hz, *C*3^{B}), 129.5 (d, $^{2}J_{CP}$ = 21.9 Hz, *C*3^{A}), 129.2 (*C*4'^{B}), 129.2 (*C*4'^{A}), 128.9 (*C*10'^{B}), 128.8 (*C*10'^{A}), 128.2 (*C*5'^{A}), 128.2 (*C*5'^{B}), 128.0 (*C*5^{AB}), 127.7 (d, $^{3}J_{CP}$ = 12.6 Hz, *C*4^{B}), 127.7 (d, $^{3}J_{CP}$ = 12.1 Hz, *C*4^{A}), 127.1 (*C*6^{B}), 127.1 (*C*6^{A}), 126.7 (*C*7^{AB}), 126.7 (*C*7'^{A}), 126.6 (*C*7'^{B}), 126.5 (*C*8^{A}), 126.5 (*C*8^{B}), 125.2 (*C*8'), 123.6 (*C*6'^{B}), 123.5 (*C*6'^{A}), 121.0 (*C*1'^{B}), 120.8 (*C*1'^{A}), 112.9 (*C*3'^{B}), 112.6 (*C*3'^{A}), 77.8 (d, $^{2}J_{CP}$ = 38.7 Hz, allyl-*C*t^{B}), 77.4 (d, $^{2}J_{CP}$ = 38.7 Hz, allyl-*C*t^{A}), 59.9 (allyl-*C*c^{A}),

59.5 (allyl-*C*c^{B}), 56.0 (O*C*H$_3$^{B}), 55.7 (O*C*H$_3$^{A}), 41.3 (d, $^{2}J_{CP}$ = 7.4 Hz, N(*C*H$_3$)$_2$^{A}), 40.7 (d, $^{2}J_{CP}$ = 7.9 Hz, N(*C*H$_3$)$_2$^{B}), 40.3 (d, $^{2}J_{CP}$ = 7.9 Hz, N(*C*H$_3$)$_2$^{B}), 40.2 (d, $^{2}J_{CP}$ = 7.9 Hz, N(*C*H$_3$)$_2$^{A}), 23.2 (allyl-*C*H$_3$) ppm. **^{31}P{^{1}H} NMR** (202 MHz, CD_2Cl_2, –25 °C): δ = isomer **A** (61%) 105.0; isomer **B** (39%) 105.4 ppm. **HRMS** (ESI$^+$): Found: *m*/*z* = 563.1446. Calculated for [M – Cl]$^+$: *m*/*z* = 563.1449.

4.4.16 Chloro(dimethyl (2'-methoxy-[1,1'-binaphthalen]-2-yl)phosphonite)(η^3-2-methylallyl)palladium (**29b**)

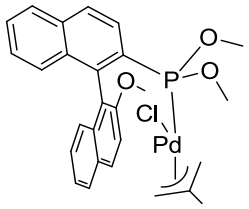

[Pd(η^3-C$_4$H$_7$)Cl]$_2$ (9.8 mg, 25 µmol) and **19b** (18.8 mg, 50 µmol) were dissolved in CD_2Cl_2 (0.7 mL) and stirred for 15 minutes. The intended complex was formed quantitatively.

^{1}H NMR (500 MHz, CD_2Cl_2, –25 °C): δ = isomer **A** 8.15 (dd, $^{3}J_{HH}$ = 8.6 Hz, $^{3}J_{HP}$ = 5.6 Hz, 1H, *H*3), 8.07 (d, $^{3}J_{HH}$ = 8.6 Hz, 1H, *H*4), 7.99-7.97 (m, 2H, *H*5'+*H*5), 7.77 (d, $^{3}J_{HH}$ = 8.1 Hz, 1H, *H*5'), 7.54 (ddd, $^{3}J_{HH}$ = 8.1 Hz, $^{3}J_{HH}$ = 6.8 Hz, $^{4}J_{HH}$ = 1.1 Hz, 1H, *H*6), 7.45 (d, $^{3}J_{HH}$ = 9.1 Hz, 1H, *H*3'), 7.30-7.21 (m, 3H, *H*6'+*H*7+*H*7'), 7.18 (d, $^{3}J_{HH}$ = 8.5 Hz, 1H, *H*8'), 7.05 (d, $^{3}J_{HH}$ = 8.5 Hz, 1H, *H*8), 3.78 (d, $^{3}J_{HP}$ = 14.2 Hz, 3H, POC*H*$_3$), 3.78 (s, 3H, OC*H*$_3$), 3.77 (m, 1H, allyl-*H*t$_{syn}$), 3.35 (d, $^{3}J_{HP}$ = 11.2 Hz, 3H, POC*H*$_3$), 2.73 (s, 1H, allyl-*H*c$_{syn}$), 1.58 (d, $^{3}J_{HP}$ = 11.2 Hz, 1H, allyl-*H*t$_{anti}$), 0.46 (s, 1H, allyl-*H*c$_{anti}$), 1.65 (s, 3H, allyl-C*H*$_3$) ppm. **^{13}C{^{1}H} NMR** (126 MHz, CD_2Cl_2, –25 °C): δ = isomer **A** 156.1 (*C*2'), 140.1 (d, $^{2}J_{CP}$ = 22.4 Hz, *C*1), 133.9 (*C*10), 133.0 (d, $^{1}J_{CP}$ = 10.6 Hz, *C*2), 132.5 (d, $^{3}J_{CP}$ = 8.4 Hz, *C*9), 131.5 (d, allyl-*C*), 130.6 (*C*4'), 128.3 (*C*8'), 128.3 (*C*5), 127.5 (*C*4), 127.9 (*C*6), 127.7 (*C*7'), 127.3 (*C*5'), 127.0 (d, $^{2}J_{CP}$ = 3.9 Hz, *C*3), 126.8 (*C*7), 126.1 (*C*8^{A}), 123.9 (*C*6'), 118.3 (d, $^{3}J_{CP}$ = 7.7 Hz, *C*1'), 112.6 (*C*3'), 76.6 (d, $^{2}J_{CP}$ = 43.5 Hz, allyl-*C*t), 56.0 (d, $^{2}J_{CP}$ = 5.8 Hz, POC*H*$_3$), 55.7 (O*C*H$_3$), 54.5 (d, $^{2}J_{CP}$ = 5.2 Hz, allyl-*C*c), 52.3 (d, $^{2}J_{CP}$ = 13.0 Hz, POC*H*$_3$), 23.4 (allyl-*C*H$_3$) ppm; resonances for *C*9' and *C*10' are obscured. **^{31}P{^{1}H} NMR** (202 MHz, CD_2Cl_2, –25 °C): δ = isomer **A** (89%) 148.9; isomer **B** (11%) 147.2 ppm. **HRMS** (NSI$^+$): Found: *m*/*z* = 533.0824. Calculated for [M – Cl]$^+$: *m*/*z* = 533.0827.

4.4.17 ((*R*)-(2'-Methoxy-[1,1'-binaphthalen]-2-yl-*κC*1')dimethylphosphine-*κP*)(η³-2-methylallyl)palladium tetrakis(3,5-bis(trifluoromethyl)phenyl)borate (**30b**)

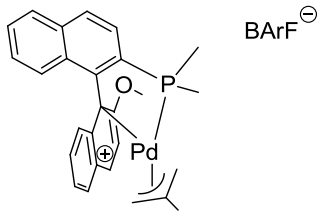

NaBArF (44.3 mg, 50.0 µmol) and **27b** (27.1 mg, 50.0 µmol) were dissolved in CH_2Cl_2 (2 mL) and stirred for 15 minutes. The reaction mixture was filtered through a layer of celite and the solvent removed *in vacuo*; the intended product was obtained as a pale yellow solid.

^{1}H NMR (500 MHz, CD_2Cl_2): δ = isomer **A**,**B** 8.17-8.11 (m, 4H, *H*4+*H*4'), 8.04 (d, $^3J_{HH}$ = 8.2 Hz, 1H, *H*5'), 8.03 (d, $^3J_{HH}$ = 8.2 Hz, 1H, *H*5'), 7.96 (m, 2H, *H*5), 7.91 (d, $^3J_{HH}$ = 9.3 Hz, 1H, *H*3'^{A}), 7.84 (d, $^3J_{HH}$ = 9.2 Hz, 1H, *H*3'^{B}), 7.76 (m, 2H, *H*3), 7.75 (s, 16H, *o*-BArF), 7.58 (s, 8H, *p*-BArF), 7.54-7.49 (m, 4H, *H*6'+*H*6), 7.43 (m, 1H, *H*7'), 7.35 (m, 1H, *H*7'), 7.19-7.14 (m, 2H, *H*7), 7.00 (d, $^3J_{HH}$ = 8.3 Hz, 1H, *H*8'), 6.89 (d, $^3J_{HH}$ = 8.3 Hz, 1H, *H*8'), 5.83 (d, $^3J_{HH}$ = 8.6 Hz, 1H, *H*8), 5.78 (d, $^3J_{HH}$ = 8.6 Hz, 1H, *H*8), 3.90 (s, 3H, OCH_3^A), 3.82 (s, 3H, OCH_3^B), 3.58 (d, $^3J_{HP}$ = 9.5 Hz, 1H, allyl-*H*t$_{anti}$), 3.44 (s, 1H, allyl-*H*c$_{syn}$), 3.23 (s, 1H, allyl-*H*c$_{syn}$), 2.71 (d, $^3J_{HP}$ = 9.5 Hz, 1H, allyl-*H*t$_{anti}$), 2.61 (s, 1H, allyl-*H*c$_{anti}$), 2.55 (dd, $^3J_{HP}$ = 5.8 Hz, $^4J_{HH}$ = 3.0 Hz, 1H, allyl-*H*t$_{syn}$), 2.47 (s, 1H, allyl-*H*c$_{anti}$), 2.06 (dd, $^3J_{HP}$ = 6.3 Hz, $^4J_{HH}$ = 3.1 Hz, 1H, allyl-*H*t$_{syn}$), 1.95 (d, $^2J_{HP}$ = 10.2 Hz, 3H, PCH_3), 1.93 (d, $^2J_{HP}$ = 10.0 Hz, 3H, PCH_3), 1.83 (s, 3H, allyl-CH_3), 1.80 (d, $^2J_{HP}$ = 10.3 Hz, 3H, PCH_3), 1.72 (d, $^2J_{HP}$ = 10.3 Hz, 3H, PCH_3), 1.10 (s, 3H, allyl-CH_3) ppm; in some cases the distinct assignment of resonances to the respective isomer was unavailable. **^{11}B NMR** (128 MHz, CD_2Cl_2): δ = –7.6 ppm. **^{13}C{^{1}H} NMR** (126 MHz, CD_2Cl_2): δ = isomer **A**,**B** 161.8 (q, $^1J_{CB}$ = 49.9 Hz, *ipso*-BArF), 155.6 (*C*2'^{A}), 154.0 (*C*2'^{B}), 140.6 (d, $^2J_{CP}$ = 27.0 Hz, *C*1), 137.0 (d, $^2J_{CP}$ = 27.0 Hz, allyl-*C*^{A}), 136.4 (d, $^2J_{CP}$ = 27.0 Hz, allyl-*C*^{B}), 136.1 (d, $^1J_{CP}$ = 30.7 Hz, *C*2), 135.8, 135.7 (d, $^1J_{CP}$ = 30.7 Hz, *C*2), 134.9 (*o*-BArF), 134.2 (*C*4'^{A}), 133.9 (*C*4'^{B}), 132.3 (*C*9'^{B}), 131.9 (d, $^3J_{CP}$ = 3.9 Hz, *C*9), 131.8 (d, $^3J_{CP}$ = 3.7 Hz, *C*9), 131.5 (*C*4), 131.4 (*C*4), 131.2 (*C*9'^{A}), 129.9 (*C*10'^{B}), 129.7 (*C*5'), 129.5 (*C*5'), 129.3, 129.0 (qq, $^2J_{CF}$ = 31.2 Hz, $^4J_{CF}$ = 2.9 Hz, *m*-BArF), 128.6 (*C*5), 128.5 (*C*6), 128.3 (*C*7), 128.3 (*C*7), 126.4 (*C*6'^{B}), 126.3 (*C*6'^{A}), 124.7 (q, $^1J_{CF}$ = 272.3 Hz, *C*F$_3$), 124.7 (*C*8), 124.5 (*C*8), 124.0, 122.6 (*C*8'^{A}), 122.0 (*C*8'^{B}), 117.5 (septet, $^3J_{CF}$ = 4.0 Hz, *p*-BArF), 115.5 (*C*3'^{B}), 115.0 (*C*3'^{A}), 105.2 (*C*1'^{B}), 104.6 (*C*1'^{A}), 98.2 (d, $^2J_{CP}$ = 30.4 Hz, allyl-*C*t), 97.6 (d, $^2J_{CP}$ = 30.7 Hz, allyl-*C*t), 57.2 (O*C*H$_3^A$), 57.0 (O*C*H$_3^B$), 52.7 (d, $^2J_{CP}$ = 2.7 Hz, allyl-*C*c^B), 52.5 (d, $^2J_{CP}$ = 2.7 Hz, allyl-*C*c^A), 22.9

(allyl-CH_3^B), 21.7 (allyl-CH_3^A), 16.2 (d, $^1J_{CP}$ = 28.9 Hz, PCH_3), 16.2 (d, $^1J_{CP}$ = 29.3 Hz, PCH_3), 15.4 (d, $^1J_{CP}$ = 28.3 Hz, PCH_3), 15.0 (d, $^1J_{CP}$ = 29.3 Hz, PCH_3) ppm; in some cases the distinct assignment of resonances to the respective isomer was unavailable. **^{19}F NMR** (376 MHz, CD_2Cl_2): δ = –62.7 ppm. **^{31}P{^{1}H} NMR** (202 MHz, CD_2Cl_2): δ = isomer **A**,**B** (1:1 ratio) 9.4, 8.7 ppm. **HRMS** (ESI^+): Found: m/z = 501.0925. Calculated for $[M - BArF]^+$: m/z = 501.0934.

4.4.18 ((*R*)-*N*,*N*,*N*',*N*'-Tetramethyl-1-(2'-methoxy-[1,1'-binaphthalen]-2-yl-κ*C*1')phosphinediamine-κ*P*)(η^3-2-methylallyl)palladium tetrakis(3,5-bis(trifluoromethyl)phenyl)borate (**31b**)

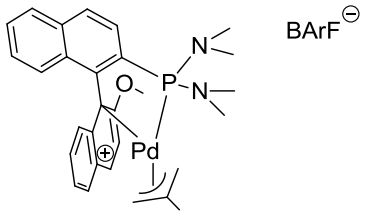

NaBArF (44.3 mg, 50.0 µmol) and **28b** (30.0 mg, 50.0 µmol) were dissolved in CH_2Cl_2 (2 mL) and stirred for 15 minutes. The reaction mixture was filtered through a layer of celite and the solvent removed *in vacuo*; the intended product was obtained as a pale yellow solid. Slow evaporation of a CH_2Cl_2 solution gave crystals which were suitable for X-ray analysis.

^{1}H NMR (500 MHz, CD_2Cl_2): δ = isomer **A**,**B** 8.12 (d, $^3J_{HH}$ = 9.2 Hz, 2H, *H*4'), 8.10 (d, $^3J_{HH}$ = 8.5 Hz, 2H, *H*4), 8.05 (d, $^3J_{HH}$ = 8.3 Hz, 1H, *H*5'), 8.03 (d, $^3J_{HH}$ = 8.3 Hz, 1H, *H*5'), 7.94 (d, $^3J_{HH}$ = 8.3 Hz, 2H, *H*5), 7.93 (d, $^3J_{HH}$ = 9.2 Hz, 1H, *H*3'), 7.85 (d, $^3J_{HH}$ = 9.2 Hz, 1H, *H*3'), 7.81 (dd, $^3J_{HH}$ = 8.5 Hz, $^3J_{HP}$ = 6.5 Hz, 2H, *H*3), 7.75 (s, 16H, *o*-BArF), 7.58 (s, 8H, *p*-BArF), 7.55-7.47 (m, 4H, *H*6'+*H*6), 7.44 (m, 1H, *H*7'), 7.36 (m, 1H, *H*7'), 7.15-7.10 (m, 2H, *H*7), 7.07 (d, $^3J_{HH}$ = 8.4 Hz, 1H, *H*8'), 6.95 (d, $^3J_{HH}$ = 8.4 Hz, 1H, *H*8'), 5.67 (d, $^3J_{HH}$ = 8.3 Hz, 1H, *H*8), 5.66 (d, $^3J_{HH}$ = 8.3 Hz, 1H, *H*8), 3.87 (s, 3H, OCH_3), 3.82 (d, $^3J_{HP}$ = 10.6 Hz, 1H, allyl-*H*t$_{anti}$), 3.78 (s, 3H, OCH_3), 3.63 (m, 1H, allyl-*H*c$_{syn}$), 3.33 (m, 1H, allyl-*H*c$_{syn}$), 2.70 (d, $^3J_{HP}$ = 14.4 Hz, 3H, NCH_3), 2.69 (d, $^3J_{HP}$ = 14.4 Hz, 3H, NCH_3), 2.68 (m, 1H, allyl-*H*t$_{anti}$), 2.61 (d, $^3J_{HP}$ = 12.2 Hz, 6H, NCH_3), 2.58 (m, 1H, allyl-*H*c$_{anti}$), 2.45 (dd, $^3J_{HP}$ = 7.4 Hz, $^4J_{HH}$ = 2.8 Hz, 1H, allyl-*H*t$_{syn}$), 2.37 (s, 1H, allyl-*H*c$_{anti}$), 1.90-1.84 (m, 4H, allyl-*H*t$_{syn}$+allyl-CH_3), 1.08 (s, 3H, allyl-CH_3) ppm; in some cases the distinct assignment of resonances to the respective isomer was unavailable. **^{11}B NMR** (128 MHz, CD_2Cl_2): δ = –7.5 ppm. **^{13}C{^{1}H} NMR** (101 MHz, CD_2Cl_2): δ = isomer **A**,**B** 161.8 (q, $^1J_{CB}$ = 50.2 Hz, *ipso*-BArF), 156.2 (*C*2'), 154.5 (*C*2'), 140.7 (d, $^1J_{CP}$ = 35.3 Hz, *C*2), 140.6 (d, $^1J_{CP}$ = 35.1 Hz, *C*2), 140.5

(d, $^{2}J_{CP}$ = 18.2 Hz, *C*1), 140.0 (d, $^{2}J_{CP}$ = 18.5 Hz, *C*1), 136.1 (m, *C*9), 135.7 (d, $^{2}J_{CP}$ = 7.8 Hz, allyl-*C*), 135.2 (d, $^{2}J_{CP}$ = 8.0 Hz, allyl-*C*), 134.8 (*o*-BArF), 134.4 (*C*4'), 134.2 (*C*4'), 133.2 (*C*9'), 132.2 (*C*9'), 132.0 (m, *C*9), 131.9 (m, *C*10), 130.6 (d, $^{3}J_{CP}$ = 3.4 Hz, *C*4), 130.5 (d, $^{3}J_{CP}$ = 3.4 Hz, *C*4), 130.1 (*C*7'), 129.8 (*C*7'), 129.5 (*C*5'), 129.3 (*C*5'), 129.2 (d, $^{5}J_{CP}$ = 0.9 Hz, *C*10'), 128.9 (d, $^{5}J_{CP}$ = 0.9 Hz, *C*10'), 128.9 (qq, $^{2}J_{CF}$ = 31.2 Hz, $^{4}J_{CF}$ = 2.9 Hz, *m*-BArF), 128.5 (*C*5+*C*6), 128.1 (*C*7), 126.6 (*C*6'), 126.3 (*C*6'), 124.7 (q, $^{1}J_{CF}$ = 272.3 Hz, *C*F$_3$), 124.5-124.3 (m, *C*3+*C*8'+*C*8), 117.5 (septet, $^{3}J_{CF}$ = 4.0 Hz, *p*-BArF), 115.6 (*C*3'), 115.1 (*C*3'), 102.5 (*C*1'), 102.4 (*C*1'), 101.0 (d, $^{2}J_{CP}$ = 34.8 Hz, allyl-*C*t), 100.1 (d, $^{2}J_{CP}$ = 34.4 Hz, allyl-*C*t), 57.0 (O*C*H$_3$), 56.8 (O*C*H$_3$), 46.0 (d, $^{2}J_{CP}$ = 5.5 Hz, allyl-*C*c), 45.7 (d, $^{2}J_{CP}$ = 5.7 Hz, allyl-*C*c), 38.1 (d, $^{2}J_{CP}$ = 9.1 Hz, N*C*H$_3$), 38.0 (d, $^{2}J_{CP}$ = 8.7 Hz, N*C*H$_3$), 37.9 (d, $^{2}J_{CP}$ = 9.1 Hz, N*C*H$_3$), 37.8 (d, $^{2}J_{CP}$ = 8.7 Hz, N*C*H$_3$), 22.9 (allyl-*C*H$_3$), 21.6 (allyl-*C*H$_3$) ppm; in some cases the distinct assignment of resonances to the respective isomer was unavailable. **^{19}F NMR** (376 MHz, CD_2Cl_2): δ = –62.7 ppm. **^{31}P{^{1}H} NMR** (202 MHz, CD_2Cl_2): δ = isomer **A**,**B** (1:1 ratio) 120.5, 120.5 ppm. **HRMS** (ESI$^+$): Found: *m*/*z* = 562.1448. Calculated for [M – BArF]$^+$: *m*/*z* = 562.1460.

4.4.19 Bis((*R*)-(2'-Methoxy-[1,1'-binaphthalen]-2-yl)dimethylphosphine)(η^3-2-methylallyl)palladium tetrakis(3,5-bis(trifluoromethyl)phenyl)borate (**32b**)

16b (17.2 mg, 50.0 µmol) and **30b** (68.5 mg, 50.0 µmol) were dissolved in CH_2Cl_2 (2 mL) and stirred for 15 minutes. The solvent was removed *in vacuo* and the intended product was obtained as a yellow solid.

^{1}H NMR (500 MHz, CD_2Cl_2): δ = 8.09 (d, $^{3}J_{HH}$ = 9.2 Hz, 1H, *H*4'^{B}), 8.09 (d, $^{3}J_{HH}$ = 9.2 Hz, 1H, *H*4'^{A}), 8.04 (d, $^{3}J_{HH}$ = 8.7 Hz, 1H, *H*4^{A}), 7.96 (d, $^{3}J_{HH}$ = 8.2 Hz, 1H, *H*5^{A}), 7.93-7.88 (m, 4H, *H*5'^{B}+*H*4^{B}+*H*5^{B}+*H*5'^{A}), 7.78 (s, 8H, *o*-BArF), 7.64 (dd, $^{3}J_{HP}$ = 11.5 Hz, $^{3}J_{HH}$ = 8.7 Hz, 1H, *H*3^{A}), 7.60 (s, 4H, *p*-BArF), 7.58-7.54 (m, 2H, *H*6^{A}+*H*6^{B}), 7.49 (d, $^{3}J_{HH}$ = 9.2 Hz, 1H, *H*3'^{A}), 7.49 (dd, $^{3}J_{HP}$ = 13.9 Hz, $^{3}J_{HH}$ = 8.7 Hz, 1H, *H*3^{B}), 7.46 (d, $^{3}J_{HH}$ = 9.2 Hz, 1H, *H*3'^{B}), 7.37 (ddd, $^{3}J_{HH}$ = 8.1 Hz, $^{3}J_{HH}$ = 6.8 Hz, $^{4}J_{HH}$ = 1.1 Hz, 1H, *H*6'^{B}), 7.33-7.24 (m, 3H, *H*7^{B}+*H*6'^{A}+*H*7^{A}), 7.22 (ddd, $^{3}J_{HH}$ = 8.5 Hz, $^{3}J_{HH}$ = 6.8 Hz, $^{4}J_{HH}$ = 1.3 Hz, 1H, *H*7'^{B}), 7.05 (d, $^{3}J_{HH}$ = 8.6 Hz, 1H, *H*8^{B}), 7.05 (ddd, $^{3}J_{HH}$ = 8.5 Hz, $^{3}J_{HH}$ = 6.8 Hz, $^{4}J_{HH}$ = 1.2 Hz, 1H, *H*7'^{A}), 7.00 (d, $^{3}J_{HH}$ = 8.6 Hz, 1H, *H*8^{A}), 6.76 (d, $^{3}J_{HH}$ = 8.5 Hz, 1H, *H*8'^{B}), 6.73 (d, $^{3}J_{HH}$ = 8.5 Hz, 1H, *H*8'^{A}), 3.79 (s, 3H, OC*H*$_3^{B}$), 3.76 (s, 3H, OC*H*$_3^{A}$), 3.65 (s, 1H, allyl-*H*$_{syn}$), 3.57 (s, 1H, allyl-*H*$_{syn}$), 1.78 (d, $^{3}J_{HP}$ = 10.1 Hz, 1H, allyl-*H*$_{anti}$), 1.74 (s, 3H, allyl-C*H*$_3$), 1.64 (d, $^{3}J_{HP}$ = 10.1 Hz, 1H, allyl-*H*$_{anti}$), 1.40 (d, $^{2}J_{HP}$ = 8.5 Hz, 3H, PC*H*$_3^{A}$), 1.21 (d, $^{2}J_{HP}$ = 9.5 Hz, 3H, PC*H*$_3$'^{A}), 1.10 (d, $^{2}J_{HP}$ = 9.0 Hz, 3H, PC*H*$_3^{B}$), 1.08 (d, $^{2}J_{HP}$ = 8.9 Hz, 3H, PC*H*$_3$'^{B}) ppm;

only one isomer was observed; labelled as A,B to distinguish between the resonances of the two ligands. **^{11}B NMR** (128 MHz, CD_2Cl_2): δ = –7.5 ppm. **^{13}C{^{1}H} NMR** (126 MHz, CD_2Cl_2): δ = 161.9 (q, $^1J_{CB}$ = 50.0 Hz, *ipso*-BArF), 155.4 ($C2'^A$), 155.1 ($C2'^B$), 139.5 (d, $^2J_{CP}$ = 7.6 Hz, $C1^A$), 139.3 (d, $^2J_{CP}$ = 3.4 Hz, $C1^B$), 137.3 (pt, $^2J_{CP}$ = 5.4 Hz, allyl-*C*), 134.9 (*o*-BArF), 134.4 (d, $^4J_{CP}$ = 2.0 Hz, $C10^A$), 134.3 (d, $^4J_{CP}$ = 2.0 Hz, $C10^B$), 134.3 ($C9'^A$), 134.2 ($C9'^B$), 133.4 (d, $^3J_{CP}$ = 1.6 Hz, $C9^A$), 133.3 (d, $^3J_{CP}$ = 2.4 Hz, $C9^B$), 131.5 ($C4'^A$), 131.4 ($C4'^B$), 130.5 (d, $^1J_{CP}$ = 41.6 Hz, $C2^A$), 129.9 (d, $^1J_{CP}$ = 41.8 Hz, $C2^B$), 129.4 (d, $^2J_{CP}$ = 24.3 Hz, $C3^B$), 129.1 ($C10'^B$), 129.0 (qq, $^2J_{CF}$ = 31.2 Hz, $^4J_{CF}$ = 2.9 Hz, *m*-BArF), 128.9 ($C10'^A$), 128.7 ($C4^A$+$C5'^A$), 128.5 ($C4^B$+$C5^B$), 128.2 ($C5^A$), 128.2 ($C6^A$+$C6^B$), 128.1 ($C5'^B$), 127.6 ($C7^A$), 127.6 ($C7^B$), 127.3 ($C7'^B$), 127.1 (d, $^2J_{CP}$ = 12.6 Hz, $C3^A$), 127.1 ($C7'^A$), 126.2 ($C8^B$), 126.1 ($C8^A$), 124.7 (q, $^1J_{CF}$ = 272.3 Hz, CF_3), 125.0 ($C8'^B$), 124.5 ($C6'^B$), 124.3 ($C8'^A$), 124.1 ($C6'^A$), 120.1 ($C1'^B$), 119.7 ($C1'^A$), 117.6 (septet, $^3J_{CF}$ = 4.0 Hz, *p*-BArF), 113.4 ($C3'^A$), 113.3 ($C3'^B$), 70.6 (d, $^2J_{CP}$ = 30.5 Hz, allyl-CH_2), 69.8 (d, $^2J_{CP}$ = 30.8 Hz, allyl-CH_2'), 56.3 (OCH_3^B), 55.9 (OCH_3^A), 23.6 (allyl-CH_3), 17.7 (dd, $^1J_{CP}$ = 27.2 Hz, $^3J_{CP}$ = 2.4 Hz, $PCH_3'^A$), 17.5 (dd, $^1J_{CP}$ = 26.9 Hz, $^3J_{CP}$ = 2.4 Hz, PCH_3^B), 16.3 (m, PCH_3^A+$PCH_3'^B$) ppm; only one isomer was observed; labelled as A,B to distinguish between the resonances of the two ligands. **^{19}F NMR** (376 MHz, CD_2Cl_2): δ = –62.7 ppm. **^{31}P{^{1}H} NMR** (202 MHz, CD_2Cl_2): δ = –2.1 (d, $^2J_{PP}$ = 43 Hz, P^A), –7.6 (d, $^2J_{PP}$ = 43 Hz, P^B) ppm; only one isomer was observed; labelled as A,B to distinguish between the resonances of the two ligands. **HRMS** (ESI^+): Found: *m*/*z* = 845.2245. Calculated for $[M - BArF]^+$: *m*/*z* = 845.2258.

4.4.20 Palladium Catalysed Asymmetric Allylic Alkylation of (*rac*)-(*E*)-1,3-Diphenylallyl Acetate

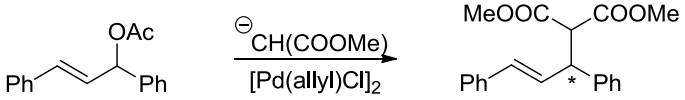

$[Pd(\eta^3\text{-}C_3H_5)Cl]_2$ (3.7 mg, 0.01 mmol) and ligand (0.04 mmol) were dissolved in CH_2Cl_2 (3ml) and stirred for 20 minutes. Subsequently the reaction was treated with a solution of (*rac*)-(*E*)-1,3-diphenylallyl acetate (126 mg, 0.5 mmol) in CH_2Cl_2 (3 mL), KOAc (5 mg, 0.05 mmol), dimethyl malonate (0.11 mL, 1.0 mmol) and N,O-bis(trimethylsilyl)acetamide (0.25 mL, 1.0 mmol). The reaction mixture was stirred at room temperature and the conversion was monitored by TLC analysis. After the appropriate reaction time the solution was diluted with Et_2O (20 ml) and washed with saturated aqueous NH_4Cl (3 × 20 ml). The organic phase was dried over $MgSO_4$. The product was purified by column chromatography

(hexane/EtOAc, 3:1, $R_f = 0.50$) on silica media (h = 13 cm, d = 2 cm) to give the final product as a colourless oil (in some cases the oil became a white solid after a few hours). The enantiomeric excess was measured by chiral HPLC (Column Daicel Chiralpak AD-H; flow rate: 1.0 mL/min; hexane/2-propanol, 90:10; retention times: (*R*) t_1 = 10.0 min, (*S*) t_2 = 13.4 min).[246]

4.5 References

193 The manuscript for publishing the content of this chapter in a peer-reviewed scientific journal is currently in preparation: A. Ficks, R. W. Harrington, L. J. Higham, Chiral MOP-Type Ligands: Structural and Electronic Impact in Palladium(II) and Platinum(II) Complexes; Applications in Asymmetric Hydrosilylation and Allylic Alkylation.

194 R. Noyori, *Angew. Chem. Int. Ed.* **2002**, *41*, 2008.

195 C. A. Tolman, *Chem. Rev.* **1977**, *77*, 313.

196 See for example: (a) O. Kühl, *Coord. Chem. Rev.* **2005**, *249*, 693; (b) T. L. Brown, K. J. Lee, *Coord. Chem. Rev.* **1993**, *128*, 89; (c) S. P. Flanagan, P. J. Guiry, *J. Organomet. Chem.* **2006**, *691*, 2125; (d) N. Fey, A. G. Orpen, J. N. Harvey, *Coord. Chem. Rev.* **2009**, *253*, 704.

197 (a) J. W. Han, T. Hayashi, *Tetrahedron*: *Asymmetry* **2010**, *21*, 2193; (b) T. Hayashi, *Acc. Chem. Res*. **2000**, *33*, 354.

198 F. Lagasse, H. B. Kagan, *Chem. Pharm. Bull.* **2000**, *48*, 315.

199 P. Kočovský, S. Vyskočil, M. Smrčina, *Chem. Rev.* **2003**, *103*, 3213, and references therein.

200 (a) T. Hayashi, S. Hirate, K. Kitayama, H. Tsuji, A. Torii, Y. Uozumi, *J. Org. Chem.* **2001**, *66*, 1441; (b) T. Hayashi, *Acta Chem. Scand.* **1996**, *50*, 259.

201 (a) E. F. Clarke, E. Rafter, H. Müller-Bunz, L. J. Higham, D. G. Gilheany, *J. Organomet. Chem.* **2011**, *696*, 3608; (b) N. Armanino, R. Koller, A. Togni, *Organometallics* **2010**, *29*, 1771; (c) B. Saha, T. V. RajanBabu, *J. Org. Chem.* **2007**, *72*, 2357; (d) X. Xie, T. Y. Zhang, Z. Zhang, *J. Org. Chem.* **2006**, *71*, 6522; (e) T. Hamada, A. Chieffi, J. Åhman, S. L. Buchwald, *J. Am. Chem. Soc.* **2002**, *124*, 1261; (f) J.-X. Chen, J. F. Daeuble, J. M. Stryker, *Tetrahedron* **2000**, *56*, 2789.

202 (a) L. Maier, in *Organic Phosphorus Compounds, Vol. 1* (Eds.: G. M. Kosolapoff, L. Maier), Wiley-Interscience, New York, 1972, pp. 4–16; (b) L. J. Higham, in

Phosphorus Compounds: Advanced Tools in Catalysis and Material Sciences, Catalysis by Metal Complexes, Vol. 37 (Eds.: M. Peruzzini, L. Gonsalvi), Springer, Germany, **2011**, pp. 1–19.

203 (a) M. Brynda, *Coord. Chem. Rev.* **2005**, *249*, 2013; (b) K. V. Katti, N. Pillarsetty, K. Raghuraman, *Top. Curr. Chem.* **2003**, *229*, 121.

204 (a) W. Henderson, S. R. Alley *J. Organomet. Chem.* **2002**, *656*, 120; (b) N. Pillarsetty, K. Raghuraman, C. L. Barnes, K. V. Katti, *J. Am. Chem. Soc.* **2005**, *127*, 331.

205 R. M. Hiney, L. J. Higham, H. Müller-Bunz, D. G. Gilheany, *Angew. Chem. Int. Ed.* **2006**, *45*, 7248.

206 A. Ficks, I. Martinez-Botella, B. Stewart, R. W. Harrington, W. Clegg, L. J. Higham, *Chem. Commun.* **2011**, *47*, 8274.

207 (a) F. Mathey, *Chem. Rev.* **1990**, *90*, 997; (b) L. D. Quin, in *A Guide to Organophosphorus Chemistry* (Ed.: L. D. Quin), John Wiley Sons, New York, 2000, pp. 234–241; (c) F. Mathey and M. Regitz, in *Phosphorus-Carbon Heterocyclic Chemistry: The Rise of a New Domain* (Ed.: F. Mathey), Elsevier Science, Amsterdam, 2001, pp. 17–55.

208 (a) M. Shi, L.-H. Chen, C.-Q. Li, *J. Am. Chem. Soc.* **2005**, *127*, 3790; (b) M. Shi, C.-Q. Li, *Tetrahedron: Asymmetry* **2005**, *16*, 1385; (c) M. Shi, X.-G. Liu, Y.-W. Guo, W. Zhang, *Tetrahedron* **2007**, *63*, 12731.

209 A. Ficks, C. Sibbald, S. Ojo, R. W. Harrington, W. Clegg, L. J. Higham, *Synthesis* **2013**, *45*, 265.

210 N. Z. Weferling, *Z. Anorg. Allg. Chem.* **1987**, *548*, 55.

211 A. Ficks, R. M. Hiney, R. W. Harrington, D. G. Gilheany, L. J. Higham, *Dalton Trans.* **2012**, *41*, 3515.

212 B. Stewart, A. Harriman, L. J. Higham, *Organometallics* **2011**, *30*, 5338.

213 (a) A. Orthaber, M. Fuchs, F. Belaj, G. N. Rechberger, C. O. Kappe, R. Pietschnig, *Eur. J. Inorg. Chem.* **2011**, 2588; (b) R. Starosta, A. Bykowska, M. Barys, A. K. Wieliczko, Z. Staroniewicz, M. Jeżowska-Bojczuk, *Polyhedron* **2011**, *30*, 2914; (c) M. Clarke, D. J. Cole-Hamilton, A. M. Z. Slawin, J. D. Woollins, *Chem. Commun.* **2000**, 2065; (d) M. L. Clarke, G. L. Holliday, A. M. Z. Slawin, J. D. Woollins, *J. Chem. Soc., Dalton Trans.* **2002**, 1093; (e) P. W. Dyer, J. Fawcett, M. J. Hanton, R. D. W. Kemmitt, R.

Padda, *Dalton Trans.* **2003**, 104; (f) J. Cheng, F. Wang, J.-H. Xu, Y. Pan, Z. Zhang, *Tetrahedron Lett.* **2003**, *44*, 7095.

214 J. Gopalakrishnan, *Appl. Organometal. Chem.* **2009**, *23*, 291.

215 (a) W. McFarlane, D. S. Rycroft, *J. Chem. Soc., Dalton Trans.* **1973**, 2162; (b) W. McFarlane, D. S. Rycroft, *J. Chem. Soc., Chem. Commun.* **1972**, 902.

216 (a) D. W. Allen, B. F. Taylor, *J. Chem. Soc., Dalton Trans.* **1982**, 51; (b) R. P. Pinnell, C. A. Megerle, S. L. Manatt, P. A. Kroon, *J. Am. Chem. Soc.* **1973**, *95*, 977.

217 P. B. Dias, M. E. Minas de Piedade, J. A. Martinho Simões, *Coord. Chem. Rev.* **1994**, *135/136*, 737.

218 A. Muller, S. Otto, A. Roodt, *Dalton Trans.* **2008**, 650.

219 (a) A. Roodt, S. Otto, G. Steyl, *Coord. Chem. Rev.* **2003**, *245*, 121; (b) S. Otto, A. Roodt, *Inorg. Chim. Acta* **2004**, *357*, 1.

220 G. Kemp, A. Roodt, W. Purcell, *Rhodium Expr.* **1995**, *12*, 21.

221 (*a*) J. Liedtke, S. Loss, G. Alcaraz, V. Gramlich, H. Grützmacher, *Angew. Chem. Int. Ed.* **1999**, *38*, 1623; (*b*) J. Liedtke, S. Loss, C. Widauer, H. Grützmacher, *Tetrahedron* **2000**, *56*, 143; (*c*) J. Liedtke, H. Rüegger, S. Loss, H. Grützmacher, *Angew. Chem. Int. Ed.* **2000**, *39*, 2478; (*d*) C. Laporte, G. Frison, H. Grützmacher, A. C. Hillier, W. Sommer, S. P. Nolan, *Organometallics* **2003**, *22*, 2202.

222 (a) H. M. Senn, D. V. Deubel, P. E. Blöchl, A. Togni, G. Frenking, *J. Mol. Struct. Theochem* **2000**, *506*, 233; (b) N. Fey, A. C. Tsipis, S. E. Harris, J. N. Harvey, A. G. Orpen, R. A. Mansson, *Chem. Eur. J.* **2006**, *12*, 291.

223 M. Carreira, M. Charernsuk, M. Eberhard, N. Fey, R. van Ginkel, A. Hamilton, W. P. Mul, A. G. Orpen, H. Phetmung, P. G. Pringle, *J. Am. Chem. Soc*. **2009**, *131*, 3078.

224 B. J. Dunne, R. B. Morris, A. G. Orpen, *J. Chem. Soc., Dalton Trans.* **1991**, 653.

225 T. E. Müller, D. M. P. Mingos, *Transition Met. Chem.* **1995**, *20*, 533.

226 For an overview of steric and electronic descriptors see: N. Fey, *Dalton Trans.* **2010**, *39*, 296.

227 J. Mathew, T. Thomas, C. H. Suresh, *Inorg. Chem.* **2007**, *46*, 10800.

228 For reviews on ^{195}Pt NMR see: (a) B. M. Still, P. G. A. Kumar, J. R. Aldrich-Wright, W. S. Price, *Chem. Soc. Rev.* **2007**, *36*, 665; (b) P. S. Pregosin, *Coord. Chem. Rev.* **1982**, *44*, 247; (c) P. S. Pregosin, *Annu. Rep. NMR Spectrosc.* **1986**, *17*, 285; (d) J. D.

Kennedy, W. McFarlane, R. J. Puddephatt, P. J. Thompson, *J. Chem. Soc., Dalton Trans.* **1976**, 874.

229 G. G. Mather, A. Pidcock, G. J. N. Rapsey, *J. Chem. Soc., Dalton Trans.* **1972**, *19*, 2095.

230 (a) P. G. Waddell, A. M. Z. Slawin, J. D. Woollins, *Dalton Trans.* **2010**, *39*, 8620; (b) C. J. Cobley, P. G. Pringle, *Inorg. Chim. Acta* **1997**, *265*, 107.

231 T. G. Appleton, H. C. Clark, L. E. Manzer, *Coord. Chem. Rev.* **1973**, *10*, 335.

232 (a) L. Rigamonti, C. Manassero, M. Rusconi, M. Manassero, A. Pasini, *Dalton Trans.* **2009**, 1206; (b) R. Münzenberg, P. Rademacher, R. Boese, *J. Mol. Struct.* **1998**, *444*, 77.

233 K. M. Anderson, A. G. Orpen, *Chem. Commun.* **2001**, 2682.

234 (a) S. B. Clendenning, P. B. Hitchcock, G. A. Lawless, J. F. Nixon, C. W. Tate, *J. Organomet. Chem.* **2010**, *695*, 717; (b) M. J. Atherton, J. Fawcett, A. P. Hill, J. H. Holloway, E. G. Hope, D. R. Russell, G. C. Saunders, R. M. J. Stead, *J. Chem. Soc., Dalton Trans.* **1997**, 1137.

235 See for example: (a) C. Breutel, P. S. Pregosin, R. Salzmann, A. Togni, *J. Am. Chem. Soc.* **1994**, *116*, 4067; (b) U. J. Scheele, M. John, S. Dechert, F. Meyer, *Eur. J. Inorg. Chem.* **2008**, 373; (c) B. E. Ketz, A. P. Cole, R. M. Waymouth, *Organometallics*, **2004**, *23*, 2835; (d) H. M. Peng, G. Song, Y. Li, X. Li, *Inorg. Chem.* **2008**, *47*, 8031; (e) S. Filipuzzi, P. S. Pregosin, M. J. Calhorda, P. J. Costa, *Organometallics* **2008**, *27*, 2949.

236 (a) T. Hayashi, H. Iwamura, M. Naito, Y. Matsumoto, Y. Uozumi, M. Miki, K. Yanagi, *J. Am. Chem. Soc.* **1994**, *116*, 775; (b) P. G. A. Kumar, P. Dotta, R. Hermatschweiler, P. S. Pregosin, A. Albinati, S. Rizzato, *Organometallics* **2005**, *24*, 1306.

237 (a) P. Kočovský, Š. Vyskočil, I. Císařová, J. Sejbal, I. Tišlerová, M. Smrčina, G. C. Lloyd-Jones, S. C. Stephen, C. P. Butts, M. Murray, V. Langer, *J. Am. Chem. Soc.* **1999**, *121*, 7714; (b) P. Dotta, P. G. A. Kumar, P. S. Pregosin, A. Albinati, S. Rizzato, *Organometallics* **2004**, *23*, 4247; (c) P. Dotta, P. G. A. Kumar, P. S. Pregosin, A. Albinati, S. Rizzato, *Helv. Chim. Acta* **2004**, *87*, 272; (d) P. Dotta, P. G. A. Kumar, P. S. Pregosin, A. Albinati, S. Rizzato, *Organometallics* **2003**, *22*, 5345; (e) I. S. Mikhel, H. Rüegger, P. Butti, F. Camponovo, D. Huber, A. Mezzetti, *Organometallics* **2008**, *27*, 2937.

238 (a) P. S. Pregosin, *Chem. Commun.* **2008**, 4875; (b) P. S. Pregosin, *Coord. Chem. Rev*. **2008**, *252*, 2156.

239 H. L. Pedersen, M. Johannsen, *J. Org. Chem.* **2002**, *67*, 7982.

240 S. E. Gibson, M. Rudd, *Adv. Synth. Catal.* **2007**, *349*, 781.

241 (a) A. Magistrato, A. Togni, U. Rothlisberger, *Organometallics* **2006**, *25*, 1151; (b) A. Magistrato, T. K. Woo, A. Togni, U. Rothlisberger, *Organometallics* **2004**, *23*, 3218.

242 K. Kitayama, Y. Uozumi, T. Hayashi, *J. Chem. Soc., Chem. Commun.* **1995**, 1533.

243 Z. Lu, S. Ma, *Angew. Chem. Int Ed.* **2008**, *47*, 258, and references therein.

244 G. Poli, G. Prestat, F. Liron, C. Kammerer-Pentier, *Top. Organomet. Chem.* **2012**, 38, 1.

245 (a) K. B. Dillon, A. E. Goeta, P. K. Monks, H. J. Shepherd, *Polyhedron* **2010**, *29*, 606; (b) W. Baratta, P. S. Pregosin, *Inorg. Chim. Acta* **1993**, *209*, 85.

246 Absolute stereochemical assignment according to literature data: H. Y. Cheung, W.-Y. Yu, T. T. L. Au-Yeung, Z. Zhou, A. S. C. Chan, *Adv. Synth. Catal.* **2009**, *351*, 1412.

Chapter 5 — MOP-Phosphonites: Introducing a Second Stereocentre

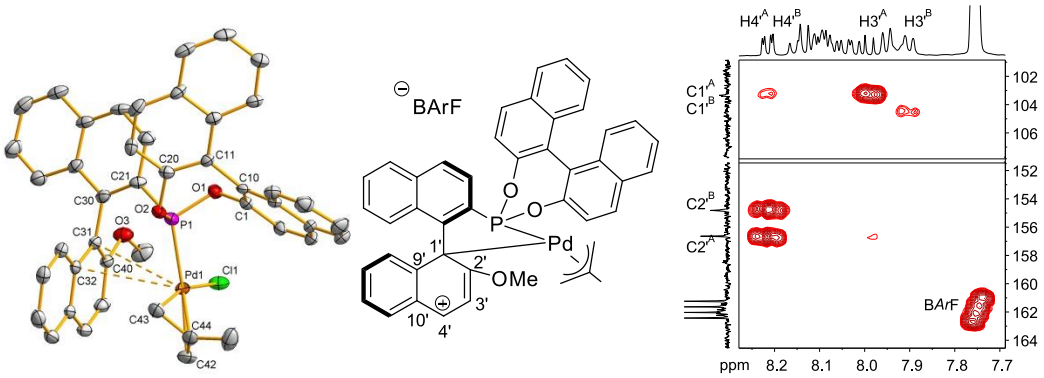

Chiral phosphonite ligands **33a**,**b** and **34a**,**b** are synthesised comprising a MOP-type backbone with a BINOL-based binaphthyl group bound to the phosphorus. Their reaction with $[Pd(\eta^3\text{-}C_4H_7)Cl]_2$ affords η^3-methallylpalladium chloride complexes **36a**,**b** and **37a**,**b** which have been isolated and structurally characterised. Solid-state and solution studies indicate subtle differences in their coordination behaviour, which ultimately affects their efficacy in the asymmetric hydrosilylation of styrene.[247]

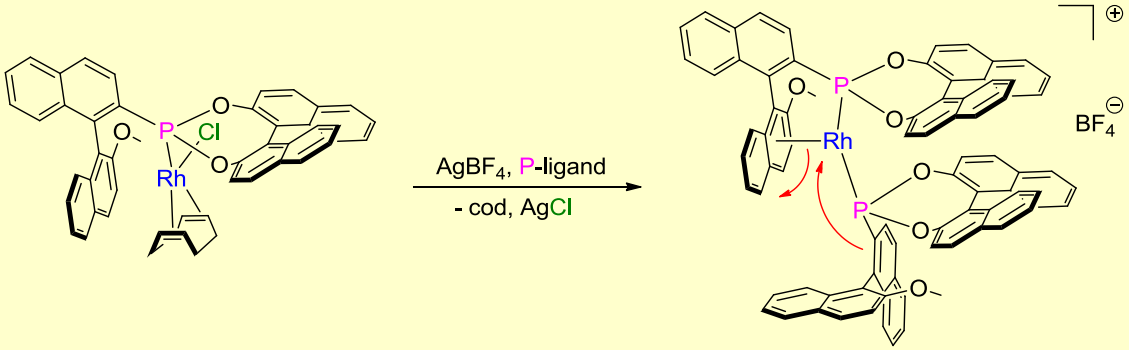

The synthesis of rhodium(I) complexes of chiral MOP-phosphonite ligands is reported. The full characterisation of stabilised 18VE complexes is provided, which demonstrates a hemilabile η^1,η^6-(σ-P, π-arene) binding mode on the arene.[248]

5.1 Introduction

Chiral monophosphorus ligands have attracted considerable attention as their transition metal complexes have been found to be valuable catalysts in a variety of organic transformations.[249] Binaphthyl-derived phosphorus ligands based on phosphine,[250] phosphoramidite[251] and phosphonite[252] architectures have all demonstrated their effectiveness in asymmetric catalysis (Figure 5.1).

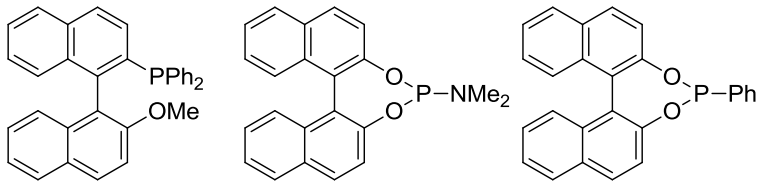

MOP **Phosphine** | **MONOPHOS** **Phosphoramidite** | **XuPhos** **Phosphonite**

Figure 5.1 Established classes of binaphthyl monophosphorus ligands.

Primary phosphines have a reputation for being difficult compounds to work with owing to their perceived high reactivity towards oxygen.[253] Hence, they are somewhat underrepresented as synthons in synthetic chemistry, despite the two P–H bonds being easily functionalised. However, a few examples of user-friendly, air-stable primary phosphines have been reported,[254] and we were the first to describe enantiopure analogues.[255] Subsequently a DFT-based model to help rationalise this stability was published by our group (Chapter 1.4.1).[256] We also recently described how air-stable, chiral primary phosphines **1a**,**b** (Chapter 2) could form novel phosphiranes with unusually high oxidative and thermal stability (Chapter 3).[257] We were therefore keen to establish whether we could transform **1a**,**b** into their dichlorophosphines, and subsequently access MOP/XuPhos-type hybrids (Figure 5.1). This work focuses on the synthesis and characterisation of a novel MOP-phosphonite ligand class. The coordination chemistry in their methallylpalladium complexes is described and we have subsequently investigated their potential as asymmetric ligands in the palladium catalysed hydrosilylation of styrene.

It has been widely recognised that MOP-type ligands can act as P,arene bidentate chelates to stabilise coordinatively unsaturated electron deficient species (see also Chapter 4.2.4).[258] As such, hemilabile arene interactions are expected to be present, or indeed imperative, in catalytic processes. Whilst palladium[259] and ruthenium[260] complexes of this class have been investigated in detail, studies on rhodium-MOP complexes remain scarce.[261] Some controversy persists about the exact nature of the ligand's coordination *via* its aryl backbone

on rhodium, as no X-ray crystal structures have been reported.[262] This is despite the demonstrated catalytic ability of Rh-MOPs in a number of important asymmetric carbon-carbon bond forming reactions of biologically relevant targets,[263] and the presence of an additional spectroscopic probe in the form of the NMR active rhodium nucleus (^{103}Rh, I = ½),[264] which better facilitates the study of these metal bonding modes. We investigated rhodium(I) and iridium(I) complexes of ligands **33a**,**b** and **34a**,**b** in particular with a view to examining the ligand-metal binding modes. Aryl side-on coordination of a MOP-phosphonite ligand was revealed for [Rh(**34b**)$_2$]BF$_4$ (**43b**) by X-ray analysis and further elucidated in solution by extended NMR experiments. Solution NMR studies also showed a dynamic behaviour of this complex, triggered by the hemilabile binding of the ligands towards the metal centre.

Furthermore, we report gold(I) complexes of these phosphonites that are accompanied by studies of their asymmetric catalytic transformations utilising this metal.

5.2 Results and Discussion

5.2.1 Ligand Synthesis

Four MOP-phosphonite ligand derivatives have each been synthesised in a straightforward two-step, one-pot reaction approach. The ligands differ in the substituent on the 2'-position of the MOP-backbone (H or OMe) and in the stereochemistry of the affiliated hydroxyl compound ((*R*)- or (*S*)-BINOL). By comparing the two pairs of diastereomeric compounds with each other, we can elucidate the effect of the second stereocentre. Previous attempts in our group for synthesising these intermediates included transformations with triphosgene,[265] phosgene[266] and *N*-chlorosuccinimide.[267] Even though the formation of the desired compounds was observed by ^{31}P NMR spectroscopy, a number of side-products usually made the work-up more difficult and lowered the yields significantly. A more convenient reagent was found in phosphorus pentachloride;[268] the chlorination occurred at room temperature in less than an hour and the only by-products formed were hydrogen chloride and phosphorus trichloride which could both be removed under reduced pressure. Subsequent addition of (*R*)-BINOL under basic conditions afforded the MOP-phosphonite hybrids **33a**,**b** as white solids (Scheme 5.1). Their diastereomers **34a**,**b** were afforded from reactions with (*S*)-BINOL, again in high yield.

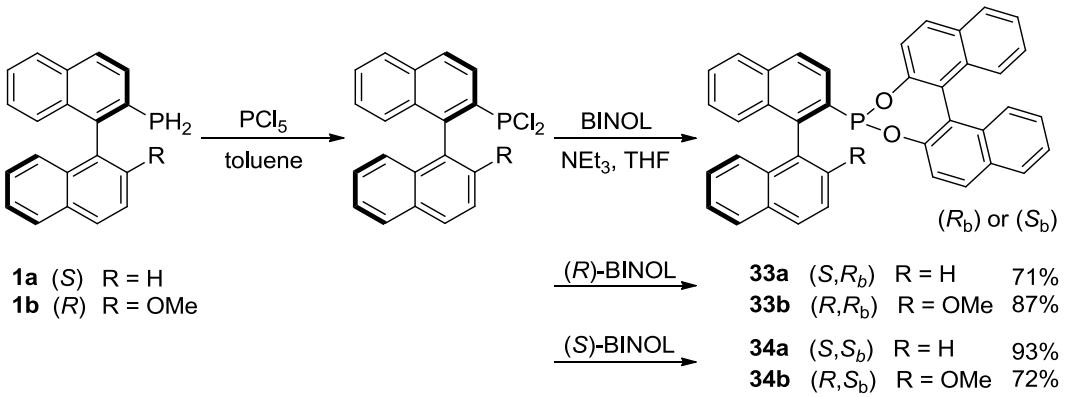

Scheme 5.1 Synthesis of the BINOL-derived phosphonites **33a**,**b** and **34a**,**b**.

The ^{31}P NMR spectroscopic data for the phosphonites are as expected, showing characteristic resonances (δ = 177.4 ppm for **33a**; 177.8 for **33b**; 175.7 ppm for **34a**; 177.9 for **34b**). All ligands could conveniently be handled in air without any apparent decomposition. However, when dissolved in unstabilised bench chloroform-d (containing trace amounts of HCl and H_2O)[269] quick hydrolysis to the corresponding phosphinates was observed. In the case of **34a** and **34b** crystals of the hydrolysis products **35a** and **35b** were obtained from NMR samples after slow evaporation of the solvent (Scheme 5.2), and the molecular structures are shown in Figure 5.2. In the absence of acid the hydrolysis occurs much slower; in fact, in stabilised bench chloroform and other common reagent grade solvents (dichloromethane, toluene, benzene) no hydrolysis products were found.

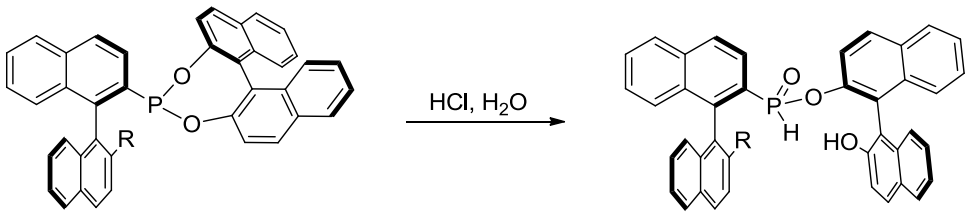

Scheme 5.2 Decomposition reaction of **34a**,**b** by trace amounts of HCl and H_2O in $CDCl_3$.

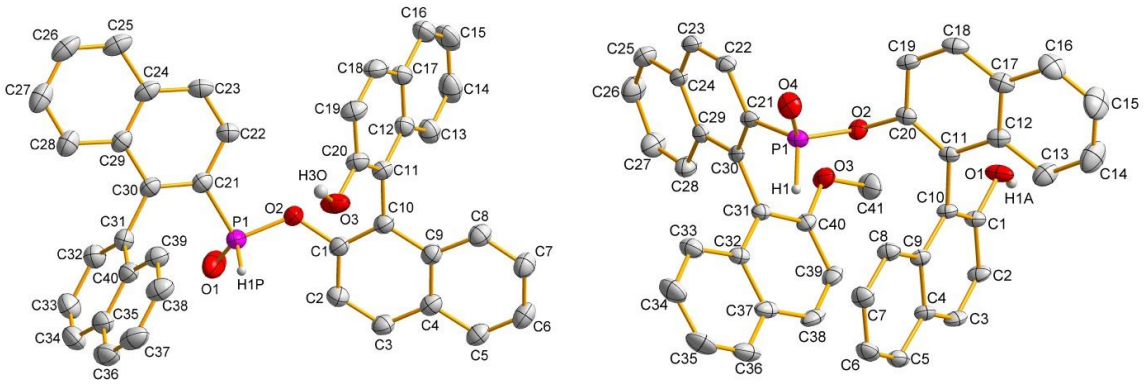

Figure 5.2 Molecular structures of **35a** (left) and **35b** (right) with 50% probability displacement ellipsoids. Hydrogen atoms have been omitted for clarity.

5.2.2 Structural and Electronic Parameters

In Chapter 4.2.2 we have introduced the assessment of structural and electronic properties of phosphorus ligands; please see that section for a more detailed explanation of the different parameters and references to relevant literature. The MOP-phosphonites discussed here have been analysed in an analogous way; the values obtained are fully comparable with those described earlier as the same experimental procedures were used. Thus, we synthesised the corresponding selenide compounds of ligands **33a**,**b**, **34a**,**b** and OMe-MOP to find out about the ligands' σ-donor strengths. The $^{1}J_{PSe}$ couplings of these compounds are among the largest that have been reported for organophosphorus selenides (Table 5.1).

Table 5.1 Structural and electronic parameters of phosphorus ligands **33a**,**b** and **34a**,**b**.

ligand	$^{1}J_{PSe}$ [a]	ν (CO_{Rh}) [b]	$^{1}J_{PPt}$ [c]	E_{HOMO} [d]	PA [e]	S4 [f]
33a	925	2004	2492	–5.49	241.9	57.6°
33b	930	2004	2509	–5.41	244.4	57.8°
34a	925	2023	2481	–5.49	242.0	57.2°
34b	925	2010	2495	–5.39	244.9	55.2°
OMe-MOP	720	1974	2554	–5.27	253.2	40.9°

[a] Coupling from the $ArP(Se)R_2$ derivative in Hertz. [b] CO-stretch of *trans*-$[RhCl(CO)(L_P)_2]$ (L_P = P-ligand) in CH_2Cl_2 in cm^{-1}. [c] Coupling of the PEt_3 ligand in *trans*-$[Pt(L_P)(PEt_3)Cl_2]$. [d] Calculated HOMO energies in eV. [e] Calculated proton affinity in kcal/mol. [f] Calculated from the optimised structure of the free ligand.

For comparison, the couplings observed for $(MeO)_2PhPSe$ and $(MeO)_3PSe$ are 876 Hz and 963 Hz respectively,[270] meaning the donor character of **33a**,**b** and **34a**,**b** (925-930 Hz) is fairly weak and mimics simple phosphites rather than typical phosphonites. The large CO stretching frequencies in *trans*-$[RhCl(CO)(L_P)_2]$ (L_P = P-ligand) complexes of **33a**,**b** and **34a**,**b** (2004-2023 cm^{-1}) are another indication for their weak net-donation properties. Interestingly, subtle

differences in these values imply a slightly stronger net-donation for the (*R*)-BINOL derived ligands **33a**,**b** compared to their (*S*)-BINOL derived counterparts **34a**,**b**.

We determined the *trans* effect of our P-ligands by measuring the $^{1}J_{PPt}$ coupling of PEt_3 in *trans*-[Pt(L_P)(PEt_3)Cl_2] complexes. We found that the *trans* effect for phosphonites **33a**,**b** and **34a**,**b** is somewhat larger than the *trans* effect in OMe-MOP. In comparison to dimethyl phosphonite ligands **19a**,**b** (2402-2407 Hz, Chapter 4) the *trans* effect is however slightly reduced.

We also carried out DFT calculations to determine the HOMO orbital energy levels and the proton affinities (PA) of ligands **33a**,**b** and **34a**,**b**. The values are similar for all ligands; the difference in HOMO energy between H (**a**) and OMe (**b**) derivatives is ~0.1 eV. Most of the HOMO orbital is distributed on the BINOL moiety of the ligands (Figure 5.3) which may be the reason for the small influence that the 2'-substituent on the MOP moiety has in regard the orbital energy. The relative magnitudes of the PA values correlate fairly well with the results for the HOMO energy levels, indicating slightly lower Lewis-basicity of the free electron pair for the H-substituted derivatives **33a** and **34a** (*cf.* Chapter 4.2.2).

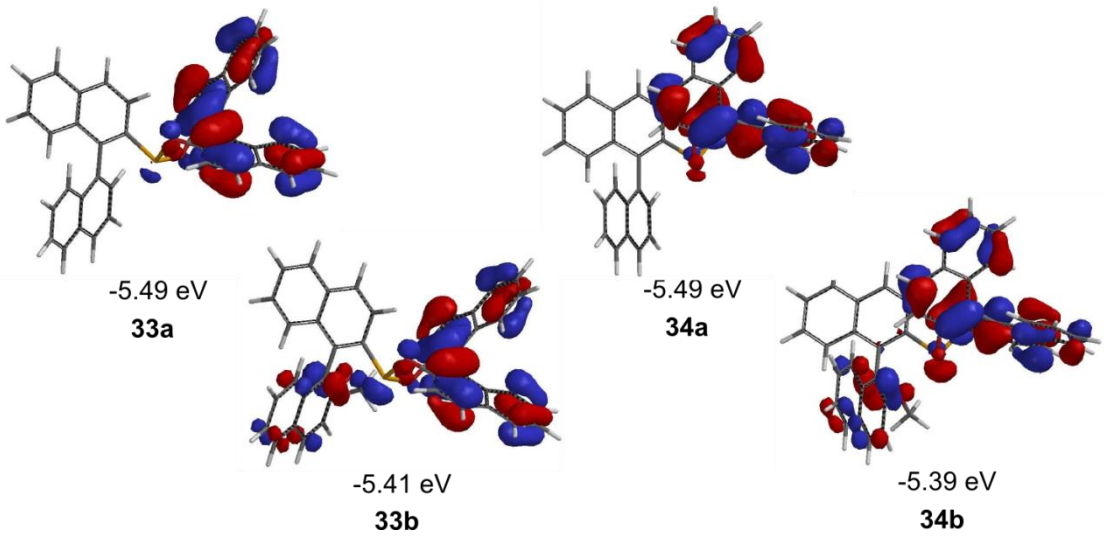

Figure 5.3 HOMO energies of **33a**,**b** and **34a**,**b** calculated at the B3LYP/6-31G* level of theory.

The steric parameter S4 was calculated from the optimised structures of the free ligands. The values are very similar to the dimethyl phosphonite ligands **19a**,**b** which have been discussed in Chapter 4. Therefore, the strain of the chelating BINOL-substituent on the phosphorus seems to have minimal influence on the geometry around the donor atom. The comparably larger S4 values in relation to OMe-MOP contribute further to the decreased donor strength as the s-character of the donor orbital is increased.

5.2.3 Palladium(II) Complexation

We next studied the coordination chemistry of the phosphonites; reaction of two equivalents of the pertinent ligand with $[Pd(\eta^3\text{-}C_4H_7)Cl]_2$ resulted in the rapid, quantitative formation of **36a**,**b** and **37a**,**b** (Scheme 5.3) as shown by NMR, HRMS and X-ray crystallography. Neat samples of the methallylpalladium complexes are stable in air for several weeks without any decomposition. In solution some minor formation of palladium black was observed when leaving the samples at room temperature for several days.

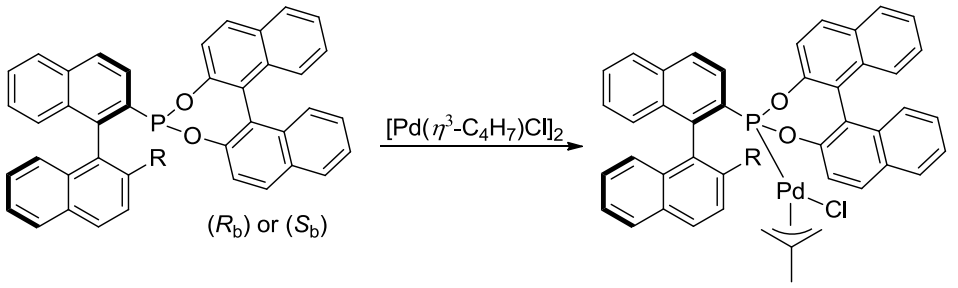

Scheme 5.3 Synthesis of the palladium phosphonite complexes **36a**,**b** and **37a**,**b**.

In all four complexes the X-ray crystal structure reveals the methyl group on the allyl fragment points towards the BINOL component of the ligand (see Figure 5.4 to Figure 5.7). The torsion angles of the two binaphthyl fragments present are significantly different from each other. The unstrained MOP portion preserves an almost right angle (90.5(4) to 101.2(3)°), whilst the torsion of the BINOL moiety is enforced by the bonding of both oxygen atoms to the phosphorus, and thus appears acutely angled (51.2(3) to 53.8(4)°). The ligands coordinate *via* the phosphorus donor atom in an expected monodentate manner to form a pseudo-square-planar configuration around the palladium. Pd–P bond lengths are similar in all complexes (2.2354(7) to 2.2542(8) Å) and are found to be shorter than for the two MOP-phosphine allylpalladium complexes previously reported (2.3098(9) and 2.3279(9) Å);[271] however, shortened Pd-P bond lengths are anticipated for phosphonite palladium complexes, due to their stronger π-acceptor character.[272]

The Pd–C(allyl) bond lengths show the dominant *trans* effect of the P-ligand relative to the chloride; the bonds *trans* to the phosphorus are about 0.1 Å longer compared to the bonds in the *cis* position. In all complexes the position of the palladium centre is face-to-face with the lower naphthyl moiety of the MOP fragment of the ligand. However, the exact position of the allylpalladium moiety is somewhat diverse. When the phosphonite consists of a (*R*)-BINOL

fragment (**36a**,**b**), the palladium is situated towards the back of the lower naphthyl ring (Figure 5.4 and Figure 5.5); in **37a**,**b**, as a consequence of the opposite BINOL stereochemistry, the metal is instead located above the front of this group (Figure 5.6, and Figure 5.7). The distance of the palladium atom from the naphthyl group ranges from 3.0653(1) Å in **36a** to 3.4458(1) Å in **37b**.

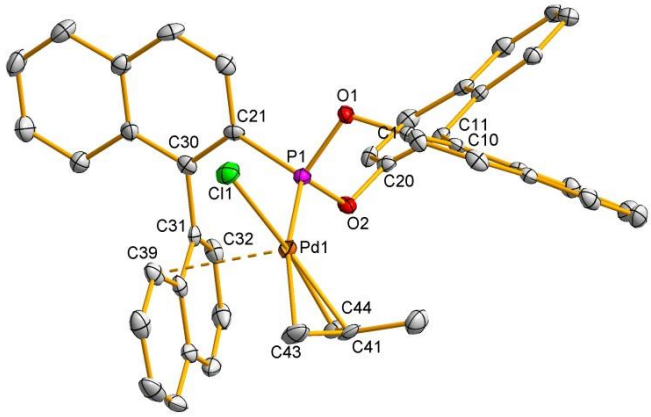

Figure 5.4 Molecular structure of **36a** with 50% probability displacement ellipsoids. Hydrogen atoms have been omitted for clarity. Selected bond distances (Å) and angles (deg): Pd–P 2.2476(7), Pd–Cl(1) 2.3854(7), Pd–C(44) 2.093(2), Pd–C(43) 2.206(2), C(41)–C(43) 1.384(4), C(41)–C(44) 1.415(4), Pd···C(39) 3.0653(1); P–Pd–Cl(1) 93.67(2), P–Pd–C(44) 98.23(9), Cl(1)–Pd–C(43) 101.60(7), C(43)–Pd–C(44) 66.68(11), C(21)–C(30)–C(31)–C(32) −101.2(3), C(1)–C(10)–C(11)–C(20) −51.2(3).

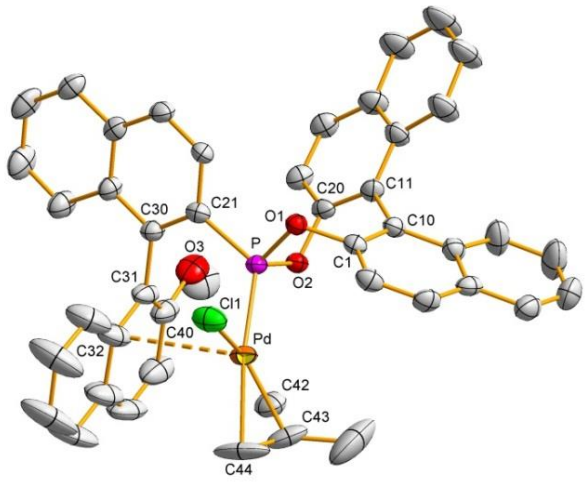

Figure 5.5 View of the molecular structure of **36b**. Hydrogen atoms and cocrystallized solvent have been omitted for clarity. Selected bond distances (Å) and angles (deg): Pd–P 2.2363(8), Pd–Cl(1) 2.3755(10), Pd–C(42) 2.104(4), Pd–C(44) 2.185(4), C(42)–C(43) 1.415(6), C(43)–C(44) 1.381(7), Pd···C(32) 3.4018(1); P–Pd–Cl(1) 93.29(3), P–Pd–C(42) 98.24(12), Cl–Pd–C(44) 101.41(16), C(42)–Pd–C(44) 67.08(19), C(21)–C(30)–C(31)–C(40) −98.0(4), C(1)–C(10)–C(11)–C(20) −52.1(4).

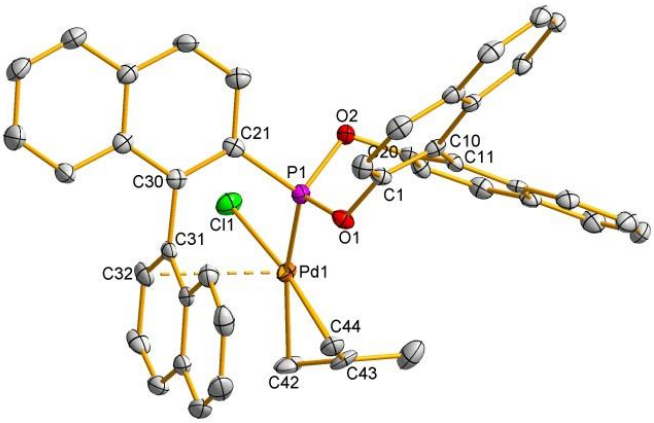

Figure 5.6 View of the molecular structure of **37a**. Hydrogen atoms have been omitted for clarity. Selected bond distances (Å) and angles (deg): Pd–P 2.2354(7), Pd–Cl(1) 2.3730(8), Pd–C(44) 2.078(3), Pd–C(42) 2.198(3), C(42)–C(43) 1.387(4), C(43)–C(44) 1.409(4), Pd···C(32) 3.1412(1); P–Pd–Cl(1) 94.51(3), P–Pd–C(44) 96.49(9), Cl(1)–Pd–C(42) 101.71(9), C(42)–Pd–C(44) 67.31(13), C(21)–C(30)–C(31)–C(32) −90.5(4), C(1)–C(10)–C(11)–C(20) 52.1(4).

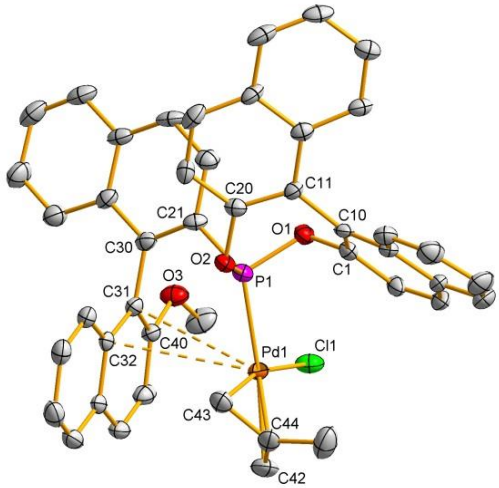

Figure 5.7 View of the molecular structure of **37b**. Hydrogen atoms and cocrystallized solvent have been omitted for clarity. Selected bond distances (Å) and angles (deg): Pd–P 2.2542(8), Pd–Cl 2.3675(7), Pd–C(43) 2.101(3), Pd–C(42) 2.177(3), C(42)–C(44) 1.402(5), C(43)–C(44) 1.412(4), Pd···C(31) 3.4458(1), Pd···C(32) 3.4793(0); P–Pd–Cl 98.46(3), P–Pd–C(43) 96.80(8), Cl–Pd–C(42) 97.23(9), C(42)–Pd–C(43) 67.39(12), C(21)–C(30)–C(31)–C(40) −98.9(3), C(1)–C(10)–C(11)–C(20) 53.8(4).

The NMR spectra of complexes **36a** and **36b** show the presence of two isomers in a 97/3 and 93/7 ratio respectively, which can be rationalised by a rotation of the allyl moiety. nOe contacts between each pair of *syn* and *anti* protons and between the *syn* allyl protons and the central methyl group, in addition to allyl proton-phosphorus coupling, allowed for a complete NMR assignment of the allyl signals (Table 5.2). The protons *trans* to the phosphorus ligand are deshielded and show coupling with ^{31}P whereas the *cis* protons are observed as singlets at higher field.[273]

Table 5.2 Selected ^{31}P and ^{1}H NMR data (δ in ppm) for complexes **36a**,**b**, **37a**,**b**, **38b** and **39b**, and the relative ratio of isomers observed (CD_2Cl_2, 21 °C, 202 and 500 MHz).

complex	P	H_t^{syn}	H_t^{anti}	H_c^{syn}	H_c^{anti}	CH_3	A/B[a]
36a	173.4 (A)	3.75	1.57	2.56	0.83	1.00	97/3
	175.7 (B)	3.96	2.64	2.96	1.53	1.42	
36b	173.6 (A)	3.73	1.63	2.60	0.85	0.92	93/7
	175.6 (B)	3.87	1.94	3.18	1.35	1.70	
38b	177.5 (A)	2.43	2.90	2.99	2.34	1.58	52/48
	178.0 (B)	2.34	3.16	3.03	2.22	1.30	
37a	172.1	4.16	2.56	2.31	0.50	0.93	100/0
37b	174.4	4.07	2.24	2.35	0.32	0.84	100/0
39b	178.9 (A)	2.19	3.76	2.82	2.32	0.96	50/50
	179.1 (B)	3.00	2.63	2.87	2.20	1.79	

[a] Determined by integration of the allyl resonances in the ^{1}H NMR.

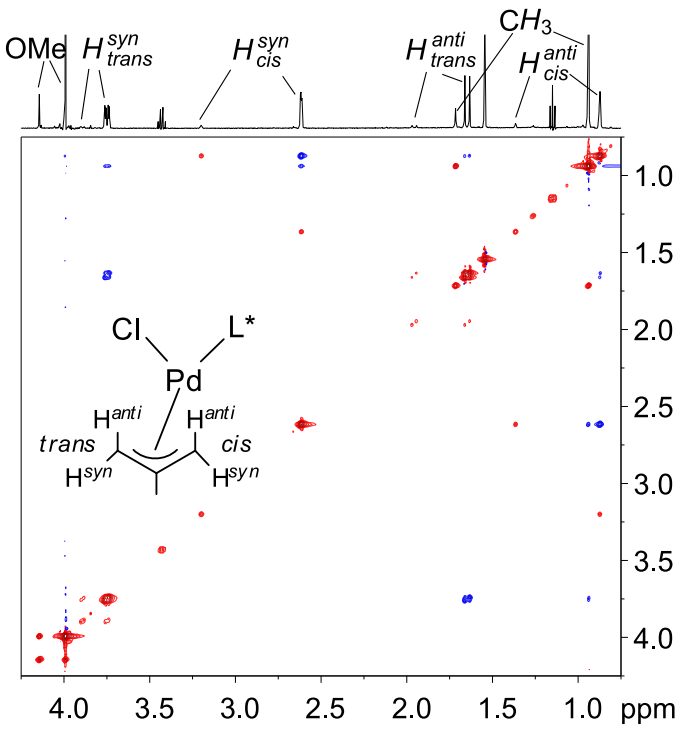

Figure 5.8 Section of the ^{1}H-NOESY spectrum of **36b** in CD_2Cl_2; two isomers were observed. nOe correlations are shown in blue, exchange correlations are shown in red. The spectrum was acquired at 21 °C, using a 500 MHz spectrometer with a mixing time of 400 ms.

The ^{13}C chemical shifts for the atoms in terminal allyl positions are consistent with those reported for similar complexes:[274] 77–79 ppm ($^{2}J_{PH} \approx 46$ Hz) for the allyl carbons *trans* to the P-donor, and 56–59 ppm ($^{2}J_{PH} \approx 5$ Hz) for the *cis* allyl carbons. The phase-sensitive ^{1}H NOESY spectrum of **36b** shows exchange peaks due to interconversion of the two isomers (Figure 5.8). Quantitative analysis of the peak integrals yielded exchange rate constant values of $k_{AB} \approx 0.1$ s^{-1} and $k_{BA} \approx 1.5$ s^{-1} at room temperature.

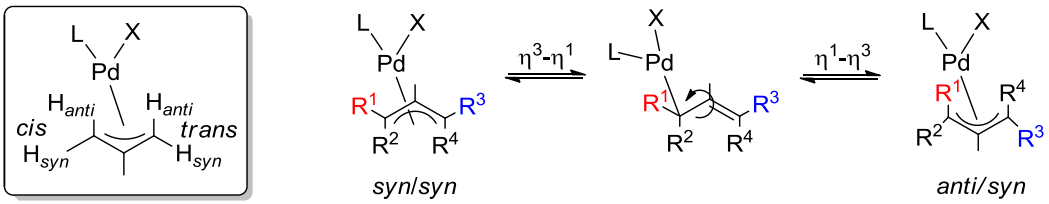

Scheme 5.4 The *syn*/*anti* exchange mechanism in allylpalladium complexes.

The selective *syn*/*anti* exchange of the allyl protons *cis* to the phosphorus is caused by the well-known η^3–η^1–η^3 mechanism (Scheme 5.4; see also Chapter 1.3.4); the protons in the *trans* position exchange *syn*/*syn* and *anti*/*anti* due to the selective opening of the allyl ligand.[274,275] The selectivity of the process is due to the stronger *trans* effect of the P-donor ligand compared to the chloro ligand. An apparent allyl rotation mechanism (*cf.* Chapter 1.3.4) requires a *syn*/*syn* and *anti*/*anti* exchange for both *cis* and *trans* allyl protons and can be ruled out here as such exchange peaks were not observed.[276] Note that conversely for complexes **37a** and **37b** only one single isomer was present in each case.

Table 5.3 Selected ^{13}C NMR data (δ in ppm) for ligands **33b** and **34b** and their palladium complexes **36b**, **37b**, **38b** and **39b** (CD_2Cl_2, 21°C).

carbon	**33b**	**36b**[a]	**38b**[b]	**34b**	**37b**	**39b**[b]
1’	118.9	118.8	104.6/n.d.[c]	119.0	118.2	103.4/104.5
2’	156.6	156.4	157.2/159.0	154.9	156.2	156.6/154.8
3’	112.8	113.1	114.9/114.5	113.0	113.5	115.3/115.9
4’	130.8	131.0	134.6/134.6	130.7	129.7	134.9/134.3
10’	128.2	127.0	128.4/128.4	128.3	128.2	129.3/130.0
9’	134.5	134.2	131.5/131.4	135.0	135.5	132.7/133.7
OMe	56.2	56.2	57.4/57.5	56.4	56.0	57.5/57.4

[a] Major isomer. [b] Two isomers were observed due to allyl rotation. [c] No distinctive assignment due to signal overlap and peak broadening.

MOP ligands can display unconventional bonding characteristics upon metal complexation, using their aromatic backbone to coordinate to a vacant metal site, as shown by several groups who observed binding in a chelating P,C-σ-donor or P,C-π-arene bidentate fashion (see Chapter 1.3.3).[271b,274,277,278] When the chloride counterions of complexes **36b** and **37b** were exchanged for the non-coordinating BArF anion to give complexes **38b** and **39b**, the C1' carbon shifted by –14.3 (**38b**) or –15.6/–14.5 ppm (for the two isomers of **39b**) to lower frequency compared to the free ligand, indicative of greater sp^3 character. The chemical shift of the C2' carbon remained almost unchanged (Table 5.3).

In agreement with studies made by Pregosin and co-workers[278b] we therefore propose a weak η^1 binding mode of the lower naphthyl ring *via* the C-1' carbon (Figure 5.9, left). The downfield shifts of 3.8 ppm in **38b** and 4.2/3.6 ppm in **39b** for the C-4' carbon also suggests it carries some of the associated positive charge of the cation, again matching the aforementioned work. A section of the ^{13}C–^{1}H HMBC spectrum of **39b** showing the indirect resonances of the C1' and C2' carbons is given (Figure 5.9, right).

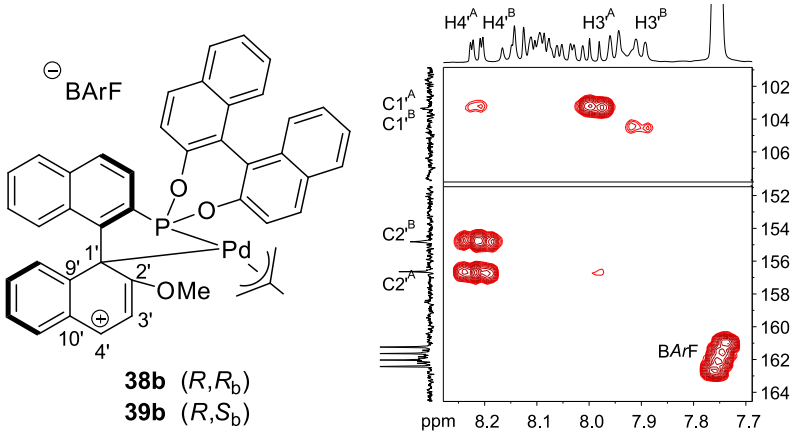

Figure 5.9 Left: Proposed binding mode in **38b** and **39b** using ^{13}C NMR data. Right: Section of the ^{13}C–^{1}H HMBC spectrum of **39b** with key C1′/H3' and C2′/H4' data shown; two isomers of **39b** (labelled A, B) are present.

5.2.4 Palladium Catalysed Allylic Alkylation

The allylic alkylation is a common benchmark reaction for asymmetric ligands in catalysis.[279] The reaction usually works best with moderately strong electron donor ligands and a number of binaphthyl based ligands have been successfully used in this transformation (see also Chapter 1.3.4).[280] We therefore did not expect very high activities for our electron-poor MOP-phosphonite ligands (*cf.* Chapter 4.2.6). As substrates we employed (*rac*)-(*E*)-1,3-diphenylallyl acetate and dimethyl malonate; further reaction conditions and results are given in Table 5.4. The catalyst activity was moderate to low; full conversion of the starting materials was achieved after 22 h (**33a**, **34a**) or 72-96 . The observed selectivities were low, yielding enantiomeric excess values of 12-21%. Interestingly the absolute configuration of the major product is reversed in the case of **34b** (*S* configuration) compared to **33a**,**b** and **34a** (*R* configuration). Hence, the configuration of the stereocentre on the BINOL moiety in **33b** and **34b** seems to have more pronounced influence on the selectivity of the reaction, while for H-MOP derivatives **33a** and **34a** the configuration on the BINOL group is less important.

Table 5.4 Palladium catalysed asymmetric allylic alkylation of (*rac*)-(*E*)-1,3-diphenylallyl acetate.

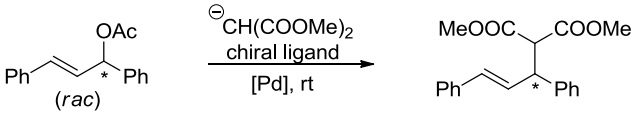

entry	ligand[a]	L:Pd ratio	reaction time[b]	yield[c]	*ee*[d]
1	**33a**	2:1	22 h	95%	12% (*R*)
2	**33b**	2:1	72 h	92%	15% (*R*)
3	**34a**	2:1	22 h	96%	21% (*R*)
4	**34b**	2:1	96 h	97%	14% (*S*)

[a] Catalyst was generated *in situ* from ligand (8.0 mol%) and $[Pd(allyl)Cl]_2$ (2.0 mol%) and reacted with (*rac*)-(*E*)-1,3-diphenylallyl acetate (0.5 mmol), dimethyl malonate (1.0 mmol), BSA (1.0 mmol) and KOAc (0.05 mmol). [b] Reaction progress was monitored by TLC analysis. [c] Isolated yield after column chromatographic workup. [d] Determined by chiral HPLC (Chiralpak AD-H); absolute configuration assigned by comparing the retention times to literature data.[281]

5.2.5 Palladium Catalysed Hydrosilylation

The catalytic activity of the newly prepared ligands was also tested in the asymmetric hydrosilylation of styrene (*cf.* Chapters 1.3.5 and 4.2.5).[282] The catalysts were generated *in situ* from allylpalladium chloride dimer and the appropriate phosphonite. To start with we chose a ligand to palladium ratio of 1:1 to form the catalyst precursors (Table 5.5, entries 1-6), as the methallylpalladium complexes **36a**,**b** and **37a**,**b** had been obtained in this way (*vide supra*). We found that the activity of the catalyst was predominantly dependent on the substituent in the 2'-position of the ligand: H-MOP derivatives **33a** and **34a** showed a higher activity (>94% conversion after 6 h, entries 1 and 3) than their corresponding OMe-MOP derivatives **33b** and **34b** (completed after 16 h, entries 2 and 4). In contrast, the selectivity was mostly determined by the configuration of the adherent BINOL group. Enantioselectivities of 80 and 79% were achieved with the (*S*)-BINOL derivatives **34a**,**b** while the (*R*)-BINOL compounds **33a**,**b** gave lower *ee* values (7 and 55%). In previous studies H-MOP ligands have been found to be more selective in this transformation than their OMe-MOP counterparts (93% vs. 14% *ee* at 0 °C),[250a] hence our results for **33a** (H-MOP derivative, low *ee*) and **34b** (OMe-MOP derivative, high *ee*) were somewhat surprising. Solid-state analysis of a H-MOP allylpalladium *phosphine* complex,[271b] found to be very selective in the same catalytic reaction,[283] shows a similar P/Pd environment to that found in the H-MOP complex [Pd(**34a**)(η^3-C_4H_7)Cl] (**37a**). In contrast, the palladium atom in [Pd(**33a**)(η^3-C_4H_7)Cl] (**36a**) is located more towards the back of the lower naphthyl ring. Thus the subtle differences in the position of the palladium atom relative to the MOP fragment in the

catalytically active species could be crucial in determining the reaction enantioselectivity, again emphasising that we are comparing pairs of diastereomers in this study.

Table 5.5 Palladium catalysed hydrosilylation of styrene.

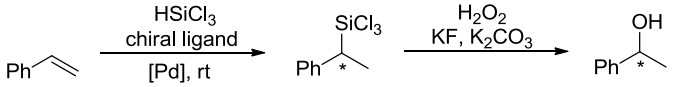

entry	ligand[a]	L:Pd	temp.	reaction time	conversion[b]	*ee*[c]
1	**33a**	1:1	rt	6 h	94%[d]	7% (*R*)
2	**33b**	1:1	rt	16 h	>99%	55% (*S*)
3	**34a**	1:1	rt	4 h	95%[d]	80% (*R*)
4	**34b**	1:1	rt	16 h	>99%	79% (*R*)
5	**34a**	1:1	0 °C	48 h	85%	62% (*R*)
6	**34a**	1:1	50 °C	2 h	93%	70% (*R*)
7	**33a**	2:1	rt	16 h	>99%	40% (*R*)
8	**33b**	2:1	rt	16 h	>99%	17% (*S*)
9	**34a**	2:1	rt	16 h	24%	79% (*R*)
10	**34b**	2:1	rt	16 h	>99%	76% (*R*)

[a] The catalyst was generated *in situ* from the ligand (0.25 mol%) and $[Pd(allyl)Cl]_2$ (0.125 mol%), and reacted with styrene (10.0 mmol) and trichlorosilane (12.0 mmol). [b] Determined by ^{1}H NMR spectroscopy. [c] Determined by chiral HPLC (Chiralcel OD); absolute configuration assigned by comparing the retention times to literature data.[284] [d] Complete conversion after additional 2 h reaction time.

For ligand **34a** we varied the temperature of the reaction to see its effect on the activity and selectivity. When the reaction temperature was reduced to 0 °C the reaction time increased to more than 48 h (entry 5). The observed selectivity was also lower compared to the same reaction at room temperature. At elevated temperature (50 °C), reaction times were shortened but again the selectivity of the reaction was reduced (entry 6). Further studies were therefore carried out at room temperature only.

According to Johannsen and co-workers proposed mechanism, the catalytic pathway for the hydrosilylation reaction can change when a high phosphorus ligand loading relative to palladium metal is present in the reaction mixture (*cf.* Chapter 1.3.5).[285] Increasing the ligand to palladium ratio to 2:1 in the catalytic transformation gave indeed different results for activities and selectivities (entries 1-4 vs. entries 7-10). Most significantly, the activity for ligand **34a** was drastically lowered, and only 24% conversion was observed after 16 h reaction time (entry 9). The enantioselectivity remained almost constant for the (*S*)-BINOL derivatives **34a**,**b** (entries 9-10), but it was changed for the (*R*)-BINOL derivatives **33a**,**b** giving a moderately better *ee* value for **33a** (entry 7), but a worse result for **33b** (entry 8). The lower reactivity for ligands **33a** and **34a** at a 2:1 L:Pd ratio might be rationalised by the steric

nature of the bulky ligand, resulting in catalyst deactivation upon coordination of a second ligand to the metal. However, further studies need to be undertaken to fully understand the catalytic mechanism as a 2:1 L:Pd ratio has been shown to improve the reaction activity for some related ligand scaffolds (see *e.g.* Chapter 4.2.5).

5.2.6 η^1,η^6-(σ-P, π-Arene) Chelated Rhodium(I) Complexes

For an initial evaluation of the coordination behaviour of MOP-phosphonite ligands **33b** and **34b** on rhodium(I) we reacted two equivalents of the respective ligand with $[Rh(\eta^4\text{-cod})Cl]_2$. The resulting complexes [Rh(**33b**)(η^4-cod)Cl] (**40b**) and [Rh(**34b**)(η^4-cod)Cl] (**41b**) were both formed quantitatively; the ^{31}P NMR spectra (Figure 5.10) show a doublet caused by coupling to the rhodium (^{103}Rh, I = ½) nucleus (**40b**: 162.9 ppm, $^1J_{PRh}$ = 223 Hz; **41b**: δ = 161.5 ppm, $^1J_{PRh}$ = 224 Hz).

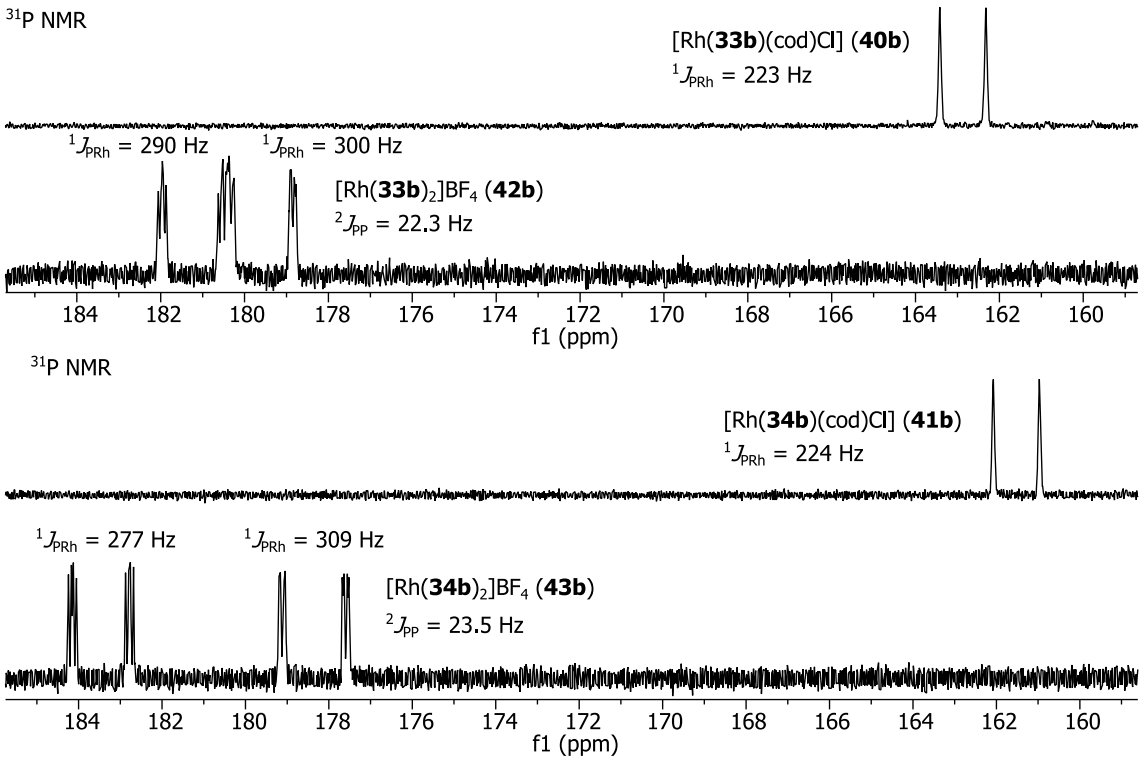

Figure 5.10: Undecoupled ^{31}P NMR (202 MHz) spectra of **40b**-**43b**. Note that in the case of **42b** and **43b** coupling to the hydrogen in the 3-position of the ligand is also resolved in the spectra.

In the case of **40b** single crystals suitable for X-ray analysis were obtained from slow diffusion of hexane into a dichloromethane solution (Figure 5.11). Typical bond lengths are found within the coordination sphere of the metal. As expected, the Rh–P distance of this *phosphonite* donor (2.2112(7) Å) is shorter than the bond lengths typically observed for aryl *phosphine* ligands (2.297–2.3607(14) Å)[286] due to their stronger π-acceptor character (the

same trend was observed for the Pd–P distances in their allylpalladium complexes; see Chapter 5.2.3).[287] The η^4-cod ligand shows the dominant *trans* effect of the phosphorus donor compared to the chloride; the alkene bond coordinated in the *cis* position is longer and closer to the rhodium compared to the alkene bound *trans* to the phosphorus atom.

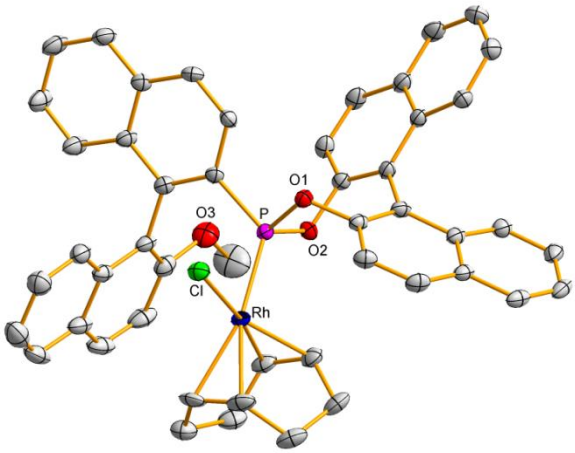

Figure 5.11 View of the molecular structure of [Rh(**33b**)(η^4-cod)Cl] (**40b**) (50% probability thermal ellipsoids). Hydrogen atoms and co-crystallised solvent are omitted for clarity.

In order to investigate the possibility of a hemilabile aryl coordination of the MOP-type ligands, we carried out an anion exchange of **40b** and **41b** from chloride to the non-coordinating tetrafluoroborate ion. Specifically, exchange of the counter ion was achieved by reacting **40b** and **41b** with $AgBF_4$ and the reaction was monitored by ^{31}P NMR spectroscopy. Initial attempts produced large amounts of oxidation and no pure product could be isolated. However when another equivalent of the appropriate ligand **33b** or **34b** was added to the reaction mixture (together with the silver salt), a clean quantitative conversion was achieved to yield [Rh(**33b**)$_2$]BF_4 (**42b**) or [Rh(**34b**)$_2$]BF_4 (**43b**) respectively; the η^4-cod ligand was thus replaced by a second phosphorus donor during the course of the reaction. Alternatively, the two compounds could also be obtained from the reaction of two equivalents of either **33b** or **34b** with [Rh(η^4-cod)$_2$]BF_4, although in some cases oxidised by-products were formed.

Crystals of **43b** suitable for crystallographic analysis were obtained from slow diffusion of diethyl ether into a dichloromethane solution (Figure 5.12). The complex contains two phosphorus ligands, one of which is coordinated in the anticipated η^1 binding mode *via* the phosphorus atom (Rh–P bond length: 2.2145(14) Å). The second ligand fills the coordination sphere of the rhodium metal by acting as η^1,η^6 chelate; in addition to the η^1-phosphorus donor (Rh–P bond length: 2.1882(14) Å), the lower naphthyl ring coordinates side-on *via* its π-system in η^6-fashion. Selected Rh–C bond lengths of the coordinated aryl group are given in

Table 5.6. The plane of the η^6-arene is only slightly distorted; the distance from its centre to the rhodium is 1.85 Å. To the best of our knowledge this is the first time that such a bonding motif of a MOP-type rhodium complex has been unveiled in the solid-state.

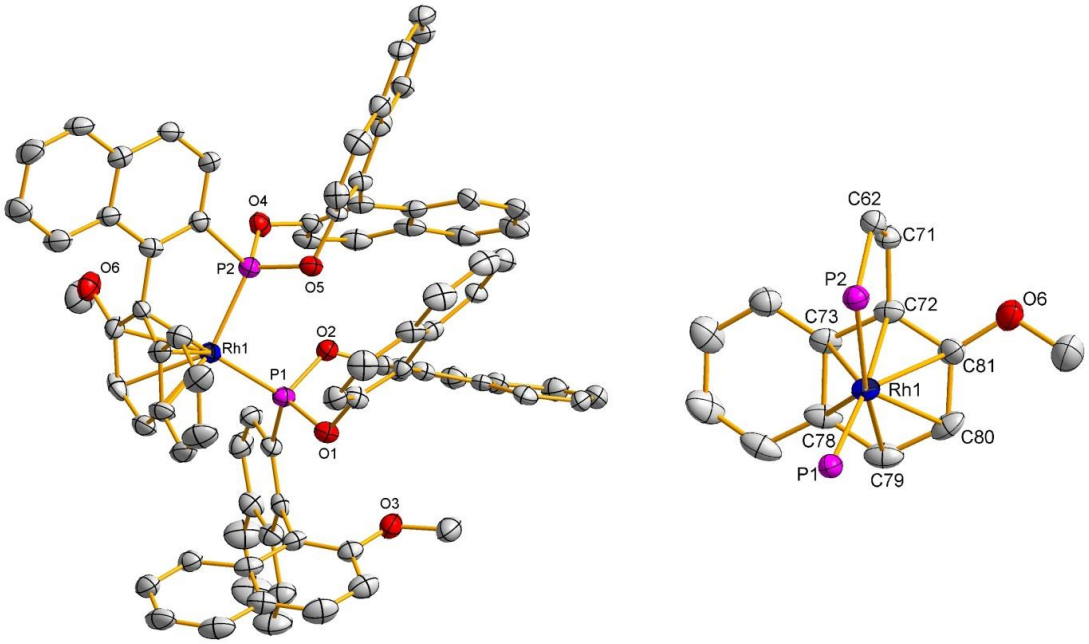

Figure 5.12 Left: View of the molecular structure of [Rh(**34b**)$_2$]BF_4 (**43b**) (50% probability thermal ellipsoids). Hydrogen atoms, the BF_4-anion and co-crystallised solvent are omitted for clarity. Right: View on the metal coordination sphere of **43b**. Selected bond distances (Å): Rh1–P1 2.2145(14), Rh1–P2 2.1882(14).

Solution NMR studies confirmed the coordination environment of the structural analysis. The $^{31}P\{^1H\}$ NMR spectra (Figure 5.10) show two doublets of doublets (**42b**: 181.3, 179.6 ppm; **43b**: δ = 183.5, 178.4 ppm) caused by the two inequivalent phosphorus atoms coupling to each other (**42b**: $^2J_{PP}$ = 22.3 Hz; **43b**: $^2J_{PP}$ = 23.5 Hz) and to the rhodium nucleus (**42b**: $^1J_{PRh}$ = 290 Hz, 300 Hz; **43b**: $^1J_{PRh}$ = 277 Hz, 309 Hz). We attribute the smaller Rh–P coupling to the η^1-bound ligand, in accord with the relative bond lengths found in the solid state (listed in the caption of Figure 5.12). In the ^{13}C NMR spectra the η^6-aryl binding situation of the coordinated carbon atoms is accompanied by a change in chemical shift to upper field. Furthermore, the coordinated C1' and C4' carbons show a doublet splitting pattern, which is most likely caused by ^2J-coupling to the respective ^{31}P nucleus in the *trans* position. The values for the respective carbon resonances of the η^1,η^6-coordinated ligand and the resonances of the non-coordinated counterparts of the η^1-bound ligand are given in Table 5.6 (**43b**) and Table 5.7 (**42b**). Sections of the ^{13}C–^1H HSQC and ^{13}C–^1H HMBC spectra of **43b** are shown in Figure 5.13.

Table 5.6 Selected Rh–C bond lengths and ^{13}C NMR resonances of **43b**.

	Rh–C [Å][a]	$^{13}C(\eta^1,\eta^6)$ [ppm][b,c]	$^{13}C(\eta^1)$ [ppm][b]
C1'	2.189(5) (C72)[d]	101.6 (15.8 Hz)[e]	118.8
C2'	2.296(5) (C81)	145.3	155.8
C3'	2.337(5) (C80)	90.1	112.3
C4'	2.324(5) (C79)	93.1 (12.7 Hz)[e]	129.9
C10'	2.477(5) (C78)	114.0	129.1
C9'	2.431(5) (C73)	122.0	133.8

[a] From X-ray data in the solid-state. [b] Solution NMR analysis (126 MHz, CD_2Cl_2, 21 °C). [c] Resonances of the (σ-P, π-arene)-coordinated ligand. [d] Carbon labelling scheme used for X-ray data. [e] Resonance appeared as doublet with the indicated coupling constant.

Table 5.7 Selected ^{13}C NMR resonances of the rhodium complexes **42b** and **44b**.

	42b		**44b**	
	$^{13}C(\eta^1,\eta^6)$ [ppm][a,b]	$^{13}C(\eta^1)$ [ppm][a]	$^{13}C(\eta^1,\eta^6)$ [ppm][a,b]	$^{13}C(\eta^1)$ [ppm][a]
C1'	100.5 (14.3 Hz)[c]	121.9	93.6 (13.1 Hz)[c]	118.7
C2'	149.1	153.8	141.4	154.3
C3'	87.5	114.2	89.5	112.4
C4'	95.8 (11.3 Hz)[c]	128.1	92.3 (9.2 Hz)[c]	130.7
C10'	112.8	128.2	120.2	128.6
C9'	118.7	134.6	123.1	134.2

[a] Solution NMR analysis (126 MHz, CD_2Cl_2, 21 °C). [b] Resonances of the (σ-P, π-arene)-coordinated ligand. [c] Resonance appeared as doublet with the indicated coupling constant.

The proton NMR spectra show the expected 48 independent aromatic resonances, from which 24 originate from each ligand. At room temperature, exchange of all 24 pairs of signals is observed in the ^1H-NOESY of **42b** and **43b** (Figure 5.14); at –50 °C the NOESY spectra showed strong positive nOe peaks without exchange. Combining the information from variable temperature NOESY experiments allowed for the unambiguous assignment of all 48 proton resonances in **42b** and **43b**. nOe contacts confirmed the solid-state structure of **43b** in solution; the solution structure of **42b** was also analysed, and the nOe signals in this case revealed a rotation of the η^1-ligand about its C2–P bond in comparison to **43b** (details are given in Figure 5.15).

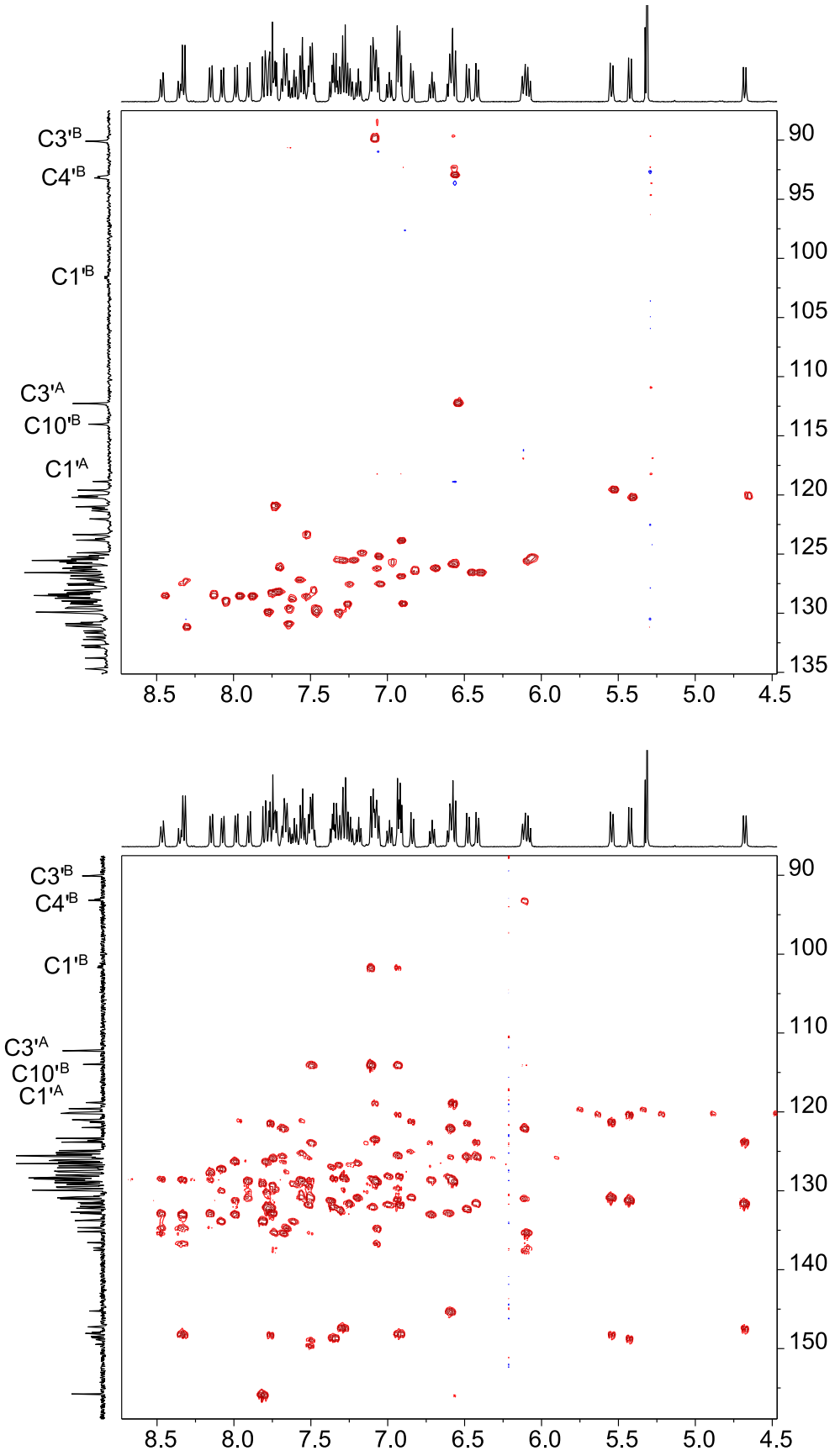

Figure 5.13 Section of the ^{13}C–^{1}H HSQC (top) and ^{13}C–^{1}H HMBC (bottom) spectra of **43b** in CD_2Cl_2 at 21 °C using a 400 MHz spectrometer. Metal coordinated carbons (labelled B) are shifted to higher field compared to their non-coordinated counterparts (labelled A).

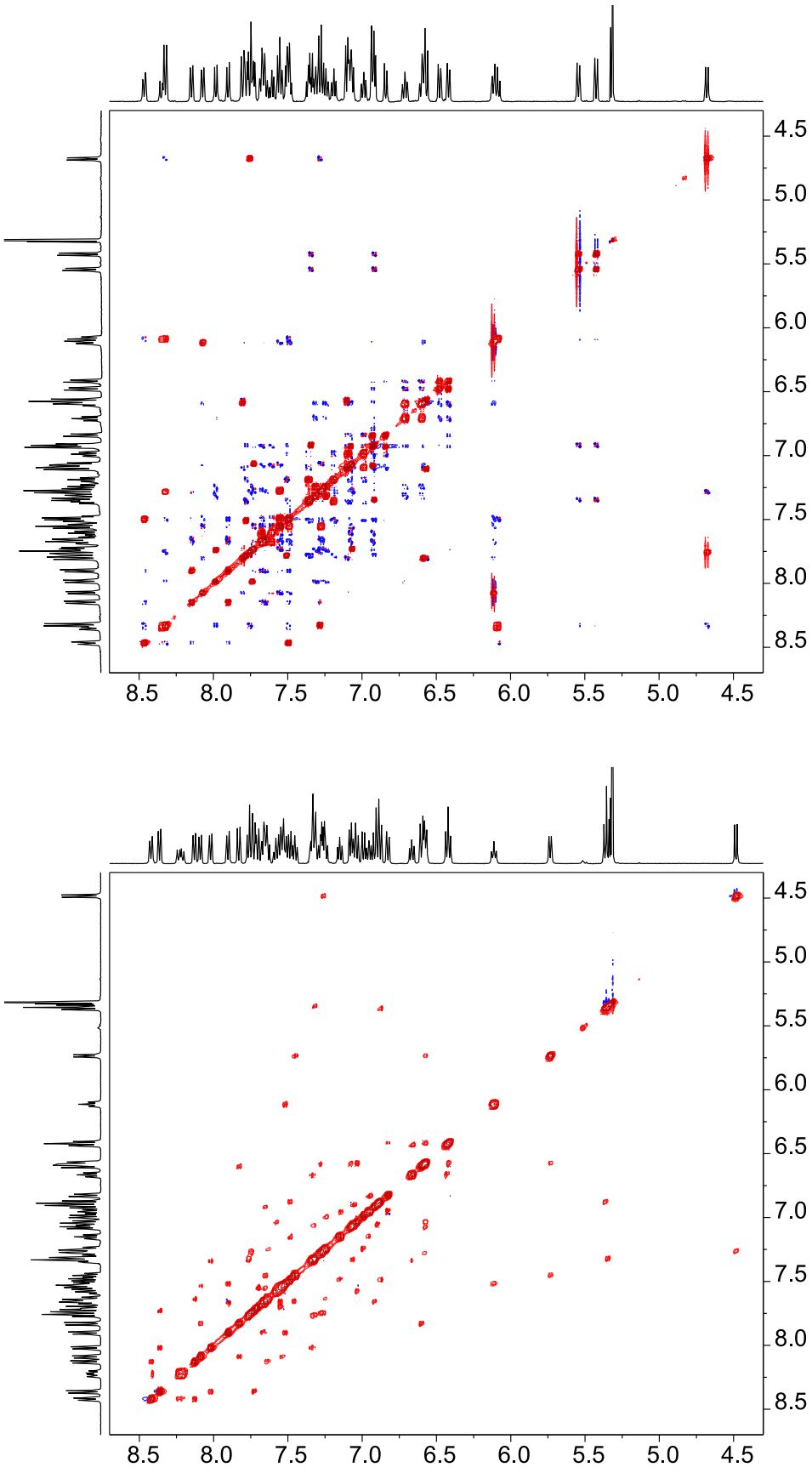

Figure 5.14 Aromatic resonances of **43b** in the ^{1}H-NOESY spectrum in CD_2Cl_2 at 21 °C (top) and –50 °C (bottom). Negative correlations are shown in blue, positive correlations are shown in red. The spectra were acquired with 2048 × 512 data points and a spectral width of 9 ppm, recorded using a 500 MHz spectrometer with a mixing time of 500 ms.

The dynamic behaviour in **42b** and **43b** is a result of the hemilabile binding of the aryl group; the side-on coordination of the η^1,η^6 chelating ligand is released while in the same instance the η^1-bound ligand coordinates as a chelate, ultimately reproducing the complex (Figure 5.16). Quantitative analysis of the ^{1}H-NOESY spectra yielded exchange rate constants of $k_{294K} = 1.2\ s^{-1}$ and $k_{273K} = 0.12\ s^{-1}$ for **43b** in dichloromethane-d2. The values only changed slightly when the experiments were carried out in chloroform-d ($k_{294K} = 1.3\ s^{-1}$) or THF-d8 ($k_{294K} = 0.9\ s^{-1}$). Thus, we propose a concerted reaction mechanism as the rate of exchange showed no increase in coordinating solvent. Comparable exchange rate values were also found for **42b** (in THF-d8: $k_{294K} = 0.9\ s^{-1}$).

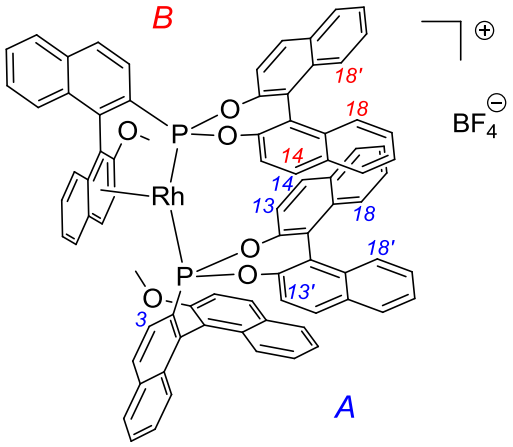

Figure 5.15 Structure of **42b** based on nOe correlations in the ^{1}H-NOESY NMR. The η^1 ligand is labelled *A*, the η^1,η^6-(σ-P, π-arene) is labelled *B*. Selected nOe contacts: $H18^A$–$H18^B$, $H13^A$–$OCH_3{}^B$, $H3^A$–$H13'^A$, $H14^B$–$H13'^A$, $H18^A$–$H18'^A$, $H18^B$–$H18'^B$.

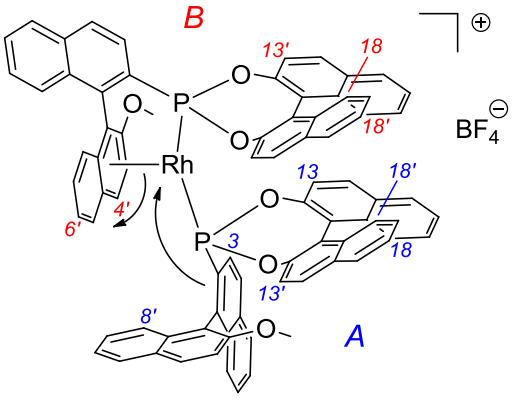

Figure 5.16 Dynamic behaviour observed in solution for **43b** (arrows). The η^1 ligand is labelled *A*, the η^1,η^6-(σ-P, π-arene) is labelled *B*. Selected nOe contacts: $H13'^B$–$OCH_3{}^B$, $H3^A$–$H13'^B$, $H3^A$–$H13^A$, $H4'^B$–$H8'^A$, $H18^B$–$H18'^B$, $H18^A$–$H18'^A$, $H13'^A$–$H6'^B$.

The Eyring equation relates the rate constant *k* and the activation free energy $\Delta G^{\ddagger}$.[288] The most common form of the Eyring equation is:

$$k = \frac{\kappa T}{h} \cdot e^{-\Delta G^{\ddagger}/RT} \quad (1)$$

where κ is the Boltzmann constant, h is Planck's constant, T is the temperature in Kelvin and R is the universal gas constant. The equation can be rewritten as:

$$\Delta G^{\ddagger} = -\ln\left(\frac{k\,h}{\kappa\,T}\right) RT \quad (2)$$

The activation free energies of **43b** in dichloromethane-d2 were calculated from selected rate constants giving values of $\Delta G^{\ddagger}_{294K}$=71.2 kJ/mol and $\Delta G^{\ddagger}_{273K}$=71.5 kJ/mol. Related studies by Mirkin and co-workers gave free energies of activation of similar magnitude for their rhodium piano-stool complexes with hemilabile arene ligands.[261f]

In order to clarify whether the phenomenon of η^6 side-on coordination to rhodium is exclusive to our bulky MOP-phosphonite ligands **42b** and **43b** or is valid for complexes of other MOP type ligands too, we utilised Hayashi's OMe-MOP ligand to synthesise the analogous $[Rh(OMe\text{-}MOP)_2]BF_4$ (**44b**) complex. Full characterisation by NMR spectroscopy revealed a similar (σ-P, π-arene)-binding situation as observed for **42b** and **43b**. Its two ^{31}P NMR resonances are observed at 50.0 and 37.2 ppm ($^1J_{PRh}$ = 217 Hz, 197 Hz; $^2J_{PP}$ = 32.1 Hz). The ^{13}C NMR resonances of the six coordinated carbon atoms show the characteristic upfield shift (shifted by 8.4 to 38.4 ppm) which is slightly less pronounced for C9' and C10' (Table 5.7). In contrast to **42b** and **43b** we detected no dynamic exchange in the ^1H NOESY NMR spectrum at room temperature, suggesting the arene-coordination is stronger in this case.

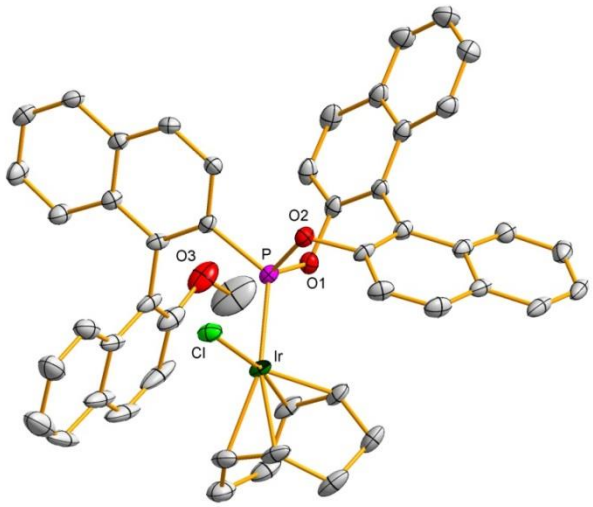

Figure 5.17 View of the molecular structure of [Ir(**33b**)(η^4-cod)Cl] (**45b**) (50% probability thermal ellipsoids). Hydrogen atoms and co-crystallised solvent are omitted for clarity.

To further understand the coordination behaviour of MOP ligands with the catalytically important group-nine transition-metals, we also reacted MOP-phosphonites **33b** and **34b** with $[Ir(\eta^4\text{-cod})Cl]_2$ in an analogous manner to the rhodium chemistry. To the best of our knowledge we were therefore able to synthesise and isolate the first iridium-MOP complexes [Ir(**33b**)(η^4-cod)Cl] (**45b**) and [Ir(**34b**)(η^4-cod)Cl] (**46b**); the ^{31}P NMR spectra show a resonance at 140.4 (**45b**) or 139.6 ppm (**46b**). The crystal structure of **45b** is depicted in Figure 5.17; bond lengths and angles are very similar to the corresponding rhodium complex **40b** (Ir–P distance: 2.2242(8) Å).

In contrast to the bonding situation found for rhodium, treatment of **45b** with silver tetrafluoroborate and an additional equivalent of **33b** gave $[Ir(\mathbf{33b})_2(\eta^4\text{-cod})]BF_4$ (**47b**). The ^{31}P NMR spectrum exhibits a single resonance at 156.3 ppm; rather than side-on coordination of the arene, the coordination sphere of the metal accommodates two equivalently bound η^1-phosphines and the η^4-cod ligand (Figure 5.18).

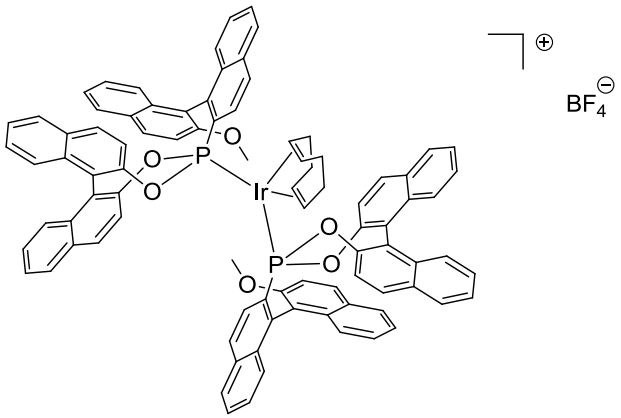

Figure 5.18 Structure of $[Ir(\mathbf{33b})_2(\eta^4\text{-cod})]BF_4$ (**47b**) based on nOe correlations in the ^{1}H-NOESY NMR.

5.2.7 Rhodium Catalysed Reactions

The rhodium catalysed asymmetric hydrogenation of (*Z*)-methyl-2-acetamido cinnamate is a common benchmark reaction for chiral ligands.[289] BINOL-based phosphonite ligands were successfully employed in this reaction whereas MOP-type compounds were hardly studied and gave inferior results (*cf.* Chapters 1.3.6 and 2.2).[290] As both of these moieties are present in **33a**,**b** and **34a**,**b** we were interested in what influence this would have on the performance of the reaction, and moreover how the two stereocentres would affect the enantioselectivity. From our coordination studies on the relevant rhodium complexes **42b** and **43b** we concluded that a) the BINOL moiety might have a significant influence on the chiral induction, as the position of the η^1-ligand notably changes when the stereocentre is inverted by rotation about

the C2–P bond (**42b** versus **43b**, *vide supra*), and b) the reactivity of the catalyst might be reduced as the coordination sphere of the rhodium is saturated by the η^6-coordination of the arene.

Indeed, we found that the reactions proceeded rather slowly; however reasonable conversions of 58% and 77% were achieved for the H-MOP derived compounds **33a** and **34a** respectively after 16 hours reaction time (Table 5.8, entries 1 and 3). The result is in accord with the study of our phosphirane ligands that also gave a higher conversion for the H-MOP-type derivative (Chapter 3.2). Better selectivities of 40-43% *ee* were achieved when the BINOL fragment was (R_b)-configured (**33a**,**b**, entries 1-2) compared to their (S_b)-configured diastereomers **34a**,**b** (entries 3-4). Thus, the enantioselectivity of the reaction was increased in relation to our phosphirane ligands (14/23% *ee*, Chapter 3.2) but is still inferior to the related phosphonite ligand **XLIII** (Figure 5.19) that carries a phenyl group instead of the MOP fragment (63% *ee*, Chapter 1.3.6).[291] It has been suggested that MOP-type rhodium complexes with side-on coordinated arene groups might hydrogenate their ligand *in situ* and thereby removing the atropisomeric axis,[262a] which would partially explain the low enantioselectivity control of this class of compounds.

Table 5.8 Rhodium catalysed hydrogenation of (*Z*)-methyl-2-acetamido cinnamate.

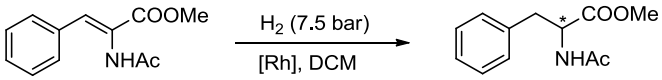

entry	catalyst[a]	conversion[b]	*ee*[c]
1	**33a**	58%	43% (*S*)
2	**33b**	12%	40% (*S*)
3	**34a**	77%	9% (*S*)
4	**34b**	17%	26% (*S*)

[a] Catalyst was generated *in situ* from ligand (8.0 mol%) and $[Rh(\eta^4\text{-cod})_2]BF_4$ (4.0 mol%) and reacted with (*Z*)-methyl-2-acetamido cinnamate (0.25 mmol) and H_2 gas (7.5 bar) in DCM (4 mL); 16 h, 21 °C. [b] Determined by ^{1}H NMR. [c] Determined by chiral HPLC (Chiralpak AD-H); absolute configuration was assigned according to literature data.[292]

As another test for the catalytic performance of our ligands we decided to carry out the rhodium catalysed addition of phenylboronic acid to 1-naphthaldehyde.[293] The reaction was first described by Miyaura and co-workers utilising MeO-MOP as the asymmetric ligand (Table 5.9, entry 1),[294] and has been the subject of increasing interest in recent years.[295] For instance, Hayashi *et al.* were able to increase the selectivity to 86% *ee* when applying the C_2-symmetric tetrafluorobenzobarrelene **LVII** as chiral ligand (Figure 5.19).[295e]

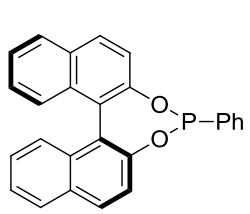

XLIII

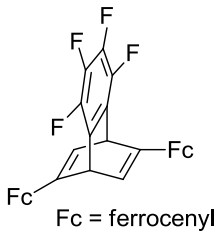

LVII

Figure 5.19 Selected ligands that have been used in rhodium(I) catalysed hydrogenations (**XLIII**) or additions of arylboronic acids to aldehydes (**LVII**).

Table 5.9 Rhodium catalysed asymmetric addition of phenylboronic acid to 1-naphthaldehyde.

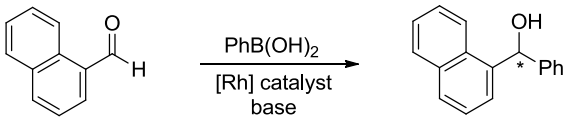

entry	ligand	Rh precursor[a]	base	solvent	time	yield[b]	*ee*[c]
1	OMe-MOP[d]	$[Rh(acac)(\eta^2\text{-}C_2H_4)_2]$	–	DME/H_2O	36 h	78%	41%
2	**33b**	$[Rh(acac)(\eta^2\text{-}C_2H_4)_2]$	–	THF	48 h	30%	20% (*R*)
3	**33b**	$[Rh(acac)(\eta^2\text{-}C_2H_4)_2]$	KOH	THF	48 h	42%	23% (*R*)
4	**33b**	$[Rh(\eta^4\text{-cod})Cl]_2$	KOH	THF	3 h	>99%	racemic
5	**33b**	$[Rh(\eta^2\text{-}C_2H_4)Cl]_2$	KOH	THF	18 h	–	–
6	**33b**	$[Rh(acac)(\eta^2\text{-}C_2H_4)_2]$	K_2CO_3	THF	48 h	55%	25% (*R*)
7	**33b**	$[Rh(acac)(\eta^2\text{-}C_2H_4)_2]$	Cs_2CO_3	THF	48 h	–	–
8	**33b**	$[Rh(acac)(\eta^2\text{-}C_2H_4)_2]$	K_3PO_4	THF	39 h	77%	28% (*R*)
9	**33b**	$[Rh(acac)(\eta^2\text{-}C_2H_4)_2]$	K_3PO_4	DME	8 h	49%	30% (*R*)
10	**33b**	$[Rh(acac)(\eta^2\text{-}C_2H_4)_2]$	K_3PO_4	dioxane	8 h	85%	34% (*R*)
11	**33a**	$[Rh(acac)(\eta^2\text{-}C_2H_4)_2]$	K_3PO_4	dioxane	72 h	29%	16% (*R*)
12	**34a**	$[Rh(acac)(\eta^2\text{-}C_2H_4)_2]$	K_3PO_4	dioxane	72 h	11%	25% (*S*)
13	**34b**	$[Rh(acac)(\eta^2\text{-}C_2H_4)_2]$	K_3PO_4	dioxane	72 h	13%	31% (*S*)

[a] Catalyst was generated *in situ* from ligand (20 µmol) and rhodium precursor (10 µmol Rh) over 30 minutes in THF (4 mL). Phenylboronic acid (122 mg, 1.0 mmol), base (2.5 M aqueous solution, 1.0 mmol) and 1-naphthaldehyde (68 µl, 0.5 mmol) were added subsequently; reaction temp.: 60 °C. [c] Determined by chiral HPLC (Chiralcel OD). [d] Values taken from ref. 294.

Initially, we adapted the reaction conditions from Miyaura's protocol using **33b** as chiral ligand. We decided to use anhydrous THF instead of DME/water as solvent to prevent hydrolysis of the phosphonite ligand, which resulted in 30% product formation with a selectivity of 20% *ee* (entry 2). In subsequent runs (entries 3-13) the water was added after the *in situ* formation of the phosphonite-rhodium complexes; we also added different base additives to promote the reaction activity (entries 3, 6-8). The best results were obtained with K_3PO_4 which gave a marked increase in yield to 77% after 39 h, as well as a slight increase in enantioselectivity (entry 8). Other rhodium precursors were tested but they were found to be inferior to $[Rh(acac)(\eta^2\text{-}C_2H_4)_2]$ (entires 3-5). We achieved a maximum selectivity of 34% *ee*

with ligand **33b** when we changed the solvent to dioxane (entry 10). We were unable to achieve better results with any of the other ligand derivatives **33a** or **34a**,**b**. Interestingly, the stereochemical configuration on the major product was reversed when the (S_b)-configured ligands **34a**,**b** were used instead of (R_b)-configured derivatives **33a**,**b**. The 2'-substituent (H in **33a** and **34a**, OMe in **33b** and **34b**) had only a minor influence on the enantioselectivities.

Although we were unable to match the performance of the reference ligand OMe-MOP, we have shown that our phosphonite ligands give moderate asymmetric induction in this rhodium catalysed reaction. Therefore, **33a**,**b** and **34a**,**b** should also be suitable ligands for related reactions like the asymmetric addition of arylylboronic acids to isatins, in which OMe-MOP achieved up to 93% *ee*.[296]

5.2.8 Gold(I) Complexation and Catalysis

Gold catalysis has received an increased amount of research interest from the beginning of the 21st century.[297] It has been realised that gold(I) complexes can act as a soft carbophilic Lewis acid towards C–C double and triple bonds and thereby they are efficient catalysts for the transformation of alkyne and allene substrates. The tolerance of functional groups is usually high as a result of the relatively low oxophilicity of the metal. Asymmetric reactions relying on homogeneous gold(I) catalysis have been challenging because of the nature of the two-coordinate linear complexes that position the substrate far away from the chiral ligand. However, good enantioselectivities have been achieved mainly using chiral bisphosphine ligands with the general structure [$(AuX)_2$(P–P)] (P–P chiral bisphosphine, X = anionic ligand).[298]

Our chiral MOP-based phosphonite ligands **33a**,**b** or **34a**,**b** are sterically demanding which we thought could be a good prerequisite for achieving asymmetric induction from their linear coordinated gold(I) complexes. Firstly, we set out to study the coordination chemistry of these ligands by reacting **33a**,**b** and **34a**,**b** with [Au(tht)Cl] to obtain the corresponding gold(I) complexes **48a**,**b** and **49a**,**b** in quantitative conversions. For complexes **48b** (Figure 5.20) and **49b** (Figure 5.21) we were able to analyse the molecular structures by X-ray diffraction. The Au–P (2.192(3)-2.200(3) Å) and Au–Cl (2.2647(13)-2.267(3) Å) bond lengths were found to be as expected for aryl-phosphonite ligated complexes.[299] They are slightly shorter than the equivalent bonds in gold(I) complexes of the BINAP ligand (Au–P 2.226(2), Au–Cl 2.290(2))[300] which is due to the stronger back bonding in the case of the phosphonites. The position of the Au-atom relative to the lower naphthyl group of the MOP-fragment is very similar in **48b** and **49b**; it is situated closest to the C2'-carbon with a distance of 3.1156(12) to

3.220(3) Å. The two reported gold(I) chloride structures of BINAP-derivatives show the C1-carbon of the naphthyl group in closest proximity, presumably due to the enhanced steric crowding caused by the coordination of two metals in those complexes.[300,301] The metal-aryl interactions in gold(I) complexes have been investigated as part of a theoretical study on biphenyl-derived P-ligands suggesting a weak η^2 side-on coordination of the aryl group.[302]

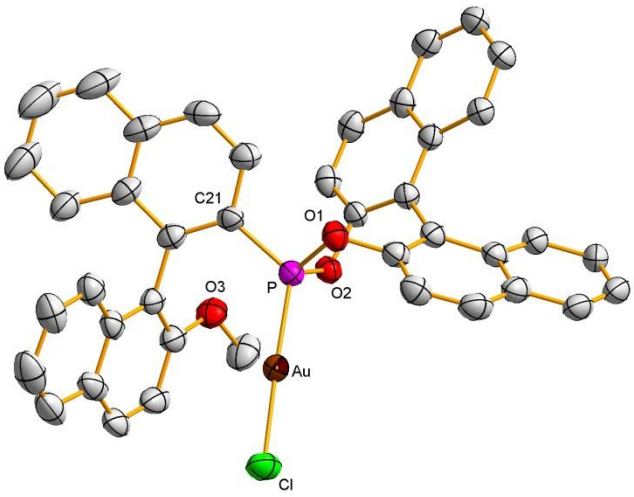

Figure 5.20 View of the molecular structure of [(**33b**)AuCl] (**48b**) with 50% probability displacement ellipsoids. Hydrogen atoms have been omitted for clarity. Selected bond distances [Å] and angles [°]: Au–P 2.1984(12), Au–Cl 2.2647(13); P-Au-Cl 177.91(5), O1-P-O2 101.94(16), O1-P-C21 98.52(17), O2-P-C21 106.88(19).

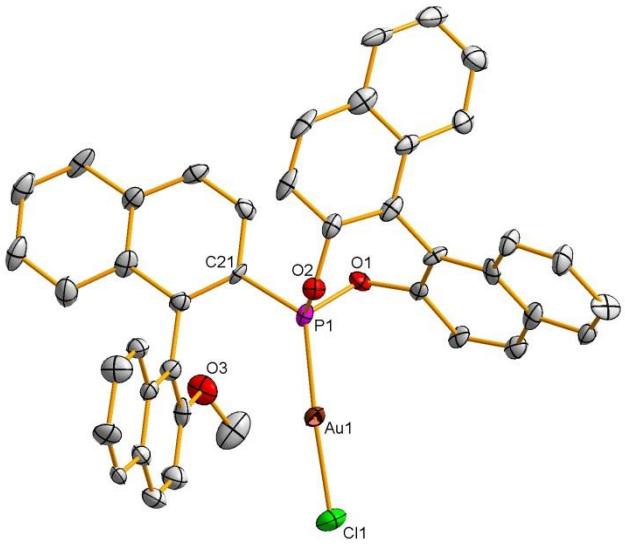

Figure 5.21 View of one of the two independent molecules of [(**34b**)AuCl] (**49b**) with 50% probability displacement ellipsoids. Hydrogen atoms have been omitted for clarity. Selected bond distances [Å] and angles [°], respective bond lengths/angles of the second molecule in brackets: Au1–P1 2.200(3) (2.192(3)), Au1–Cl1 2.267(3) (2.267(3)); P1-Au1-Cl1 173.30(12) (174.78(12)), O1-P1-O2 102.7(4) (102.1(4)), O1-P1-C21 101.2(4) (101.3(4)), O2-P1-C21 104.2(4) (103.0(4)).

We were keen to evaluate the catalytic activity of our complexes **48a**,**b** and **49a**,**b** in the gold(I) catalysed cyclopropanation of styrene.[303] The propargyl acetate coordinates to the

metal by a 1,2-carboxylate shift to form the gold(I)-carbenoid intermediate, which subsequently reacts with styrene to give the cyclopropane derivative as product (Scheme 5.5). The use of bulky ligands enabled the diastereoselective formation of the *cis*-isomers *via* the favoured intermediate with the least interaction between the alkene and the gold(I)-complex (Scheme 5.5); on the same basis a chiral ligand can support the formation of a specific *cis*-enantiomer.[304]

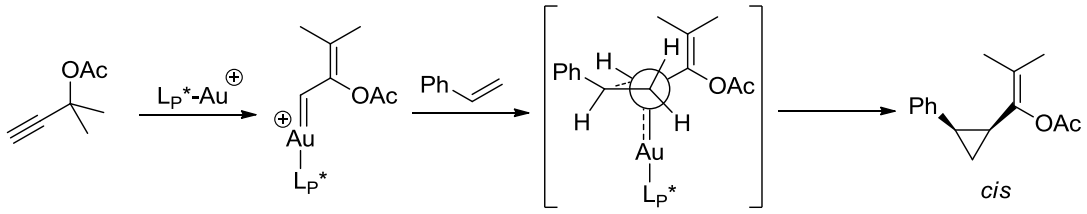

Scheme 5.5 Gold(I) catalysed cyclopropanation of styrene with propargyl acetate.

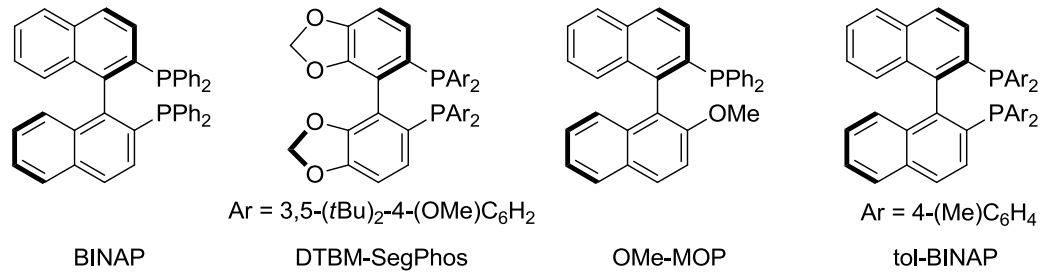

Figure 5.22 Phosphine ligands that have been used in gold(I) catalysed cyclopropanations (BINAP, DTBM-SegPhos, OMe-MOP) and alkoxycyclisations of 1,6-enynes (tol-BINAP).

Table 5.10 Catalytic cyclopropanation of styrene with propargyl acetate.

entry	ligand[a]	temp.	dr (*cis*/*trans*)[b]	yield[c]	*ee*[d]
1	BINAP[e]	rt	>20:1	85%	22%
2	DTBM-SegPhos[e]	rt	>20:1	72%	60%
3	OMe-MOP[e]	rt	>20:1	44%	5%
4	**33a** (**48a**)	rt	98:2	50%	15%
5	**33b** (**48b**)	rt	91:9	43%	14%
6	**34a** (**49a**)	rt	93:7	73%	–4%
7	**34b** (**49b**)	rt	93:7	36%	0%

[a] Catalyst was generated *in situ* from [AuCl(ligand)] (0.025 mmol) and $AgSbF_6$ (0.025 mmol) in $MeNO_2$ (4 mL) and reacted with styrene (2.0 mmol) and 2-methylbut-3-yn-2-yl acetate (0.5 mmol); 2 hours reaction time. [b] Determined by integration of the OAc resonances in the ^1H NMR. [c] Isolated yield after column chromatographic workup.[d] Determined by chiral HPLC (Chiralcel OD). [e] Values taken from ref. 303.

Toste and co-workers were the first to carry out the reaction using various mono- and bidentate P-ligands including BINAP, DTBM-SegPhos and OMe-MOP (Figure 5.22, Table

5.10). The best results were obtained using the SegPhos ligand, which gave a diastereomeric ratio of >20:1 (*cis*/*trans*) and 60% *ee* (entry 2). For our ligands **33a**,**b** and **34a**,**b** the *cis*-product was generally observed as the major isomer in agreement with the literature values (entries 4-7). The enantioselectivities of the reactions were however low; nearly racemic products were obtained from the (*S*)-BINOL substituted derivatives **34a**,**b** (entires 6-7). For the (*R*)-BINOL substituted derivatives **33a**,**b** we obtained low enantioselectivities of 15% and 14% *ee* respectively (entries 4-5), suggesting that the substituent in the 2'-position of the ligand has little influence on the enantioselectivity, and that the configurations of the two stereocentres in these ligands are better matched for this type of catalysis. The results are comparable to those of the related OMe-MOP ligand which gave a similar yield of 44% and a very low enantioselectivity of 5% *ee* (entry 3).

For a further test of the asymmetric induction of complexes **48a**,**b** and **49a**,**b** we also employed these compounds as catalysts in the alkoxycyclisation of enynes.[301] The reaction proceeds by coordination of the enyne-substrate *via* formation of gold(I)-carbene and carbocation intermediates and subsequent nucleophilic attack of the methanol solvent (Scheme 5.6).[304] Achieving a high level of asymmetric induction has been found particularly challenging for this reaction as the generated chiral centre of the substrate is located relatively far away from the gold centre.[301]

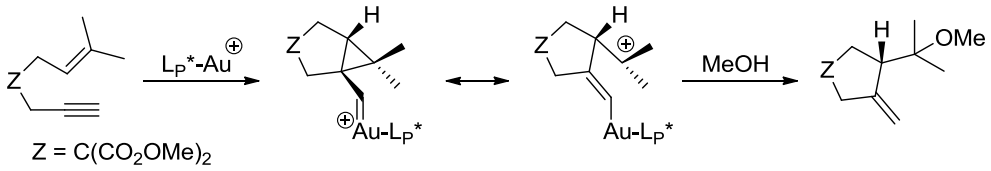

Scheme 5.6 Gold(I) catalysed alkoxycyclisation with 1,6-enynes.

Table 5.11 Catalytic alkoxycyclisation of 1,6-enynes.

entry	ligand[a]	temp.	time	yield[b]	*ee*[c]
1	tol-BINAP[d]	24 °C	7 h	91%	~2%
2	**33a** (**48a**)	rt	2.5 h	89%	2%
3	**33b** (**48b**)	rt	3 h	77%	6%
4	**34a** (**49a**)	rt	3 h	80%	–1%
5	**34b** (**49b**)	rt	2.5 h	84%	6%

[a] Catalyst was generated *in situ* from [AuCl(ligand)] (0.015 mmol) and $AgSbF_6$ (0.015 mmol) in MeOH (4 mL) and reacted with enyne (0.25 mmol). [b] Isolated yield after column chromatographic workup. [c] Determined by chiral HPLC (Chiralpak AD-H). [d] Values taken from ref. 301.

The observed activities that were achieved with our ligands **33a**,**b** and **34a**,**b** were generally good, giving complete conversions of the starting materials in less than 3 hours; very low enantioselectivities (up to 6% *ee*) were obtained in all cases (Table 5.11, entries 2-5). However, our results showed a small improvement in comparison to the tol-BINAP ligand (Figure 5.22) that only gave about 2% *ee* in this transformation (Table 5.11, entry 1).[301]

The reaction has been found to be significantly more selective for bulkier substrates (*i.e.* Z = $C(SO_2Ph)_2$) giving 43% *ee* with tol-BINAP.[301] Hence, the small improvements made with ligands **33a**,**b** and **34a**,**b** suggest that these ligands might be more viable candidates for the enantioselective transformation of bulkier 1,6-enynes.

5.3 Conclusion

In summary, we have demonstrated that the air-stable primary phosphines **1a**,**b** readily form their dichlorophosphine counterparts, which react as electrophiles with enantiopure BINOL to give novel chiral phosphonites. We have characterised each ligand as its methallylpalladium complex by NMR and X-ray crystallography, which together with detailed NMR experiments on related cationic complexes indicate the subtly different metal environment in each case and the P,C ligation of **38b** and **39b**. For the hydrosilylation of styrene, enantioselectivities of 80% were achieved, in reactions that have not yet been optimised. We have reported the first structural confirmation of a η^1,η^6-(σ-P, π-arene) chelated MOP-type ligand on rhodium(I) and the extent of the bonding has been analysed quantitatively by NOESY NMR. We were also able to synthesise the first iridium(I)-MOP complexes. The fine tuning between metal-stabilisation and catalytic activity will be the focus of future research. The asymmetric induction of the MOP-type ligands in gold(I) catalysed reactions has been very moderate. However, the initial results reported here show some potential in comparison with literature data, given the challenges of gold(I) catalysis.

5.4 Experimental Section

5.4.1 General Considerations

All air- and/or water-sensitive reactions were performed under a nitrogen atmosphere using standard Schlenk line techniques. Tetrahydrofuran and dichloromethane were dried over sodium/benzophenone and calcium hydride respectively, and distilled prior to use. Toluene (Acros) was purchased in an anhydrous state and stored over molecular sieves. Procedures for the preparation of **1a**,**b** are given in Chapter 2.4. The experimental procedures for the rhodium

catalysed hydrogenation of (*Z*)-methyl-2-acetamido cinnamate, the palladium catalysed hydrosilylation of styrene, and the palladium catalysed allylic alkylation of (*rac*)-(*E*)-1,3-diphenylallyl acetate are described in Chapters 3.4.8, 3.4.9, and 4.4.20 respectively. $[Rh(C_2H_4)_2Cl]_2$,[305] $[Rh(\eta^4\text{-cod})Cl]_2$,[306] $[Ir(\eta^4\text{-cod})Cl]_2$[307] and $[Ir(\eta^4\text{-cod})_2]BF_4$[308] were synthesised according to literature procedures. All other chemicals were used as received without further purification.

Table 5.12 Selected crystallographic data of **35a**,**b** and **36a**,**b**.

	35a	**35b**	**36a**	**36b**
formula	$C_{40}H_{27}O_3P\cdot 2C_7H_8$	$C_{42}H_{30}Cl_3O_4P$	$C_{45}H_{34}Cl_3O_2PPd$	$C_{45}H_{34}Cl_3O_2PPd$
formula wt	770.85	735.98	850.44	850.44
cryst syst	monoclinic	monoclinic	orthorhombic	orthorhombic
space group	$P2_1$	$P12_11$	$P2_12_12_1$	$P2_12_12_1$
a, Å; *α*, deg	9.377(2); 90	8.5896(2); 90	11.9353(3); 90	12.0059(4); 90
b, Å; *β*, deg	13.472(3); 93.983(3)	23.5450(5); 108.165(3)	13.7947(4); 90	13.8615(4); 90
c, Å; *γ*, deg	16.236(4); 90	9.0240(2); 90	22.2867(6); 90	22.5034(7); 90
V, Å^3	2046.1(8)	1734.08(7)	3669.37(17)	3745.0(2)
Z	2	2	4	4
ρ_{calc}, g cm^{-3}	1.251	1.410	1.539	1.508
μ, mm^{-1}	0.113	0.355	0.808	0.791
F(000)	812	760	1728	1728
T_{min}/T_{max}		0.9010/0.9324	0.97796/1.00000	0.82919/1.00000
hkl range	–9 to 12, –18 to 18, –21 to 20	–8 to 10, –29 to 30, –11 to 12	–12 to 15, –16 to 18, –27 to 28	–15 to 14, –18 to 18, –22 to 30
θ range, deg	2.5 to 27.6	2.9 to 28.5	2.9 to 28.6	2.9 to 28.6
no. of measd rflns	18683	16587	19447	21950
no. of unique rflns (R_{int})	9114 (0.0383)	7295 (0.0225)	7808 (0.0373)	8064 (0.0447)
no. of obsd rflns, $I > 2\sigma(I)$	8070	6530	6453	6146
refined params/restraints	595/330	460/1	470/0	471/0
goodness of fit	1.027	1.027	0.880	0.876
Abs. structure param.	0.08(8)	0.01(4)	–0.024(14)	–0.020(16)
R1/wR2 ($I > 2\sigma(I)$)	0.0490/0.1159	0.0308/0.0778	0.0281/0.0444	0.0311/0.0500
R1/wR2 (all data)	0.0596/0.1242	0.0355/0.0790	0.0396/0.0457	0.0509/0.0525
resid electron dens, e Å^{-3}	0.48/–0.33	0.65/–0.27	0.29/–0.41	0.64/–0.69

Table 5.13 Selected crystallographic data of **37a**,**b**, **40b** and **43b**.

	37a	**37b**	**40b**	**43b**
formula	$C_{45}H_{34}ClO_3PPd \cdot CH_2Cl_2$	$C_{49}H_{44}ClO_4PPd$	$C_{53}H_{49}ClO_4PRh$	$C_{90}H_{74}BF_4O_8P_2Rh$
formula wt	880.47	869.66	919.25	1535.15
cryst syst	orthorhombic	orthorhombic	orthorhombic	orthorhombic
space group	$P2_12_12_1$	$P2_12_12_1$	$P2_12_12_1$	$P2_12_12_1$
a, Å; α, deg	10.4065(4)	12.1370(2); 90	9.5919(3); 90	14.0434(4); 90
b, Å; β, deg	17.4563(4)	14.4938(3); 90	19.2348(5); 90	20.3321(6); 90
c, Å; γ, deg	21.7841(5)	23.2109(5); 90	23.6141(6); 90	25.7605(6); 90
V, Å^3	3957.3(2)	4083.06(14)	4356.8(2)	7355.4(3)
Z	4	4	4	4
ρ_{calc}, g cm^{-3}	1.478	1.415	1.401	1.386
μ, mm^{-1}	0.753	0.604	0.537	2.864
F(000)	1792	1792	1904	3176
T_{min}/T_{max}	0.7945/0.8639	0.8395/0.9420	0.85566/1.00000	0.71860/1.00000
hkl range	–9 to 12, –17 to 22, –21 to 29	–16 to 16, –19 to 19, –30 to 31	–11 to 12, –25 to 24, –24 to 31	–14 to 14, –21 to 21, –27 to 27
θ range, deg	3.0 to 28.6	3.0 to 28.6	3.0 to 28.5	7.7 to 54.2
no. of measd rflns	22011	48358	25484	36016
no. of unique rflns (R_{int})	8320 (0.0394)	9182 (0.0525)	9385 (0.0321)	8935 (0.0542)
no. of obsd rflns, $I > 2\sigma(I)$	7461	6798	8683	8181
refined params/restraints	463/24	509/0	542/0	961/0
goodness of fit	1.038	0.893	1.081	1.027
Abs. structure param.	0.03(2)	–0.028(16)	–0.03(2)	–0.037(7)
R1/wR2 ($I > 2\sigma(I)$)	0.0385/0.0887	0.0300/0.0548	0.0330/0.0757	0.0401/0.0986
R1/wR2 (all data)	0.0455/0.0931	0.0511/0.0575	0.0388/0.0795	0.0461/0.1031
resid electron dens, e Å^{-3}	0.38/–0.54	0.42/–0.40	0.74/–0.45	0.80/–0.50

Flash chromatography was performed on silica gel from Fluorochem (silica gel, 40-63u, 60A, LC301). Thin-layer-chromatography was performed on Merck aluminium-based plates with silica gel and fluorescent indicator 254 nm. For indicating, UV light or potassium permanganate solution (1.0 g $KMnO_4$, 6.7 g K_2CO_3, 0.1 g NaOH, 100 ml H_2O) was used. Melting points were determined in open glass capillary tubes on a Stuart SMP3 melting point apparatus. Optical rotation values were determined on an Optical Activity Polaar 2001 device. Mass spectrometry was carried out by the EPSRC National Mass Spectrometry Service Centre, Swansea. Analytical high performance liquid chromatography (HPLC) was performed on a Varian Pro Star HPLC equipped with a variable wavelength detector using a Daicel Chiralcel OD or a Chiralpak AD-H column.

Table 5.14 Selected crystallographic data of **45b**, **48b** and **49b**.

	45b	**48b**	**49b**
formula	$C_{49}H_{39}Cl_3IrO_2P$	$C_{41}H_{27}AuClO_3P\cdot CH_2Cl_2$	$C_{41}H_{27}AuClO_3P\cdot CH_2Cl_2\cdot H_2O$
formula wt	989.32	915.94	933.95
cryst syst	orthorhombic	monoclinic	triclinic
space group	$P2_12_12_1$	C2	P1
a, Å; *α*, deg	11.0978(5); 90	23.505(6); 90	9.1356(3); 108.251(4)
b, Å; *β*, deg	13.6168(6); 90	7.956(2); 100.359(2)	13.1385(6); 90.102(3)
c, Å; *γ*, deg	26.3077(12); 90	19.215(5); 90	15.5999(6); 101.515(3)
V, Å^3	3975.5(3)	3534.7(16)	1738.27(12)
Z	4	4	2
ρ_{calc}, g cm^{-3}	1.653	1.721	1.784
μ, mm^{-1}	3.642	4.109	4.554
F(000)	1968	1800	920
T_{min}/T_{max}	0.4079/0.5295	0.6384/0.8529	2/1.00000
hkl range	–13 to 13, –17 to 18, –31 to 31	–31 to 31, –6 to 10, –25 to 25	–10 to 10, –15 to 15, –18 to 18
θ range, deg	3.0 to 28.6	1.8 to 27.4	3.1 to 25.0
no. of measd rflns	25042	17861	25237
no. of unique rflns (R_{int})	8542 (0.0381)	7360 (0.0318)	12133 (0.0448)
no. of obsd rflns, $I > 2\sigma(I)$	7597	6759	11602
refined params/restraints	505/0	427/1	923/556
goodness of fit	1.035	1.017	1.046
Abs. structure param.	–0.037(5)	0.043(6)	0.007(7)
R1/wR2 ($I > 2\sigma(I)$)	0.0312/0.0585	0.0260/0.0615	0.0521/0.1274
R1/wR2 (all data)	0.0394/0.0629	0.0287/0.0625	0.0544/0.1295
resid electron dens, e Å^{-3}	0.87/–0.81	1.24/–0.98	2.55/–1.36

^{1}H NMR, ^{11}B{^{1}H} NMR, ^{13}C{^{1}H} NMR, ^{19}F NMR, and ^{31}P{^{1}H} NMR spectra were recorded on a JEOL Lambda 500 (^{1}H 500.16 MHz) or JEOL ECS-400 (^{1}H 399.78 MHz) spectrometer at room temperature (21°C) if not otherwise stated, using the indicated solvent as internal reference. Two-dimensional NMR experiments (COSY, NOESY, HSQC, HMBC) were used for the assignment of proton and carbon resonances, the numbering scheme is given in Figure 5.23. Full range NOESY spectra were acquired with 512 × 1024 data points and a spectral width of 9.0 ppm; mixing times were chosen between 10 and 500 ms. For the measurement of exchange rate constants, the proton resonances of the methoxy group were used. Peak volumes were determined manually from the NOESY spectrum using MestReNova 6, and the rate constants were calculated with an estimated error of 10% using EXSYCalc.[309] Key crystallographic data are given in Table 5.12,

Table **5.13** and Table 5.14.

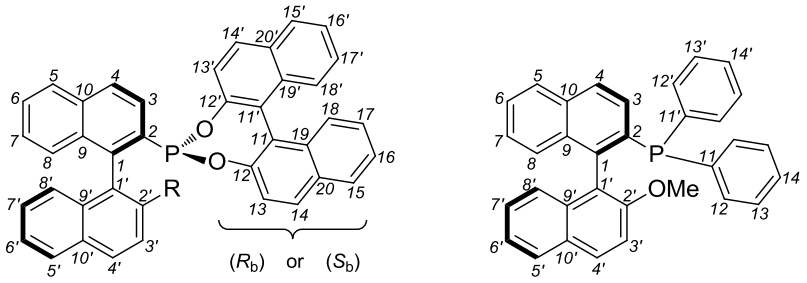

Figure 5.23 Numbering scheme used for MOP-type phosphonite compounds (left) and OMe-MOP (right).

5.4.2 (*S*,*R*b)-[1,1'-Binaphthalene]-2,2'-diyl [1,1'-binaphthalen]-2-ylphosphonite (**33a**)

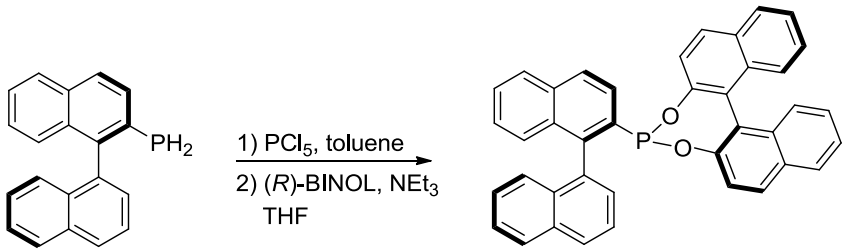

PCl_5 (458 mg, 2.20 mmol) was dissolved in toluene (8 mL). Primary phosphine **1a** (286 mg, 1.00 mmol) was added and the reaction mixture was left to stir for 45 minutes. The volatiles were removed *in vacuo* to give the corresponding dichlorophosphine ($^{31}P\{^1H\}$ NMR, $CDCl_3$: δ = 157.1 ppm) as a yellow oil. THF (8 mL), NEt_3 (448 mg, 0.64 mL, 4.40 mmol) and (*R*)-BINOL (286 mg, 1.00 mmol) were subsequently added and the solution was left to stir overnight. The volatiles were removed *in vacuo* and the crude product was filtered through a plug of silica in toluene. The title product was obtained after removal of the solvent as a white solid. (404 mg, 0.71 mmol, 71%).

MP (uncorrected): 158 °C. **^{1}H NMR** (500 MHz, CD_2Cl_2): δ = 8.06 (d, $^3J_{HH}$ = 8.3 Hz, 1H, *H*4'), 8.01 (d, $^3J_{HH}$ = 8.3 Hz, 1H, Ar*H*), 7.95-7.91 (m, 3H, *H*14+2 Ar*H*), 7.88 (d, $^3J_{HH}$ = 8.2 Hz, 1H, Ar*H*), 7.84 (dd, $^3J_{HH}$ = 7.0 Hz, $^5J_{HP}$ = 1.0 Hz, 1H, *H*2'), 7.73 (d, $^3J_{HH}$ = 8.7 Hz, 1H, *H*14'), 7.69 (dd, $^3J_{HH}$ = 8.3 Hz, $^3J_{HH}$ = 7.0 Hz, 1H, *H*3'), 7.61 (d, $^3J_{HH}$ = 8.6 Hz, 1H, *H*4), 7.56-7.52, (m, 2H, 2 Ar*H*), 7.49-7.40 (m, 4H, *H*13+3 Ar*H*), 7.38-7.31 (m, 5H, 5 Ar*H*), 7.30-7.24 (m, 3H, *H*3+2 Ar*H*), 6.91 (d, $^3J_{HH}$ = 8.7 Hz, 1H, *H*13') ppm. **^{13}C{^{1}H} NMR** (126 MHz, CD_2Cl_2): δ = 150.2 (d, $^2J_{CP}$ = 2.4 Hz, *C*12), 149.0 (d, $^2J_{CP}$ = 6.1 Hz, *C*12'), 145.0 (d, $^2J_{CP}$ = 37.2 Hz, *C*1), 136.2 (d, $^1J_{CP}$ = 38.9 Hz, *C*2), 135.0, 134.8 (d, J_{CP} = 10.0 Hz), 133.5, 133.3 (d, J_{CP} = 2.1 Hz), 133.0 (d, J_{CP} = 4.7 Hz), 132.9 (d, J_{CP} = 1.5 Hz), 132.8 (d, J_{CP} = 1.0 Hz), 131.7, 131.2, 130.9 (d, $^4J_{CP}$ = 5.8 Hz, *C*2'), 130.6 (*C*14), 129.6 (d,

$^4J_{CP}$ = 0.7 Hz, *C*14'), 129.1 (*C*4'), 128.5, 128.4, 128.3, 128.2, 127.7, 127.1 (*C*4), 127.0 (d, J_{CP} = 2.8 Hz), 126.8, 126.7, 126.6, 126.6, 126.5, 126.3, 126.3, 126.2, 125.0, 124.9 (*C*3'), 124.9, 124.7 (d, $^3J_{CP}$ = 5.7 Hz, *C*11), 124.2 (d, $^2J_{CP}$ = 2.7 Hz, *C*3), 123.8 (d, $^3J_{CP}$ = 2.6 Hz, *C*11'), 122.2 (*C*13'), 121.5 (d, $^3J_{CP}$ = 1.4 Hz, *C*13) ppm. **^{31}P{^{1}H} NMR** (202 MHz, CD_2Cl_2): δ = 177.4 ppm. **IR** (neat): ν = 3055.4 (w), 2981.3 (w), 1588.6 (w), 1505.9 (m), 1462.5 (m), 1362.2 (w), 1326.4 (m), 1228.2 (s), 1203.1 (w), 1154.9 (w), 1070.0 (m), 949.2 (s), 869.5 (w), 818.8 (s), 782.0 (m), 747.7 (s), 629.4 (m) cm^{-1}. **HRMS** (ESI$^+$, MeOH): Found: *m*/*z* = 585.1605. Calculated for $[M + H_2O]^+$: *m*/*z* = 585.1614. **OR** ($CHCl_3$, *c* = 1.0 mg/ml): $[\alpha]_D^{20}$ = +238°. **EA**: Found: C 84.49%, H 4.77%. Calculated for [M]: C 84.49%, H 4.43%.

5.4.3 (*R*,*R*$_b$)-[1,1'-Binaphthalene]-2,2'-diyl (2'-methoxy-[1,1'-binaphthalen]-2-yl)-phosphonite (**33b**)

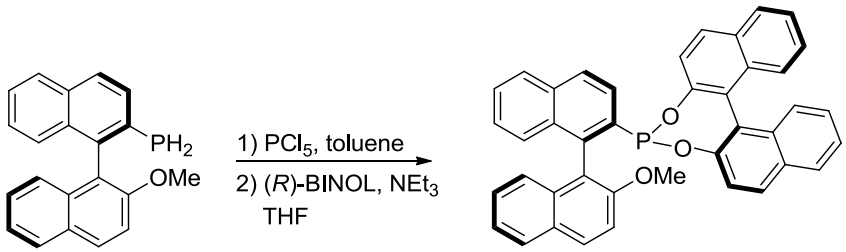

PCl_5 (458 mg, 2.20 mmol) was dissolved in toluene (8 mL). **1b** (316 mg, 1.00 mmol) was added and the reaction mixture was left to stir for 45 minutes. The volatiles were removed *in vacuo* to give the corresponding dichlorophosphine (^{31}P{^{1}H} NMR, $CDCl_3$: δ = 159.1 ppm) as yellow solid. THF (8 mL), NEt_3 (448 mg, 0.64 mL, 4.40 mmol) and (*R*)-BINOL (286 mg, 1.00 mmol) were added subsequently and the solution was left to stir overnight. The volatiles were removed *in vacuo* and the crude product was dissolved in toluene and filtered through a plug of silica. The title product was obtained after removal of the solvent as a white solid (523 mg, 0.87 mmol, 87%).

MP (uncorrected): >270 °C. **^{1}H NMR** (500 MHz, CD_2Cl_2): δ = 8.09 (d, $^3J_{HH}$ = 9.1 Hz, 1H, *H*4'), 7.94-7.90 (m, 4H, *H*5'+*H*14+*H*15'+Ar*H*), 7.89 (d, $^3J_{HH}$ = 8.2 Hz, 1H, *H*5), 7.72 (d, $^3J_{HH}$ = 8.8 Hz, 1H, *H*14'), 7.59 (d, $^3J_{HH}$ = 8.5 Hz, 1H, *H*4), 7.55 (ddd, $^3J_{HH}$ = 8.2 Hz, $^3J_{HH}$ = 5.7 Hz, $^4J_{HH}$ = 2.1 Hz, 1H, *H*6), 7.53 (d, $^3J_{HH}$ = 9.1 Hz, 1H, *H*3'), 7.47 (ddd, $^3J_{HH}$ = 8.2 Hz, $^3J_{HH}$ = 6.8 Hz, $^4J_{HH}$ = 1.2 Hz, 1H, Ar*H*), 7.44-7.40 (m, 3H, *H*13+2 Ar*H*), 7.38 (ddd, $^3J_{HH}$ = 8.2 Hz, $^3J_{HH}$ = 6.8 Hz, $^4J_{HH}$ = 1.2 Hz, 1H, Ar*H*), 7.36-7.24 (m, 6H, 6 Ar*H*), 7.23 (dd, $^3J_{HH}$ = 8.5 Hz, $^3J_{HP}$ = 1.4 Hz, 1H, *H*3), 7.02 (d, $^3J_{HH}$ = 8.5 Hz, 1H, Ar*H*), 6.93 (d, $^3J_{HH}$ = 8.8 Hz, 1H, *H*13'), 3.99 (s, 3H, OCH_3) ppm. **^{13}C{^{1}H} NMR** (126 MHz, CD_2Cl_2): δ = 156.6 (d, $^4J_{CP}$ = 3.5 Hz, *C*2'), 150.3 (d, $^2J_{CP}$ = 2.5 Hz, *C*12), 154.9 (d, $^2J_{CP}$ = 5.8 Hz, *C*12'),

141.8 (d, $^{2}J_{CP}$ = 37.5 Hz, *C*1), 136.3 (d, $^{1}J_{CP}$ = 37.7 Hz, *C*2), 135.3, 134.5 (d, $^{4}J_{CP}$ = 2.9 Hz, *C*9'), 132.9, 132.8, 132.7 (d, J_{CP} = 1.0 Hz), 131.6 (d, J_{CP} = 0.9 Hz), 131.4, 131.2, 130.8 (*C*4'), 130.5 (*C*5'), 129.5 (*C*14'), 128.7, 128.5, 128.5, 128.3 (*C*5), 128.2 (*C*10'), 128.1, 127.7, 127.1, 126.8, 126.7 (*C*4), 126.6, 126.5, 126.4 (d, J_{CP} = 2.6 Hz), 126.2, 126.1, 125.2, 124.9, 124.8, 124.5 (d, $^{2}J_{CP}$ = 2.0 Hz, *C*3), 123.8, 122.7 (*C*13), 121.6 (*C*13'), 118.9 (d, $^{3}J_{CP}$ = 10.2 Hz, *C*1'), 112.8 (*C*3'), 56.2 (s, O*C*H$_3$) ppm. **^{31}P{^{1}H} NMR** (202 MHz, CD_2Cl_2): δ = 177.8 ppm. **IR** (neat): ν = 2981.2 (w), 1619.8 (w), 1590.0 (m), 1507.0 (m), 1461.8 (m), 1431.0 (w), 1327.7 (w), 1228.2 (s), 1149.5 (w), 1078.1 (m), 947.3 (s), 866.6 (w), 820.5 (m), 799.5 (m), 746.7 (s), 686.7 (w), 630.3 (w) cm^{-1}. **HRMS** (ESI$^+$, CH_2Cl_2): Found: *m*/*z* = 599.1767. Calculated for [M + H]$^+$: *m*/*z* = 599.1771. **OR** ($CHCl_3$, *c* = 1.0 mg/ml): $[\alpha]_D^{20}$ = +444°. **EA**: Found: C 82.60%, H 4.58%. Calculated for [M]: C 82.26%, H 4.55%.

5.4.4 (*S*,*S*$_b$)-[1,1'-Binaphthalene]-2,2'-diyl [1,1'-binaphthalen]-2-ylphosphonite (**34a**)

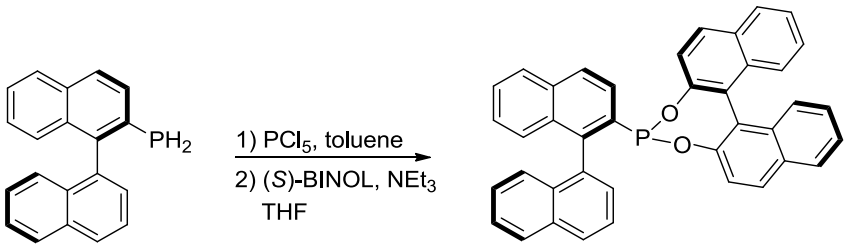

The same procedure was followed as for **33a**, except for using (*S*)-BINOL as the nucleophile. The title product was obtained as a white solid after removal of the solvent (527 mg, 0.93 mmol, 93%).

MP (uncorrected): 197 °C. **^{1}H NMR** (500 MHz, CD_2Cl_2): δ = 8.04 (d, $^{3}J_{HH}$ = 8.2 Hz, 1H, *H*4'), 7.99-7.89 (m, 4H, *H*14'+3 Ar*H*), 7.88 (d, $^{3}J_{HH}$ = 8.2 Hz, 1H, *H*5), 7.78 (d, $^{3}J_{HH}$ = 8.7 Hz, 1H, *H*14), 7.68 (dd, $^{3}J_{HH}$ = 8.2 Hz, $^{3}J_{HH}$ = 7.0 Hz, 1H, *H*3'), 7.63 (dd, $^{3}J_{HH}$ = 7.0 Hz, $^{5}J_{HP}$ = 1.2 Hz, 1H, *H*2'), 7.61 (d, $^{3}J_{HH}$ = 8.6 Hz, 1H, *H*4), 7.55 (ddd, $^{3}J_{HH}$ = 8.2 Hz, $^{3}J_{HH}$ = 5.5 Hz, $^{4}J_{HH}$ = 2.5 Hz, 1H, *H*6), 7.53-7.36 (m, 7H, *H*13'+6 Ar*H*), 7.35-7.28 (m, 3H, *H*7+*H*8+Ar*H*), 7.23-7.21 (m, 3H, *H*3+2 Ar*H*), 6.90 (d, $^{3}J_{HH}$ = 8.7 Hz, 1H, *H*13) ppm. **^{13}C{^{1}H} NMR** (126 MHz, CD_2Cl_2): δ = 150.1 (d, $^{2}J_{CP}$ = 1.9 Hz, *C*12'), 148.9 (d, $^{2}J_{CP}$ = 5.7 Hz, *C*12), 145.4 (d, $^{2}J_{CP}$ = 37.0 Hz, *C*1), 136.5 (d, $^{1}J_{CP}$ = 40.4 Hz, *C*2), 135.0 (d, J_{CP} = 7.9 Hz), 134.1 (d, J_{CP} = 2.9 Hz), 133.5, 133.0 (d, J_{CP} = 4.3 Hz), 132.9, 132.8, 131.6, 131.4, 131.2, 130.6 (*C*14'), 129.6 (*C*14), 129.4 (*C*2'), 128.7 (*C*4'), 128.5, 128.4, 128.4, 128.1 (*C*5), 127.8, 127.4 (d, J_{CP} = 2.6 Hz), 127.1 (*C*4), 127.0, 126.9, 126.8, 126.6, 126.5, 126.4, 126.2, 126.1, 125.9, 125.1 (*C*3'), 124.9, 124.8 (*C*11'), 124.3 (d, $^{2}J_{CP}$ = 2.6 Hz, *C*3), 123.6 (*C*11), 122.5 (*C*13), 121.4 (*C*13') ppm. **^{31}P{^{1}H} NMR** (202 MHz, CD_2Cl_2): δ = 175.7 ppm. **IR**

(neat): ν = 3060.6 (w), 2981.3 (w), 1588.6 (w), 1506.5 (w), 1466.0 (w), 1366.0 (w), 1330.0 (w), 1262.7 (w), 1232.0 (w), 1204.0 (w), 1141.6 (w), 1141.6 (w), 1072.2 (w), 951.6 (w), 869.5 (w), 822.7 (w), 789.4 (w), 753.7 (w), 684.6 (w), 630.2 (w) cm^{-1}. **HRMS** (EI^+): Found: m/z = 567.1514. Calculated for $[M - H]^+$: m/z = 567.1508. **OR** ($CHCl_3$, c = 1.0 mg/ml): $[\alpha]_D^{20} = -264°$.

5.4.5 (R,S_b)-[1,1'-Binaphthalene]-2,2'-diyl (2'-methoxy-[1,1'-binaphthalen]-2-yl)-phosphonite (**34b**)

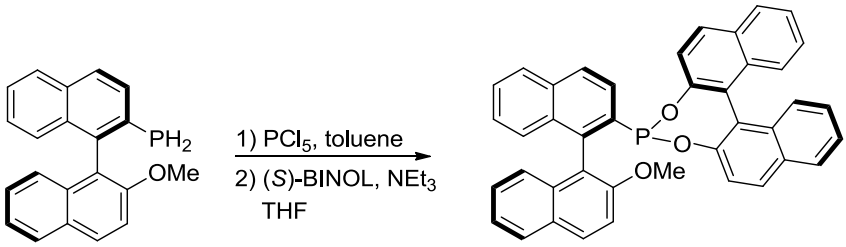

The same procedure was followed as for **33b**, except for using (*S*)-BINOL as the nucleophile. The title product was obtained as a white solid after removal of the solvent (430 mg, 0.72 mmol, 72%).

MP (uncorrected): 231 °C (decomposition). **^{1}H NMR** (500 MHz, CD_2Cl_2): δ = 8.09 (d, $^3J_{HH}$ = 9.1 Hz, 1H, *H*4'), 7.97 (d, $^3J_{HH}$ = 8.8 Hz, 1H, *H*14'), 7.93-7.90 (m, 3H, *H*15+*H*5'+*H*15'), 7.88 (d, $^3J_{HH}$ = 8.2 Hz, 1H, *H*5), 7.76 (d, $^3J_{HH}$ = 8.7 Hz, 1H, *H*14), 7.60 (d, $^3J_{HH}$ = 8.6 Hz, 1H, *H*4), 7.54 (dd, $^3J_{HH}$ = 8.0 Hz, $^{3/4}J_{HH}$ = 4.0 Hz, 1H, *H*6'), 7.52 (d, $^3J_{HH}$ = 8.8 Hz, 1H, *H*13'), 7.51 (d, $^3J_{HH}$ = 9.1 Hz, 1H, *H*3'), 7.46 (ddd, $^3J_{HH}$ = 8.0 Hz, $^3J_{HH}$ = 6.8 Hz, $^4J_{HH}$ = 1.0 Hz, 1H, *H*16), 7.42-7.35 (m, 4H, *H*18+3 Ar*H*), 7.32 (d, $^3J_{HH}$ = 4.0 Hz, 2H, *H*7'+*H*8'), 7.30 (ddd, $^3J_{HH}$ = 8.4 Hz, $^3J_{HH}$ = 6.8 Hz, $^4J_{HH}$ = 1.3 Hz, 1H, *H*17), 7.23-7.18 (m, 4H, *H*3+3 Ar*H*), 6.87 (d, $^3J_{HH}$ = 8.7 Hz, 1H, *H*13), 3.89 (s, 3H, OCH_3) ppm. **^{13}C{^{1}H} NMR** (101 MHz, CD_2Cl_2): δ = 154.9 (d, $^4J_{CP}$ = 2.9 Hz, *C*2'), 150.2 (d, $^2J_{CP}$ = 2.3 Hz, *C*12'), 149.0 (d, $^2J_{CP}$ = 5.9 Hz, *C*12), 141.9 (d, $^2J_{CP}$ = 39.2 Hz, *C*1), 136.4 (d, $^1J_{CP}$ = 38.3 Hz, *C*2), 135.3, 135.0 (*C*9'), 132.8, 132.7, 132.7, 131.6, 131.1, 130.7 (*C*4'), 130.5 (*C*14'), 129.5 (*C*14), 128.8, 128.4 (*C*15), 128.4 (*C*15'), 128.3 (*C*5'), 128.3 (*C*10'), 128.2 (*C*5), 127.7, 126.9 (*C*4), 126.8, 126.7, 126.6, 126.5, 126.4 (d, J_{CP} = 2.1 Hz), 126.2, 126.1, 125.5, 124.9, 124.8 (*C*16), 124.6 (d, J_{CP} = 2.5 Hz), 123.7, 123.6 (d, J_{CP} = 2.5 Hz), 122.5 (*C*13), 121.5 (*C*13'), 119.0 (d, $^3J_{CP}$ = 10.3 Hz, *C*1'), 113.0 (*C*3'), 56.4 (s, OCH_3) ppm. **^{31}P{^{1}H} NMR** (202 MHz, CD_2Cl_2): δ = 177.9 ppm. **IR** (neat): ν = 2980.8 (w), 1620.1 (w), 1590.2 (m), 1506.3 (m), 1462.7 (w), 1431.5 (w), 1329.8 (w), 1230.2 (s), 1203.4 (w), 1146.0 (w), 1070.1 (m), 949.5 (s), 867.8 (w), 820.8 (s), 789.7 (m), 747.2 (s), 684.7 (m), 628.8 (w) cm^{-1}. **HRMS**

(ESI$^+$, CH_2Cl_2): Found: m/z = 599.1766. Calculated for $[M + H]^+$: m/z = 599.1771. **OR** ($CHCl_3$, c = 1.0 mg/ml): $[\alpha]_D^{20} = -310°$.

5.4.6 General Procedure for the Preparation of L_P(Se)

Phosphorus ligand (L_P, 50.0 μmol) and KSeCN (14.4 mg, 100 μmol) were dissolved in THF (1 mL) and heated to 50 °C for 2 hours. The solvent was removed and the residue dissolved in $CDCl_3$. After filtration through celite the product was analysed by $^{31}P\{^1H\}$ NMR.

$^{31}P\{^1H\}$ NMR (202 MHz, $CDCl_3$): δ = **33a**(Se): 104.5 ($^1J_{PSe}$ = 925 Hz); **33b**(Se): 105.6 ($^1J_{PSe}$ = 930 Hz); **34a**(Se): 107.9 ($^1J_{PSe}$ = 925 Hz); **34b**(Se): 105.8 ($^1J_{PSe}$ = 925 Hz); OMe-MOP(Se): 38.3 ($^1J_{PSe}$ = 720 Hz) ppm.

5.4.7 General Procedure for the Preparation of *trans*-[Rh(L_P)$_2$(CO)Cl]

$[Rh(CO)_2Cl]_2$ (1.2 mg, 3.125 μmol) and phosphorus ligand (L_P, 12.5 μmol) were dissolved in CH_2Cl_2 (0.5 mL) and left to react for 10 minutes. The solvent was removed *in vacuo* and the product analysed by IR spectroscopy.

IR (CH_2Cl_2): ν = [Rh(**33a**)$_2$(CO)Cl]: 2004; [Rh(**33b**)$_2$(CO)Cl]: 2004; [Rh(**34a**)$_2$(CO)Cl]: 2023; [Rh(**34b**)$_2$(CO)Cl]: 2010; [Rh(OMe-MOP)$_2$(CO)Cl]: 1974 cm^{-1}.

5.4.8 General Procedure for the Preparation of *trans*-[Pt(L_P)(PEt$_3$)Cl$_2$]

$[Pt(PEt_3)Cl_2]_2$ (19.2 mg, 25.0 μmol) and phosphorus ligand (L_P, 50.0 μmol) were dissolved in CD_2Cl_2 (0.55 mL) and left to react for 30 minutes. The products were analysed by $^{31}P\{^1H\}$ NMR spectroscopy.

$^{31}P\{^1H\}$ NMR (202 MHz, CD_2Cl_2): δ = *trans*-[Pt(**33a**)(PEt$_3$)Cl$_2$]: 141.9 ($^1J_{PPt}$ = 3492 Hz, $^2J_{PP}$ = 624 Hz, **33a**), 10.5 ($^1J_{PPt}$ = 2492 Hz, $^2J_{PP}$ = 624 Hz, PEt$_3$); *trans*-[Pt(**33b**)(PEt$_3$)Cl$_2$]: 140.4 ($^1J_{PPt}$ = 3498 Hz, $^2J_{PP}$ = 620 Hz, **33b**), 9.2 ($^1J_{PPt}$ = 2509 Hz, $^2J_{PP}$ = 620 Hz, PEt$_3$); *trans*-[Pt(**34a**)(PEt$_3$)Cl$_2$]: 140.6 ($^1J_{PPt}$ = 3529 Hz, $^2J_{PP}$ = 621 Hz, **34a**), 10.0 ($^1J_{PPt}$ = 2481 Hz, $^2J_{PP}$ = 621 Hz, PEt$_3$); *trans*-[Pt(**34b**)(PEt$_3$)Cl$_2$]: 141.4 ($^1J_{PPt}$ = 3545 Hz, $^2J_{PP}$ = 623 Hz, **34b**), 8.6 ($^1J_{PPt}$ = 2495 Hz, $^2J_{PP}$ = 623 Hz, PEt$_3$); *trans*-[Pt(OMe-MOP)(PEt$_3$)Cl$_2$]: 25.3 ($^1J_{PPt}$ = 2440 Hz, $^2J_{PP}$ = 468 Hz, OMe-MOP), 13.7 ($^1J_{PPt}$ = 2554 Hz, $^2J_{PP}$ = 468 Hz, PEt$_3$); ppm.

5.4.9 Chloro((*S*,R_b)-[1,1'-binaphthalene]-2,2'-diyl [1,1'-binaphthalen]-2-ylphosphonite)(η³-2-methylallyl)palladium (**36a**)

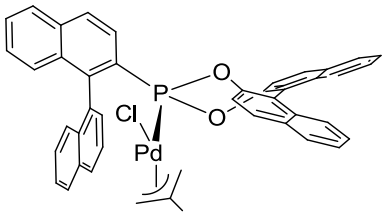

$[Pd(\eta^3\text{-}C_4H_7)Cl]_2$ (7 mg, 18 μmol) and **33a** (20 mg, 35 μmol) were dissolved in CH_2Cl_2 (1 mL) and stirred for 10 minutes. The intended complex was formed quantitatively. Slow diffusion of Et_2O into the reaction mixture yielded colorless crystals overnight, which were suitable for X-ray diffraction analysis. Yield: 25 mg (33 μmol, 93%)

MP (uncorrected): >270 °C. **^{1}H NMR** (500 MHz, CD_2Cl_2): δ = isomer **A** (97%) 7.97 (d, $^3J_{HH}$ = 8.1 Hz, 1H, *H*4'), 7.94-7.90 (m, 4H, *H*14+*H*5+*H*15+*H*15'), 7.89-7.85 (m, 2H, *H*2'+*H*5'), 7.84-7.80 (m, 2H, *H*13+*H*4), 7.78 (d, $^3J_{HH}$ = 8.9 Hz, 1H, *H*14'), 7.72 (dd, $^3J_{HH}$ = 8.6 Hz, $^3J_{HP}$ = 5.5 Hz, 1H, *H*3), 7.69 (dd, $^3J_{HH}$ = 8.1 Hz, $^3J_{HH}$ = 7.2 Hz, 1H, *H*3'), 7.58-7.55 (m, 1H, Ar*H*), 7.53-7.43 (m, 5H, *H*6'+4 Ar*H*), 7.39-7.27 (m, 5H, 5 Ar*H*), 7.18-7.13 (m, 2H, *H*13'+Ar*H*), 3.75 (dd, $^3J_{HP}$ = 9.9 Hz, $^4J_{HH}$ = 2.5 Hz, 1H, allyl-*H*t$_{syn}$), 2.56 (s, 1H, allyl-*H*c$_{syn}$), 1.57 (d, $^3J_{HP}$ = 14.1 Hz, 1H, allyl-*H*t$_{anti}$), 1.00 (s, 3H, allyl-C*H*$_3$), 0.83 (s, 1H, allyl-*H*c$_{anti}$); isomer **B** (3%), 8.00-6.99 (m, 23H, 23 Ar*H*), 6.92 (m, 1H, Ar*H*), 6.87 (m, 1H, Ar*H*), 3.96 (d, $^3J_{HP}$ = 6.8 Hz, 1H, allyl-*H*t$_{syn}$), 2.96 (m, 1H, allyl-*H*c$_{syn}$), 2.64 (d, $^3J_{HP}$ = 12.3 Hz, 1H, allyl-*H*t$_{anti}$), 1.53 (m, 1H, allyl-*H*c$_{anti}$), 1.42 (s, 3H, allyl-C*H*$_3$) ppm. **^{13}C{^{1}H} NMR** (126 MHz, CD_2Cl_2): δ = isomer **A** (97%) 149.1 (d, $^2J_{CP}$ = 5.3 Hz, *C*12), 148.6 (d, $^2J_{CP}$ = 13.2 Hz, *C*12'), 144.7 (d, $^2J_{CP}$ = 27.2 Hz, *C*1), 135.2, 134.7 (d, $^1J_{CP}$ = 9.3 Hz, *C*2), 133.5, 133.4, 133.3, 133.1, 132.6 (d, J_{CP} = 1.4 Hz), 132.2 (d, J_{CP} = 1.9 Hz), 131.9 (d, J_{CP} = 1.3 Hz), 131.5 (d, J_{CP} = 1.3 Hz), 131.1 (*C*2'), 131.0 (d, J_{CP} = 28.6 Hz, allyl-*C*), 130.7 (d, $^4J_{CP}$ = 1.1 Hz, *C*14), 130.2 (d, $^4J_{CP}$ = 1.4 Hz, *C*14'), 129.7, 129.2 (*C*4'), 128.6, 128.5, 128.3, 128.2, 128.2, 127.7 (d, $^3J_{CP}$ = 5.2 Hz, *C*4), 127.3, 127.1, 127.1, 127.0 (d, J_{CP} = 2.3 Hz), 126.9, 126.8, 126.7, 126.6, 126.4, 125.5, 125.4, 125.2 (*C*3'), 124.9 (d, $^2J_{CP}$ = 2.8 Hz, *C*3), 124.2 (d, $^3J_{CP}$ = 3.8 Hz, *C*11), 123.7 (d, $^3J_{CP}$ = 2.9 Hz, *C*11'), 122.4 (d, $^3J_{CP}$ = 2.4 Hz, *C*13), 120.4 (*C*13'), 76.8 (d, $^2J_{CP}$ = 45.3 Hz, allyl-*C*t), 56.1 (d, $^2J_{CP}$ = 5.8 Hz, allyl-*C*c), 22.4 (allyl-*C*H$_3$) ppm; signals of isomer B could not be observed. **^{31}P{^{1}H} NMR** (202 MHz, CD_2Cl_2): δ = isomer **A** (97%), 173.4; isomer **B** (3%) 175.7 ppm. **IR** (neat): ν = 3052.0 (w), 1587.6 (w), 1505.8 (m), 1460.0 (w), 1432.9 (w), 1360.3 (w), 1322.4 (m), 1220.7 (s), 1067.8 (m), 977.3 (w), 942.2 (s), 871.8

(w), 838.4 (m), 810.2 (s), 759.4 (m), 706.9 (m), 677.2 (w), 634.3 (w), 596.8 (w) cm^{-1}. **HRMS** (ESI^+, MeOH): Found: m/z = 727.1178. Calculated for $[M - Cl]^+$: m/z = 727.1176.

5.4.10 Chloro((*R*,R_b)-[1,1'-binaphthalene]-2,2'-diyl (2'-methoxy-[1,1'-binaphthalen]-2-yl)phosphonite)(η³-2-methylallyl)palladium (**36b**)

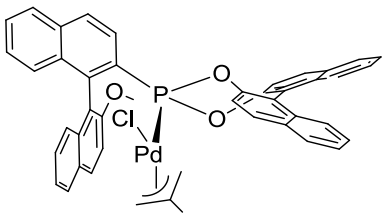

$[Pd(\eta^3\text{-}C_4H_7)Cl]_2$ (7 mg, 18 μmol) and **33b** (21 mg, 35 μmol) were dissolved in CH_2Cl_2 (1 mL) and stirred for 10 minutes. The intended complex was formed quantitatively. Slow diffusion of Et_2O into the reaction mixture yielded colorless crystals overnight, which were suitable for X-ray diffraction analysis. Yield: 26 mg (33 μmol, 93%).

MP (uncorrected): >270 °C. **^{1}H NMR** (500 MHz, CD_2Cl_2): δ = isomer **A** (93%) 7.98 (d, $^3J_{HH}$ = 9.1 Hz, 1H, *H*4'), 7.93 (dd, $^3J_{HH}$ = 8.9 Hz, $^4J_{HP}$ = 0.9 Hz, 1H, *H*13), 7.91-7.86 (m, 4H, *H*14+*H*5+*H*15+*H*15'), 7.78-7.73 (m, 2H, *H*5'+*H*4), 7.72 (d, $^3J_{HH}$ = 8.9 Hz, 1H, *H*14'), 7.63 (dd, $^3J_{HH}$ = 8.6 Hz, $^3J_{HP}$ = 5.4 Hz, 1H, *H*3), 7.55 (ddd, $^3J_{HH}$ = 8.1 Hz, $^3J_{HH}$ = 6.8 Hz, $^4J_{HH}$ = 1.1 Hz, 1H, Ar*H*), 7.50 (d, $^3J_{HH}$ = 9.1 Hz, 1H, *H*3'), 7.47-7.24 (m, 10H, 9 Ar*H*+*H*6'), 7.19 (d, $^3J_{HH}$ = 8.9 Hz, $^4J_{HP}$ = 1.0 Hz, 1H, *H*13'), 7.14 (d, $^3J_{HH}$ = 8.4 Hz, 1H, Ar*H*), 3.97 (s, 3H, OCH_3), 3.73 (dd, $^3J_{HP}$ = 10.0 Hz, $^4J_{HH}$ = 3.0 Hz, 1H, allyl-*H*t_{syn}), 2.60 (m, 1H, allyl-*H*c_{syn}), 1.63 (d, $^3J_{HP}$ = 14.1 Hz, 1H, allyl-*H*t_{anti}), 0.92 (s, 3H, allyl-CH_3), 0.85 (m, 1H, allyl-*H*c_{anti}); isomer **B** (7%) 8.05 (d, $^3J_{HH}$ = 9.1 Hz, 1H, *H*4'), 7.99-7.10 (m, 20H, 20 Ar*H*), 7.07-7.02 (m, 1H, Ar*H*), 6.97 (d, $^3J_{HH}$ = 8.9 Hz, 1H, *H*13'), 6.74 (d, $^3J_{HH}$ = 8.5 Hz, 1H, Ar*H*), 4.12 (s, 3H, OCH_3), 3.87 (m, 1H, allyl-*H*t_{syn}), 3.18 (m, 1H, allyl-*H*c_{syn}), 1.94 (d, $^3J_{HP}$ = 13.0 Hz, 1H, allyl-*H*t_{anti}), 1.70 (s, 3H, allyl-CH_3), 1.35 (m, 1H, allyl-*H*c_{anti}) ppm. **^{13}C{^{1}H} NMR** (126 MHz, CD_2Cl_2): δ = isomer **A** (93%) 156.4 (*C*2'), 149.3 (d, $^2J_{CP}$ = 5.3 Hz, *C*12), 149.1 (d, $^2J_{CP}$ = 12.9 Hz, *C*12'), 141.5 (d, $^2J_{CP}$ = 27.0 Hz, *C*1), 135.5 (d, $^1J_{CP}$ = 1.4 Hz, *C*2), 134.2 (*C*9'), 133.2 (d, J_{CP} = 7.1 Hz), 133.2 (d, J_{CP} = 8.1 Hz), 132.4 (d, J_{CP} = 1.3 Hz), 132.1 (d, J_{CP} = 1.4 Hz), 131.8 (d, J_{CP} = 8.1 Hz), 131.6 (d, J_{CP} = 1.1 Hz), 131.3 (d, $^2J_{CP}$ = 28.8 Hz, allyl-C), 131.0 (*C*4'), 130.5 (d, $^4J_{CP}$ = 1.1 Hz, *C*14), 130.1 (d, $^4J_{CP}$ = 1.3 Hz, *C*14'), 128.6, 128.5, 128.4, 128.4, 128.3, 128.2 (*C*6), 128.0, 127.5 (d, $^3J_{CP}$ = 5.3 Hz, *C*4), 127.0 (*C*10'), 127.0, 126.9 (*C*5'), 126.7, 126.4, 126.3 (d, J_{CP} = 2.3 Hz), 126.2 (*C*8), 125.4, 125.3, 125.0 (d, $^2J_{CP}$ = 2.7 Hz, *C*3), 124.5 (*C*6'), 124.4 (d, $^3J_{CP}$ = 3.8 Hz, *C*11), 123.7 (d, $^3J_{CP}$ = 3.0 Hz, *C*11'),

122.9 (d, $^{3}J_{CP}$ = 2.4 Hz, *C*13), 121.5 (*C*13'), 118.8 (d, $^{3}J_{CP}$ = 9.5 Hz, *C*1'), 113.1 (*C*3'), 77.3 (d, $^{2}J_{CP}$ = 44.9 Hz, allyl-*C*t), 56.2 (O*C*H$_3$), 56.1 (d, $^{2}J_{CP}$ = 5.3 Hz, allyl-*C*c), 22.5 (allyl-*C*H$_3$) ppm; signals of isomer **B** could not be determined due to their low intensity. **^{31}P{^{1}H} NMR** (202 MHz, CD_2Cl_2): δ = isomer **A** (93%) 173.6; isomer **B** (7%) 175.6 ppm. **IR** (neat): ν = 3065.2 (w), 1620.2 (w), 1589.0 (m), 1507.6 (m), 1463.0 (m), 1431.3 (w), 1327.7 (m), 1247.8 (s), 1223.0 (s), 1194.2 (m), 1151.8 (w), 1068.9 (w), 1021.8 (w), 943.5 (s), 873.9 (w), 839.0 (w), 807.0 (s), 743.7 (m), 677.2 (w), 637.2 (w), 597.2 (w), 597.8 (w), 560.2 (w) cm^{-1}. **HRMS** (ESI$^+$, MeOH): Found: *m*/*z* = 755.1301. Calculated for [M – Cl]$^+$: *m*/*z* = 755.1296.

5.4.11 Chloro((*S*,*S*$_b$)-[1,1'-binaphthalene]-2,2'-diyl [1,1'-binaphthalen]-2-ylphosphonite)(η^3-2-methylallyl)palladium (**37a**)

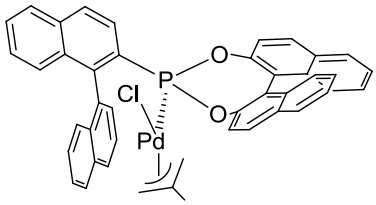

[Pd(η^3-C$_4$H$_7$)Cl]$_2$ (7 mg, 18 μmol) and **34a** (20 mg, 35 μmol) were dissolved in CH_2Cl_2 (1 mL) and stirred for 10 minutes. The intended complex was formed quantitatively. Slow diffusion of Et_2O into the reaction mixture yielded colorless crystals overnight which were suitable for X-ray diffraction analysis. Yield: 23 mg (30 μmol, 86%).

MP (uncorrected): >270 °C. **^{1}H NMR** (500 MHz, CD_2Cl_2): δ = 8.13 (d, $^{3}J_{HH}$ = 7.0 Hz, 1H, *H*2'), 7.98-7.86 (m, 7H, *H*4'+*H*15+*H*5'+*H*14'+*H*5+*H*15'+*H*13'), 7.83 (d, $^{3}J_{HH}$ = 8.8 Hz, 1H, *H*14), 7.74 (d, $^{3}J_{HH}$ = 8.7 Hz, 1H, *H*4), 7.69 (dd, $^{3}J_{HH}$ = 8.7 Hz, $^{3}J_{HH}$ = 7.0 Hz, 1H, *H*3'), 7.60-7.57 (m, 1H, Ar*H*), 7.53-7.40 (m, 7H, *H*3+6 Ar*H*), 7.36-7.23 (m, 5H, 5 Ar*H*), 7.00 (d, $^{3}J_{HH}$ = 8.7 Hz, 1H, *H*13), 4.16 (dd, $^{3}J_{HP}$ = 10.2 Hz, $^{4}J_{HH}$ = 2.8 Hz, 1H, allyl-*H*t$_{syn}$), 2.56 (d, $^{3}J_{HP}$ = 14.8 Hz, 1H, allyl-*H*t$_{anti}$), 2.31 (s, 1H, allyl-*H*c$_{syn}$), 0.93 (s, 3H, allyl-C*H*$_3$), 0.50 (s, 1H, allyl-*H*c$_{anti}$) ppm. **^{13}C{^{1}H} NMR** (126 MHz, CD_2Cl_2): δ = 149.1 (d, $^{2}J_{CP}$ = 5.3 Hz, *C*12'), 148.4 (d, $^{2}J_{CP}$ = 13.1 Hz, *C*12), 145.1 (d, $^{2}J_{CP}$ = 29.7 Hz, *C*1), 135.5, 134.5 (d, $^{1}J_{CP}$ = 9.4 Hz, *C*2), 134.3, 133.6 (d, J_{CP} = 4.7 Hz), 133.5 d, J_{CP} = 4.4 Hz), 133.3, 132.6 (d, J_{CP} = 1.4 Hz), 132.1, 131.8 (d, J_{CP} = 0.9 Hz), 131.6, 131.5 (d, $^{4}J_{CP}$ = 1.0 Hz, *C*2'), 130.8 (d, J_{CP} = 28.5 Hz, allyl-*C*), 130.7 (*C*14'), 130.2 (d, $^{4}J_{CP}$ = 1.4 Hz, *C*14), 128.6, 128.5, 128.5, 128.3, 128.1, 128.1 (*C*4'), 127.6 (d, $^{3}J_{CP}$ = 4.9 Hz, *C*4), 127.3, 127.2, 127.1, 127.0, 126.6, 126.6, 126.5, 126.3, 126.3, 126.2 (*C*3'), 125.5, 125.4, 124.5 (*C*3), 124.1 (d, $^{3}J_{CP}$ = 4.2 Hz, *C*11'), 123.5 (d, $^{3}J_{CP}$ = 2.6 Hz, *C*11), 122.5 (d, $^{3}J_{CP}$ = 2.3 Hz, *C*13'), 121.1 (d, $^{3}J_{CP}$ = 0.8 Hz, *C*13), 77.8 (d,

$^{2}J_{CP}$ = 46.5 Hz, allyl-*C*t), 57.6 (d, $^{2}J_{CP}$ = 5.3 Hz, allyl-*C*c), 22.5 (allyl-*C*H$_3$) ppm. **^{31}P{^{1}H} NMR** (202 MHz, CD_2Cl_2): δ = 172.1 ppm. **IR** (neat): ν = 3047.7 (w), 1585.8 (w), 1505.6 (m), 1461.1 (w), 1434.2 (w), 1360.9 (w), 1322.9 (m), 1269.3 (w), 1222.1 (s), 1161.0 (w), 1121.5 (w), 1068.7 (m), 1027.5 (w), 977.3 (w), 943.4 (s), 877.1 (w), 839.5 (w), 803.3 (m), 757.5 (w), 729.6 (m), 687.3 (w), 634.8 (w), 598.0 (m), 557.6 (w) cm^{-1}. **HRMS** (ESI$^+$, MeOH): Found: *m*/*z* = 725.1195. Calculated for [M – Cl]$^+$: *m*/*z* = 725.1191.

5.4.12 Chloro((*R*,*S*$_b$)-[1,1'-binaphthalene]-2,2'-diyl (2'-methoxy-[1,1'-binaphthalen]-2-yl)phosphonite)(η^3-2-methylallyl)palladium (**37b**)

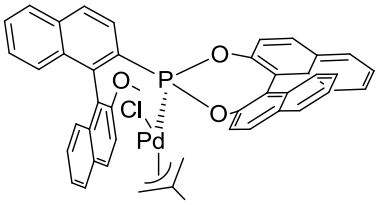

[Pd(η^3-C_4H_7)Cl]$_2$ (7 mg, 18 μmol) and **34b** (21 mg, 35 μmol) were dissolved in CH_2Cl_2 (1 mL) and stirred for 10 minutes. The intended complex was formed quantitatively. Slow diffusion of Et_2O into the reaction mixture yielded colorless crystals overnight, which were suitable for X-ray diffraction analysis. Yield: 23 mg (29 μmol, 83%).

MP (uncorrected): >270 °C. **^{1}H NMR** (500 MHz, CD_2Cl_2): δ = 8.02 (d, $^{3}J_{HH}$ = 9.1 Hz, 1H, *H*4'), 8.00-7.97 (m, 2H, *H*15+*H*13'), 7.94 (d, $^{3}J_{HH}$ = 8.9 Hz, 1H, *H*14'), 7.91 (d, $^{3}J_{HH}$ = 8.1 Hz, 1H, *H*5), 7.89 (d, $^{3}J_{HH}$ = 8.2 Hz, 1H, *H*15'), 7.86 (d, $^{3}J_{HH}$ = 8.7 Hz, 1H, *H*14), 7.83 (d, $^{3}J_{HH}$ = 8.2 Hz, 1H, *H*5'), 7.65 (d, $^{3}J_{HH}$ = 8.7 Hz, 1H, *H*4), 7.59 (ddd, $^{3}J_{HH}$ = 8.1 Hz, $^{3}J_{HH}$ = 6.6 Hz, $^{4}J_{HH}$ = 1.0 Hz, 1H, *H*6), 7.54-7.51 (m, 1H, *H*16), 7.49 (d, $^{3}J_{HH}$ = 9.1 Hz, 1H, *H*3'), 7.46-7.39 (m, 3H, 2 ArH+H16'), 7.37-7.27 (m, 7H, Ar*H*+*H*17+*H*7'+*H*6'+*H*3+*H*7+*H*18'), 7.25-7.22 (m, 1H, *H*17'), 7.00 (d, $^{3}J_{HH}$ = 8.7 Hz, 1H, *H*13), 4.07 (dd, $^{3}J_{HP}$ = 9.9 Hz, $^{4}J_{HH}$ = 3.8 Hz, 1H, allyl-*H*t$_{syn}$), 3.87 (s, 3H, OC*H*$_3$), 2.35 (s, 1H, allyl-*H*c$_{syn}$), 2.24 (d, $^{3}J_{HP}$ = 13.6 Hz, 1H, allyl-*H*t$_{anti}$), 0.84 (s, 3H, allyl-C*H*$_3$), 0.32 (s, 1H, allyl-*H*c$_{anti}$) ppm. **^{13}C{^{1}H} NMR** (126 MHz, CD_2Cl_2): δ = 156.2 (*C*2'), 149.2 (d, $^{2}J_{CP}$ = 5.3 Hz, *C*12'), 148.5 (d, $^{2}J_{CP}$ = 12.4 Hz, *C*12), 142.6 (d, $^{2}J_{CP}$ = 29.8 Hz, *C*1), 135.6 (d, $^{1}J_{CP}$ = 1.3 Hz, *C*2), 135.5 (d, $^{4}J_{CP}$ = 0.9 Hz, *C*9'), 134.0 (d, J_{CP} = 9.2 Hz), 133.1 (d, J_{CP} = 9.8 Hz), 132.7 (d, J_{CP} = 1.5 Hz), 132.1 (d, J_{CP} = 1.9 Hz), 131.8 (d, J_{CP} = 1.3 Hz), 131.6 (d, J_{CP} = 1.3 Hz), 131.3 (d, $^{2}J_{CP}$ = 26.3 Hz, allyl-C), 130.5 (d, $^{4}J_{CP}$ = 0.9 Hz, *C*14'), 130.1 (d, $^{4}J_{CP}$ = 1.3 Hz, *C*14), 129.7 (*C*4'), 128.5 (*C*15), 128.5 (*C*15'), 128.5 (*C*6), 128.3 (*C*5), 128.2 (*C*10'), 128.0 (*C*5'), 127.3 (d, $^{3}J_{CP}$ = 4.7 Hz, *C*4), 127.0, 127.0, 126.9, 126.8, 126.6, 126.6, 126.2 (*C*17'), 125.5 (*C*16), 125.3

(*C*16'), 125.3, 125.1 (d, $^{2}J_{CP}$ = 1.4 Hz, *C*3), 124.1 (d, $^{3}J_{CP}$ = 3.8 Hz, *C*11'), 123.5, 123.4 (d, $^{3}J_{CP}$ = 2.8 Hz, *C*11), 123.1 (d, $^{3}J_{CP}$ = 2.4 Hz, *C*13'), 121.4 (*C*13), 118.2 (d, $^{3}J_{CP}$ = 10.5 Hz, *C*1'), 113.5 (*C*3'), 79.3 (d, $^{2}J_{CP}$ = 46.1 Hz, allyl-*C*t), 59.0 (d, $^{2}J_{CP}$ = 4.5 Hz, allyl-*C*c), 56.0 (O*C*H$_3$), 22.3 (allyl-*C*H$_3$) ppm. **^{31}P{^{1}H} NMR** (202 MHz, CD_2Cl_2): δ = 174.4 ppm. **IR** (neat): ν = 3066.0 (w), 1619.1 (w), 1587.6 (w), 1506.6 (m), 1463.6 (m), 1429.5 (w), 1323.0 (w), 1276.0 (m), 1226.1 (s), 1199.8 (w), 1155.9 (w), 1117.7 (w), 1070.1 (m), 1028.0 (w), 946.1 (s), 867.4 (w), 833.3 (m), 814.2 (s), 751.9 (s), 706.2 (m), 686.6 (w), 634.8 (w), 606.6 (w), 560.1 (m) cm^{-1}. **HRMS** (ESI$^+$, MeOH): Found: *m*/*z* = 755.1280. Calculated for [M – Cl]$^+$: *m*/*z* = 755.1296. **EA**: Found: C 67.61%, H 5.18%. Calculated for [M + Et_2O]: C 67.67%, H 5.10%.

5.4.13 ((*R*,*R*$_b$)-[1,1'-Binaphthalene]-2,2'-diyl (2'-methoxy-[1,1'-binaphthalen]-2-yl-*κC*1')phosphonite-*κP*)(η^3-2-methylallyl)palladium tetrakis(3,5-bis(trifluoromethyl)phenyl)borate (**38b**)

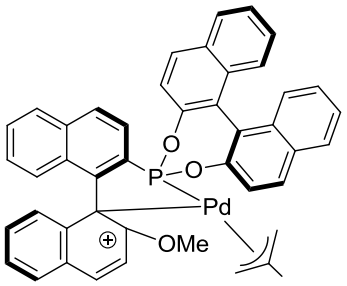

36b (30.0 mg, 37.7 μmol) and Na(BArF) (33.4 mg, 37.7 μmol) were dissolved in CH_2Cl_2 (2 mL) and stirred for 30 minutes. The reaction mixture was filtered through a layer of celite and the solvent removed in vacuo; the intended product was obtained as a yellow solid (48.9 mg, 30.1 μmol, 80%).

^{1}H NMR (500 MHz, CD_2Cl_2): δ = isomer **A**,**B** 8.27-7.23 (m, 2H, *H*4'^{B}+*H*4'^{A}), 8.14-7.98 (m, 10H, *H*5'+*H*14+*H*15'+*H*15+*H*14'), 7.93-7.89 (m, 3H, *H*5'+*H*3'^{B}), 7.86-7.80 (m, 3H, *H*3'^{A}+*H*4), 7.74 (br s, 16H, *o*-BArF), 7.63-7.51 (m, 18H, *H*6'+*H*16+*H*16'+*H*6+Ar*H*+*p*-BArF), 7.48-7.38 (m, 10H, *H*13+4 Ar*H*), 7.26-7.19 (m, 4H, *H*7+3 Ar*H*), 7.13-7.02 (m, 4H, *H*13'+*H*3), 6.06 (d, $^{3}J_{HH}$ = 8.3 Hz, 2H, *H*8), 4.06 (s, OC*H*$_3^{B}$), 4.00 (s, OC*H*$_3^{A}$), 3.16 (br d, $^{3}J_{HP}$ = 10.7 Hz, allyl-*H*t$_{anti}^{B}$), 3.03 (s, allyl-*H*c$_{syn}^{B}$), 2.99 (s, allyl-*H*c$_{syn}^{A}$), 2.90 (d, $^{3}J_{HP}$ = 13.2 Hz, allyl-*H*t$_{anti}^{A}$), 2.43 (br d, $^{3}J_{HP}$ = 8.2 Hz, allyl-*H*t$_{syn}^{A}$), 2.39 (s, allyl-*H*c$_{anti}^{A}$), 2.34 (br s, allyl-*H*t$_{syn}^{B}$), 2.22 (s, allyl-*H*c$_{anti}^{B}$), 1.58 (s, allyl-C*H*$_3^{A}$), 1.30 (s, allyl-C*H*$_3^{B}$) ppm. (A:B ratio from integration of OMe signals: 52:48). **^{11}B NMR** (160 MHz, CD_2Cl_2): δ = –7.6 ppm. **^{13}C{^{1}H} NMR** (101 MHz, CD_2Cl_2): δ = isomer **A**,**B** 161.8 (q, $^{1}J_{CB}$ = 40.8 Hz, *ipso*-BArF), 159.0 (*C*2'^{B}), 157.2 (*C*2'^{A}),

148.1 (d, $^2J_{CP}$ = 10.1 Hz, *C*12'^{B}), 148.0 (d, $^2J_{CP}$ = 11.0 Hz, *C*12'^{A}), 147.1 (d, $^2J_{CP}$ = 7.7 Hz, *C*12), 142.1 (d, $^2J_{CP}$ = 41.7 Hz, *C*1^B), 141.9 (d, $^2J_{CP}$ = 41.7 Hz, *C*1^A), 137.9 (d, $^2J_{CP}$ = 9.5 Hz, allyl-*C*^{A}), 137.0 (*C*2), 134.8 (*o*-BArF), 134.6 (*C*4'), 132.8, 132.5, 132.1, 132.0, 131.7, 131.6 (*C*14), 131.5 (*C*9'^{A}), 131.4 (*C*9'^{B}), 131.4 (*C*14'), 130.9, 130.8, 130.4, 130.3 (*C*4), 130.1 (*C*5'), 130.0, 129.8, 129.4, 128.9 (qq, $^2J_{CF}$ = 31.2 Hz, $^4J_{CF}$ = 2.8 Hz, *m*-BArF), 128.8, 128.4 (*C*10'), 127.5, 127.4, 127.3, 127.1, 127.0, 126.9, 126.5, 126.4, 126.3, 126.0, 125.0, 124.8, 124.7 (q, $^1J_{CF}$ = 273.2 Hz, *C*F$_3$), 124.1, 124.0 (d, J_{CP} = 3.4 Hz), 123.8, 123.7, 123.3, 122.5, 122.3, 120.7 (*C*3), 120.6 (*C*13'), 120.3 (*C*13), 120.1, 117.5 (septet, $^3J_{CF}$ = 4.0 Hz, *p*-BArF), 114.9 (*C*3'^{A}), 114.5 (*C*3'^{B}), 104.6 (*C*1'^{A}), 99.6 (d, $^2J_{CP}$ = 40.1 Hz, allyl-*C*t^A), 57.5 (O*C*H$_3{}^B$), 57.4 (O*C*H$_3{}^A$), 53.2 (allyl-*C*c^A), 22.4 (allyl-*C*H$_3{}^A$), 21.6 (allyl-*C*H$_3{}^B$) ppm (Not all signals could be observed due to peak broadening and overlap). **^{19}F NMR** (471 MHz, CD_2Cl_2): δ = –62.7 ppm. **^{31}P{^{1}H} NMR** (202 MHz, CD_2Cl_2): δ = isomer **A** 177.5; isomer **B** 178.0 ppm. **IR** (neat): ν = 1612.4 (w), 1588.2 (w), 1506.9 (w), 1464.1 (w), 1353.8 (m), 1273.2 (s), 1220.7 (w), 1116.5 (s), 953.5 (m), 882.6 (w), 836.8 (m), 813.3 (m), 746.2 (w), 711.9 (w), 681.4 (m), 638.0 (w), 599.2 (w) cm^{-1}. **HRMS** (ESI$^+$, MeCN): Found: *m*/*z* = 757.1287. Calculated for [M – BArF]$^+$: *m*/*z* = 757.1281.

5.4.14 ((*R*,*S*$_b$)-[1,1'-Binaphthalene]-2,2'-diyl (2'-methoxy-[1,1'-binaphthalen]-2-yl-κ*C*1')phosphonite-κ*P*)(η^3-2-methylallyl)palladium tetrakis(3,5-bis(trifluoromethyl)phenyl)borate (**39b**)

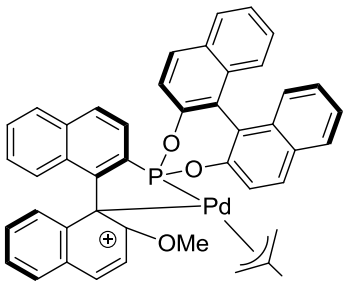

37b (29.0 mg, 36.5 µmol) and Na(BArF) (32.3 mg, 36.5 µmol) were dissolved in CH_2Cl_2 (2 mL) and stirred for 30 minutes. The reaction mixture was filtered through a layer of celite and the solvent was removed in vacuo; the intended product was obtained as a yellow solid (54.0 mg, 33.3 µmol, 91%).

^{1}H NMR (500 MHz, CD_2Cl_2): δ = isomer **A**,**B** 8.22 (d, $^3J_{HH}$ = 9.2 Hz, 1H, *H*4'^{A}), 8.21 (d, $^3J_{HH}$ = 9.2 Hz, 1H, *H*4'^{B}), 8.17-8.01 (m, 10H, *H*14+*H*14'+*H*5'+2 Ar*H*), 7.99 (d, $^3J_{HH}$ = 9.2 Hz, 1H, *H*3'^{A}), 7.96-7.89 (m, 5H, Ar*H*+*H*4+*H*3'^{B}), 7.76 (br s, 16H, *o*-BArF), 7.64-7.51 (m, 18H, 5 Ar*H*+*p*-BArF), 7.49-7.35 (m, 12H, 4.5 Ar*H*+*H*13^B+*H*13'^{A}+*H*13^A), 7.30-7.22 (m, 4H,

0.5 Ar*H*+*H*7+*H*13'^{B}), 7.20 (dd, $^{3}J_{HH}$ = 8.5 Hz, $^{3}J_{HP}$ = 6.9 Hz, 1H, *H*3^{A}), 7.10 (dd, $^{3}J_{HH}$ = 8.5 Hz, $^{3}J_{HP}$ = 6.9 Hz, 1H, *H*3^{B}), 6.09 (br d, 1H, *H*8^{B}), 6.00 (d, $^{3}J_{HH}$ = 8.6 Hz, 1H, *H*8^{A}), 3.98 (s, OC*H*$_3^{A}$), 3.89 (s, OC*H*$_3^{B}$), 3.76 (d, $^{3}J_{HP}$ = 13.6 Hz, allyl-*H*t$_{anti}^{A}$), 3.00 (br d, allyl-*H*t$_{syn}^{B}$), 2.87 (s, allyl-*H*c$_{syn}^{B}$), 2.82 (s, allyl-*H*c$_{syn}^{A}$), 2.63 (d, $^{3}J_{HP}$ = 13.5 Hz, allyl-*H*t$_{anti}^{B}$), 2.32 (s, allyl-*H*c$_{anti}^{A}$), 2.20 (br s, allyl-*H*c$_{anti}^{B}$), 2.19 (d, allyl-*H*t$_{syn}^{A}$), 1.79 (br s, allyl-C*H*$_3^{B}$), 0.96 (s, allyl-C*H*$_3^{A}$) ppm (A:B ratio from integration of OMe signals: 50:50, signals of isomer B broadened). **^{11}B NMR** (128 MHz, CD_2Cl_2): δ = –7.6 ppm. **^{13}C{^{1}H} NMR** (126 MHz, CD_2Cl_2): δ = isomer **A**,**B** 161.8 (q, $^{1}J_{CB}$ = 40.7 Hz, *ipso*-BArF), 156.6 (*C*2'^{A}), 154.8 (d, J_{CP} = 2.4 Hz, *C*2'^{B}), 148.3 (d, $^{2}J_{CP}$ = 13.5 Hz, *C*12^{A}), 148.3 (d, $^{2}J_{CP}$ = 13.3 Hz, *C*12^{B}), 147.2 (d, $^{2}J_{CP}$ = 7.1 Hz, *C*12'^{A}), 147.1 (d, $^{2}J_{CP}$ = 7.4 Hz, *C*12'^{B}), 142.4 (d, $^{2}J_{CP}$ = 43.5 Hz, *C*1^{B}), 142.2 (d, $^{2}J_{CP}$ = 41.3 Hz, *C*1^{A}), 138.9 (d, $^{2}J_{CP}$ = 10.4 Hz, allyl-*C*^{A}), 138.1 (d, *J* = 10.0 Hz, allyl-*C*^{B}), 137.1 (*C*2^{B}), 137.0 (*C*2^{A}), 134.9 (*C*4'^{A}), 134.9 (*o*-BArF), 134.3 (*C*4'^{B}), 133.7 (*C*9'^{B}), 132.8, 132.7 (*C*9'^{A}) 132.1, 131.8, 131.7, 131.6, 131.5, 130.7 (d, $^{3}J_{CP}$ = 4.7 Hz, *C*4), 130.0 (*C*10'^{B}), 129.8, 129.8, 129.7, 129.3 (*C*10'^{A}), 128.9 (qq, $^{2}J_{CF}$ = 31.6 Hz, $^{4}J_{CF}$ = 2.9 Hz, *m*-BArF), 128.7, 128.6, 128.0, 127.6, 127.4, 127.4, 127.0, 127.0, 126.6, 126.5, 126.4, 125.1, 124.8, 124.7 (q, $^{1}J_{CF}$ = 272.3 Hz, *C*F$_3$), 124.3, 124.1, 123.7 (d, $^{2}J_{CP}$ = 1.4 Hz, *C*3^{B}), 123.7 (d, $^{2}J_{CP}$ = 1.4 Hz, *C*3^{A}), 123.0, 122.3, 122.1, 120.7 (d, $^{3}J_{CP}$ = 1.0 Hz, *C*13^{B}), 120.6 (d, $^{3}J_{CP}$ = 1.0 Hz, *C*13^{A}), 120.1 (d, $^{3}J_{CP}$ = 2.1 Hz, *C*13'^{A}), 119.8 (*C*13'^{B}), 117.5 (septet, $^{3}J_{CF}$ = 4.0 Hz, *p*-BArF), 115.9 (*C*3'^{B}), 115.3 (*C*3'^{A}), 104.5 (*C*1'^{B}), 103.4 (*C*1'^{A}), 99.5 (d, $^{2}J_{CP}$ = 41.1 Hz, allyl-*C*t^{A}), 96.9 (br, allyl-*C*t^{B}), 57.6 (O*C*H$_3^{A}$), 57.3 (O*C*H$_3^{B}$), 56.4(allyl-*C*c^{B}), 54.9 (allyl-*C*c^{A}), 22.6 (allyl-*C*H$_3^{B}$), 21.5 (allyl-*C*H$_3^{A}$) ppm (Not all signals could be observed due to peak broadening and overlap). **^{19}F NMR** (376 MHz, CD_2Cl_2): δ = –62.7 ppm. **^{31}P{^{1}H} NMR** (202 MHz, CD_2Cl_2): δ = isomer **A** 178.9; isomer **B** 179.1 ppm. **IR** (neat): ν = 1612.1 (w), 1588.9 (w), 1506.1 (w), 1463.5 (w), 1353.6 (m), 1273.0 (s), 1219.8 (w), 1116.1 (s), 952.9 (m), 882.4 (w), 836.7 (m), 811.4 (m), 745.5 (w), 711.9 (w), 669.8 (m), 638.6 (w), 602.7 (w) cm^{-1}. **HRMS** (ESI^{+}, MeCN): Found: *m*/*z* = 757.1296. Calculated for [M – BArF]$^{+}$: *m*/*z* = 757.1281.

5.4.15 Chloro((*R*,*R*$_b$)-[1,1'-binaphthalene]-2,2'-diyl (2'-methoxy-[1,1'-binaphthalen]-2-yl)phosphonite)(η^4-cycloocta-1,5-diene)rhodium (**40b**)

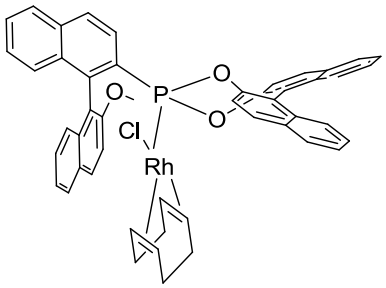

33b (21.0 mg, 35.0 μmol) and [Rh(η^4-cod)Cl]$_2$ (8.6 mg, 17.5 μmol) were dissolved in CH_2Cl_2 (1 mL) and stirred for 30 minutes. The solution was filtered and layered with Et_2O. Dark orange crystals suitable for X-ray analysis were formed overnight.

MP (uncorrected): 239 °C. **^{1}H NMR** (500 MHz, CD_2Cl_2): δ = 8.29 (d, $^3J_{HH}$ = 8.8 Hz, 1H, *H*13), 8.21 (d, $^3J_{HH}$ = 9.1 Hz, 1H, *H*4'), 8.14 (d, $^3J_{HH}$ = 8.8 Hz, 1H, *H*14), 8.02 (d, $^3J_{HH}$ = 8.3 Hz, 1H, *H*15), 7.98 (d, $^3J_{HH}$ = 8.2 Hz, 1H, *H*5'), 7.86 (m, 2H, *H*5+*H*15'), 7.73-7.65 (m, 3H, *H*3+*H*4+*H*14'), 7.60 (d, $^3J_{HH}$ = 9.1 Hz, 1H, *H*3'), 7.52-7.48 (m, 2H, *H*6+*H*16), 7.46-7.39 (m, 4H, *H*16'+*H*18+*H*18'+*H*6'), 7.33-7.29 (m, 2H, *H*17+*H*17'), 7.26-7.21 (m, 2H, *H*7'+*H*7), 7.18 (d, $^3J_{HH}$ = 8.8 Hz, 1H, *H*8'), 7.16 (d, $^3J_{HH}$ = 8.8 Hz, 1H, *H*13'), 6.92 (d, $^3J_{HH}$ = 8.7 Hz, 1H, *H*8), 5.31 (br s, 1H, cod-C*H*), 4.26 (br s, 1H, cod-C*H*), 3.95 (s, 3H, OCH_3), 2.69 (br s, 1H, cod-C*H*), 2.49 (br s, 1H, cod-C*H*), 1.88 (m, 1H, cod-CH_2), 1.50 (m, 4H, cod-CH_2), 1.32 (m, 1H, cod-CH_2), 1.21 (m, 1H, cod-CH_2), 1.13 (m, 1H, cod-CH_2) ppm. **^{13}C{^{1}H} NMR** (126 MHz, CD_2Cl_2): δ = 155.9 (*C*2'), 150.0 (d, $^2J_{CP}$ = 5.4 Hz, *C*12), 149.8 (d, $^2J_{CP}$ = 12.6 Hz, *C*12'), 140.5 (d, $^2J_{CP}$ = 24.6 Hz, *C*1), 135.1 (*C*9), 134.5 (*C*9'), 133.3 (d, $^1J_{CP}$ = 11.2 Hz, *C*2), 132.4 (m, *C*19+*C*19'), 131.8 (*C*20), 131.5 (*C*4'), 131.4 (*C*20'), 130.2 (*C*14), 129.9 (*C*14'), 129.8 (*C*8'), 129.4 (*C*10'), 128.5 (*C*15'), 128.4 (*C*15), 128.2 (*C*5), 127.8 (*C*6), 127.2 (*C*5'), 126.8 (*C*18'), 126.7 (*C*4+*C*18), 126.6 (*C*7), 126.5 (*C*7'+*C*8), 126.3 (*C*17), 126.2 (*C*17'), 125.5 (d, $^2J_{CP}$ = 2.5 Hz, *C*3), 125.4 (*C*16), 125.2 (*C*16'), 124.3 (d, $^3J_{CP}$ = 3.6 Hz, *C*11), 124.3 (*C*6'), 124.1 (d, $^3J_{CP}$ = 2.5 Hz, *C*13), 123.4 (d, $^3J_{CP}$ = 2.5 Hz, *C*11'), 121.7 (*C*13'), 119.9 (d, $^3J_{CP}$ = 7.6 Hz, *C*1'), 112.9 (*C*3'), 111.7 (dd, *J* = 15.9 Hz, *J* = 6.5 Hz, cod-*C*H), 110.1 (dd, *J* = 14.4 Hz, *J* = 5.4 Hz, cod-*C*H), 73.3 (d, *J* = 13.8 Hz, cod-*C*H), 66.8 (d, *J* = 13.6 Hz, cod-*C*H), 56.1 (O*C*H$_3$), 33.0 (d, *J* = 2.9 Hz, cod-*C*H$_2$), 31.6 (d, *J* = 2.0 Hz, cod-*C*H$_2$), 27.2 (m, cod-*C*H$_2$) ppm; the resonance for *C*10 was obscured. **^{31}P{^{1}H} NMR** (202 MHz, CD_2Cl_2): δ = 162.9 (d, $^1J_{PRh}$ = 223 Hz) ppm. **IR** (neat): ν = 3050.3 (w), 2971.5 (w), 1620.3 (w), 1589.3 (m), 1508.5 (m), 1462.2 (m), 1430.9 (w), 1326.8 (w), 1249.5 (w), 1224.1 (s), 1152.6 (w),

1073.9 (m), 944.9 (s), 868.8 (w), 807.3 (s), 746.6 (s), 695.6 (w), 673.9 (w), 636.5 (m), 598.5 (w), 559.3 (w) cm^{-1}. **UV-Vis** ($CHCl_3$, ε [L/mol/cm]): λ_{max} = 411 (~2900) nm. **HRMS** (ESI^+, MeOH): Found: *m*/*z* = 867.1257. Calculated for $[M + Na]^+$: *m*/*z* = 867.1273.

5.4.16 Chloro((*R*,*S*$_b$)-[1,1'-binaphthalene]-2,2'-diyl (2'-methoxy-[1,1'-binaphthalen]-2-yl)phosphonite)(η^4-cycloocta-1,5-diene)rhodium (**41b**)

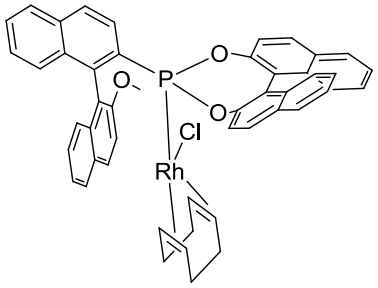

34b (21.0 mg, 35.0 μmol) and $[Rh(\eta^4\text{-cod})Cl]_2$ (8.6 mg, 17.5 μmol) were dissolved in CH_2Cl_2 (1 mL) and stirred for 30 minutes. The solution was filtered and layered with Et_2O to precipitate the product as a yellow solid overnight.

^{1}H NMR (500 MHz, CD_2Cl_2): δ = 8.29 (d, $^3J_{HH}$ = 8.8 Hz, 1H, *H*13'), 8.27 (d, $^3J_{HH}$ = 9.2 Hz, 1H, *H*4'), 8.13 (d, $^3J_{HH}$ = 8.8 Hz, 1H, *H*14'), 8.00 (d, $^3J_{HH}$ = 8.5 Hz, 1H, *H*15'), 7.99 (d, $^3J_{HH}$ = 8.5 Hz, 1H, *H*5'), 7.93 (d, $^3J_{HH}$ = 8.2 Hz, 1H, *H*15), 7.86 (d, $^3J_{HH}$ = 8.2 Hz, 1H, *H*5), 7.78 (d, $^3J_{HH}$ = 8.7 Hz, 1H, *H*14), 7.62 (m, 2H, *H*3'+*H*4), 7.58-7.52 (m, 2H, *H*3+*H*6), 7.50-7.44 (m, 2H, *H*16+*H*16'), 7.42-7.39 (m, 2H, *H*18+*H*7'), 7.37-7.23 (m, 6H, *H*6'+*H*8'+*H*17+*H*7+*H*17'+*H*18'), 7.15 (d, $^3J_{HH}$ = 8.5 Hz, 1H, *H*8), 6.99 (d, $^3J_{HH}$ = 8.8 Hz, 1H, *H*13), 5.50 (br s, 1H, cod-C*H*), 5.05 (br s, 1H, cod-C*H*), 3.80 (s, 3H, OCH_3), 2.67 (br s, 1H, cod-C*H*), 2.17 (m, 1H, cod-CH_2), 1.83 (m, 1H, cod-CH_2), 1.78 (m, 1H, cod-CH_2), 1.63 (br s, 1H, cod-C*H*), 1.49 (m, 1H, cod-CH_2), 1.42 (m, 1H, cod-CH_2), 1.22 (m, 1H, cod-CH_2), 1.14 (m, 1H, cod-CH_2), 0.94 (m, 1H, cod-CH_2) ppm. **^{13}C{^{1}H} NMR** (126 MHz, CD_2Cl_2): δ = 155.9 (*C*2'), 150.2 (d, $^2J_{CP}$ = 5.6 Hz, *C*12'), 149.3 (d, $^2J_{CP}$ = 12.6 Hz, *C*12), 141.2 (d, $^2J_{CP}$ = 26.4 Hz, *C*1), 135.2 (d, $^1J_{CP}$ = 1.4 Hz, *C*2), 135.1 (*C*9'), 133.2 (d, $^3J_{CP}$ = 11.2 Hz, *C*9), 132.8 (d, $^4J_{CP}$ = 1.4 Hz, *C*19), 132.5 (d, $^4J_{CP}$ = 2.1 Hz, *C*19'), 131.8 (d, $^5J_{CP}$ = 1.4 Hz, *C*20'), 131.3 (d, $^5J_{CP}$ = 0.9 Hz, *C*20), 131.1 (*C*4'), 130.2 (d, $^4J_{CP}$ = 1.4 Hz, *C*14'), 130.0 (d, $^4J_{CP}$ = 1.1 Hz, *C*14), 128.5 (*C*15'), 128.4 (*C*15), 128.2 (*C*5), 128.1 (*C*5'), 128.1 (*C*6), 127.0 (*C*18+*C*8), 126.9 (*C*4), 126.7 (*C*7), 126.6 (*C*17'), 126.4 (*C*17), 126.3 (*C*18'), 126.2 (*C*7'), 125.7 (*C*8'), 125.4 (*C*16'), 125.3 (*C*3), 125.3 (*C*16), 124.3 (d, $^3J_{CP}$ = 2.1 Hz, *C*13'), 123.9 (d, $^3J_{CP}$ = 4.0 Hz, *C*11'), 123.3 (*C*6'), 123.1 (d, $^3J_{CP}$ = 2.5 Hz, *C*11), 121.4 (*C*13), 119.3 (d, $^3J_{CP}$ = 8.3 Hz, *C*1'), 113.2 (*C*3'), 111.7 (dd, *J* = 15.3 Hz, *J* = 6.7 Hz, cod-*C*H), 108.4 (dd, *J* = 14.9 Hz, *J* = 5.5 Hz, cod-*C*H), 75.4 (d,

J = 13.6 Hz, cod-*C*H), 67.2 (d, *J* = 13.0 Hz, cod-*C*H), 55.9 (O*C*H$_3$), 33.1 (d, *J* = 2.5 Hz, cod-*C*H$_2$), 31.5 (d, *J* = 2.4 Hz, cod-*C*H$_2$), 27.4 (d, *J* = 1.5 Hz, cod-*C*H$_2$), 27.1 (d, *J* = 1.9 Hz, cod-*C*H$_2$) ppm; resonances for *C*10 and *C*10' were obscured. **^{31}P{^{1}H} NMR** (202 MHz, CD_2Cl_2): δ = 161.5 (d, $^{1}J_{PRh}$ = 224 Hz) ppm. **HRMS** (ESI$^+$, MeCN): Found: *m*/*z* = 809.1672. Calculated for $[M - Cl]^+$: *m*/*z* = 809.1686.

5.4.17 ((*R*,*R*$_b$)-[1,1'-Binaphthalene]-2,2'-diyl (2'-methoxy-[1,1'-binaphthalen]-2-yl)phosphonite-*κP*)((*R*,*R*$_b$)-[1,1'-binaphthalene]-2,2'-diyl (1',2',3',4',9',10'η-2'-methoxy-[1,1'-binaphthalen]-2-yl)phosphonite-*κP*)rhodium tetrafluoroborate (**42b**)

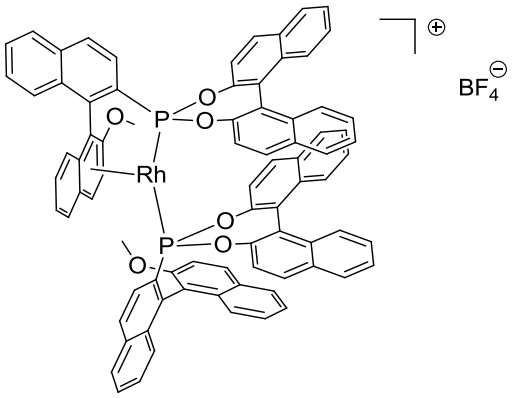

Method A: **33b** (30 mg, 50 µmol) and [Rh(η^4-cod)$_2$]BF$_4$ (10 mg, 25 µmol) were dissolved in CH_2Cl_2 (1 mL) and stirred for 30 minutes. The solution was filtered and layered with Et_2O to precipitate the product as a yellow solid overnight.

Method B: **40b** (21 mg, 25 µmol) was dissolved in CH_2Cl_2 (1 mL), $AgBF_4$ (4.8 mg, 25 µmol) and **33b** (15 mg, 25 µmol) were added and stirred for 30 minutes. The solution was filtered and concentrated *in vacuo*. The crude product was washed with Et_2O to give the product as a yellow solid.

MP (uncorrected): 267 °C (decomposition). **^{1}H NMR** (500 MHz, CD_2Cl_2): δ = 8.31 (d, $^{3}J_{HH}$ = 8.3 Hz, 1H, *H*4^{A}), 8.15 (d, $^{3}J_{HH}$ = 8.3 Hz, 1H, *H*5^{A}), 8.07 (d, $^{3}J_{HH}$ = 8.8 Hz, 1H, *H*14^{B}), 7.94 (d, $^{3}J_{HH}$ = 8.3 Hz, 1H, *H*5^{B}), 7.83 (m, 1H, *H*15^{B}), 7.83 (m, 1H, *H*8^{B}), 7.80 (m, 1H, *H*6'^{B}), 7.78 (m, 1H, *H*15'^{B}), 7.76 (m, 1H, *H*15^{A}), 7.75 (m, 1H, *H*4'^{A}), 7.75 (m, 1H, *H*14^{A}), 7.70 (m, 1H, *H*7'^{B}), 7.69 (m, 1H, *H*6^{B}), 7.64 (m, 1H, *H*6^{A}), 7.61 (m, 1H, *H*4^{B}), 7.61 (m, 1H, *H*7^{B}), 7.60 (m, 1H, *H*3'^{A}), 7.58 (m, 1H, *H*3^{A}), 7.57 (m, 1H, *H*15'^{A}), 7.45 (d, $^{3}J_{HH}$ = 8.9 Hz, 1H, *H*14'^{B}), 7.39 (d, $^{3}J_{HH}$ = 8.3 Hz, 1H, *H*5'^{B}), 7.34 (pt, J_{HH} = 7.3 Hz, 1H, *H*16'^{B}), 7.28 (m, 1H, *H*7^{A}), 7.24 (m, 1H, *H*16'^{A}), 7.23 (m, 1H, *H*3'^{B}), 7.17 (m, 1H, *H*16^{B}), 7.17 (m, 1H, *H*5'^{A}), 7.15 (m, 1H, *H*16^{A}), 7.08 (m, 1H, *H*14'^{A}), 7.08 (m, 1H, *H*8^{A}), 7.06 (m, 1H, *H*17'^{B}), 6.87 (m, 1H, *H*18'^{B}),

6.86 (m, 1H, *H*17'^{A}), 6.85 (m, 1H, *H*8'^{B}), 6.85 (m, 1H, *H*13^{B}), 6.78 (d, $^{3}J_{HH}$ = 8.6 Hz, 1H, *H*13^{A}), 6.63 (pt, J_{HH} = 7.9 Hz, 1H, *H*17^{B}), 6.54 (pt, J_{HH} = 7.9 Hz, 1H, *H*17^{A}), 6.42 (d, $^{3}J_{HH}$ = 8.6 Hz, 1H, *H*18^{B}), 6.39 (br d, $^{3}J_{HH}$ = 8.0 Hz, 1H, *H*4'^{B}), 6.34 (pt, *J* = 8.1 Hz, 1H, *H*3^{B}), 6.21 (d, $^{3}J_{HH}$ = 8.6 Hz, 1H, *H*18^{A}), 6.17 (d, $^{3}J_{HH}$ = 8.6 Hz, 1H, *H*18'^{A}), 6.17 (pt, J_{HH} = 8.6 Hz, 1H, *H*6'^{A}), 6.03 (d, $^{3}J_{HH}$ = 8.9 Hz, 1H, *H*13'^{B}), 5.76 (d, $^{3}J_{HH}$ = 8.9 Hz, 1H, *H*13'^{A}), 5.14 (d, $^{3}J_{HH}$ = 8.6 Hz, 1H, *H*8'^{A}), 4.82 (pt, J_{HH} = 7.7 Hz, 1H, *H*7'^{A}), 4.18 (s, 3H, OCH_3^{B}), 4.07 (s, 3H, OCH_3^{A}) ppm. **^{13}C{^{1}H} NMR** (126 MHz, CD_2Cl_2): δ = 153.8 (*C*2'^{A}), 150.5 (d, $^{1}J_{CP}$ = 53.0 Hz, *C*2^{B}), 149.1 (*C*2'^{B}), 148.9 (d, $^{2}J_{CP}$ = 15.5 Hz, *C*12'^{B}), 147.9 (d, $^{2}J_{CP}$ = 7.6 Hz, *C*12^{B}), 147.7 (d, $^{2}J_{CP}$ 13.2 Hz, *C*12'^{A}), 146.2 (d, $^{2}J_{CP}$ = 6.7 Hz, *C*12^{A}), 137.4 (d, $^{2}J_{CP}$ = 33.7 Hz, *C*1^{B}), 136.4 (*C*2^{A}), 135.6 (*C*1^{A}), 135.3 (*C*9^{B}), 135.0 (*C*10^{B}), 134.8 (*C*10^{A}), 134.6 (*C*9'^{A}), 132.8 (*C*9^{A}), 132.4 (*C*19^{B}+*C*19^{A}), 132.1 (*C*7'^{B}+*C*20^{B}), 131.9 (*C*19'^{B}), 131.7 (*C*19'^{A}), 131.5 (*C*20^{A}), 131.0 (*C*20'^{B}), 130.8 (*C*14^{B}+*C*20'^{A}), 130.2 (*C*4^{B}+*C*14'^{B}), 129.9 (*C*14^{A}), 129.6 (*C*6^{B}), 129.3 (*C*14'^{A}), 128.7 (*C*7^{B}), 128.5 (*C*5^{B}+*C*6^{A}), 128.4 (*C*15^{B}), 128.3 (*C*5^{A}), 128.2 (*C*6'^{B}+*C*15'^{B}+*C*15^{A}+*C*10'^{A}), 128.1 (*C*4'^{A}), 127.9 (d, *J* = 13.5 Hz, *C*4^{A}), 127.7 (*C*15'^{A}), 127.5 (*C*7^{A}), 127.4 (*C*8^{A}), 126.9 (*C*18'^{B}+*C*18^{B}), 126.6 (*C*18'^{A}+*C*3^{A}), 126.6 (*C*5'^{B}), 126.5 (*C*18^{A}), 126.4 (*C*8^{B}), 126.2 (*C*17'^{B}), 126.1 (*C*5'^{A}), 125.8 (*C*17^{B}), 125.6 (*C*17^{A}), 125.5 (*C*17'^{A}), 125.4 (*C*16^{B}), 125.3 (*C*16'^{B}+*C*16^{A}+*C*7'^{A}), 125.1 (*C*3^{B}), 124.9 (*C*16'^{A}), 123.3 (*C*8'^{B}), 123.0 (*C*6'^{A}), 122.8 (*C*8'^{A}), 122.4 (*C*11^{A}), 121.9 (*C*1'^{A}), 121.6 (*C*11^{B}), 121.3 (*C*11'^{A}), 120.9 (*C*13^{B}), 120.7 (*C*13^{A}), 120.1 (*C*13'^{B}), 120.1 (*C*11'^{B}), 119.5 (*C*13'^{A}), 118.7 (*C*9'^{B}) 114.2 (*C*3'^{A}), 112.8 (*C*10'^{B}), 100.5 (d, *J* = 14.3 Hz, *C*1'^{B}), 95.8 (d, *J* = 11.3 Hz, *C*4'^{B}), 87.5 (*C*3'^{B}), 58.1 (O*C*H$_3^{B}$), 58.1 (O*C*H$_3^{A}$). **^{31}P NMR** (202 MHz, CD_2Cl_2): δ = 181.3 (ddd, $^{1}J_{PRh}$ = 290 Hz, $^{2}J_{PP}$ = 22.3 Hz, $^{3}J_{PH}$ = 16.6 Hz, *P*^{A}), 179.6 (ddd, $^{1}J_{PRh}$ = 300 Hz, $^{2}J_{PP}$ = 22.3 Hz, $^{3}J_{PH}$ = 6.6 Hz, *P*^{B}) ppm. **IR** (neat): ν = 3058.4 (w), 1621.3 (w), 1590.9 (w), 1506.2 (m), 1463.6 (m), 1324.4 (w), 1277.9 (w), 1222.9 (s), 1154.4 (w), 1069.0 (s), 956.8 (s), 837.3 (s), 810.1 (m), 746.4 (m), 696.2 (w) cm^{-1}. **UV-Vis** ($CHCl_3$, ε [L/mol/cm]): λ_{max} = 412 (~2800) nm. **HRMS** (ESI^{+}, MeOH): Found: *m*/*z* = 1299.2432. Calculated for [M – BF_4]$^{+}$: *m*/*z* = 1299.2445.

5.4.18 ((*R*,*S*$_b$)-[1,1'-Binaphthalene]-2,2'-diyl (2'-methoxy-[1,1'-binaphthalen]-2-yl)phosphonite-*κP*)((*R*,*S*$_b$)-[1,1'-binaphthalene]-2,2'-diyl (1',2',3',4',9',10'η-2'-methoxy-[1,1'-binaphthalen]-2-yl)phosphonite-*κP*)rhodium tetrafluoroborate (**43b**)

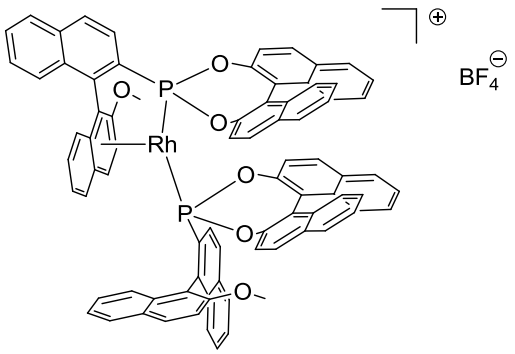

The same procedures as described for the synthesis of **42b** were utilised using **34b** as ligand. Yellow crystals suitable for X-ray analysis were formed overnight.

MP (uncorrected): >270 °C. **^{1}H NMR** (500 MHz, CD_2Cl_2): δ = 8.47 (dd, $^3J_{HH}$ = 8.6 Hz, $^4J_{HP}$ = 1.1 Hz, 1H, *H*4^A), 8.34 (dd, $^3J_{HP}$ = 13.7 Hz, $^3J_{HH}$ = 8.6 Hz, 1H, *H*3^A), 8.32 (d, $^3J_{HH}$ = 8.6 Hz, 1H, *H*14'^{B}), 8.15 (d, $^3J_{HH}$ = 8.2 Hz, 1H, *H*5^A), 8.07 (d, $^3J_{HH}$ = 8.2 Hz, 1H, *H*5'^{A}), 7.98 (d, $^3J_{HH}$ = 8.2 Hz, 1H, *H*15'^{B}), 7.90 (d, $^3J_{HH}$ = 8.2 Hz, 1H, *H*5^B), 7.80 (d, $^3J_{HH}$ = 9.1 Hz, 1H, *H*4'^{A}), 7.78 (d, $^3J_{HH}$ = 8.2 Hz, 1H, *H*15^B), 7.75 (m, 1H, *H*13'^{B}), 7.74 (m, 1H, *H*15'^{A}), 7.73 (m, 1H, *H*8^B), 7.67 (m, 3H, *H*6^A+*H*6^B+*H*7'^{B}), 7.61 (m, 1H, *H*7'^{A}), 7.55 (m, 2H, *H*6'^{A}+*H*7^B), 7.51 (m, 1H, *H*15^A), 7.50 (m, 1H, *H*4^B), 7.49 (m, 1H, *H*6'^{B}), 7.36 (m, 1H, *H*16^B), 7.34 (m, 1H, *H*14^B), 7.31 (m, 1H, *H*16'^{B}), 7.28 (m, 1H, *H*14'^{A}), 7.27 (m, 1H, *H*7^A), 7.24 (m, 1H, *H*16'^{A}), 7.19 (pt, J_{HH} = 7.5 Hz, 1H, *H*16^A), 7.10 (m, 1H, *H*3'^{B}), 7.09 (m, 1H, *H*17^B), 7.08 (m, 1H, *H*8'^{A}), 7.06 (m, 1H, *H*8^A), 6.99 (ddd, $^3J_{HH}$ = 8.6 Hz, $^3J_{HH}$ = 6.8 Hz, $^4J_{HH}$ = 1.1 Hz, 1H, *H*17^A), 6.93 (m, 2H, *H*8'^{B}+*H*18^B), 6.92 (d, $^3J_{HH}$ = 8.2 Hz, 1H, *H*14^A), 6.84 (d, $^3J_{HH}$ = 8.6 Hz, 1H, *H*18^A), 6.71 (ddd, $^3J_{HH}$ = 8.6 Hz, $^3J_{HH}$ = 6.8 Hz, $^4J_{HH}$ = 1.1 Hz, 1H, *H*17'^{B}), 6.60 (m, 1H, *H*4'^{B}), 6.59 (m, 1H, *H*17'^{A}), 6.57 (m, 1H, *H*3'^{A}), 6.48 (d, $^3J_{HH}$ = 8.6 Hz, 1H, *H*18'^{B}), 6.42 (d, $^3J_{HH}$ = 8.6 Hz, 1H, *H*18'^{A}), 6.11 (d, $^3J_{HH}$ = 8.8 Hz, 1H, *H*5'^{B}), 6.09 (dd, $^3J_{HH}$ = 8.3 Hz, $^3J_{HP}$ = 8.3 Hz, 1H, *H*3^B), 5.54 (d, $^3J_{HH}$ = 8.6 Hz, 1H, *H*13^A), 5.42 (d, $^3J_{HH}$ = 8.6 Hz, 1H, *H*13^B), 4.68 (d, $^3J_{HH}$ = 8.6 Hz, 1H, *H*13'^{A}), 4.06 (s, 3H, OCH_3^B), 1.79 (s, 3H, OCH_3^A) ppm. **^{11}B NMR** (128 MHz, CD_2Cl_2): δ = –2.0 ppm. **^{13}C{^{1}H} NMR** (126 MHz, CD_2Cl_2): δ = 155.8 (*C*2'^{A}), 149.2 (d, $^1J_{CP}$ = 56.2 Hz, *C*2^B), 148.6 (d, $^2J_{CP}$ = 12.5 Hz, *C*12^B), 148.1 (m, *C*12^A+*C*12'^{B}), 147.3 (d, $^2J_{CP}$ = 5.7 Hz, *C*12'^{A}), 145.3 (*C*2'^{B}), 137.4 (d, $^2J_{CP}$ = 32.0 Hz, *C*1^B), 136.6 (*C*1^A), 135.2 (*C*10^B), 134.9 (d, $^1J_{CP}$ = 44.1 Hz, *C*2^A), 134.7

(*C*10^{A}), 133.8 (*C*9'^{A}), 132.9 (*C*19'^{B}), 132.8 (*C*9^{A}), 132.7 (*C*19'^{A}), 132.2 (*C*20'^{B}), 132.0 (*C*19^{B}), 131.7 (*C*19^{A}), 131.5 (*C*20'^{A}), 131.1 (*C*20^{B}), 131.0 (*C*14'^{B}), 130.9 (*C*7'^{B}), 130.8 (*C*20^{A}), 130.7 (*C*9^{B}), 129.9 (*C*4'^{A}+*C*4^{B}+*C*16^{A}), 129.6 (*C*6^{B}), 129.5 (*C*6'^{B}), 129.2 (*C*14'^{A}), 129.1 (*C*14^{A}), 129.0 (*C*5'^{A}), 128.7 (*C*6^{A}+*C*10'^{A}), 128.6 (*C*7^{B}), 128.5 (*C*4^{A}+*C*15'^{B}+*C*5^{B}), 128.4 (*C*5^{A}), 128.3 (*C*15^{B}), 128.1 (*C*15'^{A}), 128.0 (*C*15^{A}), 127.6 (*C*7^{A}), 127.5 (*C*8^{A}), 127.3 (d, $^{2}J_{CP}$ = 26.0 Hz, *C*3^{A}), 127.1 (*C*7'^{A}), 126.8 (*C*18^{A}), 126.6 (*C*18'^{B}+*C*18'^{A}), 126.4 (*C*18^{B}), 126.2 (*C*17^{A}), 126.2 (*C*17'^{B}), 126.1 (*C*8^{B}), 125.8 (*C*17'^{A}), 125.7 (*C*17^{B}), 125.5 (*C*5'^{B}+*C*14^{B}+*C*16'^{A}+*C*16'^{B}), 125.2 (*C*3^{B}), 125.1 (*C*8'^{A}), 124.9 (*C*16^{B}), 123.8 (*C*8'^{B}), 123.7 (*C*11'^{A}), 123.3 (*C*6'^{A}), 122.0 (*C*9'^{B}), 121.3 (*C*11'^{B}), 121.1 (*C*11^{A}), 121.0 (*C*13'^{B}), 120.2 (*C*13'^{A}, *C*11^{B}), 120.1 (*C*13^{B}), 119.6 (*C*13^{A}), 118.9 (*C*1'^{A}), 114.0 (*C*10'^{B}), 112.3 (*C*3'^{A}), 101.6 (d, *J* = 13.1 Hz, *C*1'^{B}), 93.1 (d, *J* = 12.3 Hz, *C*4'^{B}), 90.1 (*C*3'^{B}), 58.4 (O*C*H$_3{}^{B}$), 54.6 (O*C*H$_3{}^{A}$) ppm. **^{19}F NMR** (376 MHz, CD_2Cl_2): δ = –152.9 ppm. **^{31}P NMR** (202 MHz, CD_2Cl_2): δ = 183.5 (ddd, $^{1}J_{PRh}$ = 277 Hz, $^{2}J_{PP}$ = 23.5 Hz, $^{3}J_{PH}$ = 13.7 Hz, *P*^{A}), 178.4 (ddd, $^{1}J_{PRh}$ = 309 Hz, $^{2}J_{PP}$ = 23.5 Hz, $^{3}J_{PH}$ = 8.3 Hz, *P*^{B}) ppm. **IR** (neat): ν = 3063.2 (w), 1621.2 (w), 1591.7 (w), 1506.3 (m), 1463.7 (m), 1324.2 (w), 1274.0 (m), 1223.7 (s), 1153.8 (w), 1068.9 (s), 956.1 (s), 837.0 (w), 810.1 (s), 746.6 (s), 696.3 (m) cm^{-1}. **HRMS** (ESI^{+}, MeOH): Found: *m*/*z* = 1299.2440. Calculated for [M – BF_4]$^{+}$: *m*/*z* = 1299.2445.

5.4.19 ((*R*)-(2'-Methoxy-[1,1'-binaphthalen]-2-yl)diphenylphosphine-*κP*)(1',2',3',4',9',10'η-(*R*)-(2'-methoxy-[1,1'-binaphthalen]-2-yl)diphenylphosphine-*κP*)rhodium tetrafluoroborate (**44b**)

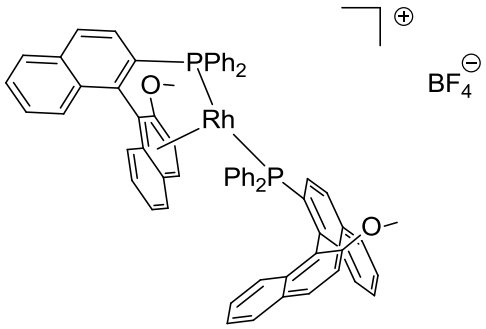

The same procedures as described for the synthesis of **42b** were utilised using OMe-MOP as ligand. The solution was filtered and layered with hexane to precipitate the product as a orange solid overnight.

^{1}H NMR (500 MHz, $CDCl_3$): δ = 7.94 (d, $^{3}J_{HH}$ = 8.2 Hz, 1H, *H*5^{B}), 7.86 (d, $^{3}J_{HH}$ = 8.0 Hz, 1H, *H*5^{A}), 7.82 (dd, $^{3}J_{HH}$ = 9.0 Hz, $^{4}J_{HP}$ = 1.3 Hz, 1H, *H*4^{B}), 7.78 (dd, $^{3}J_{HH}$ = 8.3 Hz, $^{5}J_{HP}$ = 0.8 Hz, 1H, *H*8^{B}), 7.70 (d, $^{3}J_{HH}$ = 7.5 Hz, 1H, *H*3'^{B}), 7.64 (ddd, $^{3}J_{HH}$ = 8.2 Hz,

$^{3}J_{HH}$ = 6.9 Hz, $^{4}J_{HH}$ = 1.2 Hz, 1H, *H*6^{B}), 7.60 (d, $^{3}J_{HH}$ = 8.7 Hz, 1H, *H*4^{A}), 7.57 (d, $^{3}J_{HH}$ = 8.2 Hz, 1H, *H*5'^{A}), 7.54 (ddd, $^{3}J_{HH}$ = 8.3 Hz, $^{3}J_{HH}$ = 6.9 Hz, $^{4}J_{HH}$ = 1.3 Hz, 1H, *H*7^{B}), 7.49-7.46 (m, 2H, *H*6^{A}+*H*4'^{A}), 7.38 (ddd, $^{3}J_{HH}$ = 8.3 Hz, $^{3}J_{HH}$ = 7.2 Hz, $^{4}J_{HH}$ = 1.3 Hz, 1H, *H*7'^{B}), 7.30 (m, 1H, *H*14'^{B}), 7.25 (m, 1H, *H*14^{B}), 7.17-7.12 (m, 3H, *H*6'^{B}+*H*6'^{A}+*H*7^{A}), 7.11-7.07 (m, 4H, *H*3^{B}+*H*13'^{B}+*H*14'^{A}), 7.04-6.98 (m, 4H, *H*3^{A}+*H*5'^{B}+*H*13^{B}), 6.96 (ddd, $^{3}J_{HH}$ = 8.4 Hz, $^{3}J_{HH}$ = 6.8 Hz, $^{4}J_{HH}$ = 1.3 Hz, 1H, *H*7'^{A}), 6.92-6.84 (m, 5H, *H*12'^{B}+*H*13'^{A}+*H*14^{A}), 6.81-6.73 (m, 5H, *H*12'^{A}+*H*8'^{B}+*H*3'^{A}+*H*8^{A}), 6.60-6.54 (m, 3H, *H*12^{B}+*H*8'^{A}), 6.33 (m, 2H, *H*13^{A}), 6.24-6.19 (m, 3H, *H*4'^{B}+*H*12^{A}), 3.89 (s, 3H, OC$H_3{}^{B}$), 3.61 (s, 3H, OC$H_3{}^{A}$) ppm. **^{11}B NMR** (128 MHz, CD_2Cl_2): δ = –1.6 ppm. **^{13}C{^{1}H} NMR** (126 MHz, CD_2Cl_2): δ = 154.3 (*C*2'^{A}), 145.9 (d, $^{1}J_{CP}$ = 50.3 Hz, *C*2^{B}), 141.4 (*C*2'^{B}), 139.3 (d, $^{2}J_{CP}$ = 21.6 Hz, *C*1^{B}), 137.2 (*C*1^{A}), 134.9 (d, $^{2}J_{CP}$ = 13.1 Hz, *C*12'^{A}), 134.2 (*C*9^{B}+*C*9'^{A}), 133.9 (d, $^{2}J_{CP}$ = 13.1 Hz, *C*12^{A}), 133.7 (*C*10^{A}), 133.5 (*C*9^{A}), 133.1 (d, $^{2}J_{CP}$ = 12.2 Hz, *C*12'^{B}), 132.3 (d, $^{2}J_{CP}$ = 11.7 Hz, *C*12^{B}), 132.3 (*C*11^{B}), 131.9 (*C*11^{A}), 131.4 (m, *C*3^{A}), 131.3 (*C*14'^{B}), 130.7 (*C*4'^{A}), 130.6 (*C*4^{B}+*C*14^{B}+*C*14'^{A}), 130.0 (d, $^{1}J_{CP}$ = 49.8 Hz, *C*11'^{A}), 129.6 (*C*7'^{B}), 129.4 (*C*14^{A}), 128.8 (*C*6^{B}), 128.7 (d, $^{3}J_{CP}$ = 3.7 Hz, *C*13'^{B}), 128.6 (d, $^{3}J_{CP}$ = 10.8 Hz, *C*13^{B}), 128.6 (*C*10'^{A}), 128.4 (*C*5^{B}+*C*7^{B}), 128.3 (*C*6'^{A}), 128.0 (*C*5^{A}+*C*3^{B}), 127.9 (*C*5'^{A}), 127.7 (*C*6^{A}), 127.5 (*C*13'^{A}), 127.1 (*C*7^{A}), 126.9 (d, $^{3}J_{CP}$ = 14.0 Hz, *C*4^{A}), 126.5 (*C*8^{A}), 126.5 (d, $^{3}J_{CP}$ = 3.4 Hz, *C*13^{A}), 126.2 (*C*8^{B}), 126.0 (*C*7'^{A}), 124.7 (*C*5'^{B}), 124.6 (*C*8'^{A}), 123.2 (*C*6'^{B}), 123.1 (*C*9'^{B}), 121.9 (*C*8'^{B}), 120.2 (*C*10'^{B}), 118.7 (*C*1'^{A}), 112.4 (*C*3'^{A}), 93.6 (d, *J* = 13.1 Hz, *C*1'^{B}), 92.3 (d, *J* = 9.2 Hz, *C*4'^{B}), 89.5 (*C*3'^{B}), 57.2 (O*C*$H_3{}^{B}$), 55.8 (O*C*$H_3{}^{A}$) ppm; resonances for *C*2^{A}, *C*10^{B} and *C*11'^{B} were obscured. **^{19}F NMR** (376 MHz, CD_2Cl_2): δ = –153.3 ppm. **^{31}P{^{1}H} NMR** (162 MHz, $CDCl_3$): δ = 50.0 (dd, $^{1}J_{PRh}$ = 217 Hz, $^{2}J_{PP}$ = 32.1 Hz, *P*^{B}), 37.2 (dd, $^{1}J_{PRh}$ = 197 Hz, $^{2}J_{PP}$ = 32.1 Hz, *P*^{A}) ppm. **HRMS** (ESI^+, MeOH): Found: *m*/*z* = 1039.2321. Calculated for [M – BF_4]$^+$: *m*/*z* = 1039.2336.

5.4.20 Chloro((*R*,*R*$_b$)-[1,1'-binaphthalene]-2,2'-diyl (2'-methoxy-[1,1'-binaphthalen]-2-yl)phosphonite)(η^4-cycloocta-1,5-diene)iridium (**45b**)

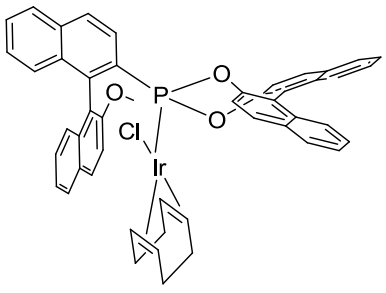

33b (28.4 mg, 50.0 μmol) and $[Ir(\eta^4\text{-cod})Cl]_2$ (16.8 mg, 25.0 μmol) were dissolved in CH_2Cl_2 (2 mL) and stirred for 30 minutes. The solution was filtered and layered with Et_2O. Dark orange crystals suitable for X-ray analysis were formed overnight.

^{1}H NMR (500 MHz, CD_2Cl_2): δ = 8.17 (d, $^3J_{HH}$ = 9.1 Hz, 1H, *H*4'), 8.10 (d, $^3J_{HH}$ = 8.8 Hz, 1H, *H*13), 8.05 (d, $^3J_{HH}$ = 8.8 Hz, 1H, *H*14), 8.00 (d, $^3J_{HH}$ = 8.9 Hz, 1H, *H*15), 7.93 (d, $^3J_{HH}$ = 8.2 Hz, 1H, *H*5'), 7.87 (d, $^3J_{HH}$ = 8.1 Hz, 1H, *H*15'), 7.87 (d, $^3J_{HH}$ = 8.1 Hz, 1H, *H*5), 7.75 (dd, $^3J_{HH}$ = 8.7 Hz, $^3J_{HP}$ = 6.3 Hz, 1H, *H*3), 7.71 (dd, $^3J_{HH}$ = 8.7 Hz, $^4J_{HP}$ = 6.3 Hz, 1H, *H*4), 7.68 (d, $^3J_{HH}$ = 8.9 Hz, 1H, *H*14'), 7.57 (d, $^3J_{HH}$ = 9.1 Hz, 1H, *H*3'), 7.52-7.41 (m, 5H, *H*6+*H*16+*H*16'+*H*18'+*H*18), 7.37-7.29 (m, 3H, *H*6'+*H*17+*H*17'), 7.24-7.18 (m, 2H, *H*7+*H*7'), 7.17 (d, $^3J_{HH}$ = 8.9 Hz, 1H, *H*13'), 7.04 (d, $^3J_{HH}$ = 8.5 Hz, 1H, *H*8'), 6.94 (d, $^3J_{HH}$ = 8.5 Hz, 1H, *H*8), 5.08 (m, 1H, cod-C*H*), 3.98 (m, 1H, cod-C*H*), 3.96 (s, 3H, OCH_3), 2.18 (m, 1H, cod-C*H*), 2.08 (m, 1H, cod-C*H*), 1.75 (m, 1H, cod-CH_2), 1.51-1.40 (m, 3H, cod-CH_2), 1.31 (m, 1H, cod-CH_2), 1.05 (m, 1H, cod-CH_2), 1.00-0.95 (m, 2H, cod-CH_2) ppm. **^{13}C{^{1}H} NMR** (101 MHz, CD_2Cl_2): δ = 155.8 (*C*2'), 149.7 (d, $^2J_{CP}$ = 4.3 Hz, *C*12), 149.6 (d, $^2J_{CP}$ = 10.9 Hz, *C*12'), 140.7 (d, $^2J_{CP}$ = 22.4 Hz, *C*1), 135.1 (*C*2), 134.6 (*C*9'), 133.2 (d, *J* = 11.7 Hz), 132.8, 132.4 (d, *J* = 1.3 Hz), 132.3 (d, *J* = 2.2 Hz), 132.2, 131.7, 131.4 (*C*4'), 129.9 (*C*14'), 129.8 (*C*14), 129.6 (*C*8'), 129.2 (*C*10'), 128.4 (*C*15), 128.4 (*C*15'), 128.1 (*C*5), 127.9 (*C*6), 127.1 (*C*5'), 126.9 (*C*4), 126.7 (*C*18), 126.7 (*C*18'), 126.6 (*C*7), 126.6 (*C*8), 126.3 (*C*17+*C*17'), 126.2 (*C*7'), 125.8 (d, $^2J_{CP}$ = 3.3 Hz, *C*3), 125.4 (*C*16), 125.2 (*C*16'), 124.5 (*C*13), 124.0 (*C*6'+*C*11), 123.3 (d, $^3J_{CP}$ = 2.7 Hz, *C*11'), 121.7 (*C*13'), 120.0 (d, $^3J_{CP}$ = 7.8 Hz, *C*1'), 112.7 (*C*3'), 102.5 (d, $^2J_{CP}$ = 18.5 Hz, cod-*C*H), 101.8 (d, $^2J_{CP}$ = 15.9 Hz, cod-*C*H), 56.1 (cod-*C*H), 56.0 (O*C*H_3), 49.7 (cod-*C*H), 33.6 (d, $^3J_{CP}$ = 3.9 Hz, cod-*C*H_2), 32.1 (d, $^3J_{CP}$ = 2.7 Hz, cod-*C*H_2), 27.9 (d, $^3J_{CP}$ = 2.3 Hz, cod-*C*H_2), 27.6 (d, $^3J_{CP}$ = 2.6 Hz, cod-*C*H_2) ppm; resonances for *C*9, *C*19, *C*19', *C*20 and *C*20' could not be specifically assigned. **^{31}P{^{1}H} NMR** (202 MHz, CD_2Cl_2): δ = 140.4 ppm. **HRMS** (ESI^+, MeCN): Found: *m*/*z* = 897.2214. Calculated for $[M - Cl]^+$: *m*/*z* = 897.2237.

5.4.21 Chloro((*R*,*S*$_b$)-[1,1'-binaphthalene]-2,2'-diyl (2'-methoxy-[1,1'-binaphthalen]-2-yl)phosphonite)(η^4-cycloocta-1,5-diene)iridium (**46b**)

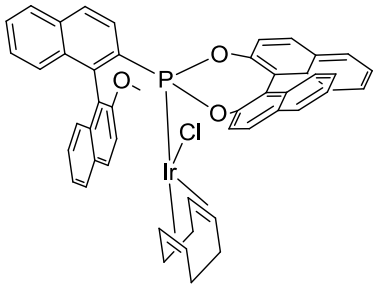

34b (30.0 mg, 50.0 μmol) and [Ir(η^4-cod)Cl]$_2$ (16.8 mg, 25.0 μmol) were dissolved in CH_2Cl_2 (2 mL) and stirred for 30 minutes. The solution was filtered and layered with Et_2O to precipitate the product as a yellow solid overnight.

^{1}H NMR (500 MHz, CD_2Cl_2): δ = 8.20 (d, $^3J_{HH}$ = 9.2 Hz, 1H, *H*4'), 8.08 (d, $^3J_{HH}$ = 8.8 Hz, 1H, *H*13'), 8.04 (d, $^3J_{HH}$ = 8.8 Hz, 1H, *H*14'), 7.97-7.92 (m, 3H, *H*15'+*H*5'+*H*15), 7.87 (d, $^3J_{HH}$ = 8.3 Hz, 1H, *H*5), 7.80 (d, $^3J_{HH}$ = 8.9 Hz, 1H, *H*14), 7.66 (d, $^3J_{HH}$ = 8.8 Hz, 1H, *H*4), 7.61 (dd, $^3J_{HH}$ = 8.7 Hz, $^3J_{HP}$ = 6.3 Hz, 1H, *H*3), 7.53 (ddd, $^3J_{HH}$ = 8.3 Hz, $^3J_{HH}$ = 6.8 Hz, $^4J_{HH}$ = 1.3 Hz, 1H, *H*6), 7.51 (d, $^3J_{HH}$ = 9.2 Hz, 1H, *H*3'), 7.49 (ddd, $^3J_{HH}$ = 8.2 Hz, $^3J_{HH}$ = 6.8 Hz, $^4J_{HH}$ = 1.3 Hz, 1H, *H*16), 7.46-7.39 (m, 4H, *H*16'+*H*7'+*H*18+*H*8'), 7.36-7.30 (m, 2H, *H*6'+*H*17), 7.29-7.23 (m, 3H, *H*7+*H*17'+*H*18'), 7.13 (d, $^3J_{HH}$ = 8.6 Hz, 1H, *H*8), 7.04 (d, $^3J_{HH}$ = 8.9 Hz, 1H, *H*13), 5.26 (m, 1H, cod-C*H*), 4.70 (m, 1H, cod-C*H*), 3.76 (s, 3H, OCH_3), 2.13 (m, 1H, cod-C*H*), 2.04 (m, 1H, cod-CH_2), 1.72 (m, 1H, cod-CH_2), 1.65 (m, 1H, cod-CH_2), 1.36-1.26 (m, 2H, cod-CH_2), 1.18 (m, 1H, cod-C*H*), 0.96-0.86 (m, 2H, cod-CH_2), 0.73 (m, 1H, cod-CH_2) ppm. **^{13}C{^{1}H} NMR** (126 MHz, CD_2Cl_2): δ = 155.6 (*C*2'), 149.8 (d, $^2J_{CP}$ = 5.8 Hz, *C*12'), 149.2 (d, $^2J_{CP}$ = 12.8 Hz, *C*12), 141.3 (d, $^2J_{CP}$ = 24.1 Hz, *C*1), 135.3 (d, $^1J_{CP}$ = 1.8 Hz, *C*2), 135.0 (*C*9'), 133.1 (d, $^3J_{CP}$ = 11.6 Hz, *C*9), 132.8 (d, $^4J_{CP}$ = 7.4 Hz, C19), 132.4 (d, $^4J_{CP}$ = 1.6 Hz, *C*19'), 131.7 (d, $^5J_{CP}$ = 1.6 Hz, *C*20'), 131.4 (d, $^5J_{CP}$ = 0.9 Hz, *C*20), 131.1 (*C*4'), 130.0 (*C*14'), 129.8 (*C*14), 128.4 (*C*15'), 128.4 (*C*15), 128.2 (*C*5'), 128.1 (*C*5), 128.1 (*C*6), 127.1 (d, $^4J_{CP}$ = 2.0 Hz, *C*8), 127.1 (*C*4), 127.0 (*C*8'+*C*18), 126.7 (*C*18'), 126.4 (*C*7), 126.3 (*C*17'), 126.2 (*C*7'), 125.8 (d, $^2J_{CP}$ = 3.1 Hz, *C*3), 125.6 (*C*17), 125.3 (*C*16'), 125.3 (*C*16), 124.7 (d, $^3J_{CP}$ = 2.7 Hz, *C*13'), 123.6 (d, $^3J_{CP}$ = 3.7 Hz, *C*11'), 123.3 (*C*6'), 123.0 (d, $^3J_{CP}$ = 2.5 Hz, *C*11), 121.4 (d, $^3J_{CP}$ = 1.4 Hz, *C*13), 119.5 (d, $^3J_{CP}$ = 8.0 Hz, *C*1'), 112.9 (*C*3'), 102.6 (d, $^2J_{CP}$ = 18.5 Hz, cod-*C*H), 99.7 (d, $^2J_{CP}$ = 17.0 Hz, cod-*C*H), 57.9 (d, $^2J_{CP}$ = 1.5 Hz, cod-*C*H), 55.7 (O*C*H_3), 50.5 (cod-*C*H), 33.4 (d, $^3J_{CP}$ = 3.5 Hz, cod-*C*H_2), 32.2 (d, $^3J_{CP}$ = 3.0 Hz, cod-*C*H_2), 27.8 (d, $^3J_{CP}$ = 2.4 Hz, cod-*C*H_2), 27.7 (d, $^3J_{CP}$ = 2.9 Hz, cod-*C*H_2)

ppm; resonances for *C*10 and *C*10' were obscured. **^{31}P{^{1}H} NMR** (202 MHz, CD_2Cl_2): δ = 139.6 ppm. **HRMS** (ESI^+, MeCN): Found: *m*/*z* = 897.2226. Calculated for $[M - Cl]^+$: *m*/*z* = 897.2237.

5.4.22 Bis((*R*,*R*$_b$)-[1,1'-binaphthalene]-2,2'-diyl (2'-methoxy-[1,1'-binaphthalen]-2-yl)phosphonite)(η^4-cycloocta-1,5-diene)iridium tetrafluoroborate (**47b**)

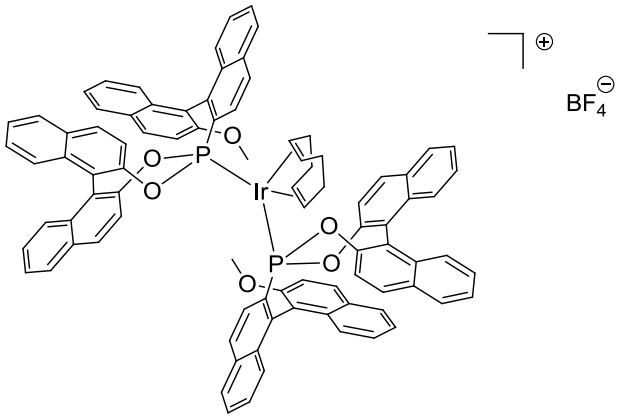

Methode A: **33b** (30.0 mg, 50.0 µmol) and $[Ir(\eta^4\text{-cod})_2]BF_4$ (12.4 mg, 25.0 µmol) were dissolved in CH_2Cl_2 (1 mL) and stirred for 30 minutes. The solution was filtered and layered with Et_2O to precipitate the product as a green solid overnight.

Methode B: **45b** (23.4 mg, 25.0 µmol) was dissolved in CH_2Cl_2 (1 mL), $AgBF_4$ (4.8 mg, 25.0 µmol) and **33b** (15.0 mg, 25.0 µmol) were added and stirred for 30 minutes. The solution was filtered and concentrated *in vacuo*. The crude product was washed with Et_2O to give the product as a green solid.

^{1}H NMR (500 MHz, $CDCl_3$): δ = 8.27 (d, $^3J_{HH}$ = 8.8 Hz, 2H, *H*14), 8.14 (d, $^3J_{HH}$ = 8.2 Hz, 2H, *H*15), 7.85 (d, $^3J_{HH}$ = 8.3 Hz, 2H, *H*5), 7.69 (d, $^3J_{HH}$ = 9.1 Hz, 2H, *H*4'), 7.61 (d, $^3J_{HH}$ = 8.1 Hz, 2H, *H*15'), 7.58-7.54 (m, 4H, *H*4+*H*16), 7.83 (pt, J_{HH} = 7.5 Hz, 2H, *H*6), 7.37-7.30 (m, 6H, *H*3+*H*16'+*H*3'), 7.24 (d, $^3J_{HH}$ = 8.8 Hz, 2H, *H*13), 7.16 (d, $^3J_{HH}$ = 8.2 Hz, 2H, *H*5'), 7.12-7.02 (m, 8H, *H*17+*H*7+*H*14'+*H*17'), 6.84 (d, $^3J_{HH}$ = 8.6 Hz, 2H, *H*8), 6.81 (d, $^3J_{HH}$ = 8.6 Hz, 2H, *H*18), 6.58 (d, $^3J_{HH}$ = 8.6 Hz, 2H, *H*18'), 6.10 (pt, J_{HH} = 7.5 Hz, 2H, *H*6'), 5.64 (m, 2H, cod-C*H*), 5.10 (d, $^3J_{HH}$ = 8.8 Hz, 2H, *H*13'), 5.08 (d, $^3J_{HH}$ = 8.5 Hz, 2H, *H*8'), 4.86 (pt, J_{HH} = 7.6 Hz, 2H, *H*7'), 4.67 (m, 2H, cod-C*H*), 3.62 (s, 6H, OCH_3), 2.73 (m, 2H, cod-CH_2), 2.57 (m, 2H, cod-CH_2), 2.15 (m, 2H, cod-CH_2), 2.00 (m, 2H, cod-CH_2) ppm. **^{13}C{^{1}H} NMR** (126 MHz, $CDCl_3$): δ = 153.2 (*C*2'), 147.6 (pt, $^2J_{CP}$ = 12.2 Hz, *C*12'), 147.2 (pt, $^2J_{CP}$ = 7.0 Hz, *C*12), 138.8 (*C*1), 134.7 (*C*10), 134.5 (*C*9'), 132.9 (pt, $^3J_{CP}$ = 8.4 Hz, *C*9), 132.8 (*C*19), 132.4 (*C*19'), 132.1 (*C*20), 131.4 (*C*20'), 130.9 (*C*14), 130.2 (*C*4'), 130.0 (*C*14'),

128.7 (*C*15), 128.6 (*C*6), 128.2 (*C*5), 128.1 (*C*4), 127.9 (*C*15'), 127.6 (*C*8), 127.6 (*C*18), 127.5 (*C*18'), 127.4 (*C*10'), 127.4 (*C*7), 126.8 (*C*17), 126.3 (*C*5'), 126.0 (*C*17'), 125.9 (*C*16), 125.5 (*C*16'), 125.4 (*C*7'), 123.5 (*C*11), 122.4 (*C*6'), 122.3 (*C*8'), 121.6 (*C*11'), 120.6 (*C*13), 119.6 (*C*13'), 119.5 (*C*1'), 111.5 (*C*3'), 99.2 (pt, $^{2}J_{CP}$ = 14.8 Hz, cod-*C*H), 94.3 (pt, $^{2}J_{CP}$ = 10.2 Hz, cod-*C*H), 55.6 (O*C*H$_3$), 33.3 (cod-*C*H$_2$), 29.3 (cod-*C*H$_2$) ppm; resonances for *C*2 and *C*3 were obscured. **^{31}P{^{1}H} NMR** (202 MHz, $CDCl_3$): δ = 156.3 ppm. **HRMS** (ESI^+, MeOH): Found: *m*/*z* = 1495.3935. Calculated for $[M - BF_4]^+$: *m*/*z* = 1495.3935.

5.4.23 ((*S*,*R*$_b$)-[1,1'-Binaphthalene]-2,2'-diyl [1,1'-binaphthalen]-2-ylphosphonite)chlorogold (**48a**)

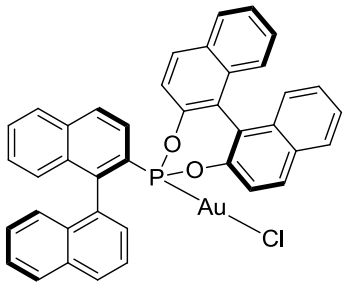

Phosphonite **33a** (29.9 mg, 50 µmol) and [AuCl(tht)] (16.0 mg, 50 µmol) were dissolved in CH_2Cl_2 (2 mL) and stirred for 15 minutes. Removal of the solvent gave the product as a colourless solid which was washed with hexane. Yield: 38 mg (95%).

^{1}H NMR (400 MHz, CD_2Cl_2): δ = 8.16 (d, $^{3}J_{HH}$ = 8.3 Hz, 1H, Ar*H*), 8.05 (d, $^{3}J_{HH}$ = 8.8 Hz, 1H, Ar*H*), 8.03 (d, $^{3}J_{HH}$ = 8.1 Hz, 1H, Ar*H*), 7.96 (d, $^{3}J_{HH}$ = 8.3 Hz, 1H, Ar*H*), 7.93 (d, $^{3}J_{HH}$ = 9.0 Hz, 1H, Ar*H*), 7.91 (d, $^{3}J_{HH}$ = 8.8 Hz, 1H, Ar*H*), 7.82 (dd, $^{3}J_{HH}$ = 7.0 Hz, *J* = 1.3 Hz, 1H, Ar*H*), 7.80 (d, $^{3}J_{HH}$ = 8.3 Hz, 1H, Ar*H*), 7.74-7.67 (m, 2H, 2 Ar*H*), 7.61 (ddd, $^{3}J_{HH}$ = 8.3 Hz, $^{3}J_{HH}$ = 6.7 Hz, *J* = 1.5 Hz, 1H, Ar*H*), 7.55-7.21 (m, 6H, 6 Ar*H*), 7.37-7.27 (m, 6H, 6 Ar*H*), 7.10 (d, $^{3}J_{HH}$ = 8.3 Hz, 1H, Ar*H*), 7.04 (dd, $^{3}J_{HH}$ = 8.8 Hz, *J* = 1.1 Hz, 1H, Ar*H*) ppm. **^{13}C{^{1}H} NMR** (101 MHz, CD_2Cl_2): δ = 147.4 (d, *J* = 7.0 Hz), 146.9 (d, *J* = 12.8 Hz), 146.3 (d, *J* = 24.7 Hz), 135.6, 134.1, 133.6, 133.3 (d, *J* = 10.4 Hz), 133.2 (d, *J* = 11.2 Hz), 132.6, 132.5, 132.3, 131.9, 130.8, 130.7, 130.2, 129.3, 129.2, 129.0, 128.8, 128.6, 128.2, 128.1, 128.0, 127.7, 127.4, 127.0, 126.9, 126.8, 126.6, 126.1, 126.0, 125.3, 124.8, 124.7, 123.6, 123.1, 120.7, 120.5 ppm. **^{31}P{^{1}H} NMR** (162 MHz, CD_2Cl_2): δ = 149.6 (d, J_{PH} = 6.1 Hz) ppm. **HRMS** (EI): Found: *m*/*z* = 800.0948. Calculated for $[M]^+$: *m*/*z* = 800.0946.

5.4.24 ((*R*,*R*$_b$)-[1,1'-Binaphthalene]-2,2'-diyl (2'-methoxy-[1,1'-binaphthalen]-2-yl)-phosphonite)chlorogold (**48b**)

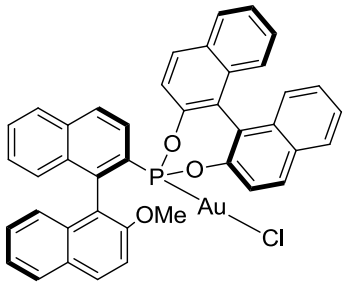

Phosphonite **33b** (29.9 mg, 50 µmol) and [AuCl(tht)] (16.0 mg, 50 µmol) were dissolved in CH_2Cl_2 (2 mL) and stirred for 15 minutes. The intended complex was formed quantitatively. Slow diffusion of Et_2O into the reaction mixture yielded colourless crystals overnight which were suitable for X-ray diffraction analysis.

^{1}H NMR (500 MHz, CD_2Cl_2): δ = 8.24 (d, $^3J_{HH}$ = 9.1 Hz, 1H, *H*4'), 8.07 (d, $^3J_{HH}$ = 9.0 Hz, 1H, Ar*H*), 8.00-7.95 (m, 3H, *H*5'+*H*15'+Ar*H*), 7.93 (d, $^3J_{HH}$ = 8.3 Hz, 1H, *H*5), 7.82 (d, $^3J_{HH}$ = 8.8 Hz, 1H, *H*14'), 7.70 (d, $^3J_{HH}$ = 8.8 Hz, J_{HP} = 2.2 Hz, 1H, *H*4), 7.63 (ddd, $^3J_{HH}$ = 8.2 Hz, $^3J_{HH}$ = 6.7 Hz, J_{HH} = 1.4 Hz, 1H, *H*6), 7.56 (d, $^3J_{HH}$ = 9.1 Hz, 1H, *H*3'), 7.56-7.49 (m, 3H, 3 Ar*H*), 7.47 (d, $^3J_{HH}$ = 8.5 Hz, 1H, Ar*H*), 7.42-7.23 (m, 8H, *H*3+*H*7+6 Ar*H*), 7.05 (d, $^3J_{HH}$ = 8.8 Hz, 1H, *H*13'), 7.86 (d, $^3J_{HH}$ = 8.5 Hz, 1H, Ar*H*), 4.02 (s, 3H, OCH_3) ppm. **^{13}C{^{1}H} NMR** (101 MHz, CD_2Cl_2): δ = 156.6 (*C*2'), 147.5 (d, *J* = 7.3 Hz), 147.2 (d, *J* = 12.9 Hz), 143.3 (d, *J* = 25.4 Hz, *C*2), 136.0 (d, *J* = 1.8 Hz), 134.7 (*C*9'), 133.1 (d, *J* = 11.6 Hz), 132.6 (d, *J* = 1.8 Hz), 132.4 (d, *J* = 1.8 Hz), 132.2 (d, *J* = 1.4 Hz), 132.1 (*C*4'), 131.9 (d, *J* = 1.4 Hz), 131.8 (d, *J* = 1.8 Hz), 130.8 (d, *J* = 1.8 Hz, *C*14'), 129.4, 129.3, 129.0, 128.8 (*C*10'), 128.6, 128.4, 128.2, 127.6 (d, *J* = 7.8 H, *C*4), 127.4 (d, *J* = 1.4 Hz), 127.4, 127.1, 127.1, 126.9 (d, *J* = 3.7 Hz), 126.8 (d, *J* = 4.2 Hz), 125.9 (d, *J* = 6.4 Hz), 124.9 (d, *J* = 4.4 Hz), 124.8, 124.1, 123.8 (d, *J* = 3.8 Hz), 123.2 (d, *J* = 3.2 Hz), 121.1 (d, J_{CP} = 1.9 Hz, *C*13'), 120.9 (d, J_{CP} = 2.9 Hz), 117.2 (d, $^2J_{CP}$ = 10.9 Hz, *C*1'), 112.6 (*C*3'), 56.2 (O*C*H_3) ppm. **^{31}P NMR** (202 MHz, CD_2Cl_2): δ = 149.9 (d, J_{PH} = 6.8 Hz) ppm. **HRMS** (EI): Found: *m*/*z* = 830.1039. Calculated for $[M]^+$: *m*/*z* = 830.1052.

5.4.25 ((*S*,*R*$_b$)-[1,1'-Binaphthalene]-2,2'-diyl [1,1'-binaphthalen]-2-ylphosphonite)chlorogold (**49a**)

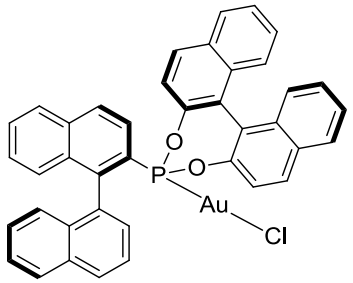

Phosphonite **34a** (29.9 mg, 50 µmol) and [AuCl(tht)] (16.0 mg, 50 µmol) were dissolved in CH_2Cl_2 (2 mL) and stirred for 15 minutes. Removal of the solvent gave the product as a colourless solid which was washed with hexane.

^{1}H NMR (400 MHz, CD_2Cl_2): δ = 8.15 (d, $^3J_{HH}$ = 7.8 Hz, 1H, Ar*H*), 8.05 (d, $^3J_{HH}$ = 8.9 Hz, 1H, Ar*H*), 8.01 (d, $^3J_{HH}$ = 8.2 Hz, 1H, Ar*H*), 7.99-7.88 (m, 5H, 5 Ar*H*), 7.78 (dd, $^3J_{HH}$ = 8.6 Hz, J = 2.1 Hz, 1H, Ar*H*), 7.64-7.57 (m, 3H, 3 Ar*H*), 7.56-7.44 (m, 5H, 5 Ar*H*), 7.39-7.31 (m, 5H, 5 Ar*H*), 7.29-7.21 (m, 2H, 2 Ar*H*), 7.11 (dd, $^3J_{HH}$ = 8.9 Hz, $^3J_{HH}$ = 1.2 Hz, 1H, Ar*H*) ppm. **^{13}C{^{1}H} NMR** (101 MHz, CD_2Cl_2): δ = 147.5 (d, J = 7.3 Hz), 147.1 (d, J = 12.7 Hz), 146.1 (d, J = 24.0 Hz), 135.8, 134.0, 133.7, 133.5 (d, J = 11.3 Hz), 133.3 (d, J = 10.2 Hz), 132.6, 132.5, 132.2, 131.9, 131.8, 131.3, 130.9, 129.9, 129.7, 129.4, 128.9, 128.8, 128.6, 128.4, 128.2, 128.1, 127.8, 127.5, 127.3, 127.1, 126.9, 126.7, 126.5, 126.1, 126.0, 124.8, 124.7, 124.1, 124.0, 123.5, 122.8, 121.0, 120.7, 117.8 ppm. **^{31}P{^{1}H} NMR** (162 MHz, CD_2Cl_2): δ = 149.5 (d, J_{PH} = 7.5 Hz) ppm. **HRMS** (EI): Found: m/z = 800.0936. Calculated for $[M]^+$: m/z = 800.0946.

5.4.26 ((*R*,*S*$_b$)-[1,1'-Binaphthalene]-2,2'-diyl (2'-methoxy-[1,1'-binaphthalen]-2-yl)-phosphonite)chlorogold (**49b**)

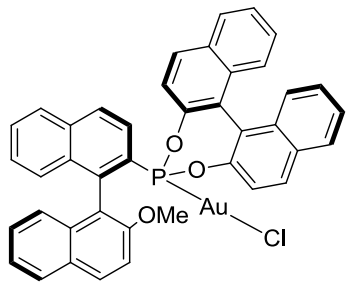

Phosphonite **34b** (29.9 mg, 50 µmol) and [AuCl(tht)] (16.0 mg, 50 µmol) were dissolved in CH_2Cl_2 (2 mL) and stirred for 15 minutes. The intended complex was formed quantitatively.

Slow evaporation of a Et_2O/CH_2Cl_2 solution yielded colourless crystals which were suitable for X-ray diffraction analysis.

^{1}H NMR (500 MHz, CD_2Cl_2): δ = 8.25 (d, $^3J_{HH}$ = 9.2 Hz, 1H, *H*4'), 8.10 (d, $^3J_{HH}$ = 8.8 Hz, 1H, Ar*H*), 7.97 (m, 2H, *H*5'+Ar*H*), 7.92 (d, $^3J_{HH}$ = 8.2 Hz, 1H, Ar*H*), 7.89 (d, $^3J_{HH}$ = 8.8 Hz, 1H, Ar*H*), 7.73 (dd, $^3J_{HH}$ = 8.8 Hz, $^3J_{HP}$ = 2.1 Hz, 1H, *H*4), 7.65-7.61 (m, 2H, 2 Ar*H*), 7.56 (d, $^3J_{HH}$ = 9.1 Hz, 1H, *H*3'), 7.55-7.34 (m, 10H, 10 Ar*H*), 7.29-7.23 (m, 2H, 2 Ar*H*), 7.16-7.13 (m, 2H, 2 Ar*H*), 3.93 (s, 3H, OC*H*$_3$) ppm. **^{13}C{^{1}H} NMR** (126 MHz, CD_2Cl_2): δ = 155.3 (*C*2'), 147.6 (d, *J* = 7.2 Hz), 147.0 (d, *J* = 12.9 Hz), 143.8 (d, *J* = 25.7 Hz, *C*2), 135.9 (d, *J* = 1.8 Hz), 134.8 (*C*9'), 133.1 (d, *J* = 11.8 Hz), 132.6, 132.6 (d, *J* = 0.9 Hz), 132.3 (d, *J* = 1.6 Hz), 131.9 (d, *J* = 1.8 Hz), 131.8 (d, *J* = 1.2 Hz), 131.6 (*C*4'), 130.8 (d, *J* = 1.5 Hz), 129.4, 128.9, 128.8, 128.7 (*C*5'), 128.6 (*C*10'), 128.3, 127.9 (d, *J* = 8.0 H), 127.6 (d, *J* = 1.4 Hz), 127.1, 127.1, 127.0, 126.9, 126.7, 126.0 (d, *J* = 2.9 Hz), 124.9 (d, *J* = 4.3 Hz), 124.8, 123.9, 123.7 (d, *J* = 3.7 Hz), 122.9 (d, *J* = 3.1 Hz), 120.9 (d, J_{CP} = 2.1 Hz), 120.8 (d, J_{CP} = 2.9 Hz), 117.3 (d, $^2J_{CP}$ = 10.8 Hz, *C*1'), 114.2 (*C*3'), 56.1 (O*C*H$_3$) ppm. **^{31}P NMR** (202 MHz, CD_2Cl_2): δ = 149.2 (d, J_{PH} = 6.7 Hz) ppm. **HRMS** (EI): Found: *m*/*z* = 830.1056. Calculated for $[M]^+$: *m*/*z* = 830.1052.

5.4.27 Rhodium-Catalysed Asymmetric Addition of Arylboronic Acids to Aldehydes

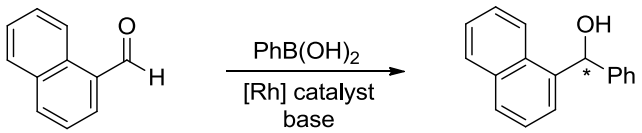

Rhodium precursor (10 µmol Rh) and ligand (20 µmol) were dissolved in THF (4 mL) and left to stir for 20 minutes. Phenylboronic acid (122 mg, 1.0 mmol), base (2.5 M aqueous solution, 1.0 mmol) and 1-naphthaldehyde (68 µl, 0.5 mmol) were added subsequently. The reaction mixture was heated to 60 °C and the conversion was followed by TLC analysis. After the stated reaction time the solvent was evaporated and the crude product was purified by column chromatography (hexane/EtOAc, 10:1) on silica media (h = 15 cm, d = 2 cm) to give the product as a colourless oil. The enantiomeric excess was measured by chiral HPLC (Column Daicel Chiralpak OD; flow rate: 1.0 mL/min; hexane/2-propanol, 80:20; retention times: (*S*) t_1 = 10.1 min, (*R*) t_2 = 19.4 min).[310]

5.4.28 Gold Catalysed Cyclopropanation of Styrene

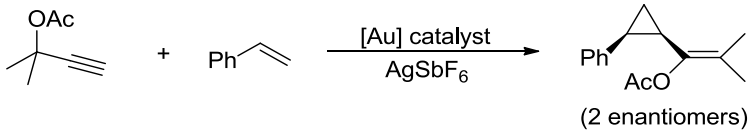

The catalyst was generated *in situ* by reacting [Au(L)Cl] (0.025 mmol, L = chiral ligand) and $AgSbF_6$ (8.6 mg, 0.025 mmol) in $MeNO_2$ (5 mL) for 30 minutes. Styrene (0.23 mL, 208 mg, 2.0 mmol) was added, followed by the addition of 2-methylbut-3-yn-2-yl acetate (0.5 mmol, 0.1 M solution in $MeNO_2$). After 2 hours reaction time the mixture was concentrated and purified by column chromatography (hexane/EtOAc, 5:1) on silica media. The diastereoselectivity was determined by ^{1}H NMR spectroscopy. The enantiomeric excess was measured by chiral HPLC (Column Daicel Chiralcel OD; flow rate: 1.0 mL/min; hexane/2-propanol, 95:5; retention times: t_1 = 5.4 min, t_2 = 6.4 min).

5.4.29 Gold Catalysed Cyclization of Enynes

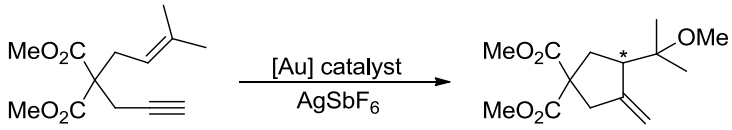

The catalyst was generated *in situ* by reacting [Au(L)Cl] (0.015 mmol, L = chiral ligand) and $AgSbF_6$ (5.2 mg, 0.015 mmol) in MeOH (4 mL) for 10 minutes. The enyne[311] (0.25 mmol, 0.0625 M solution in MeOH) was added and the reaction mixture was stirred at room temperature until full conversion was achieved. The progress of the reaction was followed by TLC analysis. The mixture was concentrated and purified by column chromatography (hexane/EtOAc, 4:1) on silica media. The enantiomeric excess was measured by chiral HPLC (Column Daicel Chiralpak AD-H; flow rate: 0.5 mL/min; hexane/2-propanol, 95:5; retention times: t_1 = 9.7 min, t_2 = 11.6 min).

5.5 References

247 This part of the chapter has been published in a peer-reviewed scientific journal: A. Ficks, R. M. Hiney, R. W. Harrington, D. G. Gilheany, L. J. Higham, *Dalton Trans.* **2012**, *41*, 3515.

248 This part of the chapter has been published in a peer-reviewed scientific journal: A. Ficks, R. W. Harrington, L. J. Higham, *Dalton Trans.* **2013**, *42*, 6302.

249 Selected review articles: (a) F. Lagasse, H. B. Kagan, *Chem. Pharm. Bull.* **2000**, *48*, 315; (b) I. V. Komarov, A. Börner, *Angew. Chem. Int. Ed.* **2001**, *40*, 1197; (c) T. Jerphagnon, J.-L. Renaud, C. Bruneau, *Tetrahedron: Asymmetry* **2004**, *15*, 2101; (d) G. Erre, S. Enthaler, K. Junge, S. Gladiali, M. Beller, *Coord. Chem. Rev.* **2008**, *252*, 471; (e) M. T. Reetz, *Angew. Chem. Int. Ed.* **2008**, *47*, 2556; (f) J. Ansell, M. Wills, *Chem. Soc. Rev.* **2002**, *31*, 259.

250 (a) J. W. Han, T. Hayashi, *Tetrahedron*: *Asymmetry* **2010**, *21*, 2193; (b) T. Hayashi, *Acc. Chem. Res*. **2000**, *33*, 354.

251 (a) J. F. Teichert, B. L. Feringa, *Angew. Chem. Int. Ed.* **2010**, *49*, 2486; (b) B. L. Feringa, *Acc. Chem. Res*. **2000**, *33*, 346.

252 Y. (A.) Xu, G. C. Clarkson, G. Docherty, C. L. North, G. Woodward, M. Wills, *J. Org. Chem*. **2005**, *70*, 8079.

253 K. V. Katti, N. Pillarsetty, K. Raghuraman, *Top. Curr. Chem.* **2003**, *229*, 121.

254 See for example: (a) M. Brynda, *Coord. Chem. Rev.* **2005**, *249*, 2013; (b) N. Pillarsetty, K. Raghuraman, C. L. Barnes, K. V. Katti, *J. Am. Chem. Soc.* **2005**, *127*, 331; (c) W. Henderson, S. R. Alley, *J. Organomet. Chem.* **2002**, *656*, 120; (d) M. Brynda, M. Geoffroy, G. Bernardinelli, *Chem. Commun.* **1999**, 961.

255 R. M. Hiney, L. J. Higham, H. Müller-Bunz, D. G. Gilheany, *Angew. Chem. Int. Ed.* **2006**, *45*, 7248.

256 B. Stewart, A. Harriman, L. J. Higham, *Organometallics* **2011**, *30*, 5338.

257 A. Ficks, I. Martinez-Botella, B. Stewart, R. W. Harrington, W. Clegg, L. J. Higham, *Chem. Commun*. **2011**, *47*, 8274.

258 (*a*) Y. Canac, R. Chauvin, *Eur. J. Inorg. Chem.* **2010**, 2325; (*b*) P. S. Pregosin, *Chem. Commun.* **2008**, 4875; (*c*) P. S. Pregosin, *Coord. Chem. Rev.* **2008**, *252*, 2156.

259 (a) P. Dotta, P. G. A. Kumar, P. S. Pregosin, A. Albinati, S. Rizzato, *Organometallics* **2004**, *23*, 4247; (b) T.-K. Zhang, D.-L. Mo, L.-X. Dai, X.-L. Hou, *Org. Lett.*, **2008**, *10*, 3689; (c) L. M. Alcazar-Roman, J. F. Hartwig, A. L. Rheingold, L. M. Liable-Sands, I. A. Guzei, *J. Am. Chem. Soc.* **2000**, *122*, 4618; (d) X. Shen, G. O. Jones, D. A. Watson, B. Bhayana, S. L. Buchwald, *J. Am. Chem. Soc.* **2010**, *132*, 11278.

260 (a) T. J. Geldbach, P. S. Pregosin, S. Rizzato, A. Albinati, *Inorg. Chim. Acta* **2006**, *359*, 962; (b) T. J. Geldbach, F. Breher, V. Gramlich, P. G. A. Kumar, P. S. Pregosin, *Inorg. Chem.* **2004**, *43*, 1920; (c) T. J. Geldbach, P. S. Pregosin, A. Albinati, *Organometallics*

2003, *22*, 1443; (d) T. J. Geldbach, D. Drago, P. S. Pregosin, *J. Organomet. Chem.* **2002**, *643-644*, 214; (e) T. J. Geldbach, P. S. Pregosin, A. Albinati, F. Rominger, *Organometallics* **2001**, *20*, 1932; (f) T. J. Geldbach, D. Drago, P. S. Pregosin, *Chem. Commun.* **2000**, 1629.

261 Selected examples of other phosphorus-alkene ligands on rhodium(I): (a) R. Shintani, R. Narui, Y. Tsutsumi, S. Hayashi, T. Hayashi, *Chem. Commun.* **2011**, *47*, 6123; (b) Z. Liu, H. Yamamichi, S. T. Madrahimov, J. F. Hartwig, *J. Am. Chem. Soc.* **2011**, *133*, 2772; (c) A. R. O'Connor, W. Kaminsky, D. M. Heinekey, K. I. Goldberg, *Organometallics* **2011**, *30*, 2105; (d) M. Montag, G. Leitus, L. J. W. Shimon, Y. Ben-David, D. Milstein, *Chem. Eur. J.* **2007**, *13*, 9043; (e) H. Werner, *Dalton Trans.* **2003**, 3829; (f) E. T. Singewald, C. A. Mirkin, A. D. Levy, C. L. Stern, *Angew. Chem. Int. Ed. Engl.* **1994**, *33*, 2473.

262 (a) M. Soleilhavoup, L. Viau, G. Commenges, C. Lepetit, R. Chauvin, *Eur. J. Inorg. Chem.* **2003**, 207; (b) E. F. Clarke, E. Rafter, H. Müller-Bunz, L. J. Higham, D. G. Gilheany, *J. Organomet. Chem.* **2011**, *696*, 3608.

263 (a) R. Shintani, M. Inoue, T. Hayashi, *Angew. Chem. Int. Ed*. **2006**, *45*, 3353; (b) T. Hayashi, M. Ishigedani, *Tetrahedron* **2001**, *57*, 2589; (c) T. Hayashi, M. Ishigedani, *J. Am. Chem. Soc.* **2000**, *122*, 976; (d) M. Sakai, M. Ueda, N. Miyaura, *Angew. Chem. Int. Ed.* **1998**, *37*, 3279.

264 (a) J. M. Ernsting, S. Gaemers, C. J. Elsevier, *Magn. Reson. Chem.* **2004**, *42*, 721; (b) L. Carlton, *Annu. Rep. NMR Spectrosc.* **2008**, *63*, 49.

265 L. Dahlenburg, A. Kaunert, *Eur. J. Inorg. Chem.* **1998**, 885.

266 W. A. Henderson Jr., S. A. Buckler, N. E. Day, M. Grayson, *J. Org. Chem.* **1961**, *26*, 4770.

267 H. Kischkel, G.-V. Röschenthaler, *Chem. Ber.* **1985**, *118*, 4842.

268 N. Weferling, *Z. Anorg. Allg. Chem.* **1987**, *548*, 55.

269 W. L. F. Armarego, C. L. L. Chai, in *Purification of Laboratory Chemicals, 5th Edition*, Elsevier Science, Burlington, **2003**, p. 163.

270 (a) W. McFarlane, D. S. Rycroft, *J. Chem. Soc., Dalton Trans.* **1973**, 2162; (b) W. McFarlane, D. S. Rycroft, *J. Chem. Soc., Chem. Commun.* **1972**, 902.

271 (a) T. Hayashi, H. Iwamura, M. Naito, Y. Matsumoto, Y. Uozumi, M Miki, K. Yanagi, *J. Am. Chem. Soc*. **1994**, *116*, 775; (b) P. G. A. Kumar, P. Dotta, R. Hermatschweiler, P. S. Pregosin, A. Albinati, S. Rizzato, *Organometallics* **2005**, *24*, 1306.

272 M. C. Bonnet, S. Agbossou, I. Tkatchenko, *Acta Cryst*. **1987**, *C43*, 445.

273 A. Grabulosa, G. Muller, J. I. Ordinas, A. Mezzetti, M. A. Maestro, M. Font-Bardia, X. Solans, *Organometallics* **2005**, *24*, 4961.

274 S. Filipuzzi, P. S. Pregosin, M. J. Calhorda, P. J. Costa, *Organometallics* **2008**, *27*, 2949, and references therein.

275 (a) C. Breutel, P. S. Pregosin, R. Salzmann, A. Togni, *J. Am. Chem. Soc.* **1994**, *116*, 4067; (b) U. J. Scheele, M. John, S. Dechert, F. Meyer, *Eur. J. Inorg. Chem.* **2008**, 373; (c) B. E. Ketz, A. P. Cole, R. M. Waymouth, *Organometallics* **2004**, *23*, 2835; (d) H. M. Peng, G. Song, Y. Li, X. Li, *Inorg. Chem*. **2008**, *47*, 8031.

276 (a) A. Guerrero, F. A. Jalon, B. R. Manzano, A. Rodriguez, R. M. Claramunt, P. Cornago, V. Milata, J. Elguero, *Eur. J. Inorg. Chem.* **2004**, 549; (b) A. Gogoll, H. Grennberg, A. Axén, *Organometallics* **1997**, *16*, 1167; (c) F. A. Jalón, B. R. Manzano, B. Moreno-Lara, *Eur. J. Inorg. Chem.* **2005**, 100; (d) V. Montoya, J. Pons, J. Garcia-Antón, X. Solans, M. Font-Bardía, J. Ros, *Organometallics* **2007**, *26*, 3183; (e) A. Ficks, C. Sibbald, M. John, S. Dechert, F. Meyer, *Organometallics* **2010**, *29*, 1117.

277 (a) P. Kočovský, Š. Vyskočil, I. Císařová, J. Sejbal, I. Tišlerová, M. Smrčina, G. C. Lloyd-Jones, S. C. Stephen, C. P. Butts, M. Murray, V. Langer, *J. Am. Chem. Soc*. **1999**, *121*, 7714; (b) P. Dotta, P. G. A. Kumar, P. S. Pregosin, A. Albinati, S. Rizzato, *Organometallics* **2004**, *23*, 4247; (c) P. Dotta, P. G. A. Kumar, P. S. Pregosin, A. Albinati, S. Rizzato, *Helv. Chim. Acta* **2004**, *87*, 272; (d) P. Dotta, P. G. A. Kumar, P. S. Pregosin, A. Albinati, S. Rizzato, *Organometallics* **2003**, *22*, 5345; (e) I. S. Mikhel, H. Rüegger, P. Butti, F. Camponovo, D. Huber, A. Mezzetti, *Organometallics* **2008**, *27*, 2937.

278 (a) P. S. Pregosin, *Chem. Commun.* **2008**, 4875; (b) P. S. Pregosin, *Coord. Chem. Rev*. **2008**, *252*, 2156.

279 G. Poli, G. Prestat, F. Liron, C. Kammerer-Pentier, *Top. Organomet. Chem.* **2012**, 38, 1.

280 (a) I. G. Rios, A. Rosas-Hernandez, E. Martin, *Molecules* **2011**, *16*, 970; (b) Z. Lu, S. Ma, *Angew. Chem. Int. Ed.* **2008**, *47*, 258.

281 Absolute stereochemical assignment according to literature data: H. Y. Cheung, W.-Y. Yu, T. T. L. Au-Yeung, Z. Zhou, A. S. C. Chan, *Adv. Synth. Catal.* **2009**, *351*, 1412.

282 (a) S. E. Gibson, M. Rudd, *Adv. Synth. Catal.* **2007**, *349*, 781; (b) L. Tietze, H. Ito, H. P. Bell, *Chem. Rev.* **2004**, *104*, 3453.

283 P. Dotta, P. G. A. Kumar, P. S. Pregosin, A. Albinati, S. Rizzato, *Organometallics* **2004**, *23*, 2295.

284 M. Ito, Y. Endo, N. Tejima, T. Ikariya, *Organometallics* **2010**, *29*, 2397.

285 H. L. Pedersen, M. Johannsen, *J. Org. Chem.* **2002**, *67*, 7982.

286 (a) J. Tiburcio, S. Bernès, H. Torrens, *Polyhedron* **2006**, *25*, 1549; (b) Q. L. Horn, D. S. Jones, R. N. Evans, C. A. Ogle, T. C. Masterman, *Acta. Cryst.* **2002**, *E58*, m51.

287 D. Selent, W. Baumann, R. Kempe, A. Spannenberg, D. Röttger, K.-D. Wiese, A. Börner, *Organometallics* **2003**, *22*, 4265.

288 K. J. Laidler, M. C. King, *J. Phys. Chem.* **1983**, *87*, 2657.

289 (a) G. Erre, S. Enthaler, K. Junge, S. Gladiali, M. Beller, *Coord. Chem. Rev.* **2008**, *252*, 471; (b) Y.-M. Li, F.-Y. Kwong, W.-Y. Yu, A. S. C. Chan, *Coord. Chem. Rev.* **2007**, *251*, 2119; (c) W. Zhang, Y. Chi, X. Zhang, *Acc. Chem. Res.* **2007**, *40*, 1278; (d) W. Tang, X. Zhang, *Chem. Rev.* **2003**, *103*, 3029.

290 S. Gladiali, F. Grepioni, S. Medici, A. Zucca, Z. Berente, L. Kollár, *Eur. J. Inorg. Chem.* **2003**, 556.

291 C. Claver, E. Fernandez, A. Gillon, K. Heslop, D. J. Hyett, A. Martorell, A. G. Orpen, P. G. Pringle, *Chem. Commun.* **2000**, 961.

292 A. Zanotti-Gerosa, C. Malan, D. Herzberg, *Org. Lett.* **2001**, *3*, 3687.

293 For a review on rhodium-catalysed asymmetric arylations see: P. Tian, H.-Q. Dong, G.-Q. Lin, *ACS Catal.* **2012**, *2*, 95.

294 M. Sakai, M. Ueda, N. Miyaura, *Angew. Chem. Int. Ed.* **1998**, *37*, 3279.

295 (a) S. Morikawa, K. Michigami, H. Amii, *Org. Lett.* **2010**, *12*, 2520; (b) H.-F. Duan, J.-H. Xie, W.-J. Shi, Q. Zhang, Q.-L. Zhou, *Org. Lett.* **2006**, *8*, 1479; (c) H.-F. Duan, J.-H. Xie, X.-C. Qiao, L. X. Wang, Q.-L. Zhou, *Angew. Chem. Int. Ed.* **2008**, *47*, 4351; (d) R. B. C. Jagt, P. Y. Toullec, J. G. de Vries, B. L. Feringa, A. J. Minnaard, *Org. Biomol. Chem.* **2006**, *4*, 773; (e) T. Nishimura, H. Kumamoto, M. Nagaosa, T. Hayashi, *Chem. Commun.* **2009**, 5713; (f) T. Noël, K. Vandyck, J. van der Eycken, *Tetrahedron* **2007**,

63, 12961; (g) W. Duan, Y. Ma, B. Qu, L. Zhao, J. Chen, C. Song, *Tetrahedron: Asymmetry* **2012**, *23*, 1369.

296 R. Shintani, M. Inoue, T. Hayashi, *Angew. Chem. Int. Ed.* **2006**, *45*, 3353.

297 For recent reviews see: (a) P. Belmont, E. Parker, *Eur. J. Org. Chem.* **2009**, 6075; (b) H. C. Shen, *Tetrahedron* **2008**, *64*, 7847; (c) J. Muzart, *Tetrahedron* **2008**, *64*, 5815; (d) E. Jiménez-Núñez, A. M. Echavarren, *Chem. Rev.* **2008**, *108*, 3326; (e) A. S. K. Hashmi, *Chem. Rev.* **2007**, *107*, 3180; (f) D. J. Gorin, F. D. Toste, *Nature* **2007**, *446*, 395; (g) A. S. K. Hashmi, G. J. Hutchings, *Angew. Chem. Int. Ed.* **2006**, *45*, 7896.

298 For recent reviews see: (a) A. Pradal, P. Y. Toullec, V. Michelet, *Synthesis* **2011**, *10*, 1501; (b) S. Sengupta, X. Shi, *ChemCatChem* **2010**, *2*, 609; (c) N. Bongers, N. Krause, *Angew. Chem. Int. Ed.* **2008**, *47*, 2178; (d) R. A. Widenhoefer, *Chem. Eur. J.* **2008**, *14*, 5382.

299 (a) M. Freytag, J. Grunenberg, P. G. Jones, R. Schmutzler, *Z. Anorg. Allg. Chem.* **2008**, *634*, 1256; (b) W. Xu, J. P. Rourke, J. J. Vittal, R. J. Puddephatt, *Inorg. Chem.* **1995**, *34*, 323.

300 J. W. Bats, M. Hamzic, A. S. K. Hashmi, *Acta Cryst.* **2007**, *E63*, m2344.

301 M. P. Muňoz, J. Adrio, J. C. Carretero, A. M. Echavarren, *Organometallics* **2005**, *24*, 1293.

302 M. Touil, B. Bechem, A. S. K. Hashmi, B. Engels, M. A. Omary, H. Rabaâ, *J. Mol. Struc. (Theochem)* **2010**, *957*, 21.

303 M. J. Johansson, D. J. Gorin, S. T. Staben, F. D. Toste, *J. Am. Chem. Soc.* **2005**, *127*, 18002.

304 For the mechanism of the reaction see also: P. Pérez-Galán, E. Herrero-Gómez, D. T. Hog, N. J. A. Martin, F. Maseras, A. M. Echavarren, *Chem. Sci.* **2011**, *2*, 141, and references therein.

305 R. Cramer, *Inorg. Synth.* **1990**, *28*, 86.

306 G. Giordano, R. H. Crabtree, *Inorg. Synth.* **1990**, *28*, 88.

307 J. L. Herde, J. C. Lambert, C. V. Senoff, *Inorg. Synth.* **1974**, *15*, 18.

308 T. G. Schenck, J. M. Downes, C. R. C. Milne, P. B. Mackenzie, H. Boucher, J. Whelan, B. Bosnich, *Inorg. Chem.* **1985**, *24*, 2334.

309 J. C. Cobas, M. Martín-Pastor, *EXSYCalc 1.0*; Mestrelab Research, Escondido, CA, 2007.

310 Absolute stereochemical assignment according to literature data: H.-F. Duan, J.-H. Xie, W.-J. Shi, Q. Zhang, Q.-L. Zhou, *Org. Lett.* **2006**, *8*, 1479.

311 J. W. Faller, P. P. Fontaine, *J. Organomet. Chem.* **2006**, *691*, 1912.

Chapter 6 — Phosphonodichalcogenoites and Phosphaalkenes

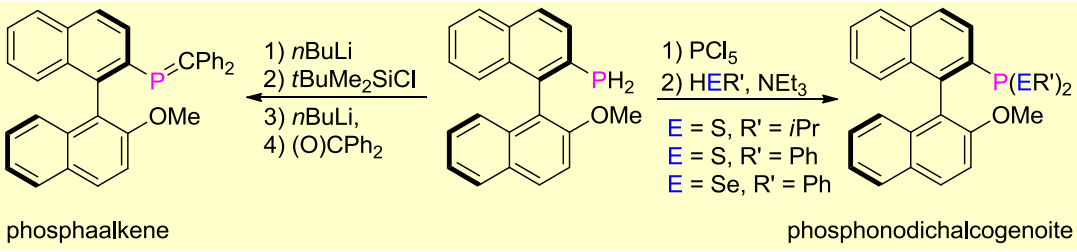

A series of chiral phosphonodichalcogenoite ligands and their corresponding gold(I) complexes were prepared and characterised by NMR and HRMS. Four representative X-ray crystal structures are reported. The ligands coordinate *via* their P-atom in a nearly linear fashion to the AuCl fragment. Furthermore, we synthesised a highly reactive MOP-phosphaalkene in a one-pot reaction sequence from the corresponding primary phosphine.

6.1 Introduction

Primary phosphines based on the MOP-type architecture have been developed in our labs.[312] They are stable towards air-oxidation and their synthesis from enantiopure BINOL in 4-5 steps has been optimised and was carried-out on a multigram scale (Chapter 2).[313] Subsequently we have successfully employed these compounds as chiral ligand precursors to access a variety of phosphorus functionalised ligands, e.g. phosphiranes (Chapter 3-4),[314] dimethylphosphines (Chapter 4), bis(dimethylamino)phosphines (Chapter 4) and phosphonites (Chapter 4-5).[315] While phosphorus-donor ligands carrying C, N, or O substituents are fairly common, organothio- and organoseleno-phosphorus compounds have rarely been studied, and only a small number of their transition metal complexes have been crystallographically analysed.[316] The coordination chemistry of trialkyltrithiophosphites has been summarised in the literature,[317] however their specific donor/acceptor properties in comparison to more typical ligand entities are largely unknown.[318] Hence, we were keen on using our primary phosphine precursors to prepare these more exotic ligands and subsequently study their metal coordination. Here we report the synthesis of phosphono-dithioite and phosphonodiselenoite ligands based on the MOP-scaffold and their coordination chemistry on gold(I). The compounds have been unambiguously characterised by NMR spectroscopy and in some cases by X-ray crystallography; for the selenium containing

compounds we report ^{77}Se NMR data which can give further insights into the coordination properties of those ligands.

Phosphaalkenes are low-coordinate compounds that possess a phosphorus-carbon double bond.[319] As expected for an element of the third period this double bond is normally very reactive and therefore usually requires steric stabilisation to be viable at ambient conditions. Chemical bonds of this type posess extremely low lying π* orbitals, and the strong π-acceptor property of the phosphorus lone-pair allows for the stabilisation of electron rich metal centres upon coordination. Consequently compounds of this type have been used as ligands in a number of catalytic processes.[319a,b,320] Furthermore, synthetic methodologies have been developed that enable P=C bonds to be polymerised leading to new phosphine-containing macromolecules that have applications in polymer-supported catalysis.[321] In the second part of this chapter we report the synthesis of an unusual MOP-phosphaalkene (Ar–P=CPh_2) which is highly reactive towards thermal decomposition.

6.2 Results and Discussion

6.2.1 Phosphonodichalcogenoites

We synthesised the novel phosphonite ligands **50a**,**b** as well as phosphonodithioites **51a**,**b** and **52a**,**b** and phosphonodiselenoite **53b** in a two-step, one-pot reaction procedure (Scheme 6.1) that we had used before to access various other MOP-type ligands. Primary phosphines **1a**,**b** were first treated with phosphorus pentachloride to generate the respective dichlorophosphines *in situ*. Further reactions were carried out in the same reaction vessel by adding the appropriate alcohol, thiol or selenol reagents. Conversions were usually quantitative so that the overall yields were only lowered during purification.

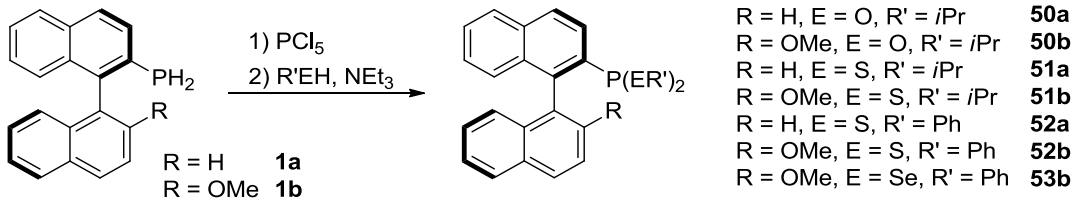

Scheme 6.1 Synthesis of phosphonodichalcogenoites from primary phosphines *via* dichlorophosphines.

Phosphonite ligands **50a**,**b** are moisture sensitive and therefore should be stored under an inert atmosphere. The ^{31}P NMR spectra show the expected resonances at 151.6 (**50a**) and 153.7 ppm (**50b**). Phosphonodithioites **51a**,**b** and **52a**,**b** are air-stable compounds as they

showed no sign of oxidation or hydrolysis even after prolonged exposure to air and moisture. Their resonances in the ^{31}P NMR spectra are shifted to higher field compared to **50a**,**b**. The aryl-dithioite signals were observed at 82.0 (**52a**) or 72.0 ppm (**52b**) while the alkyl-derivatives **51a**,**b** were found further upfield at 54.2 ppm in each case. For **51b** we were able to obtain crystals suitable for X-ray diffraction (Figure 6.1). The asymmetric unit contains two independent molecules with similar structural parameters; the positions of the isopropyl groups are slightly disordered. The P–S bond lengths compare well to those reported for other arylphosphonodithioites (2.101(2) to 2.122(1) Å).[322]

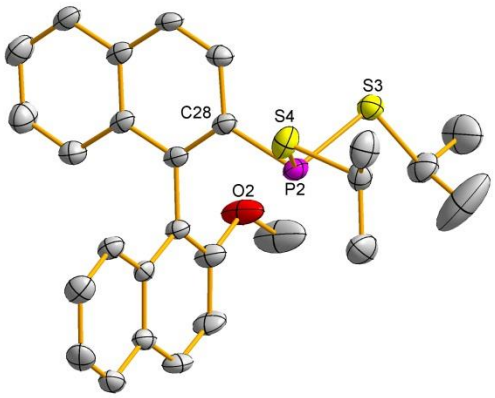

Figure 6.1 View of one of the two independent molecules of **51b** in the asymmetric unit with 50% probability displacement ellipsoids. Hydrogen atoms have been omitted for clarity. Selected bond distances [Å] and angles [°], respective bond lengths/angles of the second molecule in brackets: P2–S3 2.1169(8) (2.1125(9)), P2–S4 2.1192(8) (2.1176(8)), P2–C28 1.8232(19) (1.831(2)); S3-P2-S4 103.54(3) (103.44(4)), S3-P2-C28 99.78(6) (100.56(7)), S4-P2-C28 95.05(7) (94.75(7)).

Phosphonodiselenoite **53b** exhibits similar properties to **51a**,**b** and **52a**,**b**; it is stable towards air and moisture in the solid state, however it will decompose in solution within a number of days accompanied by formation of a dark grey residue. In the ^{31}P NMR spectrum the resonance of **53b** at 72.0 ppm is accompanied by satellite peaks caused by coupling to the ^{77}Se nucleus (Figure 6.2). The coupling of the two selenium atoms to the phosphorus is equivalent within measuring accuracy. The satellites appear as a doublet with a $^{1}J_{PSe}$ coupling constant at 224 Hz. Its magnitude compares well to the coupling constants found for Me_2PSeMe (205 Hz),[323] *t*BuP(2-SePy)$_2$ (228 Hz),[316d] and the ferrocene derivative $Fe(C_5H_4Se)_2PPh$ (247 Hz).[324] The chemical shifts of the two selenium atoms in the ^{77}Se NMR are inequivalent; the two resonances were observed as doublets at 361.2 and 348.8 ppm (Figure 6.2). From the satellite peaks in the selenium NMR spectra (due to their low intensity these are hardly recognisable in Figure 6.2) we were able to determine the reciprocal coupling of the two selenium atoms ($^{2}J_{Se,Se}$ = 71 Hz).

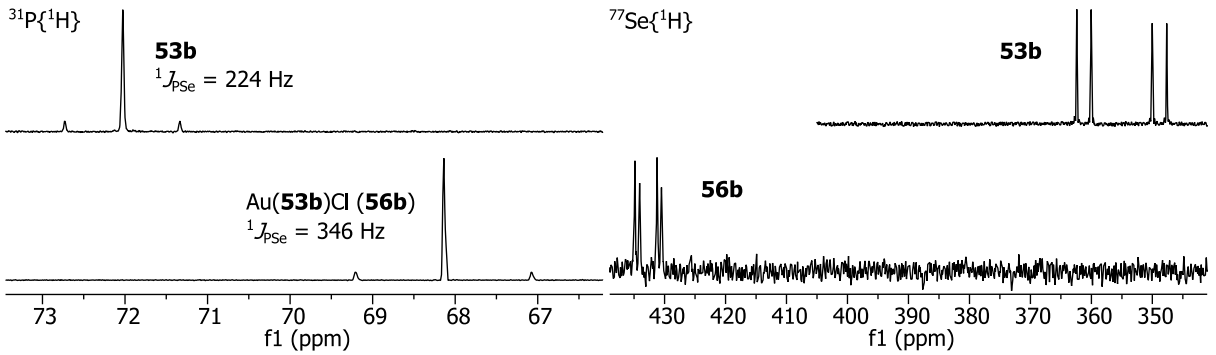

Figure 6.2 Left: $^{31}P\{^1H\}$ NMR (162 MHz) spectra of **53b** and Au(**53b**)Cl (**56b**). The satellite peaks are caused by coupling to the ^{77}Se nucleus. Right: $^{77}Se\{^1H\}$ NMR (95 MHz) spectra of **53b** and **56b**.

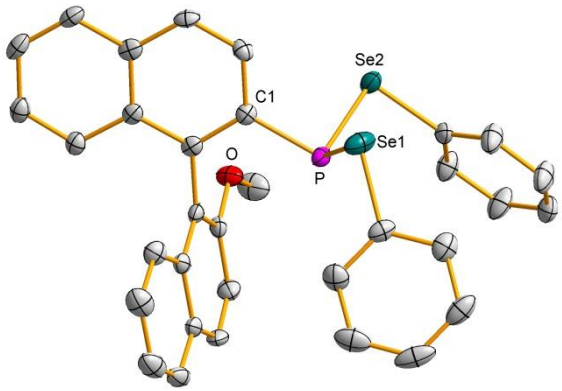

Figure 6.3 View of the molecular structure of **53b** with 50% probability displacement ellipsoids. Hydrogen atoms have been omitted for clarity. Selected bond distances [Å] and angles [°]: Se1–P 2.2785(9), Se2–P 2.2672(9), P–C1 1.826(3); Se1-P-Se2 105.05(4), Se1-P-C1 100.55(9), Se2-P-C1 95.50(10).

Crystals suitable for X-ray crystallographic analysis were obtained from slow evaporation of an ethyl acetate/hexane solution (Figure 6.3). As expected, the Se–P bond lengths at 2.2785(9) and 2.2672(9) Å in **53b** are significantly longer than the P–S bonds in **51b** (*vide supra*), but shorter than the Se–P bonds found in the carborane derivative **LVIII** (Figure 6.4) which is, to the best of our knowledge, the only other structurally characterised example of an $ArP(SeR)_2$ binding motif (2.3106(15) and 2.3061(16) Å).[325] The P–C1 distance and the intervalence angles around the phosphorus are comparable to those found for the dithioite derivative **51b**.

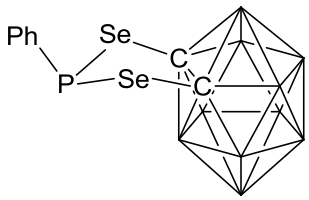

LVIII

Figure 6.4 Phosphonodiselenoite **LVIII** is a rare example of a structurally characterised $ArP(SeR)_2$ binding motif.

For testing the coordination behaviour of our phosphonodichalcogenoites **51b-53b** we synthesised their corresponding gold(I) complexes (Scheme 6.2). The quantitative formation of **54b-56b** was achieved by reacting the appropriate ligand with [AuCl(tht)] (tht = tetrahydrothiophene). The ^{31}P NMR spectral resonances of **54b** (78.8 ppm) and **55b** (101.3 ppm) are shifted to lower field while an upfield shift is observed for **56b** (68.1 ppm) compared to the free ligands respectively. Satellite peaks due to coupling of the phosphorus to selenium ($^{1}J_{PSe}$ = 346 Hz) were observed in the case of **56b**. The coupling constant increased by 120 Hz compared to the free ligand, indicating strengthened P–Se bonding in the gold complex (Figure 6.2). The ^{77}Se resonances were shifted to lower field compared to the free ligands, appearing at 433.0 ppm and 432.3 ppm.

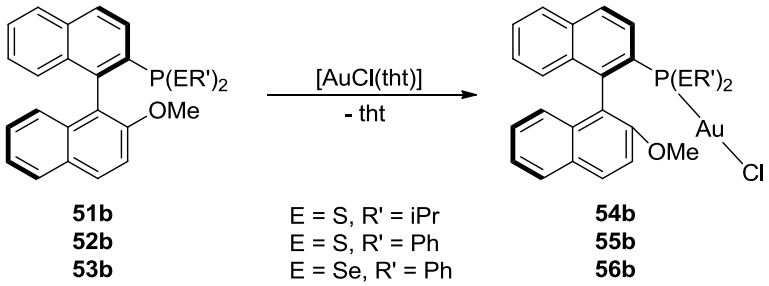

Scheme 6.2 Synthesis of the MOP-phosphonodichalcogenoite gold(I) complexes **54b**, **55b** and **56b**.

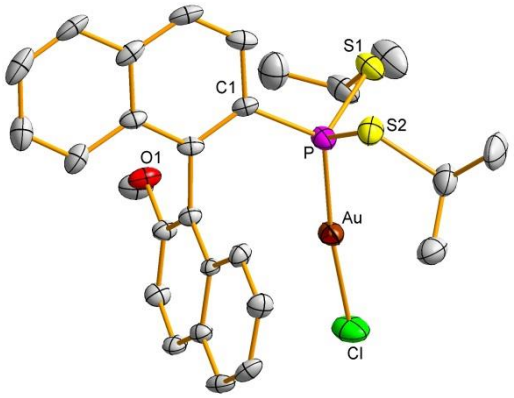

Figure 6.5 View of the molecular structure of [(**51b**)AuCl] (**54b**) with 50% probability displacement ellipsoids. Hydrogen atoms have been omitted for clarity. Selected bond distances [Å] and angles [°]: Au–P 2.2201(16), Au–Cl 2.2710(17), P–S1 2.091(2), P–S2 2.086(3), P–C1 1.825(6); Cl-Au-P 173.51(7), S1-P-S2 102.55(10), S1-P-C1 108.31(19), S2-P-C1 97.24(19).

We were able to obtain single crystals suitable for X-ray diffraction of **54b** (Figure 6.5) and **55b** (Figure 6.6) from slow evaporation of a dichloromethane solution. The asymmetric unit of **55b** contains three molecules which differ in the orientation of their phenyl groups. The P–S distances range from 2.086(3) to 2.108(3) with the slightly longer bonds being observed for **55b**. In comparison to the free ligand **51b**, the P–S bond lengths in **54b** are shortened by

about 0.03 Å and thus they follow the same trend as the phosphorus-selenium coupling constants suggested in ligand **53b** and gold(I) complex **56b**. The Au–P distance is longer in the isopropyl-derivative **54b** (2.2201(16) Å) compared to phenyl-derivative **55b** (2.206(2)-2.2138(18) Å). Structurally related compounds from the literature have Au–P bond lengths at 2.2184(16) Å ($(PhS)_3PAuCl$),[316c] 2.2352(8) Å ($(MeS)_3PAuCl$)[316c] and 2.237(2) Å (*t*BuP(2-SePy)$_2$AuCl).[316d]

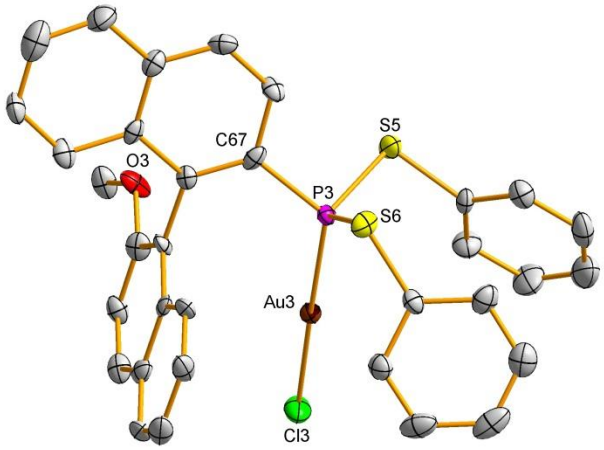

Figure 6.6 View of one of the two independent molecules of [(**52b**)AuCl] (**55b**) in the asymmetric unit with 50% probability displacement ellipsoids. Hydrogen atoms have been omitted for clarity. Selected bond distances [Å] and angles [°], respective bond lengths/angles of the second molecule in brackets: Au3–P3 2.2138(18) (2.206(2), 2.2116(18)), Au3–Cl3 2.2745(18) (2.273(3), 2.2703(18)), P3–S5 2.092(3) (2.096(3), 2.100(3)), P3–S6 2.104(3) (2.108(3), 2.106(3)), P3–C67 1.806(8) (1.810(8), 1.823(8)); P3-Au3-Cl3 175.71(8) (172.75(13), 178.09(7)), S5-P3-S6 109.24(11) (107.66(14), 100.34(11)), S5-P3-C67 100.0(3) (104.2(3), 100.2(3)), S6-P3-C67 97.0(3) (97.8(3), 105.7(3)).

6.2.2 Phosphaalkenes

For the synthesis of phosphaalkene **57b** we adapted a procedure that was first described by Yoshifuji and co-workers.[326] Primary phosphine **1b** was reacted with one equivalent of *n*-butyllithium, followed by the addition of *tert*-butyldimethylsilyl chloride to form the corresponding silyl substituted secondary phosphine. Further reaction in the same pot with *n*-butyllithium and benzophenone afforded the desired product **57b** in 77% yield after chromatographic purification (Scheme 6.3).

The formation of **57b** was clearly indicated by the characteristic carbon resonance at low field and its splitting due to coupling to the phosphorus nucleus (192.2 ppm, $^1J_{CP}$ = 43.5 Hz); the ^{31}P NMR showed a resonance at very low field (223.6 ppm). The compound was found to be very reactive and decomposed at room temperature within hours. Therefore we were unable to carry out coordination studies or indeed obtain a crystal structure. However, we have shown that the synthesis of the chiral phosphaalkene **57b** can be easily achieved and this result will

foster further studies in collaboration with Derek Gates, an expert in the field of low-valent phosphorus compounds and their polymerisation.[321]

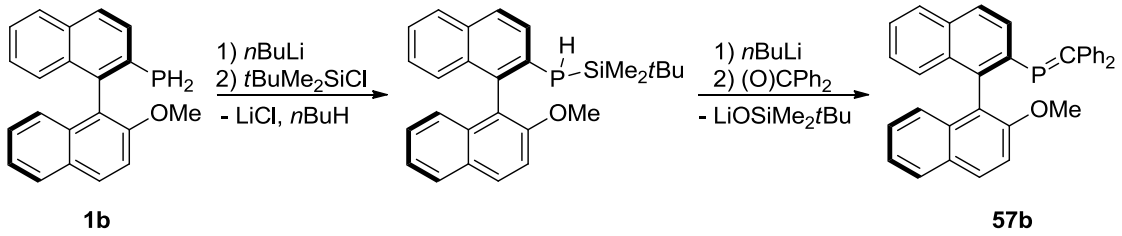

1b **57b**

Scheme 6.3 Synthetic route to phosphaalkene **57b**.

6.3 Conclusion

In summary we have synthesised novel MOP-type phosphonodichalcogenoites which are easily prepared in one-pot procedures from their parent primary phosphines. We have established that these ligands coordinate onto gold(I) and analysed two representative examples of phosphonodithioite complexes by X-ray crystallography. The coordination of the phosphonodiselenoite results in a larger ^{31}P-^{77}Se coupling and a downfield shift of the selenium resonances.

In the second part of this chapter we have shown the synthesis of a MOP-phosphaalkene which is highly reactive and decomposes under ambient conditions. Although we were unable to carry out any coordination studies, this compound might be a suitable substrate for the synthesis of chiral phosphorus functionalised polymers with possible applications in asymmetric catalysis.

6.4 Experimental Section

6.4.1 General Considerations

All air and/or water sensitive reactions were performed under a nitrogen atmosphere using standard Schlenk line techniques. THF (Na/benzophenone ketyl), toluene (Na) and CH_2Cl_2 (CaH) were dried and distilled prior to use. Flash chromatography was performed on silica gel from Fluorochem (silica gel, 40-63 μm, 60A, LC301). Thin-layer chromatography was performed on Merck aluminium-based plates with silica gel and fluorescent indicator 254 nm. ^{1}H, $^{13}C\{^{1}H\}$, $^{31}P\{^{1}H\}$ and $^{77}Se\{^{1}H\}$ NMR spectra were recorded on a JEOL Lambda 500 (^{1}H 500.16 MHz) or JEOL ECS-400 (^{1}H 399.78 MHz) spectrometer at room temperature (21°C) if not otherwise stated using the indicated solvent as internal reference. ^{77}Se chemical shifts

are given relative to Ξ(^{77}Se) = 19.071513 MHz. If necessary the assignment of signals was done by using two-dimensional NMR experiments (COSY, NOESY, HSQC, HMBC). Infrared spectra were recorded on a Varian 800 FT-IR spectrometer. Mass spectrometry was carried out by the EPSRC National Mass Spectrometry Service Centre, Swansea. The preparations of **1a**,**b** are described in the Experimental Section of Chapter 2 (**1a**,**b**). All other chemicals were used as purchased without further purification. Key crystallographic data are given in Table 6.1.

Table 6.1 Selected crystallographic data for compound **51b**, **53b**, **54b** and **55b**.

	51b	**53b**	**54b**	**55b**
formula	$C_{27}H_{29}OPS_2$	$C_{33}H_{25}OPSe_2$	$C_{27}H_{28}AuClOPS_2$	$C_{33}H_{25}AuClOPS_2$
formula wt	464.59	626.42	696.00	765.04
cryst syst	monoclinic	orthorhombic	orthorhombic	orthorhombic
space group	$P2_1$	$P2_12_12_1$	$P2_12_12_1$	$P2_12_12_1$
a, Å; α, deg	16.5205(9); 90	10.1464(4); 90	7.9141(15); 90	8.7934(3); 90
b, Å; β, deg	8.3250(3); 113.808(6)	11.5518(5); 90	18.420(4); 90	21.8830(4); 90
c, Å; γ, deg	19.7757(9); 60	23.3402(11); 90	18.715(4); 90	47.3991(9); 90
V, Å^3	2488.4(2)	2735.7(2)	2728.2(10)	9120.8(4)
Z	4	4	4	12
ρ_{calc}, g cm^{-3}	1.240	1.521	1.694	1.671
μ, mm^{-1}	0.295	2.787	5.250	5.142
F(000)	984	1256	1364	4488
T_{min}/T_{max}	0.95643/1.00000	0.4886/0.7680	0.6218/0.6218	0.2329/0.4262
hkl range	–20 to 21, –11 to 8, –26 to 27	–12 to 13, –15 to 10, –23 to 30	–8 to 10, –23 to 24, –24 to 25	–10 to 11, –28 to 29, –63 to 58
θ range, deg	3.2 to 29.6	2.8 to 28.6	1.5 to 27.4	3.0 to 28.6
no. of measd rflns	16333	10547	26174	55181
no. of unique rflns (R_{int})	9568 (0.0221)	5596 (0.0309)	6652 (0.0523)	19632 (0.0513)
no. of obsd rflns, $I > 2\sigma(I)$	7766	5015	6289	17911
refined params/restraints	622/537	335/0	299/0	1057/0
goodness of fit	0.961	1.035	1.012	1.103
Abs. structure param.	–0.02(4)	–0.004(7)	0.097(8)	0.014(5)
R1/wR2 ($I > 2\sigma(I)$)	0.0346/0.0826	0.0317/0.0616	0.0633/0.0880	0.0470/0.0917
R1/wR2 (all data)	0.0453/0.0855	0.0402/0.0657	0.0651/0.0891	0.0538/0.0939
resid electron dens, e Å^{-3}	0.38/–0.34	0.48/–0.54	2.54/–1.42	2.35/–2.77

6.4.2 (*S*)-Diisopropyl [1,1'-binaphthalen]-2-ylphosphonite (**50a**)

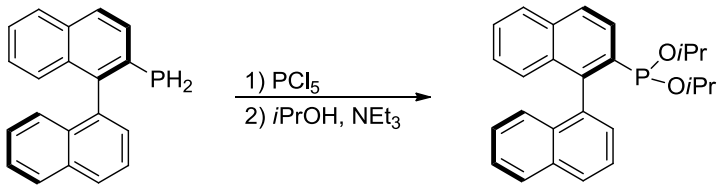

PCl_5 (458 mg, 2.20 mmol) was dissolved in toluene (8 mL). Primary phosphine **1a** (286 mg, 1.00 mmol) was added and the reaction mixture was left to stir for 45 minutes. The volatiles were removed *in vacuo* to give the corresponding dichlorophosphine ($^{31}P\{^1H\}$ NMR, $CDCl_3$: $\delta = 157.1$ ppm) as a yellow oil. CH_2Cl_2 (8 mL), NEt_3 (233 mg, 0.31 mL, 2.20 mmol) and isopropanol (132 mg, 0.17 mL, 2.20 mmol) were added subsequently and the solution was left to stir overnight. The volatiles were removed *in vacuo* and the crude product was dissolved in toluene. The title compound was obtained, after filtration and removal of the solvent, as a yellow oil (quantitative conversion).

^{1}H NMR (500 MHz, $CDCl_3$): $\delta = 8.13$ (dd, $^3J_{HH} = 8.5$ Hz, $^3J_{PH} = 2.7$ Hz, 1H, *H*3), 7.99 (d, $^3J_{HH} = 8.5$ Hz, 1H, *H*4), 7.97 (d, $^3J_{HH} = 8.3$ Hz, 1H, *H*4'), 7.93 (d, $^3J_{HH} = 8.3$ Hz, 1H, *H*5), 7.91 (d, $^3J_{HH} = 8.3$ Hz, 1H, *H*5'), 7.60 (dd, $^3J_{HH} = 8.3$ Hz, $^3J_{HH} = 6.9$ Hz, 1H, *H*3'), 7.51 (d, $^3J_{HH} = 6.9$ Hz, 1H, *H*2'), 7.48-7.43 (m, 2H, *H*6'+*H*6), 7.23 (m, 3H, 3 Ar*H*), 7.18 (d, $^3J_{HH} = 8.3$ Hz, 1H, Ar*H*), 4.12 (m, 1H, *i*Pr-C*H*), 3.77 (m, 1H, *i*Pr'-C*H*), 1.20 (d, $^3J_{HH} = 6.3$ Hz, 3H, *i*Pr-CH_3), 1.91 (d, $^3J_{HH} = 6.3$ Hz, 3H, *i*Pr-CH_3), 1.08 (d, $^3J_{HH} = 6.2$ Hz, 3H, *i*Pr'-CH_3), 0.69 (d, $^3J_{HH} = 6.2$ Hz, 3H, *i*Pr'-CH_3) ppm. **^{13}C{^{1}H} NMR** (126 MHz, $CDCl_3$): $\delta = 141.9$, 141.6, 140.1, 136.3, 134.2, 133.8, 133.4, 133.0, 129.3 (*C*2'), 128.3 (*C*4'), 128.2 (*C*5), 128.0 (*C*5'), 127.7 (*C*4), 127.1, 126.9, 126.7 (*C*6'), 126.1, 125.9 (*C*6), 125.6 (d, $^3J_{CP} = 4.3$ Hz, *C*1'), 125.0 (*C*3'), 71.2 (d, $^2J_{CP} = 21.1$ Hz, *i*Pr'-*C*H), 71.0 (d, $^2J_{CP} = 18.0$ Hz, *i*Pr-*C*H), 24.8 (d, $^3J_{CP} = 4.8$ Hz, *i*Pr-*C*H_3), 24.6 (d, $^3J_{CP} = 3.4$ Hz, *i*Pr-*C*H_3), 24.5 (d, $^3J_{CP} = 4.3$ Hz, *i*Pr'-*C*H_3), 24.0 (d, $^3J_{CP} = 5.3$ Hz, *i*Pr'-*C*H_3) ppm. **^{31}P{^{1}H} NMR** (202 MHz, $CDCl_3$): $\delta = 151.6$ ppm. **IR** (neat): $\nu = 3055.4$ (w), 2971.4 (w), 2873.7 (w), 1590.9 (w), 1505.6 (w), 1451.4 (w), 1368.5 (m), 1229.0 (m), 1166.4 (w), 1113.2 (m), 1014.8 (w), 970.0 (s), 943.2 (s), 858.9 (s), 820.9 (w), 801.9 (w), 781.7 (m), 746.4 (s), 688.5 (m), 631.5 (w) cm^{-1}. **OR** ($CHCl_3$, $c = 1.0$ mg/ml): $[\alpha]_D^{20} = -40°$.

6.4.3 (*R*)-Diisopropyl (2'-Methoxy-[1,1'-binaphthalen]-2-yl)phosphonite (**50b**)

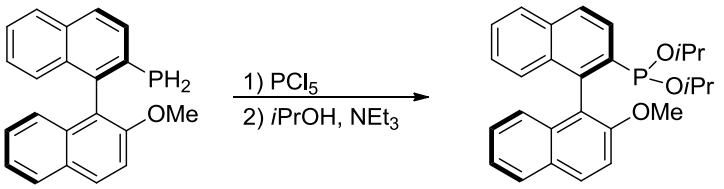

PCl_5 (458 mg, 2.20 mmol) was dissolved in toluene (8 mL). **1b** (316 mg, 1.00 mmol) was added and the reaction mixture was left to stir for 45 minutes. The volatiles were removed *in vacuo* to give the corresponding dichlorophosphine ($^{31}P\{^1H\}$ NMR, $CDCl_3$: δ = 159.1 ppm) as yellow solid. CH_2Cl_2 (8 mL), NEt_3 (233 mg, 0.31 mL, 2.20 mmol) and isopropanol (132 mg, 0.17 mL, 2.20 mmol) were added subsequently, and the solution was left to stir overnight. The volatiles were removed *in vacuo* and the crude product was dissolved in toluene. The title product was obtained, after filtration and removal of the solvent, as a white solid (191 mg, 0.44 mmol, 44%).

MP (uncorrected): 96 °C. **^{1}H NMR** (500 MHz, $CDCl_3$): δ = 8.19 (dd, $^3J_{HH}$ = 8.3 Hz, $^3J_{PH}$ = 2.8 Hz, 1H, *H*3), 8.04 (d, $^3J_{HH}$ = 9.2 Hz, 1H, *H*4'), 8.03 (d, $^3J_{HH}$ = 8.3 Hz, 1H, *H*4), 7.94 (d, $^3J_{HH}$ = 8.3 Hz, 1H, *H*5), 7.88 (d, $^3J_{HH}$ = 8.3 Hz, 1H, *H*5'), 7.48 (ddd, $^3J_{HH}$ = 8.3 Hz, $^3J_{HH}$ = 5.5 Hz, $^4J_{HH}$ = 2.7 Hz, 1H, *H*6), 7.46 (d, $^3J_{HH}$ = 9.2 Hz, 1H, *H*3'), 7.32 (ddd, $^3J_{HH}$ = 8.3 Hz, $^3J_{HH}$ = 6.7 Hz, $^4J_{HH}$ = 1.2 Hz, 1H, *H*6'), 7.28-7.25 (m, 2H, *H*7+*H*8), 7.21 (ddd, $^3J_{HH}$ = 8.3 Hz, $^3J_{HH}$ = 6.7 Hz, $^4J_{HH}$ = 1.2 Hz, 1H, *H*7'), 7.05 (d, $^3J_{HH}$ = 8.3 Hz, 1H, *H*8'), 4.19 (m, 1H, *i*Pr-C*H*), 3.80 (s, 3H, OCH_3), 3.74 (m, 1H, *i*Pr'-C*H*), 1.29 (d, $^3J_{HH}$ = 6.0 Hz, 3H, *i*Pr-CH_3), 1.21 (d, $^3J_{HH}$ = 6.0 Hz, 3H, *i*Pr-CH_3), 1.06 (d, $^3J_{HH}$ = 6.0 Hz, 3H, *i*Pr'-CH_3), 0.64 (d, $^3J_{HH}$ = 6.0 Hz, 3H, *i*Pr'-CH_3) ppm. **^{13}C{^{1}H} NMR** (126 MHz, $CDCl_3$): δ = 155.0 (*C*2'), 140.6 (d, $^2J_{CP}$ = 14.3 Hz, *C*1), 138.4 (d, $^1J_{CP}$ = 36.3 Hz, *C*2), 134.9, 134.6, 132.8, 130.0 (*C*4'), 129.2, 128.9, 128.4, 128.2 (*C*5), 127.8 (*C*5'), 127.7 (*C*4), 126.5, 126.4, 126.1 (*C*8'), 125.9 (d, $^2J_{CP}$ = 3.5 Hz, *C*3), 123.6 (*C*6'), 121.0 (d, $^3J_{CP}$ = 8.4 Hz, *C*1'), 113.3 (*C*3'), 71.0 (d, $^2J_{CP}$ = 19.0 Hz, *i*Pr'-*C*H), 70.9 (d, $^2J_{CP}$ = 20.8 Hz, *i*Pr-*C*H), 56.4 (s, O*C*H_3), 24.8 (d, $^3J_{CP}$ = 4.7 Hz, *i*Pr-*C*H_3), 24.7 (d, $^3J_{CP}$ = 4.3 Hz, *i*Pr-*C*H_3), 24.5 (d, $^3J_{CP}$ = 4.3 Hz, *i*Pr'-*C*H_3), 23.9 (d, $^3J_{CP}$ = 5.3 Hz, *i*Pr'-*C*H_3) ppm. **^{31}P{^{1}H} NMR** (202 MHz, $CDCl_3$): δ = 153.7 ppm. **IR** (neat): ν = 3055.4 (w), 2969.8 (w), 1621.4 (w), 1592.8 (m), 1509.0 (m), 1462.4 (w), 1370.4 (w), 1270.3 (m), 1250.1 (m), 1221.9 (w), 1115.9 (w), 1080.6 (m), 1052.8 (w), 1019.0 (w), 971.9 (s), 945.0 (s), 859.1 (m), 808.0 (s), 747.8 (s), 688.5 (w), 633.1 (w) cm^{-1}. **HRMS** (NSI$^+$, MeCN): Found: *m*/*z* = 433.1929. Calculated for [M + H]$^+$: *m*/*z* = 433.1927. **OR** ($CHCl_3$, *c* = 1.0 mg/ml): $[\alpha]_D^{20}$ = –20°.

6.4.4 (*S*)-Diisopropyl [1,1'-binaphthalen]-2-yl)phosphonodithioite (**51a**)

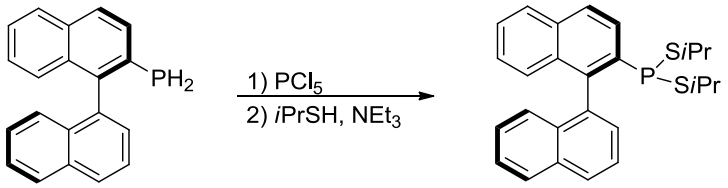

PCl_5 (458 mg, 2.20 mmol) was dissolved in toluene (8 mL). Primary phosphine **1a** (286 mg, 1.00 mmol) was added and the reaction mixture was left to stir for 45 minutes. The volatiles were removed *in vacuo* to give the corresponding dichlorophosphine ($^{31}P\{^1H\}$ NMR, $CDCl_3$: $\delta = 157.1$ ppm) as a yellow oil. CH_2Cl_2 (8 mL), NEt_3 (233 mg, 0.31 mL, 2.20 mmol) and 2-propanethiol (168 mg, 0.20 mL, 2.20 mmol) were added subsequently and the solution was left to stir overnight. The volatiles were removed *in vacuo* and the crude product was dissolved in toluene. The title product was obtained, after filtration and removal of the solvent, as a yellow oil (quantitative conversion).

^{1}H NMR (400 MHz, $CDCl_3$): $\delta = 8.14$ (d, $^3J_{HH} = 8.5$ Hz, 1H, *H*3), 7.99 (d, $^3J_{HH} = 8.5$ Hz, 1H, *H*4'), 7.98 (d, $^3J_{HH} = 8.5$ Hz, 1H, *H*4), 7.95 (d, $^3J_{HH} = 8.5$ Hz, 1H, *H*5), 7.90 (d, $^3J_{HH} = 8.5$ Hz, 1H, *H*5'), 7.59 (dd, $^3J_{HH} = 8.5$ Hz, $^3J_{HH} = 6.9$ Hz, 1H, *H*3'), 7.50 (d, $^3J_{HH} = 6.9$ Hz, 1H, *H*2'), 7.48 (m, 1H, *H*6'), 7.45 (m, 1H, *H*6), 7.24 (m, 3H, 3 Ar*H*), 7.18 (m, 1H, Ar*H*), 2.96 (dsept, $^3J_{HH} = 6.9$ Hz, $^3J_{PH} = 6.9$ Hz, 1H, *i*Pr-C*H*), 2.64 (dsept, $^3J_{HH} = 6.9$ Hz, $^3J_{PH} = 6.9$ Hz, 1H, *i*Pr'-C*H*), 1.25 (d, $^3J_{HH} = 6.8$ Hz, 3H, *i*Pr-CH_3), 1.23 (d, $^3J_{HH} = 6.8$ Hz, 3H, *i*Pr-CH_3), 1.06 (d, $^3J_{HH} = 6.8$ Hz, 3H, *i*Pr'-CH_3), 0.88 (d, $^3J_{HH} = 6.8$ Hz, 3H, *i*Pr'-CH_3) ppm. **^{13}C{^{1}H} NMR** (101 MHz, $CDCl_3$): $\delta = 140.7$ (d, $^1J_{CP} = 38.9$ Hz, *C*2), 137.0 (d, $^2J_{CP} = 22.8$ Hz, *C*1), 136.8 (d, $^3J_{CP} = 10.0$ Hz, *C*1'), 134.0, 133.5, 133.1 (d, $J_{CP} = 2.6$ Hz), 132.8 (d, $J_{CP} = 6.6$ Hz), 129.2, 129.1 (*C*3), 128.9 (d, $J_{CP} = 4.9$ Hz), 128.7 (*C*2'), 128.5, 128.2, 128.0 (*C*5'), 127.4 (d, $J_{CP} = 3.0$ Hz), 126.9 (d, $J_{CP} = 5.5$ Hz), 126.6, 126.2, 126.0, 125.1 (*C*3'), 38.4 (d, $^2J_{CP} = 22.7$ Hz, *i*Pr'-*C*H), 38.3 (d, $^2J_{CP} = 20.6$ Hz, *i*Pr-*C*H), 25.6 (d, $^3J_{CP} = 6.3$ Hz, *i*Pr-*C*H_3), 25.2 (d, $^3J_{CP} = 6.4$ Hz, *i*Pr-*C*H_3), 25.2 (d, $^3J_{CP} = 4.6$ Hz, *i*Pr'-*C*H_3), 25.1 (d, $^3J_{CP} = 5.7$ Hz, *i*Pr'-*C*H_3) ppm. **^{31}P{^{1}H} NMR** (162 MHz, $CDCl_3$): $\delta = 54.2$ ppm. **IR** (neat): $\nu = 3044.3$ (w), 2956.3 (m), 2921.4 (w), 2860.3 (w), 1500.2 (w), 1446.9 (m), 1363.9 (m), 1314.5 (w), 1237.4 (m), 1152.9 (m), 1050.7 (w), 1014.8 (w), 867.9 (w), 801.5 (s), 780.2 (s), 745.6 (s), 686.7 (w), 628.7 (m), 605.3 (w) cm^{-1}. **HRMS** (EI^+): Found: $m/z = 434.1289$. Calculated for $[M]^+$: $m/z = 434.1286$. **OR** ($CHCl_3$, $c = 1.0$ mg/ml): $[\alpha]_D^{20} = +148°$.

6.4.5 (*R*)-Diisopropyl (2'-Methoxy-[1,1'-binaphthalen]-2-yl)phosphonodithioite (**51b**)

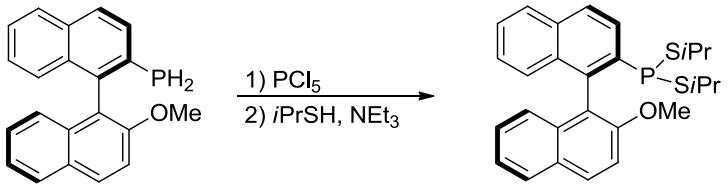

PCl_5 (458 mg, 2.20 mmol) was dissolved in toluene (8 mL). Primary phosphine **1b** (316 mg, 1.00 mmol) was added and the reaction mixture was left to stir for 45 minutes. The volatiles were removed *in vacuo* to give the corresponding dichlorophosphine ($^{31}P\{^1H\}$ NMR, $CDCl_3$: δ = 159.1 ppm) as yellow solid. CH_2Cl_2 (8 mL), NEt_3 (233 mg, 0.31 mL, 2.20 mmol) and 2-propanethiol (168 mg, 0.20 mL, 2.20 mmol) were added subsequently and the solution was left to stir overnight. The volatiles were removed *in vacuo* and the crude product was dissolved in toluene. The title product was obtained, after filtration and removal of the solvent, as a white solid (435 mg, 0.93 mmol, 93%).

MP (uncorrected): 155 °C. **^{1}H NMR** (500 MHz, $CDCl_3$): δ = 8.17 (dd, $^3J_{HH}$ = 8.5 Hz, $^3J_{PH}$ = 1.8 Hz, 1H, *H*3), 8.02 (d, $^3J_{HH}$ = 9.1 Hz, 1H, *H*4'), 7.98 (d, $^3J_{HH}$ = 8.5 Hz, 1H, *H*4), 7.89 (d, $^3J_{HH}$ = 8.2 Hz, 1H, *H*5), 7.86 (d, $^3J_{HH}$ = 8.2 Hz, 1H, *H*5'), 7.46 (ddd, $^3J_{HH}$ = 8.2 Hz, $^3J_{HH}$ = 6.4 Hz, $^4J_{HH}$ = 1.6 Hz, 1H, *H*6), 7.43 (d, $^3J_{HH}$ = 9.1 Hz, 1H, *H*3'), 7.29 (ddd, $^3J_{HH}$ = 8.2 Hz, $^3J_{HH}$ = 6.7 Hz, $^4J_{HH}$ = 1.2 Hz, 1H, *H*6'), 7.23 (m, 2H, *H*7+*H*8), 7.18 (ddd, $^3J_{HH}$ = 8.3 Hz, $^3J_{HH}$ = 6.7 Hz, $^4J_{HH}$ = 1.3 Hz, 1H, *H*7'), 6.97 (d, $^3J_{HH}$ = 8.3 Hz, 1H, *H*8'), 3.78 (s, 3H, OCH_3), 2.98 (dsept, $^3J_{HH}$ = 6.7 Hz, $^3J_{PH}$ = 6.7 Hz, 1H, *i*Pr-C*H*), 2.47 (dsept, $^3J_{HH}$ = 6.7 Hz, $^3J_{PH}$ = 6.7 Hz, 1H, *i*Pr'-C*H*), 1.28 (d, $^3J_{HH}$ = 6.7 Hz, 3H, *i*Pr-CH_3), 1.22 (d, $^3J_{HH}$ = 6.7 Hz, 3H, *i*Pr-CH_3), 0.96 (d, $^3J_{HH}$ = 6.7 Hz, 3H, *i*Pr'-CH_3), 0.73 (d, $^3J_{HH}$ = 6.7 Hz, 3H, *i*Pr'-CH_3) ppm. **^{13}C{^{1}H} NMR** (126 MHz, $CDCl_3$): δ = 154.7 (d, $^4J_{CP}$ = 2.5 Hz, *C*2'), 137.5 (d, $^1J_{CP}$ = 39.9.5 Hz, *C*2), 137.2 (d, $^2J_{CP}$ = 22.6 Hz, *C*1), 134.2, 134.2, 132.6, 130.2 (*C*4'), 129.1 (*C*3), 128.9, 128.5 (*C*4), 128.2 (*C*5), 127.8 (*C*5'), 126.8 (*C*6), 126.5 (*C*7+*C*8), 126.1 (*C*7'), 123.6 (*C*6'), 121.0 (d, $^3J_{CP}$ = 9.9 Hz, *C*1'), 112.9 (*C*3'), 56.2 (s, OCH_3), 38.3 (d, $^2J_{CP}$ = 22.1 Hz, *i*Pr'-*C*H), 38.2 (d, $^2J_{CP}$ = 21.0 Hz, *i*Pr-*C*H), 25.6 (d, $^3J_{CP}$ = 6.6 Hz, *i*Pr-*C*H_3), 25.2 (d, $^3J_{CP}$ = 5.5 Hz, *i*Pr-*C*H_3), 24.9 (d, $^3J_{CP}$ = 5.5 Hz, *i*Pr'-*C*H_3), 24.8 (d, $^3J_{CP}$ = 6.6 Hz, *i*Pr'-*C*H_3) ppm. **^{31}P{^{1}H} NMR** (202 MHz, $CDCl_3$): δ = 54.2 ppm. **IR** (neat): ν = 2961.4 (w), 2925.4 (w), 1622.0 (w), 1593.9 (m), 1508.1 (m), 1458.0 (m), 1334.7 (w), 1270.3 (s), 1251.8 (s), 1150.5 (m), 1080.9 (m), 1051.1 (m), 1020.0 (w), 871.2 (w), 806.4 (s), 751.7 (s), 686.0 (m), 627.0 (m) cm^{-1}. **HRMS** (NSI^+, MeCN): Found: *m*/*z* = 465.1469. Calculated for $[M + H]^+$: *m*/*z* = 465.1470. **OR** ($CHCl_3$, *c* = 1.0 mg/ml): $[\alpha]_D^{20}$ = +20°.

6.4.6 (*S*)-Diphenyl [1,1'-binaphthalen]-2-yl)phosphonodithioite (**52a**)

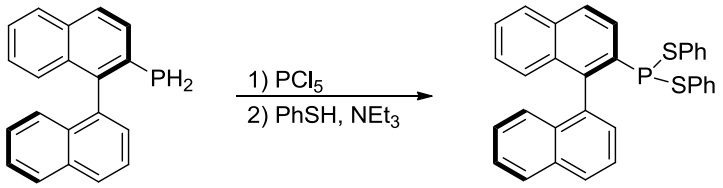

PCl_5 (458 mg, 2.20 mmol) was dissolved in toluene (8 mL). Primary phosphine **1a** (286 mg, 1.00 mmol) was added and the reaction mixture was left to stir for 45 minutes. The volatiles were removed *in vacuo* to give the corresponding dichlorophosphine ($^{31}P\{^1H\}$ NMR, $CDCl_3$: δ = 157.1 ppm) as a yellow oil. CH_2Cl_2 (8 mL), NEt_3 (233 mg, 0.31 mL, 2.20 mmol) and thiophenol (231 mg, 0.21 mL, 2.10 mmol) were added subsequently and the solution was left to stir overnight. The volatiles were removed *in vacuo* and the crude product was dissolved in toluene. The title product was obtained, after filtration and removal of the solvent, as a yellow oil (quantitative conversion).

MP (uncorrected): 115 °C. **^{1}H NMR** (500 MHz, CD_2Cl_2): δ = 8.18 (dd, $^3J_{HH}$ = 8.5 Hz, $^3J_{HP}$ = 1.1 Hz, 1H, *H*3), 8.08 (d, $^3J_{HH}$ = 8.5 Hz, 1H, *H*4), 8.00-7.97 (m, 2H, *H*5+*H*4'), 7.95 (d, $^3J_{HH}$ = 8.2 Hz, 1H, *H*5'), 7.57-7.50 (m, 3H, *H*3'+*H*6+Ph*H*), 7.47 (ddd, $^3J_{HH}$ = 8.2 Hz, $^3J_{HH}$ = 6.6 Hz, $^4J_{HH}$ = 1.1 Hz, 1H, *H*6'), 7.43 (dd, $^3J_{HH}$ = 7.0 Hz, $^4J_{HH}$ = 1.2 Hz, 1H, *H*2'), 7.33-7.28 (m, 2H, *H*7+Ph*H*), 7.27-7.13 (m, 6H, 3 Ph*H*+*H*7'+*H*8+*H*8'), 7.08 (m, 1H, Ph*H*), 6.98 (m, 2H, 2 Ph*H*), 6.93 (d, $^3J_{HH}$ = 8.2 Hz, 2H, 2 Ph*H*) ppm. **^{13}C{^{1}H} NMR** (126 MHz, CD_2Cl_2): δ = 142.3 (d, $^1J_{CP}$ = 38.9 Hz, *C*2), 136.0 (d, $^3J_{CP}$ = 10.5 Hz, *C*1'), 135.0 (d, $^2J_{CP}$ = 28.7 Hz, *C*1), 134.4, 133.5, 133.4 (d, J_{CP} = 5.8 Hz, Ph*C*), 133.3 (d, J_{CP} = 5.6 Hz, Ph*C*), 133.1 (d, J_{CP} = 5.6 Hz), 133.0 (d, J_{CP} = 2.8 Hz), 132.9 (d, J_{CP} = 6.3 Hz), 129.2 (*C*2'), 129.1 (d, J_{CP} = 4.3 Hz), 129.0 (Ph*C*), 128.8 (*C*4'), 128.8 (*C*4), 128.7 (Ph*C*), 128.4 (*C*3), 128.3 (*C*5'), 128.1 (*C*5), 127.7 (d, J_{CP} = 2.0 Hz), 127.6, 127.5 (d, J_{CP} = 2.0 Hz), 127.4 (*C*6), 127.3, 127.2 (d, J_{CP} = 3.4 Hz), 126.8 (*C*7), 126.5, 126.3, 126.1 (*C*6'), 125.1 (*C*3') ppm. **^{31}P{^{1}H} NMR** (162 MHz, CD_2Cl_2): δ = 82.0 ppm. **IR** (neat): ν = 3054.0 (w), 1580.0 (w), 1499.9 (w), 1474.4 (m), 1438.3 (m), 1365.0 (w), 1318.5 (w), 1163.6 (w), 1118.4 (w), 1021.8 (m), 901.5 (w), 869.2 (w), 810.0 (m), 781.0 (m), 738.2 (s), 683.8 (s), 628.9 (m), 605.3 (w) cm^{-1}. **HRMS** (NSI$^+$, MeOH): Found: *m*/*z* = 503.1052. Calculated for $[M + H]^+$: *m*/*z* = 503.1052. **OR** ($CHCl_3$, *c* = 1.0 mg/ml): $[\alpha]_D^{20}$ = +236°.

6.4.7 (*R*)-Diphenyl (2'-Methoxy-[1,1'-binaphthalen]-2-yl)phosphonodithioite (**52b**)

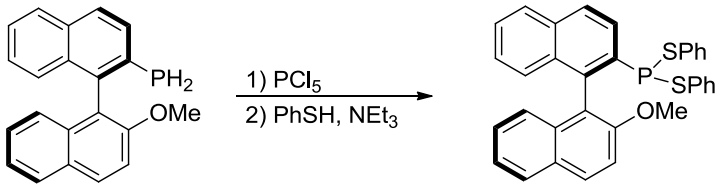

PCl_5 (458 mg, 2.20 mmol) was dissolved in toluene (8 mL). Primary phosphine **1b** (316 mg, 1.00 mmol) was added and the reaction mixture was left to stir for 45 minutes. The volatiles were removed *in vacuo* to give the corresponding dichlorophosphine ($^{31}P\{^1H\}$ NMR, $CDCl_3$: δ = 159.1 ppm) as a yellow solid. CH_2Cl_2 (8 mL), NEt_3 (233 mg, 0.31 mL, 2.20 mmol) and thiophenol (231 mg, 0.21 mL, 2.10 mmol) were added subsequently and the solution was left to stir overnight. The volatiles were removed *in vacuo* and the crude product was filtered through a plug of silica media in toluene. The title product was obtained, after filtration and removal of the solvent, as a pale yellow solid (527 mg, 0.93 mmol, 99%).

MP (uncorrected): 162 °C. **^{1}H NMR** (500 MHz, CD_2Cl_2): δ = 8.16 (d, $^3J_{HH}$ = 8.3 Hz, $^3J_{HP}$ = 1.3 Hz, 1H, *H*3), 8.06 (d, $^3J_{HH}$ = 8.3 Hz, 1H, *H*4), 8.04 (d, $^3J_{HH}$ = 9.2 Hz, 1H, *H*4'), 7.98 (d, $^3J_{HH}$ = 8.3 Hz, 1H, *H*5), 7.89 (d, $^3J_{HH}$ = 8.3 Hz, 1H, *H*5'), 7.55 (ddd, $^3J_{HH}$ = 8.3 Hz, $^3J_{HH}$ = 6.7 Hz, $^4J_{HH}$ = 1.3 Hz, 1H, *H*6), 7.53-7.50 (m, 1H, Ph*H*), 7.41 (d, $^3J_{HH}$ = 9.2 Hz, 1H, *H*3'), 7.34-7.13 (m, 8H, 4 Ph*H*+*H*6'+*H*7+*H*7'+*H*8), 7.10-7.06 (m, 1H, Ph*H*), 6.98-6.94 (m, 3H, 2 Ph*H*+*H*8'), 6.81 (d, $^3J_{HH}$ = 8.5 Hz, 2H, 2 Ph*H*), 3.67 (s, 3H, OCH_3) ppm. **^{13}C{^{1}H} NMR** (126 MHz, CD_2Cl_2): δ = 154.7 (d, $^4J_{CP}$ = 2.9 Hz, *C*2'), 138.9 (d, $^1J_{CP}$ = 38.5 Hz, *C*2), 135.2 (d, $^2J_{CP}$ = 28.9 Hz, *C*1), 134.5, 134.0 (d, J_{CP} = 2.7 Hz), 133.8 (d, J_{CP} = 13.8 Hz), 133.5 (d, J_{CP} = 14.5 Hz), 133.3 (d, J_{CP} = 5.5 Hz, Ph*C*), 132.7 (d, J_{CP} = 6.3 Hz, Ph*C*), 130.6 (*C*4'), 129.2, 128.9, 128.7, 128.6 (*C*4), 128.5 (*C*3), 128.3 (*C*5), 128.0 (*C*5'), 127.6, 127.5, 127.4 (*C*6), 127.3, 126.8, 126.7, 125.4 (*C*8'), 123.6 (*C*6'), 120.0 (d, $^3J_{CP}$ = 10.3 Hz, *C*1'), 112.9 (*C*3'), 56.1 (O*C*H$_3$) ppm. **^{31}P{^{1}H} NMR** (202 MHz, CD_2Cl_2): δ = 82.8 ppm. **IR** (neat): ν = 3054.6 (w), 1618.8 (w), 1576.3 (w), 1510.0 (w), 1471.4 (m), 1437.9 (m), 1333.6 (w), 1269.5 (m), 1251.1 (w), 1148.8 (w), 1079.0 (m), 1051.3 (w), 1020.7 (w), 905.3 (w), 810.9 (s), 741.9 (s), 688.0 (s), 627.9 (w) cm^{-1}. **HRMS** (NSI$^+$, CH_2Cl_2): Found: *m*/*z* = 533.1152. Calculated for [M + H]$^+$: *m*/*z* = 533.1157. **OR** ($CHCl_3$, *c* = 1.0 mg/ml): $[\alpha]_D^{20}$ = +110°.

6.4.8 (*R*)-Diphenyl (2'-methoxy-[1,1'-binaphthalen]-2-yl)phosphonodiselenoite (**53b**)

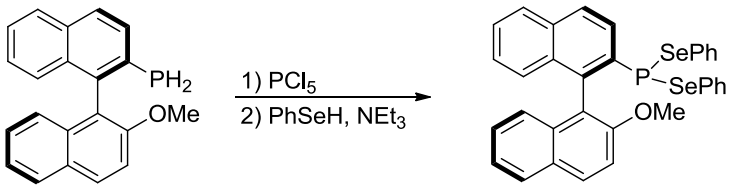

PCl_5 (458 mg, 2.20 mmol) was dissolved in toluene (8 mL). Primary phosphine **1b** (316 mg, 1.00 mmol) was added and the reaction mixture was left to stir for 45 minutes. The volatiles were removed *in vacuo* to give the corresponding dichlorophosphine ($^{31}P\{^1H\}$ NMR, $CDCl_3$: $\delta = 159.1$ ppm) as yellow solid. CH_2Cl_2 (8 mL), NEt_3 (448 mg, 0.64 mL, 4.40 mmol) and benzeneselenol (330 mg, 0.31 mL, 2.10 mmol) were added subsequently and the solution was left to stir overnight. The volatiles were removed *in vacuo* and the crude product was purified by column chromatography (hexane/EtOAc, 5:1) on a silica media and subsequent crystallisation by slow evaporation of the solvent. The title product was obtained as pale yellow crystals (383 mg, 0.61 mmol, 61%).

MP (uncorrected): 178 °C. **^{1}H NMR** (400 MHz, $CDCl_3$): $\delta = 8.15$ (dd, $^3J_{HH} = 8.5$ Hz, $^3J_{HP} = 1.1$ Hz, 1H, *H*3), 7.98 (d, $^3J_{HH} = 9.1$ Hz, 1H, *H*4'), 7.97 (d, $^3J_{HH} = 8.5$ Hz, 1H, *H*4), 7.92 (d, $^3J_{HH} = 8.2$ Hz, 1H, *H*5), 7.84 (d, $^3J_{HH} = 8.2$ Hz, 1H, *H*5'), 7.49 (ddd, $^3J_{HH} = 8.3$ Hz, $^3J_{HH} = 6.7$ Hz, $^4J_{HH} = 1.4$ Hz, 1H, *H*6), 7.36-7.20 (m, 6H, 2 Ph*H*+*H*3'+*H*6'+*H*7+*H*8), 7.18-7.12 (m, 2H, Ph*H*+*H*7'), 7.11-7.02 (m, 3H, 3 Ph*H*), 6.95 (d, $^3J_{HH} = 8.6$ Hz, 1H, *H*8'), 6.92-6.89 (m, 4H, 4 Ph*H*), 3.62 (s, 3H, OCH_3) ppm. **^{13}C{^{1}H} NMR** (101 MHz, $CDCl_3$): $\delta = 154.9$ (d, $^4J_{CP} = 2.1$ Hz, *C*2'), 138.3 (d, $^1J_{CP} = 39.1$ Hz, *C*2), 134.5 (m, Ph*C*), 134.4 (m, Ph*C*), 133.9, 132.7, 131.6, 130.5 (*C*4'), 130.2 (*C*3), 129.7, 129.3, 128.9, 128.7, 128.6 (*C*4), 128.2 (*C*5), 127.9 (*C*5'), 127.4, 127.2 (*C*6), 126.9, 126.8, 125.6 (*C*8'), 123.6 (*C*6'), 120.3 (d, $^3J_{CP} = 10.3$ Hz, *C*1'), 113.0 (*C*3'), 56.3 (OCH_3) ppm. **^{31}P{^{1}H} NMR** (162 MHz, $CDCl_3$): $\delta = 72.0$ (s with ^{77}Se satellites, $^1J_{SeP} = 224$ Hz) ppm. **^{77}Se{^{1}H} NMR** (95 MHz, $CDCl_3$): $\delta = 361.2$ (d with ^{77}Se satellites, $^1J_{SeP} = 224$ Hz, $^2J_{SeSe} = 71$ Hz), 348.8 (d with ^{77}Se satellites, $^1J_{SeP} = 224$ Hz, $^2J_{SeSe} = 71$ Hz) ppm. **IR** (neat): $\nu = 2981.1$ (w), 1617.7 (w), 1510.1 (m), 1473.1 (m), 1437.4 (m), 1332.2 (w), 1269.3 (s), 1149.0 (m), 1079.5 (s), 1050.8 (w), 1017.7 (m), 804.8 (w), 810.3 (s), 748.6 (s), 688.8 (s), 627.1 (w) cm^{-1}. **HRMS** (NSI^+, MeOH): Found: $m/z = 619.0137$. Calculated for $[M + H]^+$: $m/z = 619.0133$. **OR** ($CHCl_3$, $c = 1.0$ mg/ml): $[\alpha]_D^{20} = +130°$. **TLC** (silica gel; hexane:ethyl acetate, 5:1): $R_f = 0.5$.

6.4.9 ((*R*)-Diisopropyl (2'-Methoxy-[1,1'-binaphthalen]-2-yl)phosphonodithioite-*κP*)chlorogold (**54b**)

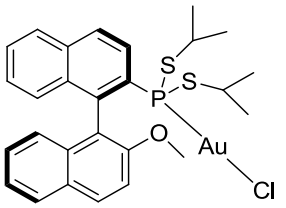

48b (23.2 mg, 50 µmol) and [AuCl(tht)] (16.0 mg, 50 µmol) were dissolved in CH_2Cl_2 (2 mL) and stirred for 15 minutes. Removal of the solvent gave the product as a colourless solid which was washed with hexane.

^{1}H NMR (500 MHz, $CDCl_3$): δ = 8.26 (dd, $^3J_{PH}$ = 10.6 Hz, $^3J_{HH}$ = 8.8 Hz, 1H, *H*3), 8.23 (d, $^3J_{HH}$ = 9.1 Hz, 1H, *H*4'), 8.07 (dd, $^3J_{HH}$ = 8.8 Hz, $^4J_{PH}$ = 1.9 Hz, 1H, *H*4), 7.93 (d, $^3J_{HH}$ = 8.2 Hz, 1H, *H*5), 7.93 (d, $^3J_{HH}$ = 8.2 Hz, 1H, *H*5'), 7.55 (m, 1H, *H*6), 7.48 (d, $^3J_{HH}$ = 9.1 Hz, 1H, *H*3'), 7.34-7.27 (m, 2H, *H*6'+*H*7), 7.19 (ddd, $^3J_{HH}$ = 8.5 Hz, $^3J_{HH}$ = 6.8 Hz, $^4J_{HH}$ = 1.2 Hz, 1H, *H*7'), 7.15 (d, $^3J_{HH}$ = 8.5 Hz, 1H, *H*8), 6.82 (d, $^3J_{HH}$ = 8.5 Hz, 1H, *H*8'), 3.82 (s, 3H, OCH_3), 3.59-3.48 (m, 1H, *i*Pr-C*H*), 3.22-3.11 (m, 1H, *i*Pr'-C*H*), 1.40 (dd, $^3J_{HH}$ = 6.7 Hz, $^3J_{PH}$ = 1.2 Hz, 3H, *i*Pr-CH_3), 1.30 (d, $^3J_{HH}$ = 6.6 Hz, 3H, *i*Pr-CH_3), 1.29 (d, $^3J_{HH}$ = 6.5 Hz, 3H, *i*Pr'-CH_3), 1.04 (d, $^3J_{HH}$ = 6.9 Hz, 3H, *i*Pr'-CH_3) ppm. **^{13}C{^{1}H} NMR** (126 MHz, $CDCl_3$): δ = 154.9 (*C*2'), 140.1 (d, $^2J_{CP}$ = 19.2 Hz, *C*1), 135.0 (d, $^4J_{CP}$ = 2.2 Hz, *C*10), 134.1 (*C*10'), 133.3 (d, $^3J_{CP}$ = 10.6 Hz, *C*9), 131.6 (*C*4'), 129.5 (d, $^1J_{CP}$ = 54.8 Hz, *C*2), 129.2 (*C*9'), 128.9 (d, $^3J_{CP}$ = 9.6 Hz, *C*4), 128.7 (*C*5'), 128.5 (*C*6), 128.2 (*C*5), 127.5 (*C*8), 127.4 (*C*7), 127.3 (*C*3), 126.8 (*C*7'), 125.2 (*C*8'), 123.9 (*C*6'), 118.8 (d, $^3J_{CP}$ = 10.1 Hz, *C*1'), 113.5 (*C*3'), 56.0 (s, OCH_3), 44.1 (d, $^2J_{CP}$ = 2.1 Hz, *i*Pr'-*C*H), 43.7 (d, $^2J_{CP}$ = 1.9 Hz, *i*Pr-*C*H), 25.7 (d, $^3J_{CP}$ = 4.8 Hz, *i*Pr'-*C*H_3), 25.2 (d, $^3J_{CP}$ = 6.1 Hz, *i*Pr'-*C*H_3), 25.1 (d, $^3J_{CP}$ = 5.7 Hz, *i*Pr-*C*H_3), 24.8 (d, $^3J_{CP}$ = 7.6 Hz, *i*Pr-*C*H_3) ppm. **^{31}P {^{1}H} NMR** (202 MHz, $CDCl_3$): δ = 78.8 ppm. **HRMS** (NSI^+, MeCN): Found: *m*/*z* = 719.0634. Calculated for $[M + Na]^+$: *m*/*z* = 719.0644.

6.4.10 ((*R*)-Diphenyl (2'-Methoxy-[1,1'-binaphthalen]-2-yl)phosphonodithioite-*κP*)chlorogold (**55b**)

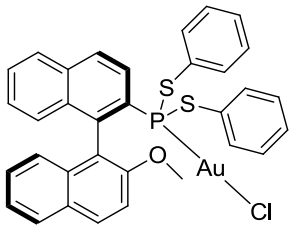

49b (18.6 mg, 35 µmol) and [AuCl(tht)] (11.2 mg, 35 µmol) were dissolved in CH_2Cl_2 (2 mL) and stirred for 15 minutes. Removal of the solvent gave the product as a colourless solid which was washed with hexane.

^{1}H NMR (500 MHz, $CDCl_3$): δ = 8.18 (d, $^3J_{HH}$ = 9.1 Hz, 1H, *H*4'), 8.04 (dd, $^3J_{HH}$ = 8.6 Hz, $^3J_{HP}$ = 8.6 Hz, 1H, *H*3), 8.01 (dd, $^3J_{HH}$ = 8.6 Hz, $^4J_{HP}$ = 3.0 Hz, 1H, *H*4), 7.97 (d, $^3J_{HH}$ = 8.2 Hz, 1H, *H*5), 7.92 (d, $^3J_{HH}$ = 8.2 Hz, 1H, *H*5'), 7.60 (ddd, $^3J_{HH}$ = 8.2 Hz, $^3J_{HH}$ = 6.7 Hz, $^4J_{HH}$ = 1.2 Hz, 1H, *H*6), 7.45-7.42 (m, 2H, 2 Ph*H*), 7.40-7.24 (m, 7H, *H*3'+*H*6'+*H*7+4 Ph*H*), 7.20 (m, 6H, *H*7'+*H*8+4 Ph*H*), 6.76 (d, $^3J_{HH}$ = 8.4 Hz, 1H, *H*8'), 3.73 (s, 3H, OCH_3) ppm. **^{13}C{^{1}H} NMR** (126 MHz, $CDCl_3$): δ = 155.2 (*C*2'), 141.5 (d, $^2J_{CP}$ = 19.4 Hz, *C*1), 136.4 (d, J_{CP} = 4.7 Hz), 136.2 (d, J_{CP} = 5.1 Hz), 135.2 (d, $^4J_{CP}$ = 2.2 Hz, *C*10), 134.1 (*C*10'), 133.4 (d, $^3J_{CP}$ = 10.3 Hz, *C*9), 131.7 (*C*4'), 130.3 (d, J_{CP} = 3.5 Hz), 130.2 (d, J_{CP} = 3.5 Hz), 129.8 (d, J_{CP} = 2.8 Hz), 129.7 (d, J_{CP} = 2.8 Hz), 129.2, 129.1, 128.8 (*C*6), 128.8 (*C*5'), 128.6 (d, $^4J_{CP}$ = 9.2 Hz, *C*4), 128.2 (*C*5), 127.6 (d, J_{CP} = 1.5 Hz), 127.5 (d, J_{CP} = 2.5 Hz), 127.4 (d, $^3J_{CP}$ = 6.4 Hz, *C*3), 127.1 (*C*7'), 124.8 (*C*8'), 123.9 (*C*6'), 118.2 (d, $^3J_{CP}$ = 10.4 Hz, *C*1'), 113.4 (*C*3'), 56.2 (s, OCH_3) ppm. **^{31}P{^{1}H} NMR** (202 MHz, $CDCl_3$): δ = 101.3ppm. **HRMS** (APCI, solid): Found: *m*/*z* = 532.1071. Calculated for $[M - AuCl]^+$: *m*/*z* = 532.1079.

6.4.11 ((*R*)-Diphenyl (2'-methoxy-[1,1'-binaphthalen]-2-yl)phosphonodiselenoite-*κP*)chlorogold (**56b**)

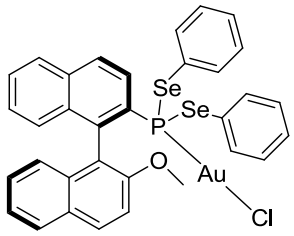

50b (22.0 mg, 35 µmol) and [AuCl(tht)] (11.2 mg, 35 µmol) were dissolved in CH_2Cl_2 (2 mL) and stirred for 15 minutes. Removal of the solvent gave the product as a colourless solid which was washed with hexane.

^{1}H NMR (400 MHz, $CDCl_3$): δ = 8.16 (d, $^3J_{HH}$ = 9.1 Hz, 1H, *H*4'), 7.94-7.89 (m, 3H, *H*5+*H*4+*H*5'), 7.85 (dd, $^3J_{PH}$ = 10.2 Hz, $^3J_{HH}$ = 8.8 Hz, 1H, *H*3), 7.58-7.50 (m, 3H, *H*6+ 2 Ph*H*), 7.40-7.36 (m, 2H, Ph*H*+*H*3'), 7.34-7.21 (m, 7H, *H*6'+*H*7+*H*8+4 Ph*H*), 7.17-7.09 (m, 4H, *H*7'+3 Ph*H*), 6.69 (d, $^3J_{HH}$ = 8.5 Hz, 1H, *H*8'), 3.73 (s, 3H, OCH_3) ppm. **^{13}C{^{1}H} NMR** (101 MHz, $CDCl_3$): δ = 155.1 (*C*2'), 140.6 (d, $^2J_{CP}$ = 17.5 Hz, *C*1), 137.3 (d, *J* = 4.0 Hz), 137.0 (d, *J* = 4.0 Hz), 135.1 (d, *J* = 1.3 Hz), 133.9, 133.4 (d, *J* = 9.9 Hz), 131.6 (*C*4'), 130.1,

129.9, 129.3, 128.8 (*C*4+*C*5), 128.6 (*C*6), 128.3 (*C*3), 127.8 (*C*5), 127.5 (*C*7), 127.1 (*C*7'), 124.7 (*C*8'), 123.9 (*C*6'), 118.4 (d, $^{3}J_{CP}$ = 9.3 Hz, *C*1'), 113.3 (*C*3'), 56.2 (s, O*C*H$_3$), ppm. **^{31}P{^{1}H} NMR** (162 MHz, $CDCl_3$): δ = 68.1 (s with ^{77}Se satellites, $^{1}J_{SeP}$ = 346 Hz) ppm. **^{77}Se{^{1}H} NMR** (95 MHz, $CDCl_3$): δ = 433.0 (d, $^{1}J_{SeP}$ = 346 Hz), 432.3 (d, $^{1}J_{SeP}$ = 343 Hz) ppm. **HRMS** (APCI, solid): Found: *m*/*z* = 621.9995. Calculated for [M – AuCl]$^{+}$: *m*/*z* = 622.0015.

6.4.12 (*R*)-(Diphenylmethylene)(2'-methoxy-[1,1'-binaphthalen]-2-yl)phosphine (**57b**)

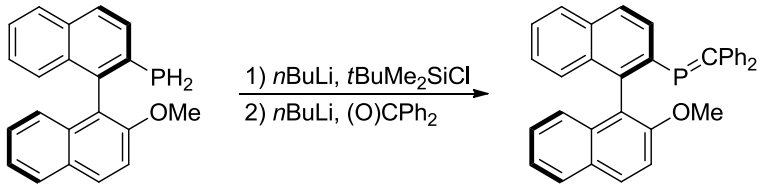

Primary phosphine **1b** (100 mg, 0.316 mmol) was dissolved in THF (4 mL) and cooled to –78 °C. *n*-Butyllithium (0.14 mL, 2.5 M in hexane, 0.348 mmol) was added and the orange-red solution was stirred for 5 minutes, warmed-up to room temperature, and stirred for additional 15 minutes. *tert*-Butyldimethylsilyl chloride (53 mg, 0.348 mmol) was added and the reaction mixture was stirred at room temperature for 30 minutes. *n*-Butyllithium (0.14 mL, 2.5 M in hexane, 0.384 mmol) was added and the solution was stirred for 15 minutes at room temperature and then cooled to –78 °C. Benzophenone (64 mg, 0.348 mmol) was added and the reaction was allowed to warm-up to ambient temperature and stirred for 1 hour. The reaction was slowly quenched with trimethylsilyl chloride (0.05 mL) and stirred for 15 minutes before the volatiles were removed *in vacuo*. Purification was performed by column chromatography (cyclohexane/CH_2Cl_2, 2:1) on a silica media (w = 2 cm, h = 20 cm) to yield the intended product as a yellow solid (117 mg, 0.243 mmol, 77%).

^{1}H NMR (500 MHz, $CDCl_3$): δ = 7.99 (d, $^{3}J_{HH}$ = 9.0 Hz, 1H, *H*4'), 7.86 (d, $^{3}J_{HH}$ = 8.0 Hz, 1H, *H*5'), 7.76 (d, $^{3}J_{HH}$ = 8.0 Hz, 1H, Ar*H*), 7.46 (d, $^{3}J_{HH}$ = 8.5 Hz, 1H, Ar*H*), 7.44 (d, $^{3}J_{HH}$ = 9.0 Hz, 1H, *H*3'), 7.42 (m, 1H, Ar*H*), 7.35-7.32 (m, 3H, 3 Ar*H*), 7.30-7.11 (m, 12H, 12 Ar*H*), 7.08 (d, $^{3}J_{HH}$ = 8.5 Hz, 1H, Ar*H*), 3.88 (s, 3H, OC*H*$_3$) ppm. **^{13}C{^{1}H} NMR** (126 MHz, $CDCl_3$): δ = 192.2 (d, $^{1}J_{CP}$ = 43.5 Hz, P=*C*Ph$_2$), 155.7 (*C*2'), 145.2 (d, J_{CP} = 25.1 Hz), 143.6 (d, J_{CP} = 13.8 Hz), 141.4 (d, $^{1}J_{CP}$ = 42.8 Hz, *C*2), 140.7 (d, J_{CP} = 20.8 Hz), 134.1, 133.5, 133.0 (d, J_{CP} = 4.5 Hz), 132.5, 130.7, 130.6, 130.4, 130.2, 130.0, 129.1, 128.9, 128.8, 128.4, 128.2, 128.1, 128.0, 127.9, 127.6, 126.9, 126.7, 126.5, 126.1, 126.0, 125.5, 123.8, 121.5 (d, $^{3}J_{CP}$ = 7.1 Hz, *C*1'), 113.4 (*C*3'), 56.4 (s, O*C*H$_3$) ppm. **^{31}P{^{1}H} NMR**

(202 MHz, $CDCl_3$): $\delta = 223.6$ ppm. **HRMS** (NSI^+, CH_2Cl_2): Found: $m/z = 513.1601$. Calculated for $[M + O_2 + H]^+$: $m/z = 513.1614$. **TLC** (silica gel; cyclohexane/DCM, 2:1): $R_f = 0.4$.

6.5 References

312 R. M. Hiney, L. J. Higham, H. Müller-Bunz, D. G. Gilheany, *Angew. Chem. Int. Ed.* **2006**, *45*, 7248.

313 A. Ficks, C. Sibbald, S. Ojo, R. W. Harrington, W. Clegg, L. J. Higham, *Synthesis* **2013**, *45*, 265.

314 A. Ficks, I. Martinez-Botella, B. Stewart, R. W. Harrington, W. Clegg, L. J. Higham, *Chem. Commun.* **2011**, *47*, 8274.

315 (a) A. Ficks, R. W. Harrington, L. J. Higham, manuscript in preparation; (b) A. Ficks, R. W. Harrington, L. J. Higham, *Dalton Trans.* **2013**, *42*, 6302; (c) A. Ficks, R. M. Hiney, R. W. Harrington, D. G. Gilheany, L. J. Higham, *Dalton Trans.* **2012**, *41*, 3515.

316 (a) L. I. Kursheva, O. N. Kataeva, S. V. Perova, E. S. Batyeva, O. G. Sinyashin, R. Freilich, *Russ. J. Gen. Chem.* **2005**, *75*, 851; (b) I. Macías-Arce, M. C. Puerta, P. Valerga, *Eur. J. Inorg. Chem.* **2010**, 1767; (c) C. E. Strasser, S. Cronje, H. Schmidbaur, H. G. Raubenheimer, *J. Organomet. Chem.* **2006**, *691*, 4788; (d) J. Laube, S. Jäger, C. Thöne, *Eur. J. Inorg. Chem.* **2001**, 1983; (e) O. N. Kataeva, I. A. Litvinov, V. A. Naumov, L. I. Kursheva, E. S. Batyeva, *Inorg. Chem.* **1995**, *34*, 5171; (f) P. G. Jones, A. K. Fischer, L. Frolova, R. Schmutzler, *Acta Cryst.* **1998**, *C54*, 1842; (g) C. E. Strasser, S. Cronje, H. G. Raubenheimer, *Acta Cryst.* **2009**, *E65*, m86; (h) N. L. Keder, R. K. Shibao, H. Eckert, *Acta Cryst.* **1992**, *C48*, 1670.

317 O. N. Kataeva, D. B. Krivolapov, A. T. Gubaidullin, I. A. Litvinov, L. I. Kursheva, S. A. Katsyuba, *J. Mol. Struct.* **2000**, *554*, 127.

318 O. Sinyashin, V. Milyukov, A. Zverev, A. Plyamovatyi, R. Mukhamadeeva, E. Batyeva, A. Ginzburg, V. Sokolov, *Phosphorus, Sulfur, Silicon* **1996**, *109–110*, 137.

319 Review articles about phosphaalkenes: (a) P. Le Floch, *Coord. Chem. Rev.* **2006**, *250*, 627; (b) L. Weber, *Angew. Chem. Int. Ed.* **2002**, *41*, 563; (c) L. Weber, *Eur. J. Inorg. Chem.* **2000**, 2425; (d) L. N. Markovski, V. D. Romanenko, *Tetrahedron* **1989**, *45*, 6019.

320 See for example: (a) A. Hayashi, M. Okazaki, F. Ozawa, R. Tanaka, *Organometallics* **2007**, *26*, 5246; (b) E. Deschamps, B. Deschamps, J. L. Dormieux, L. Ricard, N. Mézailles, P. Le Floch, *Dalton Trans.* **2006**, 594; (c) J. Dugal-Tessier, G. R. Dake, D. P. Gates, *Angew. Chem. Int. Ed.* **2008**, *47*, 8064.

321 For a recent review see: J. I. Bates, J. Dugal-Tessier, D. P. Gates, *Dalton Trans.* **2010**, *39*, 3151.

322 (a) P. L. Folkins, B. R. Vincent, D. N. Harpp, *Tetrahedron Lett.* **1991**, *32*, 7009; (b) N. Burford, B. W. Royan, A. Linden, T. S. Cameron, *J. Chem. Soc., Chem. Commun.* **1988**, 842.

323 W. McFarlane, J. A. Nash, *J. Chem. Soc. D* **1969**, 913.

324 A. G. Osborne, R. E. Hollands, R. F. Bryan, S. Lockhart, *J. Organomet. Chem.* **1985**, *288*, 207.

325 B. Wrackmeyer, Z. G. Hernández, R. Kempe, M. Herberhold, *Z. Anorg. Allg. Chem.* **2007**, *633*, 851.

326 (a) M. Yoshifuji, K. Toyota, I. Matsuda, T. Niitsu, N. Inamoto, *Tetrahedron* **1988**, *44*, 1363; (b) A. Termaten, M. van der Sluis, F. Bickelhaupt, *Eur. J. Org. Chem.* **2003**, 2049.